VOLUME: 15 NO: 3 YEAR: 2018

ISSN: 1304-530X

TURKISH JOURNAL OF PHARMACEUTICAL SCIENCES

An Official Journal of the Turkish Pharmacists' Association, Academy of Pharmacy

TURKISH
JOURNAL OF PHARMACEUTICAL SCIENCES

TURKISH
JOURNAL OF PHARMACEUTICAL SCIENCES

AIMS AND SCOPE

The Turkish Journal of Pharmaceutical Sciences is the only scientific periodical publication of the Turkish Pharmacists' Association and has been published since April 2004.
Turkish Journal of Pharmaceutical Sciences is an independent international open access periodical journal based on double-blind peer-review principles. The journal is regularly published 3 times a year and the publication language is English. The issuing body of the journal is Galenos Yayinevi/Publishing House.
The aim of Turkish Journal of Pharmaceutical Sciences is to publish original research papers of the highest scientific and clinical value at an international level.
The target audience includes specialists and physicians in all fields of pharmaceutical sciences.
The editorial policies are based on the "Recommendations for the Conduct, Reporting, Editing, and Publication of Scholarly Work in Medical Journals (ICMJE Recommendations)" by the International Committee of Medical Journal Editors (2016, archived at http://www.icmje.org/) rules.

Editorial Independence

Turkish Journal of Pharmaceutical Sciences is an independent journal with independent editors and principles and has no commerical relationship with the commercial product, drug or pharmaceutical company regarding decisions and review processes upon articles.

ABSTRACTED/INDEXED IN

Web of Science-Emerging Sources Citation Index (ESCI)
SCOPUS SJR
Directory of Open Access Journals (DOAJ)
ProQuest
Chemical Abstracts Service (CAS)
EBSCO
EMBASE
Analytical Abstracts
International Pharmaceutical Abstracts (IPA)
Medicinal & Aromatic Plants Abstracts (MAPA)
TÜBİTAK/ULAKBİM TR Dizin
Türkiye Atıf Dizini
UDL-EDGE

OPEN ACCESS POLICY

This journal provides immediate open access to its content on the principle that making research freely available to the public supports a greater global exchange of knowledge.
Open Access Policy is based on the rules of the Budapest Open Access Initiative (BOAI) http://www.budapestopenaccessinitiative.org/. By "open access" to peer-reviewed research literature, we mean its free availability on the public internet, permitting any users to read, download, copy, distribute, print, search, or link to the full texts of these articles, crawl them for indexing, pass them as data to software, or use them for any other lawful purpose, without financial, legal, or technical barriers other than those inseparable from gaining access to the internet itself. The only constraint on reproduction and distribution, and the only role for copyright in this domain, should be to give authors control over the integrity of their work and the right to be properly acknowledged and cited.

CORRESPONDENCE ADDRESS

Editor-in-Chief, Feyyaz ONUR, Prof.Dr.
Address: Lokman Hekim University, Faculty of Pharmacy, Department of Analytical Chemistry, 06100 Tandoğan-Ankara, TURKEY
E-mail: onur@pharmacy.ankara.edu.tr

PERMISSION

Requests for permission to reproduce published material should be sent to the editorial office. Editor-in-Chief, Prof. Dr. Feyyaz ONUR

ISSUING BODY CORRESPONDING ADDRESS

Issuing Body : Galenos Yayınevi
Address: Molla Gürani Mah. Kaçamak Sk. No: 21/1, 34093 İstanbul, TURKEY
Phone: +90 212 621 99 25 Fax: +90 212 621 99 27
E-mail: info@galenos.com.tr

INSTRUCTIONS FOR AUTHORS

Instructions for authors are published in the journal and on the website http://turkjps.org

MATERIAL DISCLAIMER

The author(s) is (are) responsible for the articles published in the JOURNAL.
The editor, editorial board and publisher do not accept any responsibility for the articles.

Publisher Contact
Address: Molla Gürani Mah. Kaçamak Sk. No: 21/1 34093 İstanbul, Turkey
Phone: +90 (212) 621 99 25
Fax: +90 (212) 621 99 27
E-mail: info@galenos.com.tr/yayin@galenos.com.tr
Web: www.galenos.com.tr

Printing at: Üniform Basım San. ve Turizm Ltd. Şti.
Matbaacılar Sanayi Sitesi 1. Cad. No: 114 34204 Bağcılar, İstanbul, Turkey
Phone: +90 (212) 429 10 00
Printing date: November 2018
ISSN: 1304-530X
E-ISSN: 2148-6247

TURKISH
JOURNAL OF PHARMACEUTICAL SCIENCES

INSTRUCTIONS TO AUTHORS

Turkish Journal of Pharmaceutical Sciences is the official double peer-reviewed publication of The Turkish Pharmacists' Association. This journal is published every 4 months (3 issues per year; April, August, December) and publishes the following articles:

• Research articles

• Reviews (only upon the request or consent of the Editorial Board)

• Preliminary results/Short communications/Technical notes/Letters to the Editor in every field or pharmaceutical sciences.

The publication language of the journal is English.

The Turkish Journal of Pharmaceutical Sciences does not charge any article submission or processing charges.

A manuscript will be considered only with the understanding that it is an original contribution that has not been published elsewhere.

The Journal should be abbreviated as "Turk J Pharm Sci" when referenced.

The scientific and ethical liability of the manuscripts belongs to the authors and the copyright of the manuscripts belongs to the Journal. Authors are responsible for the contents of the manuscript and accuracy of the references. All manuscripts submitted for publication must be accompanied by the Copyright Transfer Form [copyright transfer]. Once this form, signed by all the authors, has been submitted, it is understood that neither the manuscript nor the data it contains have been submitted elsewhere or previously published and authors declare the statement of scientific contributions and responsibilities of all authors.

Experimental, clinical and drug studies requiring approval by an ethics committee must be submitted to the JOURNAL with an ethics committee approval report including approval number confirming that the study was conducted in accordance with international agreements and the Declaration of Helsinki (revised 2013) (http://www.wma.net/en/30publications/10policies/b3/). The approval of the ethics committee and the fact that informed consent was given by the patients should be indicated in the Materials and Methods section. In experimental animal studies, the authors should indicate that the procedures followed were in accordance with animal rights as per the Guide for the Care and Use of Laboratory Animals (http://oacu.od.nih.gov/regs/guide/guide.pdf) and they should obtain animal ethics committee approval.

Authors must provide disclosure/acknowledgment of financial or material support, if any was received, for the current study.

If the article includes any direct or indirect commercial links or if any institution provided material support to the study, authors must state in the cover letter that they have no relationship with the commercial product, drug, pharmaceutical company, etc. concerned; or specify the type of relationship (consultant, other agreements), if any.

Authors must provide a statement on the absence of conflicts of interest among the authors and provide authorship contributions.

All manuscripts submitted to the journal are screened for plagiarism using the 'iThenticate' software. Results indicating plagiarism may result in manuscripts being returned or rejected.

The Review Process

This is an independent international journal based on double-blind peer-review principles. The manuscript is assigned to the Editor-in-Chief, who reviews the manuscript and makes an initial decision based on manuscript quality and editorial priorities. Manuscripts that pass initial evaluation are sent for external peer review, and the Editor-in-Chief assigns an Associate Editor. The Associate Editor sends the manuscript to at least two reviewers (internal and/or external reviewers). The reviewers must review the manuscript within 21 days. The Associate Editor recommends a decision based on the reviewers' recommendations and returns the manuscript to the Editor-in-Chief. The Editor-in-Chief makes a final decision based on editorial priorities, manuscript quality, and reviewer recommendations. If there are any conflicting recommendations from reviewers, the Editor-in-Chief can assign a new reviewer.

The scientific board guiding the selection of the papers to be published in the Journal consists of elected experts of the Journal and if necessary, selected from national and international authorities. The Editor-in-Chief, Associate Editors may make minor corrections to accepted manuscripts that do not change the main text of the paper.

In case of any suspicion or claim regarding scientific shortcomings or ethical infringement, the Journal reserves the right to submit the manuscript to the supporting institutions or other authorities for investigation. The Journal accepts the responsibility of initiating action but does not undertake any responsibility for an actual investigation or any power of decision.

The Editorial Policies and General Guidelines for manuscript preparation specified below are based on "Recommendations for the Conduct, Reporting, Editing, and Publication of Scholarly Work in Medical Journals (ICMJE Recommendations)" by the International Committee of Medical Journal Editors (2016, archived at http://www.icmje.org/).

Preparation of research articles, systematic reviews and meta-analyses must comply with study design guidelines:

CONSORT statement for randomized controlled trials (Moher D, Schultz KF, Altman D, for the CONSORT Group. The CONSORT statement revised recommendations for improving the quality of reports of parallel group randomized trials. JAMA 2001; 285: 1987-91) (http://www.consort-statement.org/);

PRISMA statement of preferred reporting items for systematic reviews and meta-analyses (Moher D, Liberati A, Tetzlaff J, Altman DG, The PRISMA Group. Preferred Reporting Items for Systematic Reviews and Meta-Analyses: The PRISMA Statement. PLoS Med 2009; 6(7): e1000097.) (http://www.prisma-statement.org/);

STARD checklist for the reporting of studies of diagnostic accuracy (Bossuyt PM, Reitsma JB, Bruns DE, Gatsonis CA, Glasziou PP, Irwig LM, et al., for the STARD Group. Towards complete and accurate reporting of studies of diagnostic accuracy: the STARD initiative. Ann Intern Med 2003;138:40-4.) (http://www.stard-statement.org/);

STROBE statement, a checklist of items that should be included in reports of observational studies (http://www.strobe-statement.org/);

MOOSE guidelines for meta-analysis and systemic reviews of observational studies (Stroup DF, Berlin JA, Morton SC, et al. Meta-analysis of observational studies in epidemiology: a proposal for reporting Meta-analysis of observational Studies in Epidemiology (MOOSE) group. JAMA 2000; 283: 2008-12).

Authorship

Each author should have participated sufficiently in the work to assume public responsibility for the content. Any portion of a manuscript that is critical to its main conclusions must be the responsibility of at least 1 author.

TURKISH
JOURNAL OF PHARMACEUTICAL SCIENCES

INSTRUCTIONS TO AUTHORS

GENERAL GUIDELINES

Manuscripts can only be submitted electronically through the Journal Agent website (http://journalagent.com/tjps/) after creating an account. This system allows online submission and review.

The manuscripts are archived according to ICMJE, Web of Science-Emerging Sources Citation Index (ESCI), SCOPUS, Chemical Abstracts, EBSCO, EMBASE, Analytical Abstracts, International Pharmaceutical Abstracts, MAPA(Medicinal & Aromatic Plants Abstracts), Tübitak/ Ulakbim Turkish Medical Database, Türkiye Citation Index Rules.

Format: Manuscripts should be prepared using Microsoft Word, size A4 with 2.5 cm margins on all sides, 12 pt Arial font and 1.5 line spacing.

Abbreviations: Abbreviations should be defined at first mention and used consistently thereafter. Internationally accepted abbreviations should be used; refer to scientific writing guides as necessary.

Cover letter: The cover letter should include statements about manuscript type, single-Journal submission affirmation, conflict of interest statement, sources of outside funding, equipment (if applicable), for original research articles.

The ORCID (Open Researcher and Contributor ID) number of the all authors should be provided while sending the manuscript. A free registration can be done at http://orcid.org.

REFERENCES

Authors are solely responsible for the accuracy of all references.

In-text citations: References should be indicated as a superscript immediately after the period/full stop of the relevant sentence. If the author(s) of a reference is/are indicated at the beginning of the sentence, this reference should be written as a superscript immediately after the author's name. If relevant research has been conducted in Turkey or by Turkish investigators, these studies should be given priority while citing the literature.

Presentations presented in congresses, unpublished manuscripts, theses, Internet addresses, and personal interviews or experiences should not be indicated as references. If such references are used, they should be indicated in parentheses at the end of the relevant sentence in the text, without reference number and written in full, in order to clarify their nature.

References section: References should be numbered consecutively in the order in which they are first mentioned in the text. All authors should be listed regardless of number. The titles of Journals should be abbreviated according to the style used in the Index Medicus.

Reference Format

Journal: Last name(s) of the author(s) and initials, article title, publication title and its original abbreviation, publication date, volume, the inclusive page numbers. Example: Collin JR, Rathbun JE. Involutional entropion: a review with evaluation of a procedure. Arch Ophthalmol. 1978;96:1058-1064.

Book: Last name(s) of the author(s) and initials, book title, edition, place of publication, date of publication and inclusive page numbers of the extract cited.

Example: Herbert L. The Infectious Diseases (1st ed). Philadelphia; Mosby Harcourt; 1999:11;1-8.

Book Chapter: Last name(s) of the author(s) and initials, chapter title, book editors, book title, edition, place of publication, date of publication and inclusive page numbers of the cited piece.

Example: O'Brien TP, Green WR. Periocular Infections. In: Feigin RD, Cherry JD, eds. Textbook of Pediatric Infectious Diseases (4th ed). Philadelphia; W.B. Saunders Company;1998:1273-1278.

Books in which the editor and author are the same person: Last name(s) of the author(s) and initials, chapter title, book editors, book title, edition, place of publication, date of publication and inclusive page numbers of the cited piece. Example: Solcia E, Capella C, Kloppel G. Tumors of the exocrine pancreas. In: Solcia E, Capella C, Kloppel G, eds. Tumors of the Pancreas. 2nd ed. Washington: Armed Forces Institute of Pathology; 1997:145-210.

TABLES, GRAPHICS, FIGURES, AND IMAGES

All visual materials together with their legends should be located on separate pages that follow the main text.

Images: Images (pictures) should be numbered and include a brief title. Permission to reproduce pictures that were published elsewhere must be included. All pictures should be of the highest quality possible, in

JPEG format, and at a minimum resolution of 300 dpi.

Tables, Graphics, Figures: All tables, graphics or figures should be enumerated according to their sequence within the text and a brief descriptive caption should be written. Any abbreviations used should be defined in the accompanying legend. Tables in particular should be explanatory and facilitate readers' understanding of the manuscript, and should not repeat data presented in the main text.

MANUSCRIPT TYPES

Original Articles

Clinical research should comprise clinical observation, new techniques or laboratories studies. Original research articles should include title, structured abstract, key words relevant to the content of the article, introduction, materials and methods, results, discussion, study limitations, conclusion references, tables/figures/images and acknowledgement sections. Title, abstract and key words should be written in both Turkish and English. The manuscript should be formatted in accordance with the above-mentioned guidelines and should not exceed 16 A4 pages.

Title Page: This page should include the title of the manuscript, short title, name(s) of the authors and author information. The following descriptions should be stated in the given order:

1. Title of the manuscript (Turkish and English), as concise and explanatory as possible, including no abbreviations, up to 135 characters

2. Short title (Turkish and English), up to 60 characters

3. Name(s) and surname(s) of the author(s) (without abbreviations and academic titles) and affiliations

4. Name, address, e-mail, phone and fax number of the corresponding author

5. The place and date of scientific meeting in which the manuscript was presented and its abstract published in the abstract book, if applicable

Abstract: A summary of the manuscript should be written in both Turkish and English. References should not be cited in the abstract. Use of abbreviations should be avoided as much as possible; if any abbreviations are used, they must be taken into consideration

INSTRUCTIONS TO AUTHORS

independently of the abbreviations used in the text. For original articles, the structured abstract should include the following sub-headings:

Objectives: The aim of the study should be clearly stated.

Materials and Methods: The study and standard criteria used should be defined; it should also be indicated whether the study is randomized or not, whether it is retrospective or prospective, and the statistical methods applied should be indicated, if applicable.

Results: The detailed results of the study should be given and the statistical significance level should be indicated.

Conclusion: Should summarize the results of the study, the clinical applicability of the results should be defined, and the favorable and unfavorable aspects should be declared.

Keywords: A list of minimum 3, but no more than 5 key words must follow the abstract. Key words in English should be consistent with "Medical Subject Headings (MESH)" (www.nlm.nih.gov/mesh/MBrowser.html). Turkish key words should be direct translations of the terms in MESH.

Original research articles should have the following sections:

Introduction: Should consist of a brief explanation of the topic and indicate the objective of the study, supported by information from the literature.

Materials and Methods: The study plan should be clearly described, indicating whether the study is randomized or not, whether it is retrospective or prospective, the number of trials, the characteristics, and the statistical methods used.

Results: The results of the study should be stated, with tables/figures given in numerical order; the results should be evaluated according to the statistical analysis methods applied. See General Guidelines for details about the preparation of visual material.

Discussion: The study results should be discussed in terms of their favorable and unfavorable aspects and they should be compared with the literature. The conclusion of the study should be highlighted.

Study Limitations: Limitations of the study should be discussed. In addition, an evaluation of the implications of the obtained findings/ results for future research should be outlined.

Conclusion: The conclusion of the study should be highlighted.

Acknowledgements: Any technical or financial support or editorial contributions (statistical analysis, English/Turkish evaluation) towards the study should appear at the end of the article.

References: Authors are responsible for the accuracy of the references. See General Guidelines for details about the usage and formatting required.

Review Articles

Review articles can address any aspect of clinical or laboratory pharmaceuticals. Review articles must provide critical analyses of contemporary evidence and provide directions of or future research. Most review articles are commissioned, but other review submissions are also welcome. Before sending a review, discussion with the editor is recommended.

Reviews articles analyze topics in depth, independently and objectively. The first chapter should include the title in Turkish and English, an unstructured summary and key words. Source of all citations should be indicated. The entire text should not exceed 25 pages (A4, formatted as specified above).

CORRESPONDENCE

All correspondence should be directed to the Turkish Journal of Pharmaceutical Sciences editorial board;

Post: Turkish Pharmacists' Association

Address: Willy Brandt Sok. No: 9 06690 Ankara, TURKEY

Phone: +90 312 409 8136

Fax: +90 312 409 8132

Web Page: http://turkjps.org/home/

E-mail: onur@pharmacy.ankara.edu.tr

TURKISH
JOURNAL OF PHARMACEUTICAL SCIENCES

CONTENTS

Original articles

TURKISH
JOURNAL OF PHARMACEUTICAL SCIENCES

CONTENTS

TURKISH
JOURNAL OF PHARMACEUTICAL
SCIENCES

Volume: 15, No: 3, Year: 2018

CONTENTS

Original articles

Turk J Pharm Sci 2018;15(3):231-237
DOI: 10.4274/tjps.50479

ORIGINAL ARTICLE

Structure Elucidation and Antimicrobial Activities of Secondary Metabolites from the Flowery Parts of *Verbascum mucronatum* Lam.

Verbascum mucronatum Lam.'ın Çiçekli Kısımlarından Elde Edilen Sekonder Metabolitlerin Yapı Tayini ve Antimikrobiyal Aktiviteleri

Çiğdem KAHRAMAN[1*], İffet İrem TATLI[2], Didem KART[3], Melike EKİZOĞLU[3], Zeliha Şükran AKDEMİR[1]

[1]Hacettepe University, Faculty of Pharmacy, Department of Pharmacognosy, Ankara, Turkey
[2]Hacettepe University, Faculty of Pharmacy, Department of Pharmaceutical Botany, Ankara, Turkey
[3]Hacettepe University, Faculty of Pharmacy, Department of Pharmaceutical Microbiology, Ankara, Turkey

ABSTRACT

Objectives: To determine the secondary metabolites from *Verbascum mucronatum* Lam. and evaluate their antimicrobial activity.

Materials and Methods: Antimicrobial activities of the isolated metabolites were determined using broth microdilutions against the bacteria (*Escherichia coli* ATCC 25922, *Enterococcus faecalis* ATCC 29212, *Pseudomonas aeruginosa* ATCC 27853, *Staphylococcus aureus* ATCC 29213) and fungi (*Candida albicans* ATCC 90028, *Candida krusei* ATCC 6258, *Candida parapsilosis* ATCC 90018).

Results: Four iridoid glycosides; ajugol (1), aucubin (2), lasianthoside I (3), catalpol (4), two triterpenic saponins; ilwensisaponin C (5), ilwensisaponin A (=mimengoside A) (6), and one phenylethanoid glycoside; verbascoside (=acteoside) (7) were isolated from the water soluble parts of the methanolic extract gained flowery parts of *V. mucronatum* Lam.

Conclusion: Within the obtained compounds, ajugol and ilwensisaponin A showed moderate antimicrobial activity, especially against fungi.

Key words: *Scrophulariaceae*, *Verbascum mucronatum* Lam., secondary metabolites, antimicrobial activity

ÖZ

Amaç: Bu çalışmada *Verbascum mucronatum* Lam.'ın sekonder metabolitlerinin belirlenmesi ve antimikrobiyal aktivitelerinin değerlendirilmesi amaçlanmıştır.

Gereç ve Yöntemler: İzole edilen metabolitlerin, bakteri (*Escherichia coli* ATCC 25922, *Enterococcus faecalis* ATCC 29212, *Pseudomonas aeruginosa* ATCC 27853, *Staphylococcus aureus* ATCC 29213) ve mantarlara (*Candida albicans* ATCC 90028, *Candida krusei* ATCC 6258, *Candida parapsilosis* ATCC 90018) karşı antimikrobiyal aktiviteleri sıvı mikrodilüsyon yöntemiyle belirlenmiştir.

Bulgular: *V. mucronatum* Lam.'ın çiçekli kısımlarının metanol ektresinin suda çözünen kısımlarından, dört iridoit glikoziti, ajugol (1), okubin (2), lasiantozit I (3), katalpol (4); iki triterpenik saponin, ilvensisaponin C (5), ilvensisaponin A (=mimengozit A) (6) ve bir feniletanoit glikoziti, verbaskozit (=akteozit) (7) izole edilmiştir.

Sonuç: Elde edilen bileşikler içinde ajugol ve ilvensisaponin A, özellikle mantarlara karşı zayıf antimikrobiyal aktivite göstermiştir.

Anahtar kelimeler: *Scrophulariaceae*, *Verbascum mucronatum* Lam., sekonder metabolitler, antimikrobiyal aktivite

INTRODUCTION

Verbascum is a widespread genus of the family *Scrophulariaceae*, which comprises more than 300 species of the world's flora.[1] This genus is represented by 233 species, 196 of which are endemic in Turkish flora.[2-4] Infusions prepared with the leaves and flowers of *Verbascum* species have been used as an expectorant and mucolytic[5] wound healer[6] for the treatment of hemorrhoids and rheumatism[7] in folk medicine. Turker and Camper[8] showed that *Klebsiella pneumoniae* and *Staphylococcus aureus* showed sensitivity to Mullein (*Verbascum thapsus*), which may explain why Mullein is used in folk medicine to

*Correspondence: E-mail: cigdemm@hacettepe.edu.tr, Phone: +90 544 622 77 27 ORCID-ID: orcid.org/0000-0001-8096-0738
Received: 16.05.2017, Accepted: 17.08.2017

treat respiratory disorders (caused by *K. pneumoniae* and *S. aureus*) and urinary tract infections (caused by *K. pneumoniae*). Antibacterial and antifungal activities of *Verbascum* L. species have been previously reviewed and the activity of the genus against several bacteria and fungi has been revealed.[9] The antimicrobial activity of *Verbascum mucronatum* has also been determined using disc diffusion tests by our research group.[10] In addition, *V. mucronatum* Lam. has been used as a Hemostatic in Turkish traditional medicine.[11]

Previous investigations on Turkish *Verbascum* L. species by our research group led to the isolation and characterization of a number of secondary metabolites such as iridoids, monoterpene glucosides, saponins, phenylethanoids, neolignans, and flavonoid glycosides.[12-16] As a part of our ongoing studies on the secondary metabolites of *Verbascum* L. species, we have now investigated the methanolic extract of the flowery parts of *V. mucronatum*, and isolated four iridoids; ajugol (**1**), aucubin (**2**), lasianthoside I (**3**), catalpol (**4**), two saponins; ilwensisaponin C (**5**) and ilwensisaponin A (**6**), along with a phenylethanoid glycoside, verbascoside (=acteoside) (**7**) by means of various chromatographic techniques (Figure 1). The current paper deals with the isolation and structure elucidation of the compounds (**1**-**7**) from the title plant and the evaluation of their antimicrobial activities.

MATERIALS AND METHODS

General experimental procedures

The ultraviolet (UV) spectra (λ_{max}) were recorded on a Agilent 8453 spectrophotometer. The infrared (IR) spectra (ν_{max}) were determined on a Perkin Elmer 2000 fourier transform (FT)-IR spectrophotometer. The 1D and 2D nuclear magnetic resonance (NMR) spectra were obtained on a Bruker Avance DRX 500 and 400 FT spectrometer operating at 500 and 400 MHz for ^{1}H NMR, and 125 and 100 MHz for ^{13}C NMR. For the ^{13}C NMR spectra, multiplicities were determined using distortionless enhancement with a polarization transfer (DEPT) experiment. LC-ESIMS data were obtained using a Bruker BioApex FT-mass spectrometry instrument in the ESI mode. Reversed-phase material (C-18, LiChroprep 25-40 µm) and polyamide were used for vacuum liquid chromatography (VLC), reversed-phase material (C-18, LiChroprep 25-40 µm) was used for middle pressure liquid chromatography (MPLC), and Si gel (230-400 mesh) (Merck) was used for column chromatography (CC). Pre-coated silica gel 60 F_{254} aluminum sheets (Merck) were used for thin-layer chromatography (TLC); developing systems, $CHCl_3$-MeOH-H_2O (61:32:7 and 80:20:2). Plates were examined using UV fluorescence and sprayed with 1% vanillin in concentrated H_2SO_4, followed by heating at 105°C for 1-2 min.

Plant material

V. mucronatum Lam. was collected from Aksaray, 17 km from Aksaray to Ulukışla, in July 2007. A voucher specimen has been deposited in the Herbarium of the Faculty of Science, Gazi University, Ankara, Turkey (GAZI 10097). The flowery parts of the plant, which were air dried in the shade, were used in the phytochemical studies.

Extraction and isolation

Air-dried and powdered flowery parts of the plant (586.2 g) were extracted with MeOH (3x2.5 L). The MeOH extract was evaporated to dryness in vacuo to yield 70.4 g of crude extract, then MeOH extract was dissolved with 100 mL distilled water and partitioned in $CHCl_3$ (2x100 mL). H_2O and $CHCl_3$ phases were evaporated to dryness in vacuo to yield 65.8 g H_2O and 3.6 g $CHCl_3$ extracts. The H_2O phase was fractionated using CC on polyamide (150 g) using H_2O-MeOH (100:0→0:100) (each 500 mL), respectively, to yield 6 fractions (Frs. A-F). Fraction D (4.9 g), eluted with 75% methanol, was subjected to VLC using reversed-phase material (C-18, LiChroprep 25-40 µm, 150 g), using MeOH-H_2O mixtures (0-100%) to give catalpol (**4**) (62.1 mg), aucubin (**2**) (139.3 mg), ajugol (**1**) (48.6 mg), Fr. D3 (1.19 g) and Fr. D4 (625.3 mg). Frs. D3 and D4 were rechromatographed. Fr. D3 was applied to MPLC using reversed-phase material (C-18, LiChroprep 25-40 µm) using MeOH-H_2O mixtures (100:0→30-70) to yield ilwensisaponin C (**5**) (14.7 mg), ilwensisaponin A (**6**) (51.5 mg), and lasianthoside I (**3**) (6.7 mg). Fr. D4 was rechromatographed on a silica gel column (55 mg) and eluted $CHCl_3$-MeOH (70:30→60:40) mixtures to give verbascoside (=acteoside) (**7**) (14.8 mg).

Antimicrobial activity-broth microdilution method

Antibacterial and antifungal activities were determined using the broth microdilution test as recommended by Clinical and Laboratory Standards Institute.[17,18] Plant extracts were tested against four bacteria including two Gram-positive (*S. aureus* ATCC 29213, *Enterococcus faecalis* ATCC 29212) and two Gram-negative microorganisms (*Escherichia coli* ATCC 25922, *Pseudomonas aeruginosa* ATCC 27853), as well as for antifungal activities against three yeasts (*Candida albicans* ATCC 90028, *Candida krusei* ATCC 6258, *Candida parapsilosis* ATCC 90018). The antibacterial activity test was performed in Mueller-Hinton broth (MHB, Difco Laboratories, Detroit, MI, USA); for antifungal test, RPMI-1640 medium with L-glutamine (ICN-Flow, Aurora, OH, USA), buffered with MOPS buffer (ICN-Flow, Aurora, OH, USA) was used. The inoculum densities were approximately 5×10^5 CFU/mL and 0.5-2.5×10^3 CFU/mL for bacteria and fungi, respectively.

Each plant extract was dissolved in 2.44 mL DMSO. Finally, two-fold concentrations were prepared in the wells of the microtiter plates, between 1024-1 µg/mL. Ampicillin and fluconazole were used as reference antibiotics for bacteria and fungi, respectively (64-0.0625 µg/mL). Microtiter plates were incubated at 35°C for 18-24 h for bacteria and 48 h for fungi. After the incubation period, minimum inhibitory concentration (MIC) values were defined as the lowest concentration of the extracts that inhibits the visible growth of the microorganisms.

RESULTS

Ajugol (1): UV λ_{max} (MeOH) 220 nm, IR (KBr) ν_{max} 3410 (OH), 1660 (C=C) cm^{-1}, Positive ion LC-ESIMS m/z 371 $[M+Na]^+$ (calc. for $C_{15}H_{24}O_9$), ^{1}H NMR (400 MHz, DMSO-d_6) of **1**: δ_H 6.10 (1H, dd, *J*=6/1.6 Hz, H-3), 5.29 (1H, d, *J*=2 Hz, H-1), 4.78 (1H, dd, *J*=6/2.8 Hz, H-4), 4.43 (1H, d, *J*=7.6 Hz, H-1'), 3.71 (1H, d, *J*=2.8 Hz, H-6), 3.71-3.65 (2H, *, H-6'), 3.05-2.93 (1H, *, H-2', H-3', H-4', H-5'), 2.47 (1H, m, H-5), 2.32 (1H, t, *J*=10 Hz, H-9), 1.84 (1H,

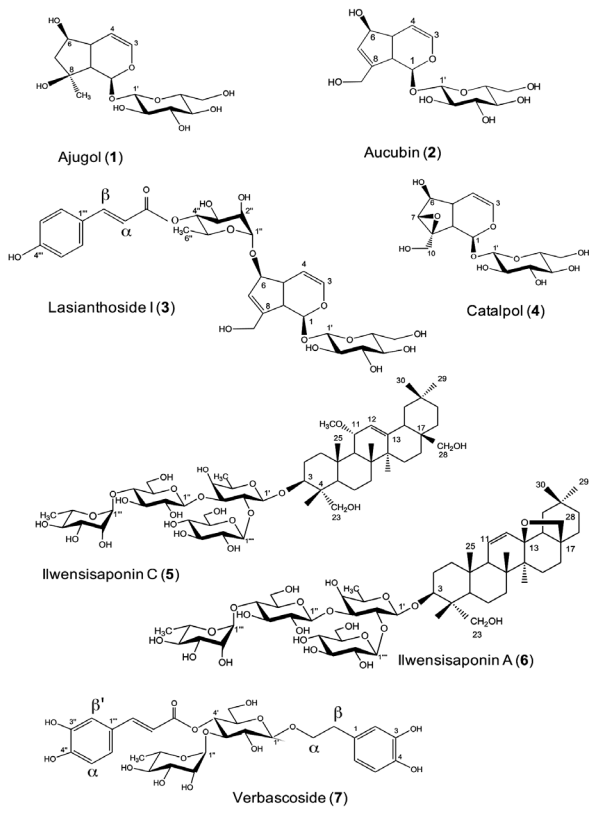

Figure 1. Isolated secondary metabolites from *Verbascum mucronatum* Lam.

Table 1. ^{13}C NMR (DMSO-d_6) data of compounds of 1, 2, 3 and 4

	2 (100 MHz)	3 (125 MHz)	4 (100 MHz)	1 (100 MHz)
C/H atom	δ_C (ppm)	δ_C (ppm)	δ_C (ppm)	δ_C (ppm)
Aglycone				
1	95.9	96.0	93.8	92.1
3	140.6	141.1	140.7	139.3
4	105.6	104.8	103.8	105.7
5	45.2	42.8	37.8	40.7
6	81.1	87.5	77.8	77.8
7	129.8	125.6	61.2	50.6
8	146.8	149.4	65.3	77.7
9	47.0	47.3	42.6	50.5
10	60.1	59.9	59.5	25.7
Glc at C-1				
1'	98.7	100.1	98.3	98.1
2'	74.0	73.9	73.8	73.8
3'	77.3	77.2	76.8	76.1
4'	70.7	70.7	70.6	70.7
5'	77.8	77.6	77.6	77.4
6'	61.7	61.6	61.7	61.7

Compound 3: Rha at C-6, 98.6 (C-1''), 74.3 (C4''), 71.4 (C-2''), 68.8 (C-3''), 67.0 (5''), 18.0 (C-6''); **Acyl moiety,** 166.8 (C=O), 161.0 (C-4'''), 145.2 (C-β), 133.0 (1'''), 130.7 (C-2'''), 130.7 (C-6'''), 116.3 (C-3'''), 116.3 (C-5'''), 115.4 (C-α)

dd, *J*=12.8/6.0 Hz, H-7b), 1.63 (1H, dd, *J*=13.2/6.0 Hz, H-7a), 1.13 (3H, s, H-10), and ^{13}C NMR (100 MHz, DMSO-d_6) (see Table 1).

Aucubin (2): UV λ_{max} (MeOH) 205 nm, (KBr) ν_{max} 3275 (OH), 1650 (C=C) cm^{-1}, Positive ion LC-ESIMS m/z 369 [M+Na]$^+$ (calc. for $C_{15}H_{22}O_9$), ^{1}H NMR (400 MHz, DMSO-d_6) of **2**: δ_H 6.30 (1H, dd, *J*=4.8/1.6 Hz, H-3), 5.65 (1H, bs, H-7) 5.01 (1H, d, *J*=4.8 Hz, H-4), 4.95 (1H, d, *J*=5.6 Hz, H-1), 4.85 (1H, d, *J*=7.7 Hz, H-1'), 4.40, (1H, d, *J*=6.4 Hz, H-6), 4.14 (1H, dd, *J*=12.4/4.0 Hz, H-10b), 3.96 (1H, dd, *J*=12.4/4.0 Hz, H-10a), 3.66 (1H, dd, *J*=12.8/4.8 Hz, H-6'a), 3.42 (1H, dd, *J*=12.0/4.8 Hz, H-6'b), 3.16 (1H, m, H-3'), 3.11 (1H, m, H-4'), 3.04 (1H, m, H-5'), 3.00 (1H, m, H-2'), 2.72 (1H, t, *J*=7.2 Hz, H-9), 2.50 (1H, m, H-5), and ^{13}C NMR (100 MHz, DMSO-d_6) (see Table 1).

Lasianthoside I (3): UV λ_{max} (MeOH) 216, 277 nm, IR (KBr) ν_{max} 3405 (OH), 1704 (C=O), 1655 (C=C), 1508, 1451 (aromatic ring) cm^{-1}, Positive ion LC-ESIMS m/z 611 [M+Na]$^+$ (calc. for $C_{30}H_{38}O_{15}$), ^{1}H NMR (400 MHz, DMSO-d_6) of **3:** δ_H 6.37 (1H, dd, *J*=4.8/1.2 Hz, H-3), 5.26 (1H, d, *J*=4.4 Hz, H-4), 5.10 (1H, d, *J*=4.0 Hz, H-1), 4.91 (1H, d, *J*=7.6 Hz, H-1'), 4.18 (1H, d, *J*=6.0 Hz, H-10b), 3.86 (1H, d, *J*=4 Hz, H-6'b), 3.78 (1H, t, *J*=6.8 Hz, H-6), 3.66 (1H, *, H-10a), 3.64 (1H, dd, *J*=10.8/6.4 Hz, H-6'a), 3.35 (1H, s, H-7), 2.31 (1H, t, *J*=7.6 Hz, H-9), 3.13-3.19 (1H, *, H-3', H-4', H-5'), 3.02 (1H, dd, *J*=10/6.4 Hz, H-2'), 2.12 (1H, m, H-5), and ^{13}C NMR (125 MHz, DMSO-d_6) (see Table 1).

Catalpol (4): UV λ_{max} (MeOH) nm 208 nm, IR (KBr) ν_{max} 3450 (OH), 1670 (C=C) cm^{-1}, Positive ion LC-ESIMS m/z 385 [M+Na]$^+$ (calc. for $C_{15}H_{22}O_{10}$), ^{1}H NMR (400 MHz, DMSO-d_6) of **4**: δ_H 6.37 (1H, dd, *J*= 4.8/1.2 Hz, H-3), 5.26 (1H, d, *J*=4.4 Hz, H-4), 5.10 (1H, d, *J*=4.0 Hz, H-1), 4.91, (1H, d, *J*=7.6 Hz, H-1'), 4.18 (1H, d, *J*=6.0 Hz, H-10b), 3.86 (1H, d, *J*=4 Hz H-6'b), 3.78 (1H, t, *J*=6.8 Hz, H-6), 3.66 (1H, *, 10a), 3.64 (1H, dd, *J*=10.8/6.4 Hz, H-6'a), 3.35 (1H, s, H-7), 3.13-3.19 (*, H-3', H-4', H-5'), 3.02 (1H, dd, *J*=10/6.4 Hz, H-2'), 2.31 (1H, t, *J*=7.6 Hz, H-9), 2.12 (1H, m, H-5), and ^{13}C NMR (100 MHz, DMSO-d_6) (see Table 1).

Ilwensisaponin C (5): UV λ_{max} (MeOH) 205 nm, IR (KBr) ν_{max} 3400 (OH), 1665 (C=C) cm^{-1}, Positive ion LC-ESIMS m/z 1127 [M+Na]$^+$ (calc. for $C_{55}H_{92}O_{22}$), ^{1}H NMR (400 MHz, pyridine) of **5**: δ_H 5.78 (1H, bs, H-1'''), 5.54 (1H, d, *J*=7.0 Hz, H-1''''), 5.46 (1H, bs, H-12), 5.21 (1H, d, *J*=7.0 Hz, H-1''), 4.91 (1H, d, *J*=6.6 Hz, H-1'), 4.35 (1H, *, H-2'), 4.33 (1H, *, H-23b), 4.10 (1H, *, H-2''''), 4.10 (1H, *, H-3), 3.89 (1H, *, H-2''), 3.82 (1H, *, H-11), 3.81 (1H, d, *J*=11.7 Hz, H-28b), 3.69 (1H, d, *J*=8.3 Hz, H-23a), 3.57 (1H, d, *J*=10.2 Hz, H-28a), 1.68 (3H, d, *J*=5.5 Hz, H-6'''), 1.35 (3H, d, *J*=4.8 Hz, H-6'), 1.30 (3H, s, H-27), 1.08 (3H, s, H-24), 1.07 (3H, s, H-25), 0.96 (3H, s, H-26), 0.95 (3H, s, H-30), 0.88 (3H, s, H-29), CH_3O: 3.21 (3H, s), and ^{13}C NMR (125 MHz, pyridine) (see Table 2).

Ilwensisaponin A (6): UV λ_{max} (MeOH) 206 nm, IR (KBr) ν_{max} 3434 (OH), 1645 (C=C) cm^{-1}, Positive ion LC-ESIMS m/z 1095 [M+Na]$^+$ (calc. for $C_{54}H_{88}O_{21}$), ^{1}H NMR (500 MHz, pyridine) of **6**: δ_H 5.94 (1H, d, *J*=10.4 Hz, H-11), 5.77 (1H, d, *J*=1.5 Hz, H-1'''), 5.53 (1H, *, H-12), 5.20 (1H, d, *J*=7.6 Hz, H-1''), 5.53 (1H, d, *J*=7.9 Hz, H-1''''), 4.91 (1H, d, *J*=7.7 Hz, H-1'), 4.58 (1H, *, H-2'''), 4.34 (1H, *, H-23b), 4.25 (1H, *, H-2'), 4.11 (1H, *, H-3), 4.05 (1H, *, H-2''''), 3.90 (1H, *, H-2''), 3.72 (1H, *, H-28b), 3.70 (1H, *, H-23a), 3.33

Table 2. ^{13}C NMR (125 MHz, pyridine-d5/5, CD_3OD/6) data of compounds 5 and 6

	5	6		5	6
C/H atom	δ_C (ppm)	δ_C (ppm)	C/atom	δ_C (ppm)	δ_C (ppm)
Aglycone			Sugar units		
1	40.2	38.0	Fuc at C-3		
2	22.9	25.6	1'	104.2	104.7
3	83.0	84.0	2'	77.0	77.1
4	44.1	45.9	3'	85.0	85.7
5	48.1	46.0	4'	72.2	72.2
6	18.5	18.0	5'	70.6	70.7
7	31.9	31.0	6'	17.3	17.0
8	37.6	42.6	Glc at Fuc C-3'		
9	52.8	54.1	1''	105.1	105.1
10	35.8	37.0	2''	75.6	75.4
11	76.2	132.9	3''	77.8	76.1
12	122.6	131.9	4''	78.4	79.3
13	148.1	86.9	5''	77.2	76.4
14	43.6	44.1	6''	61.4	63.5
15	26.7	26.0	Rha at Glc C-4''		
16	26.4	26.5	1'''	102.8	102.9
17	42.2	40.0	2'''	72.8	72.7
18	42.5	52.8	3'''	72.6	71.3
19	47.1	38.3	4'''	74.0	73.8
20	31.4	31.0	5'''	70.5	70.7
21	33.3	34.0	6'''	18.5	18.5
22	34.8	32.0	Glc at Fuc C-2'		
23	64.8	64.5	1''''	104.0	103.5
24	13.4	12.6	2''''	76.2	75.4
25	18.0	19.0	3''''	78.8	76.8
26	18.7	22.0	4''''	72.2	73.5
27	26.4	20.0	5''''	76.5	78.3
28	68.9	78.3	6''''	63.3	61.8
29	33.5	34.0			
30	24.0	24.0			
OCH_3	54.1	-			

(1H, d, *J*=6.2 Hz, H-28a), 1.68 (1H, d, *J*=6.1 Hz, H-6'''), 1.38 (3H, bs, H-6'), 1.31 (3H, s, H-26), 1.04 (3H, s, H-24), 0.98 (3H, s, H-27), 0.96 (3H, s, H-25), 0.87 (3H, s, H-29), 0.82 (3H, s, H-30), and ^{13}C NMR (125 MHz, CD_3OD) (see Table 2).

Verbascoside (Acteoside) (7): UV λ_{max} (MeOH) 220, 332 nm, IR (KBr) ν_{max} 3392 (OH), 1699 (C=O), 1631 (C=C), 1604, 1525 (aromatic ring) cm^{-1}, Positive ion LC-ESIMS m/z 647 $[M+Na]^+$ (calc. for $C_{29}H_{36}O_{15}$), ^1H NMR (500 MHz, DMSO-d_6) of **7**: δ_H 7.48 (1H, d, *J*=15.8 Hz, H-β'), 7.04 (1H, s, H-2'''), 6.97 (1H, d, *J*=7.5 Hz, H-6'''), 6.79 (1H, d, *J*=7.7 Hz, H-5'''), 6.67 (1H, bs, H-2), 6.67 (1H, bs, H-5), 6.52 (1H, d, *J*=7.5 Hz, H-6), 6.20 (1H, d, *J*=15.8 Hz, H-α'), 5.07 (1H, bs, H-1''), 4.75 (1H, t, *J*=9.4 Hz, H-4'), 4.37 (1H, d, *J*=7.7 Hz, H-1'), 3.72 (1H, *, H-2''), 3.91, (1H, m, H-α_b), 3.67, (1H, m, H-α_a), 2.73 (2H, s, H-β), 3.68 (1H, *, H-3'), 3.45-3.70 (2H, *, H-6'), 3.45 (1H, *, H-5'), 3.36 (1H, *, H-5''), 3.35 (1H, *, H-3''), 3.26 (1H, t, *J*=8.3 Hz, H-2'), 3.15 (1H, *, H-4''), 1.00 (3H, d, *J*=5.8 Hz, H-6''), and ^{13}C NMR (125 MHz, $CDCl_3$) (see Table 3).

*(*overlapped*)

The methanolic extract of the flowery part of *V. mucronatum* and isolated compounds possessed moderate antimicrobial activity, especially against fungi. Iridoid glycoside ajugol was found to be the most active compound against *C. albicans* and *C. parapsilosis* with an MIC value of 64 µg/mL, as well as ilwensisaponin A inhibited *C. albicans* and *C. krusei* with the same MIC value as ajugol. These active compounds were found to be much more effective against fungi than the *V. mucronatum* extract (Table 4).

Table 3. ^{13}C NMR (125 MHz, $CDCl_3$) data of compound 7

	7		
C/atom	δ_C (ppm)	C/atom	
Aglycone		Rha at Glc C-3'	
1	131.5	1''	103.1
2	117.2	2''	72.3
3	146.7	3''	72.1
4	144.3	4''	73.9
5	116.7	5''	70.5
6	120.5	6''	18.9
α	71.4	Acyl moiety	
β	35.9	1'''	127.7
		2'''	115.6
Glc		3'''	146.9
1'	104.3	4'''	149.9
2'	76.3	5'''	116.4
3'	81.7	6'''	122.2
4'	70.7	α'	114.7
5'	76.1	β'	148.1
6'	62.7	C=O	168.3

DISCUSSION

Compound **1** was isolated as a white amorphous powder with the molecular formula $C_{15}H_{24}O_9$ (LC-ESIMS *m/z* 371 $[M+Na]^+$). An iridoid enolether system (220 nm) in UV spectrum; hydroxyl group (3410 cm^{-1}) and double-bond (1660 cm^{-1}) absorption bands in IR spectra were observed. Compound **1** was identified as ajugol when comparing ^1H and ^{13}C NMR spectra with those of ajugol.[19]

Compound **2** (see Figure 1) was isolated as white amorphous powder with the molecular formula $C_{15}H_{22}O_9$ (LC-ESIMS *m/z* 369 $[M+Na]^+$). An iridoid enolether system (205 nm) in UV spectrum; hydroxyl group (3275 cm^{-1}) and double-bond (1650 cm^{-1}) absorption bands in IR spectra were observed. Compound **2** was identified as aucubin when comparing ^1H and ^{13}C NMR spectra with those of aucubin.[20,21]

Compound **3** (see Figure 1) was isolated as a white amorphous powder with the molecular formula $C_{30}H_{38}O_{15}$ (LC-ESIMS *m/z* 661 $[M+Na]^+$). The presence of an iridoid enolether system (216 nm) and an aromatic acid (277 nm) moiety in UV spectrum and absorption bands for a hydroxyl group (3405 cm^{-1}), a conjugated ester carbonyl (1704 cm^{-1}), a double-bond (1655 cm^{-1}) and an aromatic ring (1451 cm^{-1}, 1508 cm^{-1}) in IR spectra were observed. The ^1H and ^{13}C NMR spectra of **3** were similar to those of lasianthoside I. Based on this evidence, compound **3** was identified as lasianthoside I.[22]

Compound **4** (Figure 1) was isolated as a white amorphous powder with the molecular formula $C_{15}H_{22}O_{10}$ (LC-ESIMS *m/z* 385 $[M+Na]^+$). Its UV spectrum supported the presence of an iridoid enolether system (208 nm) and absorption bands were for a hydroxyl group (3450 cm^{-1}), and a double-bond (1670 cm^{-1})

Table 4. Minimum inhibitory concentrations (µg/mL) of the methanolic extract and the secondary metabolites

	Bacteria				Fungi		
	Staphylococcus aureus	*Enterococcus faecalis*	*Escherichia coli*	*Pseudomonas aeruginosa*	*Candida albicans*	*Candida krusei*	*Candida parapsilosis*
	ATCC 29213	ATCC 29212	ATCC 25922	ATCC 27853	ATCC 90028	ATCC 6258	ATCC 22019
Verbascum mucronatum-MeOH extract	256	128	256	256	256	128	128
Ajugol	128	256	128	128	64	128	64
Aucubin	256	512	512	256	128	256	256
Lasianthoside I	>512	512	512	512	256	512	256
Catalpol	256	512	512	256	256	256	256
Ilwensisaponin C	>512	>512	512	512	256	512	256
Ilwensisaponin A	256	>512	>512	512	64	64	128
Verbascoside	256	512	512	256	256	256	256
Ampicillin	1	8	2	-	-	-	-
Fluconazole	-	-	-	-	1	64	8

in the IR spectra were observed. The ^{1}H and ^{13}C NMR spectra of compound **4** were similar to those of catalpol. Thus, compound **4** was identified as catalpol.[23]

Compounds **5** and **6** (Figure 1) were obtained as amorphous compounds with molecular weights of 1104 {LC-ESIMS: *m/z* 1127 ([M+Na]$^{+}$)}, and 1072 {LC-ESIMS: *m/z* 1095 ([M+Na]$^{+}$)}, as calculated for $C_{55}H_{92}O_{22}$ and $C_{54}H_{88}O_{21}$, respectively.

In their IR spectra, the observed absorbances were consistent with the presence of olefinic double bonds. The ^{1}H and ^{13}C NMR data of compounds **5** and **6** suggested that they had similar structures, possessing the same sugar moieties but differing in their aglycones.

In the ^{1}H NMR spectrum of compound **5**, characteristic resonances for anomeric protons were observed at δ_H 4.91 (*d*, *J*= 6.6 Hz), 5.21 (*d*, *J*= 7.0 Hz), 5.54 (*d*, *J*= 7.0 Hz), 5.78 (*bs*), and, in the ^{13}C NMR spectrum, anomeric carbons at δ_c 104.2 (β-D-fucopyranose), 105.1 (β-D-glucopyranose-inner), 104.0 (β-D-glucopyranose-terminal) and 102.8 (α-L-rhamnopyranose), as well as 2 proton signals at δ_H 1.35 (*d*, *J*= 4.8 Hz) and 1.68 (*d*, *J*= 5.5 Hz), arising from the secondary methyl groups in the sugar moieties. By means of HMBC correlations, the sequence of the saccharidic chain was determined as [α-L-rhamnopyranosyl-(1→4)-β-D-glucopyranosyl-(1→3)]-[β-D-glucopyranosyl-(1→2)]-β-D fucopyranoside.

The ^{1}H NMR of compound **5** showed 6 tertiary methyl signals at δ_H 0.88, 0.95, 0.96, 1.07, 1.08 and 1.30. The proton signal at δ_H 3.21 (3H) was attributed to methoxy protons, and δ_H 5.46 (*br s*) to the olefinic proton of the aglycone. It was determined that the aglycone was an oleanane-Δ^{12} type confirmed by presence of δ_c 122.6 and 148.1 signals in the ^{13}C NMR spectrum. The assignment of the remaining NMR signals was achieved by means of ^{1}H-^{1}H COSY, HMQC, and HMBC experiments.

The location of the methoxy group was determined using HMBC correlations between methoxy protons and C-11, whereas a chemical shift of C-11 (δ_c 76.2) was also evident. From the chemical shift of C-11 (δ_c 76.2) in compound **5**, it can be concluded that the methoxyl group had an α-configuration as reported for saikosaponin-b_4.[24] The H-3 methine proton, H-23 and H-28 methylene protons showed downfield shifts due to hydroxy substitutions.

Consequently, the structure was elucidated to be 3-*O*-{[α-L-rhamnosyl-(1→4)-(β-D-glucopyranosyl-(1→3)]-β-D-glucopyranosyl]-(1→2)-β-D-fucopyranosyl-11-methoxy-olean-12-ene-3β,23,28-triol (=ilwensisaponin C).[25]

Compound **6** was distinguished from compound **5** by differences in the aglycone parts in ^{1}H and ^{13}C NMR spectra.

The ^{1}H NMR of compound **6** showed 6 tertiary methyl signals at δ_H 0.82, 0.87, 0.96, 0.98, 1.04 and 1.31. The olefinic protons H-11 and H-12 were determined at 5.94 (*br d*, *J*= 10.4 Hz), δ_c 132.9 and δ_H 5.53 (*), δ_c 131.9, respectively. Thus, aglycone was identified as an oleanane-Δ^{11} type and no signals of a methoxy group in ^{1}H and ^{13}C NMR spectra of compound **6** were observed compared with those of compound **5**.

Due to presence of an oxo-bridge between C-28 and C-13, a chemical shift of C-28 methylene protons (δ_H 3.33-3.72) appeared in the higher field in comparison with those of C-23 hydroxylated methylene protons (δ_H 3.70-4.34). Based on this evidence, the aglycone of compound **6** was determined as 13β, 28-epoxyolean-11-ene-3β,23-diol.[26]

As a result, the structure of compound **6** was determined as 3-*O*-{[α-L-rhamnosyl-(1→4)-(β-D-glucopyranosyl-(1→3)]-β-D-glucopyranosyl]-(1→2)-β-D-fucopyranosyl}-13β,28-epoxyolean-11-ene-3β,23-diol (=ilwensisaponin A[25]=mimengoside A).[27]

Compound **7** (Figure 1) was obtained as an amorphous powder. Its structure was identified as verbascoside by comparing its ^{1}H and DEPT-^{13}C NMR data with previously published data and by direct comparison with the authentic sample on a TLC plate.

It has been reported that *Verbascum* L. species contained diverse iridoid glycosides such as ajugol[5,13], aucubin[28], lasianthoside I[22] and catalpol[23]; saponins such as ilwensisaponin C[13] and ilwensisaponin A[13]; and phenylethanoid glycosides such as verbascoside.[13] Ilwensisaponin A has previously been found to be active against *Aspergillus fumigatus*;[29] it showed moderate antifungal activity in the current study.

CONCLUSIONS

This paper is the first to report the presence of these compounds from *V. mucronatum* Lam. Our continuing studies will be of assistance in clarifying the chemotaxonomic classification of the genus *Verbascum* L. On the other hand, when the antimicrobial activity results were evaluated, the higher activities of ajugol and ilwensisaponin A than the *V. mucronatum* extract suggest that more active compounds may be found in further phytochemical studies.

ACKNOWLEDGEMENTS

The authors would like to thank Prof. Dr. Hayri Duman, Gazi University, Faculty of Science, Department of Botany, Etiler, Ankara, Turkey, for the authentication of the plant specimen.

Conflict of Interest: No conflict of interest was declared by the authors.

REFERENCES

1. Tutin TG. Flora Europaea Vol 3. Cambridge; University Press; 1972.
2. Davis PH, Mill RR, Tan K. Flora of Turkey and the East Aegean Islands. Edinburg; University Press; 1988.
3. Ekim T, *Verbascum* L. In: Güner A, Özhatay N, Ekim T, Başer KHC, eds. Flora of Turkey and East Aegean Islands. Edinburg University Press; 2000:193-194.
4. Huber-Morath A, *Verbascum* L. In: Davis P, ed. Flora of Turkey and the East Aegean Islands. Edinburgh University Press; 1978:461-463.
5. Baytop A. Therapy with Medicinal Plants in Turkey (Past and Present). Nobel Tip Kitabevleri Ltd; 1999.
6. Sezik E, Yeşilada E, Honda G, Takaishi Y, Takeda Y, Tanaka T. Traditional medicine in Turkey X. Folk medicine in Central Anatolia. J Ethnopharmacol. 2001;75:95-115.

7. Tuzlaci E, Alparslan DF. Turkish folk medicinal plants, part V: Babaeski (Kırklareli). J Pharm Istanbul University. 2007;39:11-23.
8. Turker AU, Camper ND. Biological activity of common mullein, a medicinal plant. J Ethnopharmacol. 2002;82:117-125.
9. Tatli I, Akdemir ZS. Traditional uses and biological activities of *Verbascum* species. FABAD J Pharm Sci. 2006;31:85-96.
10. Kahraman C, Ekizoglu M, Kart D, Akdemir ZS, Tatli I. Antimicrobial activity of some *Verbascum* species growing in Turkey. FABAD J Pharm Sci. 2011;36:11-15.
11. Cubukcu B, Atay M, Sarıyar G, Ozhatay N. Folk medicines in Aydın. Journal of Traditional and Folcloric Drugs. 1994;1:1-58.
12. Akdemir ZS, Tatli I, Bedir E, Khan IA. Two new iridoid glucosides from *Verbascum salviifolium* Boiss. Z Naturforsch B. 2005;60:113-117.
13. Tatli I, Akdemir ZŞ, Bedir E, Khan IA. Saponin, iridoid, phenylethanoid and monoterpene glycosides from *Verbascum pterocalycinum* var. *mutense*. Turk J Chem. 2004;28:111-122.
14. Akdemir ZŞ, Tatli I, Bedir E, Khan IA. Neolignan and phenylethanoid glycosides from *Verbascum salviifolium* boiss. Turk J Chem. 2004;28:621-628.
15. Akdemir ZS, Tatli I, Bedir E, Khan IA. Iridoid and phenylethanoid glycosides from *Verbascum lasianthum*. Turk J Chem. 2004;28:227-234.
16. Akdemir ZS, Tatli II, Bedir E, Khan IA. Antioxidant flavonoids from *Verbascum salviifolium* boiss. FABAD J Pharm Sci. 2004;28:71-75.
17. Wayne P. Reference method for broth dilution antifungal susceptibility testing of yeasts: Approved standard. 3rd ed. M 27-A3 ed: Clinical and Laboratory Standards Institute; 2008.
18. Wayne P. Methods for dilution antimicrobial susceptibility tests for bacteria that grow aerobically: Approved standard. 8th ed. M 07-A8 ed: Clinical and Laboratory Standards Institute; 2008.
19. Pardo F, Perich F, Torres R, Delle Monache F. Phytotoxic iridoid glucosides from the roots of *Verbascum thapsus*. J Chem Ecol. 1998;24:645-653.
20. Bianco A, Passacantilli P, Polidori G. 1H and 13CNMR data of C-6 epimeric iridoids. Org Magn Resonance. 1983;21:460-461.
21. Chaudhuri RK, Sticher O. New iridoid glucosides and a lignan diglucoside from *Globularia alypum* L. Helv Chim Acta. 1981;64:3-15.
22. Tatli I, Khan IA, Akdemir ZS. Acylated iridoid glycosides from the flowers of *Verbascum* lasianthum Boiss. ex Bentham. Z Naturforsch B. 2006;61:1183-1187.
23. Tatli I, Akdemir ZS, Bedir E, Khan IA. 6-O-alpha-L-rhamnopyranosylcatalpol derivative iridoids from *Verbascum cilicicum*. Turk J Chem. 2003;27:765-772.
24. Ishii H, Seo S, Tori K, Tozyo T, Yoshimura Y. The Structures of Saikosaponin-E and Acetylsaikosaponins, minor components isolated from *Bupleurum falcatum* L. determined by C-13 Nmr-spectroscopy. Tetrahedron Lett. 1977:1227-1230.
25. Calis I, Zor M, Basaran AA, Wright AD, Sticher O. Ilwensisaponin A, B, C and triterpene saponins from *Scrophularia ilwensis*. Helv Chim Acta. 1993;76:1352-1360.
26. Tori K, Yoshimura Y, Seo S, Sakurawi K, Tomita Y, Ishii H. Carbon-13 NMR spektra of saikogenins. Stereochemical dependence in hydroxilation effects upon carbon-13 chemical shifts of oleanene-type triterpenoids. Tetrahedron Lett. 1976;17:4163-4166.
27. Ding N, Yahara S, Nohara T. Structure of mimengosides A and B, new triterpenoid glycosides from *Buddleja* flos produced in China. Chem Pharm Bull. 1992;40:780-782.
28. Akdemir ZS, Tatli I, Bedir E, Khan IA. Acylated iridoid glycosides from *Verbascum* lasianthum. Turk J Chem. 2004;28:101-109.
29. Tatlı I, Akdemir Z. Antimicrobial and antimalarial activities of secondary metabolites from some Turkish *Verbascum* species. FABAD J Pharm Sci. 2005;30:84-92.

Turk J Pharm Sci 2018;15(3):238-247
DOI: 10.4274/tjps.52724

ORIGINAL ARTICLE

Biofabrication of Copper Nanoparticles: A Next-generation Antibacterial Agent Against Wound-associated Pathogens

Bakır Nanopartiküllerin Biyofabrikasyonu: Yara ile İlişkili Patojenlere Karşı Yeni Nesil Antibakteriyel Ajan

Pallavi Singh CHAUHAN, Vikas SHRIVASTAVA*, Rajesh Singh TOMAR*

Amity University, Amity Institute of Biotechnology, Madhya Pradesh, India

ABSTRACT

Objectives: Impaired wound healing is a major complication. A few factors such as blood glucose level, poor circulation, immune system deficiency, and infection are the root causes of impaired wound healing. The aim of the present study was to bio-synthesize copper nanoparticles with potential antibacterial activity against wound-associated pathogens.

Materials and Methods: Copper nanoparticles were fabricated using the sol-gel method with the mixing of *Syzigium cumini* leaf extract in metal salt solution. The particles were then later characterized using UV spectroscopy, SEM, TEM, FTIR, and XRD, and evaluated for their antibacterial activity and its MIC against four wound-associated pathogens.

Results: The results obtained from TEM, SEM, and XRD characterization showed that the particle size was below 100 nm and of spherical shape. FTIR analysis showed the possibility of various biomolecules, which have a role in capping and stabilizing copper nanoparticles. The particles synthesized showed antibacterial activity against four wound-associated pathogens (*P. mirabilis, S. saprophyticus, S. pyogenes,* and *P. aeruginosa*).

Conclusion: The biosynthesized copper nanoparticles showed potent antimicrobial activity, thus the antibacterial activity of the synthesized copper nanoparticles could be used in several biomedical applications. Additionally, they can be exploited as a better therapeutic agent for treating infection seen in impaired diabetic wounds. The particles synthesized by the biological route are eco-friendly, less toxic, feasible, and cost effective.

Key words: Nanoparticles, sol-gel process, biosynthesis, characterization, wound-associated pathogens, biomedical applications

ÖZ

Amaç: Düzgün olmayan yara iyileşmesi önemli bir komplikasyondur. Kan glukoz düzeyi, zayıf dolaşım, bağışıklık sistemi eksikliği ve enfeksiyon gibi birkaç faktör düzgün seyretmeyen iyileşmenin temel nedenleridir. Bu çalışmanın amacı, yara ile ilişkili patojenlere karşı potansiyel antibakteriyel aktivitesi olan bakır nanopartiküllerin biyosentetik olarak üretilmesidir.

Gereç ve Yöntemler: Bakır nanopartikülleri, *Syzigium cumini* yaprak ekstresinin metal tuzu çözeltisi ile karıştırılmasıyla sol-jel yöntemi kullanılarak üretildi. Parçacıklar daha sonra UV spektroskopisi, SEM, TEM, FTIR ve XRD kullanılarak karakterize edildi ve antibakteriyel aktiviteleri yara ile ilişkili olan dört patojene karşı MIC değerleri belirlenerek araştırıldı.

Bulgular: TEM, SEM ve XRD karakterizasyonlarından elde edilen sonuçlar, parçacık boyutunun 100 nm'nin altında ve küresel şekilde olduğunu göstermiştir. FTIR analizi, bakır nanopartiküllerin kapatılmasında ve stabilize edilmesinde rol oynayan çeşitli biyomoleküllerin olasılığını göstermiştir. Sentezlenen parçacıklar, yara ile ilişkili dört patojene karşı (*P. mirabilis, S. saprophyticus, S. pyogenes* ve *P. aeruginosa*) antibakteriyel aktivite göstermiştir.

Sonuç: Biyosentezlenmiş bakır nanopartiküller güçlü antimikrobiyal aktivite göstermiştir, bu nedenle sentezlenmiş bakır nanopartikülleri antibakteriyel aktiviteleri için çeşitli biyomedikal uygulamalarda kullanılabilir. Bununla birlikte, iyileşmeyen diyabetik yaralarda görülen enfeksiyonu tedavi etmek için daha iyi bir terapötik ajan olarak kullanılabilirler. Biyolojik yolla sentezlenen parçacıklar çevre dostu, daha az toksik, uygulanabilir ve uygun maliyetlidir.

Anahtar kelimeler: Nanopartiküller, sol-jel süreci, biyosentez, karakterizasyon, yara ilişkili patojenler, biyomedikal uygulamalar

*Correspondence: **E-mail:** rstomar@amity.edu, vshrivastava@gwa.amity.edu, **ORCID-ID:** orcid.org/0000-0002-2412-5145, orcid.org/0000-0001-5838-3129
Received: 18.05.2017, **Accepted:** 09.11.2017

INTRODUCTION

Impaired or delayed wound healing is a major complication seen in various patients, especially in patients with diabetes.[1,2] There are several factors responsible for impaired wound healing, such as poor circulation,[3] diabetic neuropathy.[4,5] immune system deficiency,[6,7] infection, and stiffness of the arteries,[8] which lowers the supply of blood, nutrients, and oxygen to tissues and ultimately lowers the efficiency of white blood cells to fight against infection.[9] These factors may lead to impaired wound healing,[10,11] thus close monitoring is very essential.[12] The poor replication of immune cells is a sign of infection development, which ultimately lowers rate of wound healing.[13]

Since ancient times, metals have been known to have good antimicrobial activity, thus in daily life metals have been used for disinfecting water,[14] preservation of victuals.[15] During World War 2, the Japanese dropped metal coins into water and milk to treat dysentery.[16]

In India, nanobiotechnology is providing an incipient insight in employing Indian greeneries, which is a great source of various plant products used in Ayurveda for the synthesis of eco-friendly and non-hazardous nanoparticles.[17] Particles smaller than 100 nm are considered as nanoparticles, which have unique particle size along with advanced physical, chemical, and biochemical properties.[18] Both physical and chemical methods are a commercial way of synthesizing metal nanoparticles, which are hazardous to the environment, thus it is imperative to develop an economically and commercially feasible as well environmentally sustainable route for synthesizing metal nanoparticles to meet demand.[19] These phyto fabrications of metal nanoparticles undergo a highly controlled single-step protocol with green principles.[20] Phytoconstituents present in plant extracts can be used to synthesize metal nanoparticles in a single step.[21] Studies have shown that a few metal nanoparticles have consequential wound rejuvenating activity.[22] Thus, this study may provide insight into methods for nanoparticles synthesis and a direction for future research in impaired wound treatment.

MATERIALS AND METHODS

Material requirement

Copper sulfate metal salt was purchased from Fisher-Scientific. Nutrient agar and nutrient broth was purchased from HiMedia Ltd. *P. aeruginosa* (MTCC No. 3542), *S. saprophyticus* (MTCC N0. 6155), *S. pyogenes* (MTCC No. 5969) and *P. mirabilis* (MTCC No. 3310) were the standard cultures, which were procured from the Institute of Microbial Technology, Chandigarh, India.

Materials used for bioreduction of metal nanoparticles are *Syzigium cumini* leaf extract, double-distilled water, ethanol, magnetic beads, conical flask, and test tubes etc.

The study were approved by the Institutional Animal Ethics Committee Jiwaji University (protocol number: EAC/JU/27, date: 28/01/17).

Method

Preparation of leaf extract and phytochemical profiling

Syzigium cumini plant leaves were used for the study, which were collected, air dried, and then coarsely powdered. Extraction was performed using ethanol as a solvent in a soxhlet extractor. The extract was than concentrated. The phytochemical profiling of the plant leaf extract was performed using an alkaloids test (Mayer's test), flavonoids test, glycosides test, steroids test (Salkowski's test), cardiac glycosides test (Keller-Killiani's test), saponins test, resins test, phenols test (ferric chloride test), tannins test ($FeCl_3$/lead acetate test), and a terpenoid test.[23]

Biosynthesis of copper nanoparticles

0.01 M of copper sulphate was prepared and then mixed properly by placing it on magnetic stirrer. *Syzigium cumini* leaf extract was used for the purpose of reduction, where plant phytochemicals may themselves act as capping agents. The solution was then sanctioned for mixing on magnetic stirrer at a temperature of 60-70°C. After 2 hours, the sample was accumulated and sanctioned to centrifuge at 14,000 rpm. Pellets were collected and then washed three times by means of ethanol and then kept for drying on a dry bath. Samples were then collected and sanctioned for further characterization.

Characterization of copper nanoparticles

The synthesized nanoparticles were characterized using ultraviolet (UV)-visible spectrophotometry, a Fourier-transform infrared (FTIR) spectrophotometer Model RZX (Perkin Elmer), scanning electron microscope (SEM) Model JSM6100 (Joel) with image analyzer, an X-ray diffractometer (XRD) (powder method), and transmission electron microscope (TEM) Hitachi (H-7500).

Antimicrobial activity of copper nanoparticles

Antimicrobial susceptibility testing of bio-synthesized copper nanoparticles was performed using the Kirby-Bauer well diffusion method,[24,25] where Mueller-Hinton Agar was taken as a medium, the well diameter was 5 mm and the amount of material used was 30 µL. McFarland standard (0.5)[26] was used. *P. mirabilis, S. saprophyticus, S. pyogenes,* and *P. aeruginosa* were the four different wound-associated pathogens against which the antimicrobial potential of copper nanoparticles was tested. A solvent blank was used as a negative control. Pre-existing drug (povidone iodine), metal salt solution, and *Syzigium cumini* plant leaf extract were used as positive controls.

Minimum inhibitory concentration (MIC) of copper nanoparticles

The MIC of the bio-synthesized copper nanoparticles was then calculated at different concentrations (0.1 mg/mL, 0.3 mg/mL, 0.5 mg/mL, 0.7 mg/mL, and 0.9 mg/mL) against *P. mirabilis, S. saprophyticus, S. pyogenes,* and *P. aeruginosa* using the broth dilution method in nutrient broth. The concentration of culture was adjusted to 0.2 at 568 nm (1×10^8 CFU/mL, 0.5 McFarland's standard). Positive and negative controls were used as standard. MICs were denoted by analyzing the turbidity of the tubes. A small aliquot of the sample (approx. 50 µL) from the culture tubes showing the least or no turbidity was taken and poured on an agar plate for 24 h at the optimum temperature for bacterial growth and was examined for growth. The experiment was performed in triplicate.[27,28]

RESULTS AND DISCUSSION

Availability of phyto chemicals in Syzigium cumini leaf extract

The qualitative estimation of plant extract was performed and the results showed the availability of various phyto chemicals, which are presented in Table 1.

Nanoparticles synthesis and visible observation changes

There are three main phases of metal nanoparticle synthesis using plant extracts i.e. the activation phase, which includes metal ion reduction and then their nucleation, the second is the growth phase, which involves coalescence of small nanoparticles, and the last is the termination phase, which provides the final shape to the nanoparticles. Various studies have shown that in the bio-reduction, when the metal salt (copper sulfate) is dissolved in distilled water, it soon gets dissociated into its ionic form i.e. Cu^{2+} and SO_4^{2-}. After mixing the plant extract into the metal salt solution, there is a possibility that the chemical functional groups present within the plant extract interact with metal ions (Cu^{2+}) and reduce it to its zerovalent state (Cu^0), thus leading to the formation of metallic copper nuclei followed by the growth phase, leaving the rest of the components as by-product.[29]

Thus, the addition of plant extract converts the bulk of the copper to copper nanoparticles, leaving the by-product aside, and ultimately changes the color of the solution. After integration of the plant extract to the metal salt solution, the color of the copper sulfate salt solution turns from bluish-greenish to brownish-reddish, which can be seen in Figure 1A and 1B. Bio-reduction and bio-sorption are the two major steps required for nanoparticle synthesis, by using various phyto products such as plant phytochemicals, carboxylic and amino groups, proteins, and carbohydrates.[30] The colorimetric changes given by nanoparticles are due to the property of quantum confinement, which is a size-dependent property of nanoparticles that affects the optical properties of the nanoparticles.[31-33] The resulting color change may be due to the quantum confinement property of copper nanoparticles.

Table 1. The qualitative estimation of phytoconstituents in *Syzigium cumini* leaf extract

S. No.	Phytoconstituents	Availability in ethanol extract
1.	Flavonoids	+
2.	Alkaloids	+
3.	Glycosides	+
4.	Steroids	+
5.	Phenols	+
6.	Terpenoid	+
7.	Saponins	-
8.	Resins	+
9.	Tannins	+
10.	Cardiac glycosides	-
11.	Phytosterols and triterpenoids	+
12.	Carbohydrates	+
13.	Fixed oils and fats	-

UV spectroscopy

Applied electromagnetic fields cause the excitation of surface plasmons on the periphery of nanoparticles, which leads to the occurrence of the phenomena called surface plasmon resonance.[34] The UV absorption apex range of copper nanoparticles is 573-600 nm.[35,36] The result obtained from UV-Vis spectra (Figure 2) showed the absorption peak approximately at 582 nm, indicating the formation of copper nanoparticles. An additional peak of 558 nm was also obtained. A broad absorption peak at 582 nm is due to the surface plasmon resonance absorption band along with free electronic vibrations of copper nanoparticles in resonance with a light wave.[37]

FTIR spectroscopy

FTIR is a characterization technique that is used to quantify the vibration frequencies (Table 2) of bonds in the molecule,

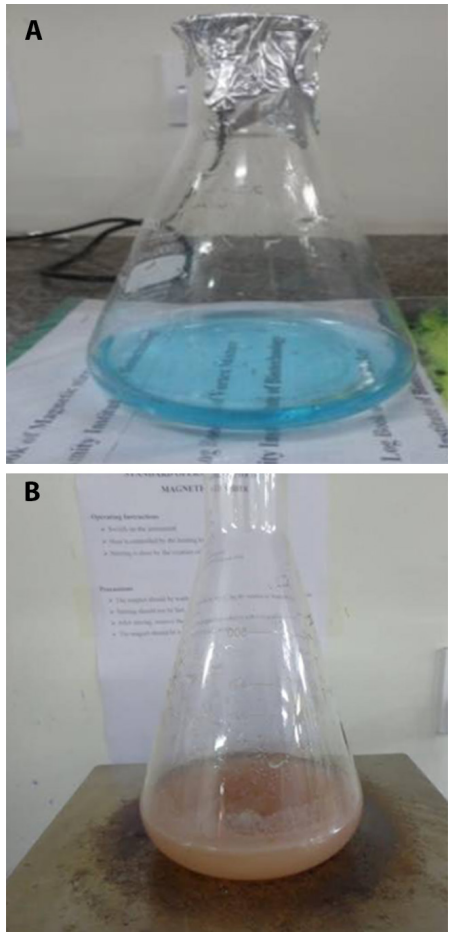

Figure 1. A) Visible observation of copper sulfate salt solution before adding plant leaf extract. B) Visible observation of copper sulfate salt solution after adding plant leaf extract

which can be seen in (Figure 3). FTIR analysis is performed to understand the vibrational kinetics of atoms or molecules, and to identify the possible phytoconstituents responsible for the reduction, as well as capping of reduced copper nanoparticles along with the nature of surface adsorbents.[38-40] The alternate modification by such adsorbents (functional groups) may generate different properties. The FTIR spectra due to such adsorbents over the surface of the nanoparticles thus show a number of absorption peaks, each peak designating the availability of particular functional groups present in the plant extract.[41] It is thus possible to understand the oxidation levels of synthesized nanoparticles prepared at different partial oxygen pressures. From FTIR data, it is possible to study the oxidation levels of nanoparticles prepared at different partial oxygen pressures.[42]

Previous studies have shown that terpenoids are often associated with nanoparticles as analysed in FTIR spectroscopy results. Also, terpenoids have an essential role in transforming metal ions into nanoparticles[43] by dissociating eugenol OH-group protons, thus generating structures that can be further oxidized, leading to the reduction of metal ions, and ultimately the formation of nanoparticles.[44] The flavonoid tautomeric shift, i.e. from enol to keto, results in the release of reactive hydrogen, resulting in the reduction of metal ions and nanoparticle formation.[45] In plant sugars, by means of the nucleophilic addition of OH-, oxidization of the aldehyde group to a carboxyl group occurs, which leads to metal ion reduction and nanoparticle synthesis.[46] Similarly, different functional groups have different mechanisms for nanoparticle synthesis. The exact mechanism behind nanoparticle synthesis is still unknown and this area thus needs further exploration.

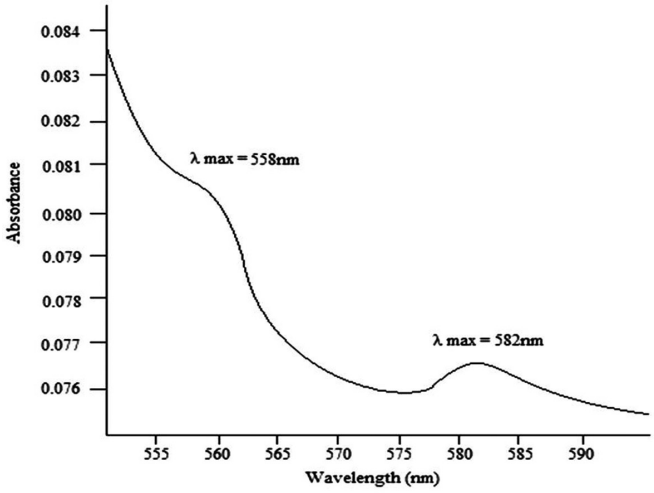

Figure 2. UV analysis of copper nanoparticles

Table 2. Vibrational frequencies of functional groups of possible phytoconstituents obtained by FTIR analysis

S. no.	Frequency (cm^{-1})	Possible functional groups
1.	3377.6 cm^{-1}	O-H stretch vibration of phenols
2.	1632.12 cm^{-1}	N-H bend of primary amines
3.	1514.13 cm^{-1}	N-O asymmetric stretch vibration of nitro compounds
4.	1198.6 cm^{-1}, 1117.3 cm^{-1}, and 1107.3 cm^{-1}	C-N stretch vibration of aliphatic amines
5.	864.11 cm^{-1}	N-H bond of primary and secondary amines
6.	803.11 cm^{-1}, 676.10 cm^{-1}, and 626.8 cm^{-1}	C-Cl stretch vibration of alkyl halides
7.	594.9 cm^{-1}	Cu-O stretching vibration

FTIR: Fourier-transform infrared spectroscopy

XRD analysis

X-ray diffraction patterns of copper nanoparticles were recorded using an XRD (powder method), which can be seen in Figure 4. Debye-Scherer's equation i.e. $D=0.9\ \lambda/\beta\ \cos\theta$, was habituated to calculate the size of copper nanoparticles, where D represents crystalline size, λ represents wavelength of X-ray, β represents full width at half maximum of the diffraction peak and θ represents Bragg's angle. At 2θ values, a number of Bragg reflection peaks were observed at 26.79, 32.4, 35.5, 36.4, 44.1, 48.7, 50.6, 58.3 and 75.6, which were indexed to (111), (110), (002), (111), (200), (202), (200), (202) and (220) crystallographic planes of face-centred cubic, (JCPDS, File No. 04-0836 and JCPDS No. 45-0937). Additional peaks obtained seen during XRD analysis (35.09, 35.90 and 36.52) revealed the availability of CuO nanoparticles and 47.49 revealed the availability of Cu_2O nanoparticles, which may have occurred due to exposure of the nanoparticles to the surrounding environment during characterization. The estimated particle size was below 100 nm (calculated using Debye-Scherer's equation). The width of the peaks obtained in XRD pattern is cognate to the crystallite size of the particle.[47] The small size of the nanoparticles synthesized thus increases their high surface area, and surface area to volume ratio.[48]

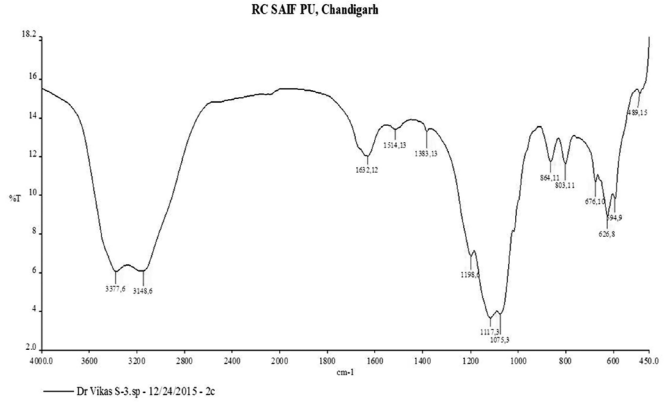

Figure 3. FTIR analysis of copper nanoparticles

TEM and SEM analysis

The synthesized nanoparticles had spherical or ellipsoidal symmetry. The copper nanoparticles were smaller than 100 nm, which can be seen in Figure 5. The obtained result supports the result obtained in TEM analysis, which can be seen in Figure 6. Both TEM and SEM confirmed the presence of copper nanoparticles (i.e. size <100 nm).

Antimicrobial activity of copper nanoparticles

Antimicrobial activity of the copper nanoparticles revealed that they had consequential antibacterial activity against wound-associated pathogens as compared with the plant extract and pre-subsisting drug (povidone iodine), which can be seen in Figures 7A-H. The biosynthesized copper nanoparticles exhibited good antibacterial activity against *P. mirabilis*, *S. saprophyticus*, *S. pyogenes*, and *P. aeruginosa* (i.e. 16 mm, 15 mm, 14 mm, and 12 mm, respectively).

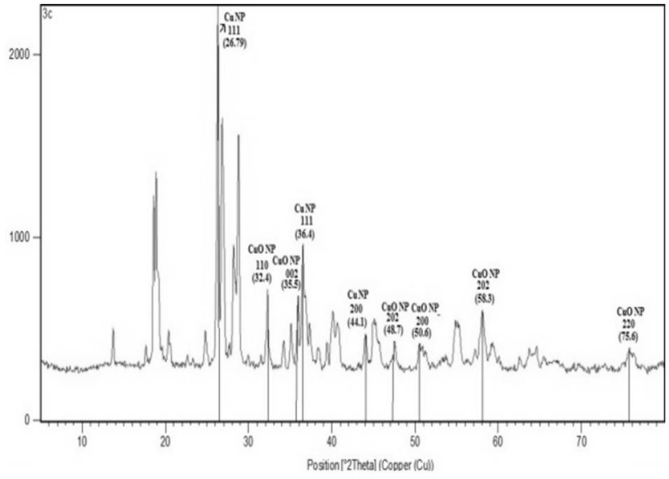

Figure 4. XRD analysis of copper nanoparticles

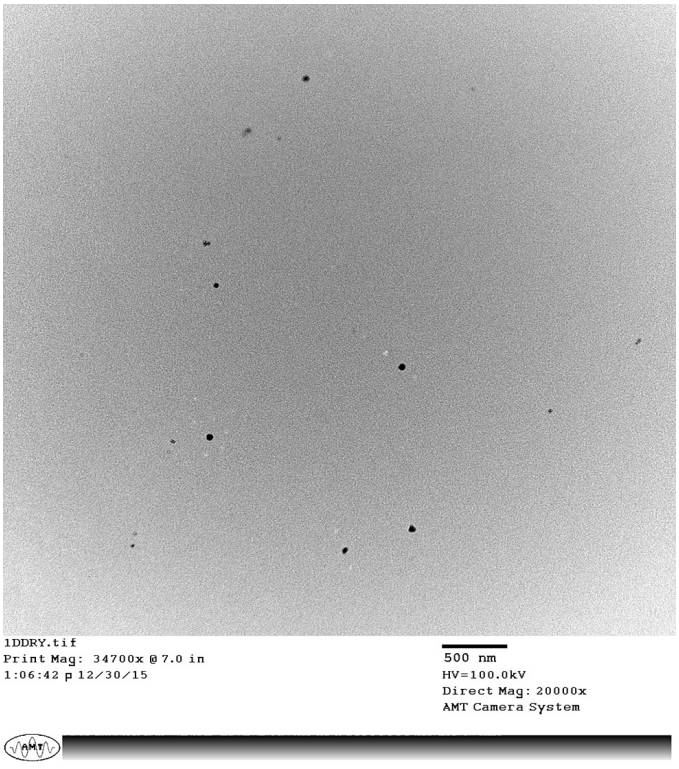

Figure 5. TEM analysis of copper nanoparticles (below 100 nm)

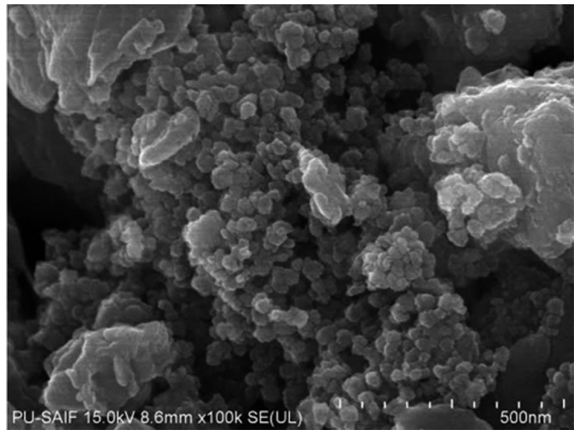

Figure 6. SEM analysis of copper nanoparticles

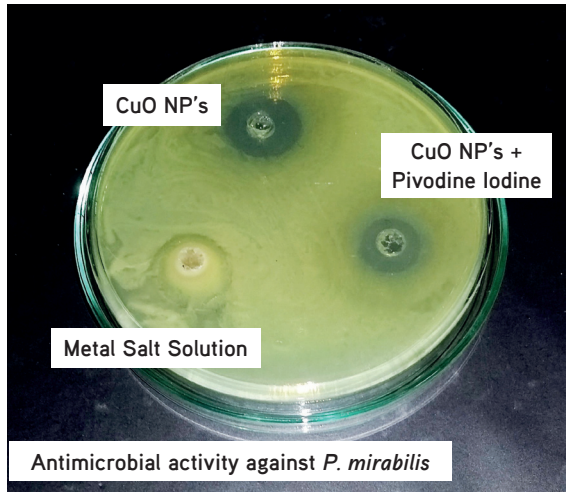

Figure 7. A) Antibacterial activity of copper nanoparticles against *P. mirabilis*

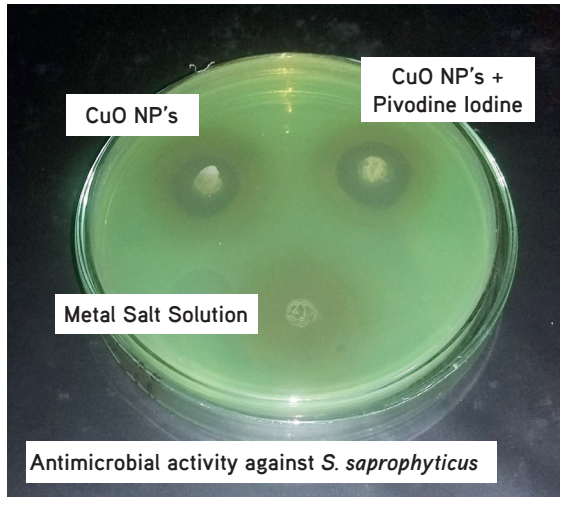

Figure 7. B) Antibacterial activity of copper nanoparticles against *S. saprophyticus*

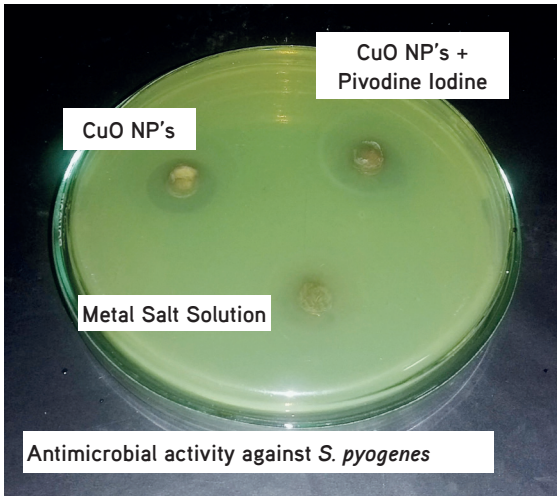

Figure 7. C) Antibacterial activity of copper nanoparticles against *S. pyogenes*

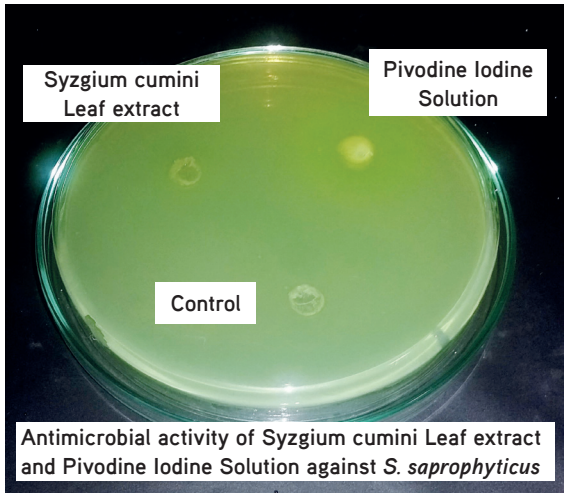

Figure 7. F) Antibacterial activity of plant leaf extract and povidone iodine against *S. saprophyticus*

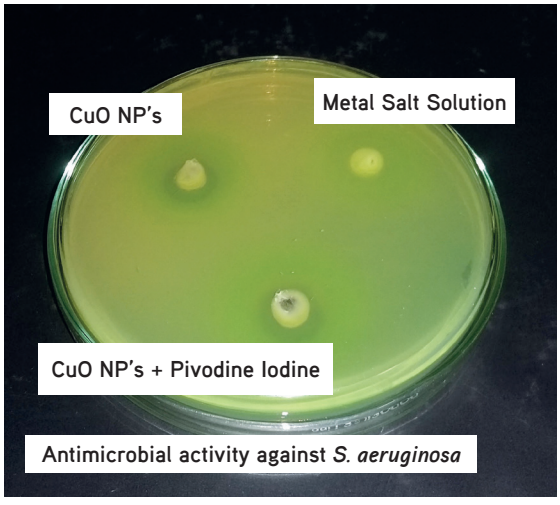

Figure 7. D) Antibacterial activity of copper nanoparticles against *P. aeruginosa*

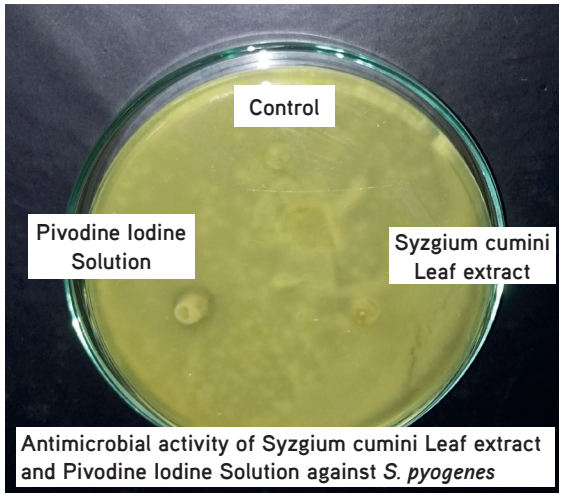

Figure 7. G) Antibacterial activity of plant leaf extract and povidone iodine against *S. pyogenes*

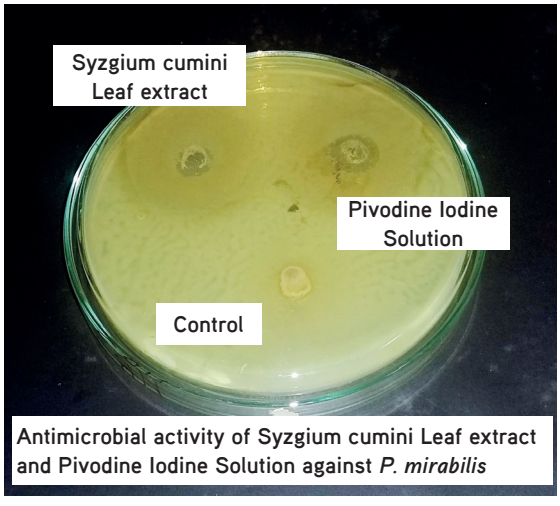

Figure 7. E) Antibacterial activity of plant leaf extract and povidone iodine against *P. mirabilis*

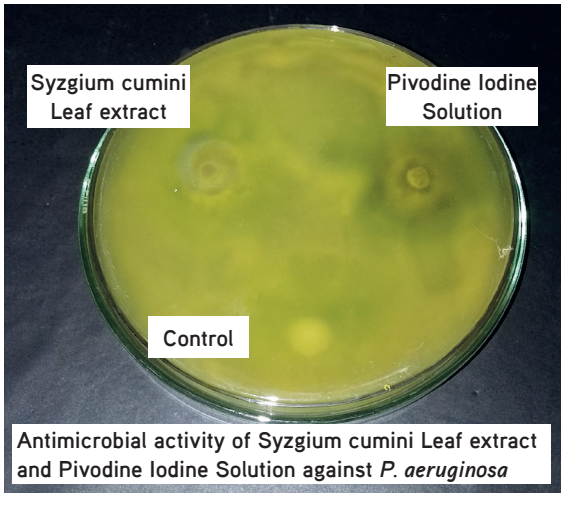

Figure 7. H) Antibacterial activity of Plant leaf extract and povidone iodine against *P. aeruginosa*

Table 3. Bacterial growth at different concentration of copper nanoparticles

Dilution for same bacterial concentration	Sets	Bacterial growth at different concentrations of copper nanoparticles				
		0.9 mg/mL	0.7 mg/mL	0.5 mg/mL	0.3 mg/mL	0.1 mg/mL
P. mirabilis	Set 1	-	-	-	+	+
	Set 2	-	-	-	+	+
	Set 3	-	-	-	+	+
S. saprophyticus	Set 1	-	-	+	+	+
	Set 2	-	-	-	+	+
	Set 3	-	-	-	+	+
S. pyogenes	Set 1	-	-	-	+	+
	Set 2	-	-	-	+	+
	Set 3	-	-	+	+	+
P. aeruginosa	Set 1	-	-	-	+	+
	Set 2	-	-	+	+	+
	Set 3	-	-	+	+	+

+: Turbidity due to microbial growth, -: No turbidity

The biosynthesized copper nanoparticles + pre-subsisting drug (povidone iodine) also exhibited good antibacterial activity against *P. mirabilis, S. saprophyticus, S. pyogenes,* and *P. aeruginosa* (20 mm, 17 mm, 18 mm, and 14 mm, respectively). Integration with povidone iodine exhibited less activity against *P. mirabilis, S. saprophyticus,* and *S. pyogenes* (11 mm, 8 mm, 8 mm), but no activity against *P. aeruginosa.* Moreover, the metal salt solution exhibited less activity against *P. mirabilis* and *S. saprophyticus* (10 mm, 9 mm) and no activity against *S. pyogenes* and *P. aeruginosa*.

MIC and minimum bacterial concentration of copper nanoparticles

The MIC and minimum bacterial concentration of copper nanoparticles was evaluated analysing the turbidity of the culture tubes. Culture tubes containing nanoparticles ranging from 0.1 mg/mL to 0.5 mg/mL showed bacterial growth, whereas no growth was seen in culture tubes containing nanoparticles 0.7 mg/mL and 0.9 mg/mL. A small aliquot of the sample poured on an agar plate showed no bacterial growth when allowed to grow for 24 hours in optimum temperature conditions, showing a bactericidal property of the copper nanoparticles at this particular concentration. Thus, it can be concluded that both the MIC (Table 3) and minimum bacterial concentration (Table 4) of the copper nanoparticles were effective at a concentration of 0.7 mg/mL.

The antibacterial activity results revealed that copper nanoparticles and copper nanoparticles + pre-existing drug acted as potent antibacterial agents against wound-associated pathogens when compared with pre-subsisting drug (povidone iodine), copper sulfate salt solution, and plant extract used for nanoparticle synthesis. The potential antimicrobial activity of the synthesized copper nanoparticles may be due to the grain size of the nanoparticles having a high surface to volume ratio.

Table 4. Minimum bactericidal concentrations of copper nanoparticles

Dilution of copper nanoparticles	Sets	Different concentration of copper nanoparticles	
		0.9 mg/mL	0.7 mg/mL
P. mirabilis	Set 1	-	-
	Set 2	-	-
	Set 3	-	-
S. saprophyticus	Set 1	-	-
	Set 2	-	-
	Set 3	-	-
S. pyogenes	Set 1	-	-
	Set 2	-	-
	Set 3	-	-
P. aeruginosa	Set 1	-	-
	Set 2	-	-
	Set 3	-	-

+: Bacterial growth, -: No bacterial growth

Nanoparticles are known to have bactericidal activity the ability to reduce flora without affecting surrounding tissue.[49] Antimicrobial agents have two modes of action, they are either bactericidal or bacteriostatic.[50] The antibacterial properties of such agents can be used to fight infectious diseases by reducing bacterial load. There is a significant difference between strains of bacteria, thus the use of antibacterial

agents should also be specific to the respective strains. Nanoparticles thus exert toxic effects against bacteria.[51] There are several factors that affect the antimicrobial activity of nanoparticles against various microbial species, some of which are discussed below.

The cell wall protects the cell from damage and rupture because it provides stability, protection, rigidity, and shape to the cell. Tolerance as well as susceptibility is dependent on the structure of the cell wall, and there are several factors that affect the tolerability as well as susceptibility to nanoparticles such as bacterial growth rate and biofilm formation.[52]

The bacterial growth rate is another factor that affects the tolerance of bacteria against nanoparticles. Susceptibility of fast-growing bacteria is more for nanoparticles and antibiotics as compared with slow-growing bacteria (in relation to the expression of stress-response genes).[53]

The formation of biofilm (adhesion of microbial species to a solid surface together with matrix secretion covering them) by bacteria is a major drawback for antibacterial drugs as well as for nanoparticles to fight against bacteria. The interaction of biofilm as well as nanoparticles is dependent on their electrostatic properties.[54]

CONCLUSIONS

The plant leaf extract we used showed great capability to synthesis copper nanoparticles at optimum temperature conditions. The UV absorption peak at 582.00 nm designates the synthesis of copper nanoparticles. The SEM and TEM studies were used with the aim at deciphering the morphology and size of the particle. FTIR studies showed the bio fabrication of the copper nanoparticles by the action of different phytochemicals with its different functional groups present in the extract solution. The XRD patterns showed the purity, phase composition, and nature of the synthesised nanoparticles. The following study justified the synthesis of stable nanoparticles, which could be due to the presence of capping and stabilizing materials such as flavonoids and terpenoids within the plant extract.

Additionally, the bio-synthesized copper nanoparticles showed potential antimicrobial activity against four different wound-associated pathogens as compared with the pre-subsisting drug povidone iodine. Thus the present work focuses on highlighting approaches of bio reduction approaches to synthesize copper nanoparticles using plant extract and antibacterial activity of synthesized nanoparticles. Various studies have already reported the synthesis of metal nanoparticles using physical and chemical methods, but the methods generally employed rigorous chemicals and stringent protocols, which are hazardous to the environment. Thus it is important to develop a protocol that is simple, cost-effective, eco-friendly, with the ability for scale up. The exact mechanism of metal nanoparticles synthesis using plant products is still not clear, but there are several studies which somehow focus on the possible mechanisms behind it. Bio-reduction and bio-sorption are two major steps required for nanoparticles synthesis, governed by the use of various phyto products such as plant phytochemicals, carboxylic and amino groups, proteins and carbohydrates. Accordingly, the present study may support proper wound management with special reference to antimicrobial activity of bio-fabricated copper nanoparticles.

Conflict of Interest: No conflict of interest was declared by the authors.

REFERENCES

1. Williams DRR. The economics of diabetes cre: a global perspective. In: International textbook of diabetes mellitus. Wiley Blackwell; Chichester, UK; 2015.
2. Simon RR, Marks V, Leeds, AR, Anderson JW. A comprehensive review of oral glucosamine use and effects on glucose metabolism in normal and diabetic individuals. Diabetes Metab Res Rev. 2011;27:14-27.
3. Cade WT. Diabetes-related microvascular and macrovascular diseases in the physical therapy setting. Phys Ther. 2008;88:1322-1335.
4. Callaghan BC, Cheng HT, Stables CL, Smith AL, Feldman EL. Diabetic neuropathy: clinical manifestations and current treatments. Lancet Neurol. 2012;11:521-534.
5. Bansal V, Kalita J, Misra UK. Diabetic neuropathy. Postgrad Med J. 2006;964:95-100.
6. Geerlings SE, Hoepelman AI. Immune dysfunction in patients with diabetes mellitus (DM). FEMS Immunol Med Microbiol. 1999;26:259-265.
7. Restrepo BI, Camerlin AJ, Rahbar MH, Wang W, Restrepo MA, Zarate I, Mora-Guzmán F, Crespo-Solis JG, Briggs J, McCormick JB, Fisher-Hoch SP. Cross-sectional assessment reveals high diabetes prevalence among newly-diagnosed tuberculosis cases. Bull World Health Organ. 2011;89:352-359.
8. Lin LY, Liao YC, Lin HF, Lee YS, Lin RT, Hsu CY, Juo SH. Determinants of arterial stiffness progression in a Han-Chinese population in Taiwan: a 4-year longitudinal follow-up. BMC Cardiovasc Disord. 2015;15:100.
9. Jiang H, Yan WH, Li CJ, Wang AP, Dou JT, Mu YM. Elevated White Blood Cell Count Is Associated with Higher risk of glucose metabolism disorders in middle-aged and elderly Chinese people. Int J Environ Res Public Health. 2014;11:5497-5509.
10. Guo S, DiPietro LA. Factors Affecting Wound Healing. J Dent Res. 2010;89:219-229.
11. Said G. Diabetic neuropathy. Handbook Clin Neurol. 2013;115:579-589.
12. Yazdanpanah L, Nasiri M, Adarvishi S. Literature review on the management of diabetic foot ulcer. World J Diabetes. 2015;6:37-53.
13. Casqueiro J, Casquerio J, Alves C. Infections in patients with diabetes mellitus: A review of pathogenesis. Indian J Endocrinol Metab. 2012;16(Suppl 1):27-36.
14. Gehrke I, Geiser A, Somborn-Schulz A. Innovations in nanotechnology for water treatment. Nanotechnol Sci Appl. 2015;8:1-17.
15. Malhotra B, Keshwani A, Kharkwal H. Antimicrobial food packaging: potential and pitfalls. Front Microbiol. 2015;6:611.
16. Lemire JA, Harrison JJ, Turner RJ. Antimicrobial activity of metals: mechanisms, molecular targets and applications. Nat Rev Microbiol. 2013;11:371-384.

17. Ahmed S, Ahmad M, Swami BL, Ikram S. A review on plants extract mediated synthesis of silver nanoparticles for antimicrobial applications: A green expertise. J Adv Res. 2016;7:17-28.

18. The Royal Society and The Royal Academy of Engineering. Nanoscience and nanotechnologies: opportunities and uncertainties. London; UK, 2004.

19. Chung IM, Park I, Seung-Hyun K, Thiruvengadam M, Rajakumar G. Plant-mediated synthesis of silver nanoparticles: Their characteristic properties and therapeutic applications. Nanoscale Res Lett. 2016;11:40.

20. He Y, Du Z, Lv H, Jia Q, Tang Z, Zheng X, Zhang K, Zhao F. Green synthesis of silver nanoparticles by Chrysanthemum morifolium Ramat. extract and their application in clinical ultrasound gel. Int J Nanomedicine. 2013;8:1809-1815.

21. Koga H, Kitaoka T. One-step synthesis of gold nanocatalysts on a microstructured paper matrix for the reduction of 4-nitrophenol. Chem Eng J. 2011;168:420-425.

22. Loomba L, Scarabelli T. Metallic nanoparticles and their medicinal potential. Part II: aluminosilicates, nanobiomagnets, quantum dots and cochleates. Ther Deliv. 2013;4:1179-1196.

23. Senguttuvan J, Paulsamy S, Karthika K. Phytochemical analysis and evaluation of leaf and root parts of the medicinal herb, Hypochaeris radicata L. for *in vitro* antioxidant activities. Asian Pac J Trop Biomed. 2014;4(Suppl 1):359-367.

24. Durán N, Nakazato G, Seabra AB. Antimicrobial activity of biogenic silver nanoparticles, and silver chloride nanoparticles: an overview and comments. Appl Microbiol Biotechnol. 2016;100:6555-6570.

25. Bhatia D, Mittal A, Malik DK. Antimicrobial activity of PVP coated silver nanoparticles synthesized by Lysinibacillus varians. 3 Biotech. 2016;6:196.

26. Omara st. MIC and MBC of Honey and Gold Nanoparticles against methicillin-resistant (MRSA) and vancomycin-resistant (VRSA) coagulase-positive *S. aureus* isolated from contagious bovine clinical mastitis. Journal of Genetic Engineering and Biotechnology. 2017;15:219-230.

27. Krishnan R, Arumugam V, Vasaviah SK. The MIC and MBC of silver nanoparticles against Enterococcus faecalis - A Facultative Anaerobe. J Nanomed Nanotechnol. 2015;6:285.

28. Cavassin ED, de Figueiredo LF, Otoch JP, Seckler MM, de Oliveira RA, Franco FF, Marangoni VS, Zucolotto V, Levin AS, Costa SF. Comparison of methods to detect the *in vitro* activity of silver nanoparticles (AgNP) against multidrug resistant bacteria. J Nanobiotechnology. 2015;13:64.

29. Cerda JS, Gómez HB, Núñezc GA, Riveroa IA, Poncea YG, López LZ. A green synthesis of copper nanoparticles using native cyclodextrins as stabilizing agents. Journal of Saudi Chemical Society. 2017;21:341-348.

30. Makarov VV, Love AJ, Sinitsyna, OV, Makarova SS, Yaminsky IV, Taliansky ME, Kalinina NO. "Green" Nanotechnologies: Synthesis of Metal Nanoparticles Using Plants. Acta Naturae. 2014;6:35-44.

31. Bhumi G, Linga Rao M, Savithramma N. Green synthesis of silver nanoparticles from the leaf extract of adhatoda vasica nees. And assessment of its antibacterial activity. Asian journal of Pharmaceutical and Clinical Research. 2015;8:62-67.

32. Banerjee P, Nath D. A phytochemical approach to synthesize silver nanoparticles for non-toxic biomedical application and study on their antibacterial efficacy. Nanosci Technol. 2015;2:1-14.

33. Smith AM, Nie S. Semiconductor nanocrystals: Structure, properties, and band gap engineering. Acc Chem Res. 2010;43:190-200.

34. Vaidyanathan R, Kalishwaralal K, Gopalram S, Gurunathan S. Nanosilver--the burgeoning therapeutic molecule and its green synthesis. Biotechnol Adv. 2009;27:924-937.

35. Rahimi P, Hashemipour H, Zadeh Me, Ghader S. Experimental investigation on the synthesis and size control of copper nanoparticle via chemical reduction method. Int J Nanosci. 2010;6:144-149.

36. Rama BP, Prajna PS, Vinita PM, Pavithra S. Antimicrobial activities of soap and detergents. Adv Biores. 2011;2:52-56.

37. Ukiya M, Akihisa T, Yasukawa K, Kasahara Y, Kimura Y, Koike K, Nikaido T, Takido M. Constituents of Compositae Plants. 2. Triterpene diols, triols, and their 3-O-fatty acid esters from edible Chrysanthemum flower extract and their anti-inflammatory effects. J Agric Food Chem. 2001;49:3187-3197.

38. Mukherjee B, Santra K, Pattnaik G, Ghosh S. Preparation, characterization and *in vitro* evaluation of sustained release protein-loaded nanoparticles based on biodegradable polymers. Int J Nanomedicine. 2008;3:487-496.

39. Prathna TC, Chandrasekaran N, Raichur AM, Mukherjee A. Biomimetic synthesis of silver nanoparticles by Citrus limon (lemon) aqueous extract and theoretical prediction of particle size. Colloid Surf B Biointerfaces. 2011;82:152-159.

40. Cunha-Filho MS, Martínez-Pacheco R, Landín M. Compatibility of the antitumoral beta-lapachone with different solid dosage forms excipients. J Pharm Biomed Anal. 2007;45:590-598.

41. Baharara J, Ramezani T, Divsalar A, Mousavi M, Seyedarabi A. Induction of apoptosis by green synthesized gold nanoparticles through activation of Caspase-3 and 9 in human cervical cancer cell. Avicenna J Med Biotechnol. 2016;8:75-83.

42. Yallapu MM, Othman SF, Curtis ET, Bauer NA, Chauhan N, Kumar D, Jaggi M, Chauhan SC. Curcumin-loaded magnetic nanoparticles for breast cancer therapeutics and imaging applications. Int J Nanomedicine. 2012;7:1761-1779.

43. Shankar SS, Ahmad A, Pasricha R, Sastry M. Bioreduction of chloroaurate ions by geranium leaves and its endophytic fungus yields gold nanoparticles of different shapes. Mater Chem. 2003;13:1822-1846.

44. Singh AK, Talat M, Singh DP, Srivastava ON. Biosynthesis of gold and silver nanoparticles by natural precursor clove and their functionalization with amine group. J Nanoparticle Res. 2010;12:1667-1675.

45. Ahmad N, Sharma S, Alam MK, Singh VN, Shamsi SF, Mehta BR, Fatma A. Rapid synthesis of silver nanoparticles using dried medicinal plant of basil. Colloids Surf B Biointerfaces. 2010;81:81-86.

46. Shiv Shankar S, Ahmad A, Pasricha R, Sastry MJ. Bioreduction of chloroaurate ions by geranium leaves and its endophytic fungus yields gold nanoparticles of different shapes. Mater Chem. 2003;13:1822-1846.

47. Sarma H, Sarma KC. X-ray Peak Broadening Analysis of ZnO Nanoparticles Derived by Precipitation method. International Journal of Scientific and Research Publications. 2014;4:1-7.

48. Venkateswarlu K, Sreekanth D, Sandhyarani M, Muthupandi V, Bose AC, Rameshbabu N. X-ray peak profile analysis of nanostructured hydroxyapatite and fluorapatite. International Journal of Bioscience, Biochemistry and Bioinformatics. 2012;2:389-393.

49. McDonnell G, Russell AD. Antiseptics and disinfectants: Activity, action, and resistance. Clin Microbiol Rev. 1999;12:147-179.

50. Pankey GA, Sabath LD. Clinical relevance of bacteriostatic versus bactericidal mechanisms of action in the treatment of Gram-positive bacterial infections. Clin Infect Dis. 2004;38:864-870.

51. Dorobantu L, Fallone C, Noble A, Veinot J, Guibin B, Ma G, Goss GG, Burrell RE. Toxicity of silver nanoparticles against bacteria, yeast, and algae. Journal of Nanoparticle Research. 2015;17:172.

52. Palanisamy NK, Ferina N, Amirulhusni AN, Mohd-Zain Z, Hussaini J, Ping LJ, Durairaj R. Antibiofilm properties of chemically synthesized silver nanoparticles found against *Pseudomonas aeruginosa*. J Nanobiotechnology. 2014;12:2.

53. Claudi B, Spröte P, Chirkova A, Personnic N, Zankl J, Schürmann N, Schmidt A, Bumann D. Phenotypic variation of Salmonella in host tissues delays eradication by antimicrobial chemotherapy. Cell. 2014;158:722-733.

54. Stewart PS. Mechanisms of antibiotic resistance in bacterial biofilms. Int J Med Microbiol. 2002;292:107-113.

Turk J Pharm Sci 2018;15(3):248-255
DOI: 10.4274/tjps.44227

ORIGINAL ARTICLE

Design and Development of Crystallo-co-agglomerates of Ritonavir for the Improvement of Physicochemical Properties

Fizikokimyasal Özelliklerin İyileştirilmesi için Ritonavirin Kristalo-Koaglomeratlarının Tasarımı ve Geliştirilmesi

Nilesh M. MAHAJAN[1]*, Ashwini D. MALGHADE[1], Nitin G. DUMORE[1], Raju R. THENGE[2]

[1]Dadasaheb Balpande College of Pharmacy, Department of Pharmaceutics, Maharashtra, India
[2]Dr. Rajendra Gode College of Pharmacy, Maharashtra, India

ABSTRACT

Objectives: The aim of the present study was to obtain CCA of ritonavir to improve the solubility, dissolution rate, and other physicochemical properties.

Materials and Methods: Ritonavir agglomerates were prepared using the CCA technique. Acetone-water containing HPMC K-15, PEG-6000, PVP K-30 was used as the crystallization medium. The agglomerates were evaluated for saturation solubility, micromeritic properties, yield, and drug content. The agglomerates were also characterized using FTIR, DSC, XRPD and SEM.

Results: The growth of particle size and the spherical form of the agglomerates resulted in the formation of products with good flow and packing properties. The improved compaction properties of the agglomerated crystals were due to the fragmentation that occurred during compression. DSC and XRD studies showed that ritonavir particles crystallized in the presence of HPMC, PEG-6000, PVP K-30 and diluents did not undergo structural modifications. The solubility and dissolution rate of ritonavir agglomerates were improve compare to pure ritonavir.

Conclusion: CCA was successfully applied to improve the physicochemical properties of ritonavir.

Key words: Crystallo-co-agglomeration, solubility, dissolution, ritonavir

ÖZ

Amaç: Bu çalışmanın amacı, çözünürlük, çözünme hızı ve diğer fizikokimyasal özelliklerini iyileştirmek için ritonavirin CCA'larını elde etmektir.

Gereç ve Yöntemler: Ritonavir aglomeraları, CCA tekniği kullanılarak hazırlandı. Kristalizasyon ortamı olarak HPMC K-15, PEG-6000, PVP K-30 içeren aseton-su kullanıldı. Aglomeratlar, doygunluk çözünürlüğü, mikromeritik özellikler, verim ve etkin madde içeriği açısından değerlendirildi. Aglomeratlar ayrıca FTIR, DSC, XRPD ve SEM kullanılarak karakterize edildi.

Bulgular: Aglomeratların partikül büyüklüğünün ve küresel formunun büyümesi, iyi akış ve paketleme özelliklerine sahip ürünlerin oluşumu ile sonuçlandı. Aglomere olmuş kristallerin iyileşmiş sıkıştırma özellikleri, sıkıştırma sırasında meydana gelen parçalanmadan kaynaklanmıştır. DSC ve XRD çalışmaları, HPMC, PEG-6000, PVP K-30 ve seyrelticilerin varlığında kristalleşen ritonavir partiküllerinin yapısal modifikasyonlara maruz kalmadığını gösterdi. Ritonavir aglomeratlarının çözünürlüğü ve çözünme hızı, saf ritonavir ile karşılaştırılır derecede gelişti.

Sonuç: Ritonavirin fizikokimyasal özelliklerini iyileştirmek için kristalo-koaglomerasyonu başarıyla uygulanmıştır.

Anahtar kelimeler: Kristalo-koaglomerasyon, çözünürlük, çözünme, ritonavir

*Correspondence: **E-mail:** nmmahajan78@gmail.com, **ORCID-ID:** orcid.org/0000-0002-2928-0769
Received: 29.06.2017, **Accepted:** 07.09.2017

INTRODUCTION

Crystal engineering is the design and synthesis of molecular solid-state structures with desired properties, based on an understanding and exploitation of intermolecular interactions.[1] The two main strategies currently in use for crystal engineering are based on hydrogen bonding and coordination complexation.[2] With advances in power technology, different attempts have been made to design primary and secondary particles of substances for several applications. Enlargement of particle size is an important process in the manufacturing of tablets that imparts some degree of functionality to particles such as improvements in flowabililty, solubility, dissolution, micromeritic, compression, and compressibility properties. Different techniques for enlargement of particle size are important tools for modifying primary and secondary properties of pharmaceutical substances.[3] Nowadays, several new techniques combining granulation and crystallization are being developed to improve particle properties. There are various conventional processes used to enlarge particle size and involve the wider acceptability, but recently, non conventional techniques of particle size enlargement have been developed including extrusion-spheronization, melt solidification, melt granulation, melt extrusion, and spherical crystallization. These techniques are advantageous because of the lower number of unit operations and are economical in terms of processing cost, and depend on the desired properties of enlarged particle and physico-chemical properties of drug and excipients.[4] Crystal engineering design techniques are widely used in pharmaceutical industries to modify primary (e.g., particle size, shape, crystal habit, crystal form, density, porosity, dust generation) as well as secondary (e.g., flowability, compressibility, compatibility, consolidation, reduced adhesion of formulation to the processing equipment, reduction in air entrapment during processing) properties of pharmaceuticals. In particular, improvement in the efficiency of the manufacturing process and a high degree of particle functionality can be achieved by these techniques.[5] Crystallo-co-agglomeration (CCA) is a novel particle engineering technique, which aggregates crystals of drugs in the form of small spherical particles using excipients and solvents to develop an intermediate material with improved micromeritic and mechanical properties, solubility, and dissolution. The rate of dissolution of the drug from the agglomerates or compacts thereof can be improved and modified by using suitable excipients during the process of preparation of agglomeration.[6] The present work reports a CCA technique used to prepare agglomerates of ritonavir, an antiviral drug, the crystalline form consisting of long needles, which otherwise has low bulk density, very poor flow property as well as compressibility, and very low solubility in water, which makes direct compression difficult. Excipients to be incorporated in the formation of agglomerates should have an affinity toward the bridging liquid. Talc, due to its hydrophobicity, undergoes preferential wetting with bridging liquids and is a suitable excipient for incorporation in agglomerates. Apart from talc, various hydrophilic and hydrophobic polymers have been used to study their effect on physicochemical and physicomechanical properties.

MATERIALS AND METHODS

Ritonavir was obtained as a gift sample from Emcure Pvt. Ltd, Pune, hydroxypropyl methyl cellulose (HPMC) K-15, polyethylene glycol (PEG)-6000 polyvinylpyrrolidone (PVP) K-30, talc, acetone and dichloromethane were purchased from Lobachem, Mumbai, India. All the solvents used were of analytical grade.

The study was approved by the Committee for the Purpose of Control and Supervision of Experiments on Animals (registration number: 1426/PO/Re/S/11/CPCSEA, 01.08.2016)

Preparation of CCA

Different agglomerates were prepared of the compositions shown in Table 1. Ritonavir agglomerates were prepared using a three solvent system comprising acetone: dichloromethane:

Table 1. Formulation of batches of crystallo-co-agglomerates of ritonavir

Sr. no	Material used / Batches	A-1 0.5% w/v g/mL	A-2 0.75% w/v g/mL	A-3 1% w/v g/mL	B-1 0.5% w/v g/mL	B-2 0.75% w/v g/mL	B-3 1% w/v g/mL	C-1 0.5% w/v g/mL	C-2 0.75% w/v g/mL	C-3 1% w/v g/mL
1	Ritonavir	1	1	1	1	1	1	1	1	1
2	PEG-6000	0.5	0.75	1	--	--	--	--	--	--
3	PVP K-30	--	--	--	0.5	0.75	1	--	--	--
4	HPMC K-15	--	--	--	--	--	--	0.5	0.75	1
6	Talc	0.3	0.35	0.4 g	0.3	0.35	0.4	0.3	0.35	0.4
7	Tween 80	0.4	0.4	0.4	0.4	0.4	0.4	0.4	0.4	0.4
8	Dichloromethane	2	2	2	2	2	2	2	2	2
9	Acetone	q.s	q.s	q.s	q.s	q.s	q.s	q.s	q.s	q.s
10	Water	q.s	q.s	q.s	q.s	q.s	q.s	q.s	q.s	q.s

PEG: Polyethylene glycol, PVP: Polyvinylpyrrolidone, HPMC: Hydroxypropyl methyl cellulose

water (acetone as good solvent, dichloromethane as bridging liquid and water as bad solvent, respectively). Polymers were dissolved in a vessel in a sufficient amount of distilled water. Then, talc and Tween 80 were added under stirring conditions at 600 rpm maintained at 10°C. Ritonavir was dissolved in acetone. The latter solution was added immediately to the dispersion containing dissolved polymer under constant stirring conditions (600 rpm) and kept at room temperature. The stirring was continued for 20 min and the bridging liquid dichloromethane was added dropwise to obtain agglomerates, which were then set aside overnight. Then obtained agglomerates were filtered and dried. Three batches (A-1, A-2, A-3, B-1, B-2, B-3, C-1, C-2, C-3) were prepared by changing the concentration of excipients (0.5, 0.75 and 1 % w/v).

Characterization of agglomerates

Saturation solubility studies

To evaluate the increase in the solubility of agglomerates, saturation solubility measurements were conducted. An excess amount drug or agglomerates was added to a 50 mL conical flask containing distilled water. The system was agitated on a rotary shaker for 48 h at 100 rpm, maintained at room temperature, and filtered. The filtrate was suitably diluted and analyzed at 201 nm using an ultraviolet (UV) visible spectrophotometer (UV-1800, Shimadzu, Japan).[7]

Micromeretic study

The flow properties of agglomerates were determined in terms of angle of repose, bulk density, tapped density, Carr's index, and Hausner's ratio. The angle of repose was determined using the fixed funnel method, whereas Carr's index and the Hausner ratio were calculated from bulk and tapped densities. The Hausner ratio was taken as a ratio of tapped density to bulk density.

Angle of repose

The angle of repose has been used to characterize the flow properties of solids. It is a characteristic related to inter particulate friction or resistance to movement between particles. This is the maximum angle possible between the surface of pile of powder or granules and the horizontal plane.

$\tan\theta = h / r$

$\theta = \tan^{-1} h / r$

Where, = angle of repose, h= height of heap, r= radius of base of heap circle.

Method: A funnel was fixed at a height approximately 2-4 cm over a platform. The drug powder was slowly passed along the wall of funnel till the tip of the formed powder cone just touched the tip of the funnel stem. The angle of repose was then determined by measuring the height of the cone of powder and the radius of the circular base of the powder heap.[8]

Compressibility index and Hausner's ratio

In recent years, the compressibility index and the closely-related Hausner ratio, which are simple and quick, have become the most popular methods of predicting powder flow characteristics. The compressibility index has been proposed as an indirect measure of bulk density, size and shape, surface area, moisture content, and cohesiveness of materials because all of these can influence the observed compressibility index. The compressibility index and Hausner's ratio are determined by measuring both bulk density and the tapped density of agglomerates.[9]

Compressibility index= Tapped density - Bulk density / Tapped density × 100

Hausner's ratio= Tapped density / Bulk density.

Production yield (%)

The production yields were calculated as the weight percentage of the final product after drying, with respect to the initial total amount of ritonavir and polymer used for the preparations.[8]

$$\text{Production yield \%} = \frac{\text{Practical mass (CCA)}}{\text{Theoretical mass (polymer+drug)}} \times 100$$

Drug content

Ten milligrams of agglomerates were accurately weighed in a 100 mL volumetric flask and the volume was adjusted to 100 mL with methanol (100 µg/mL), serving as a test solution. Standard solution was sonicated for 5 min and analyzed at 238 nm using a UV spectrophotometer.[10]

Fourier-transformation infrared (FTIR) spectroscopy

The study was conducted with an intention to check the compatibility of polymers such as HPMC K-15M, PEG-6000, and PVP K-30 with ritonavir. Also, it helps to check the suitability of polymer for the preparation of agglomerates. FTIR spectra were obtained using a Shimadzu FTIR spectrometer (Thermo Fisher, Japan). The samples of pure drug and physical mixture such as Ritonavir and HPMC K-15, PEG-6000, PVP K-30 were prepared. The scanning range was kept from 4000 to 500 cm^{-1}[8].

Scanning electron microscopy (SEM)

The surface morphology of the optimized formulations was studied using a SEM (JSM 6390, JEOL) operated at an accelerating voltage of 10 kV and obtained micrographs were examined at differentmagnifications.[11]

X-ray diffraction (XRD) of powder

The X-ray powder diffraction (XRPD) patterns were recorded on the XRD (PW 1729, Philips, Netherland). The samples were irradiated with monochromatised Cu K-α radiation (1.542A°) and analyzed between 10-50° 2θ. The voltage and current used were 30 kV and 30 mA, respectively. The range and chart of speed were CPS and 5 mm/2 respectively[11].

Differential scanning calorimetry (DSC)

The thermal behavior of the drug-loaded agglomerates was studied using a differential scanning calorimeter (Mettler Toledo) at a heating rate of 10°C/min. The measurements were performed at a heating range of 20-250°C under nitrogen atmospheres.[11]

Dissolution studies

The dissolution rate studies were conducted in 900 mL of pH 6.8 phosphate buffer (simulated intestinal fluid) at 50 rpm and maintained at 37±0.5°C in a dissolution apparatus (Model Electrolab Dissolution tester USP TDT-08L) using the paddle method. One hundred milligram equivalent quantity agglomerates were added to the dissolution medium and the samples were withdrawn at appropriate time intervals up to 90 mins. The samples were immediately filtered through a 0.45-µm membrane filter, suitably diluted, and analyzed spectrophotometrically at 201 nm. The data obtained from dissolution studies were statistically validated.[12]

RESULTS AND DISCUSSION

Ritonavir was crystallized from acetone-water and agglomerated with diluents. In this process, the crystallization of the drug was performed by the addition of a solution to the anti-solvent phase (water). Acetone served as good solvent and the bridging liquid and aqueous phase as the non-solvent. The saturation solubility of prepared agglomerate with HPMC K-15 showed the highest solubility compared with pure ritonavir, as shown in Table 2.

The spherically agglomerated crystals, produced in yields generally within the range 55-80% (Table 2), were produced simultaneously as crystallization was completed. As both phases (acetone and aqueous) contained the diluents, then it is likely that it was distributed both inside the agglomerates (intragranularly) and outside the agglomerate (extragranularly), attached to the surface.

Micromeritic of agglomerates

The micromeritic properties, such as flowability of agglomerates, are shown in Table 2. It shows that the flowability represented in terms of the angle of repose, Carr's index and Hausner's ratio of agglomerates was much improved compared with those of the original drug. Statistical analysis showed that the angle of repose and Carr's index for both agglomerates reduced significantly in comparison with the original drug. The Hausner's ratio for both agglomerates was found to be less than 1.52, indicating improvement in their flow properties. The poor flow properties of pure ritonavir might be attributed to it being amorphous in nature. These findings proved that the flowability of agglomerates was preferably improved as compared with the pure drug.

Morphology of agglomerates

An SEM examination confirmed that the starting material was markedly smaller in particle size than any of the treated crystals. Similar results were obtained in other studies using CCA procedures for other drugs. Ritonavir exhibits platy crystal habit, which was distributed at CCA formation. Prominent changes were observed with formulation C-1 as compared with A-1 and B-1. Although all formulations showed formation of agglomerates in the SEM images in Figure 1A-D, as evident from the adherence of the polymer and talc on to the crystal surface of drug.

FTIR spectroscopy

The FTIR spectra of samples are shown in Figure 2A-D. There was no considerable change in the positions of characteristic absorption bands and bonds of various functional groups present in the drug. This observation clearly suggests that the

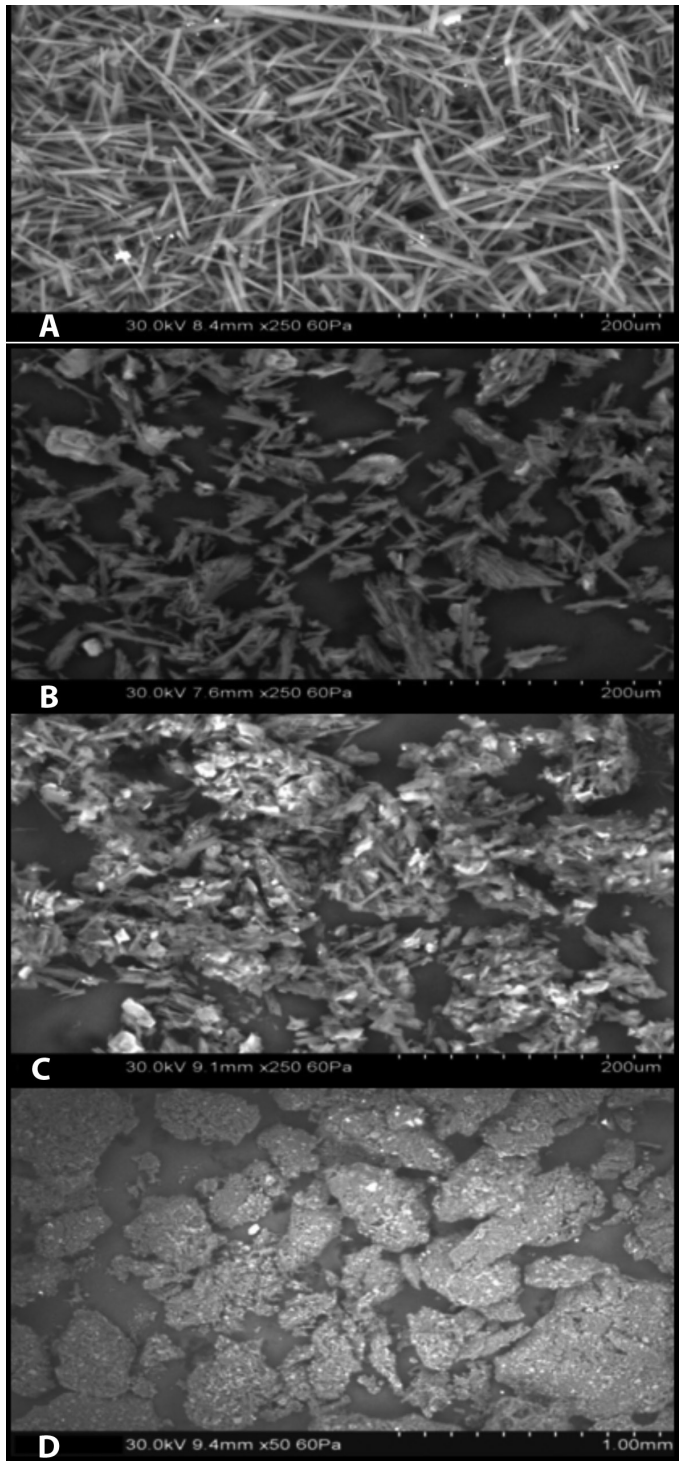

Figure 1. A) Scanning electron microscopy of pure drug (ritonavir). B) Scanning electron microscopy of crystallo-co-agglomeration of formulation A-1. C) Scanning electron microscopy of crystallo-co-agglomeration of formulation B-1. D) Scanning electron microscopy of crystallo-co-agglomeration of formulation C-1

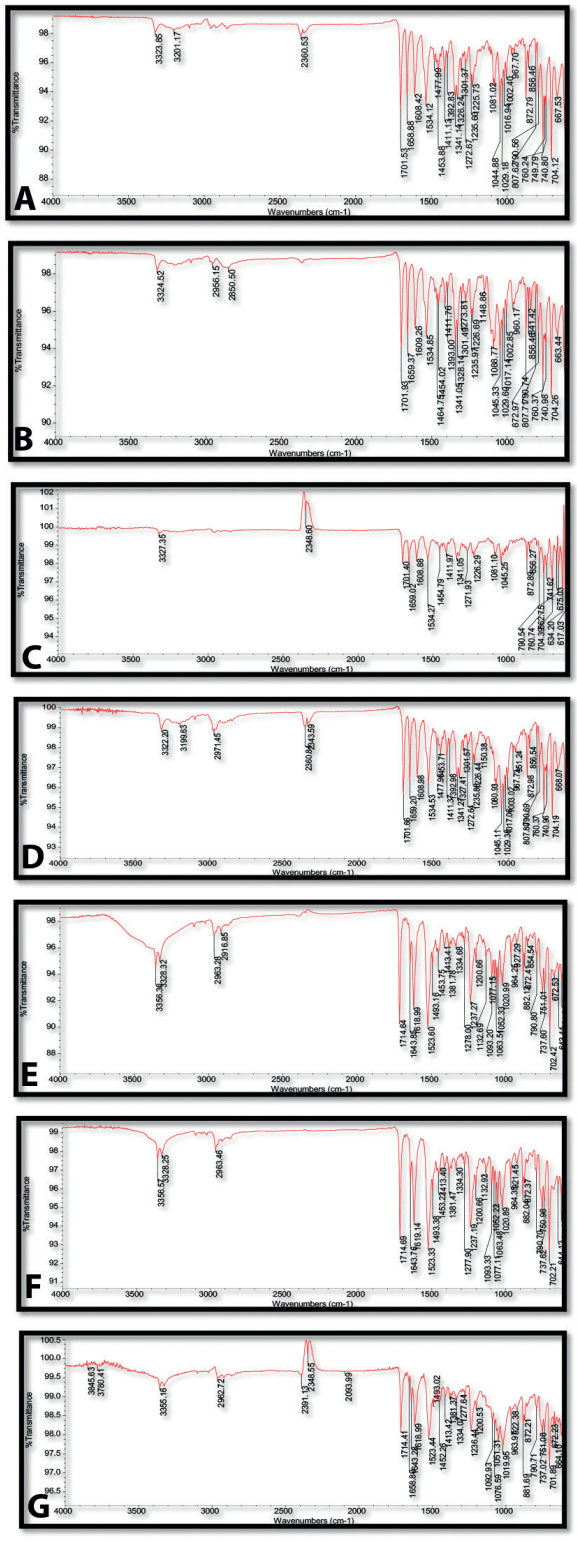

Figure 2. A) Fourier-transformation infrared spectrum of pure drug (ritonavir). B) Fourier-transformation infrared spectrum of physical mixture (polyethylene glycol-6000: ritonavir). C) Fourier-transformation infrared spectrum of physical mixture (polyvinylpyrrolidone K-30: ritonavir). D) Fourier-transformation infrared spectrum of physical mixture (hydroxypropylmethylcellulose K-15: ritonavir). E) Fourier-transformation infrared spectrum of formulation A-1. F) Fourier-transformation infrared spectrum of formulation B-1. G) Fourier-transformation infrared spectrum of formulation C-1

drug remained in its normal form with no prominent change in its characteristics, even in its physical mixture and formulation. The results of the FTIR spectra indicated the absence of any well-defined interaction between drug, diluents, and polymer, as shown in Table 3.

XRD

XRD is a powerful technique for determining the presence of polymorphs, crystal habit modification in drug crystals, and generation of new crystal forms during CCA. Every crystalline solid phase has a unique (XPRD) pattern, which can form the basis for its identification. The XRPD pattern in the 10-80˚, 2θ range showed that the diffraction peaks, characterstics of ritonavir were detectable in crystalline sample i.e. CCA sample, Figure 3A-D, suggesting that the particles crystallized in the presence of polymers, and talc did not undergo structural changes or modification. However, the difference in the relative intensities of their peaks and some new identification peaks over an extended range may be attributed to the difference in the crystallinity or particle size of the sample.

DSC

DSC can be combined with XRPD to determine the polymorphic composition of pharmaceutical powders, if two or more polymorphs are present. The uniformity of crystalline structure in all batches was confirmed by the DSC. All the formulations, irrespective of the polymer and concentration used, showed a sharp melting endotherm that started at 120-121˚C with a flat baseline, which indicated that the material was not degraded by hydration, salvation or any crystalline changes. Also, it shows no interaction of drug with polymers during crystalline changes. There was no appreciable change in the melting endotherm of CCA compared with that of pure drug. The DSC results (Figure 4A-G) also revealed little amorphization of ritonavir when prepared in the form of agglomerates with HPMC K-15, PEG-6000, and PVP K-30. This is evident by a decrease in the enthalpy changes of agglomerates when compared with that of pure drug (ritonavir) -408.25 mJ/mg and that for CCA of formulation of A-1, B-1 and C-1 were -27.75 mJ/mg, -32.1818 mJ/mg and -49.77 mJ/mg, respectively.

Dissolution rate

The dissolution rate of pure ritonavir and its agglomerates are shown in Figure 5. The dissolution rates of the agglomerates were significantly different from pure ritonavir. Dissolution rate enhancement of ritonavir agglomerates were due to the presence of polymers, which may improve the wettability of the drug. The agglomerates with HPMC K-15, PVP-K30, and PEG-600 had 95.70%, 93.00%, and 89.22% drug release compared with pure drug, 55.64%.

CONCLUSIONS

CCA of ritonavir with different hydrophilic polymers such as PEG-6000, PVP K-30, and HPMC K-15 showed an improvement in the solubility, dissolution rate, and flowability as compared with pure drug. Solid state characterization of drug and CCA showed satisfactory results; FTIR proved compatibility, SEM

Table 2. Evaluation parameters of crystallo-co-agglomerates of ritonavir

Batches	Saturation solubility (mg/mL)	Hauser's ratio	Carr's index	Angle of repose (°)	Drug content (% w/w)	Production yields (%)
Pure drug	0.040	1.52	34	30.39	---	---
A-1	0.202	1.12	11	22.58	75	66.66
A-2	0.221	1.09	8	23.02	79.82	69.23
A-3	0.239	1.09	8	23.02	79.98	55.80
B-1	0.175	1.20	18	19.29	84.96	69.40
B-2	0.200	1.10	9	19.64	95.71	62.19
B-3	0.203	1.13	11	19.29	95	55.54
C-1	0.245	1.19	16	25.12	81	78.33
C-2	0.252	1.07	7	21	95	64.61
C-3	0.255	1.18	15	21.65	95.1	60.23

Table 3. Interpretation of FTIR spectra

Material	Peak (cm^{-1})	Functional group	Physical mixture			Formulation code		
			PEG-6000 + ritonavir	PVP K-30 + ritonavir	HPMC K-15 + ritonavir	A-1	B-1	C-1
Ritonavir	704.12	C-S stretching vibration	704.26	704.39	704.19	702.40	702.58	702.21
	790.56	C-C stretching vibration	790.74	790.54	790.96	790.87	790.73	790.51
	1235.60	C=O bending vibration	1235.97	1226.29	1235.88	1235.79	1235.19	1235.19
	1411.13	C-NH_3 stretching vibration	1411.76	1411.97	1411.37	1411.80	1411.31	1411.07
	1658.88	C=C stretching vibration	1658.33	1659.02	1659.20	1643.32	1658.20	1659.07

PEG: Polyethylene glycol, PVP: Polyvinylpyrrolidone, HPMC: Hydroxypropyl methyl cellulose, FTIR: Fourier-transformation infrared

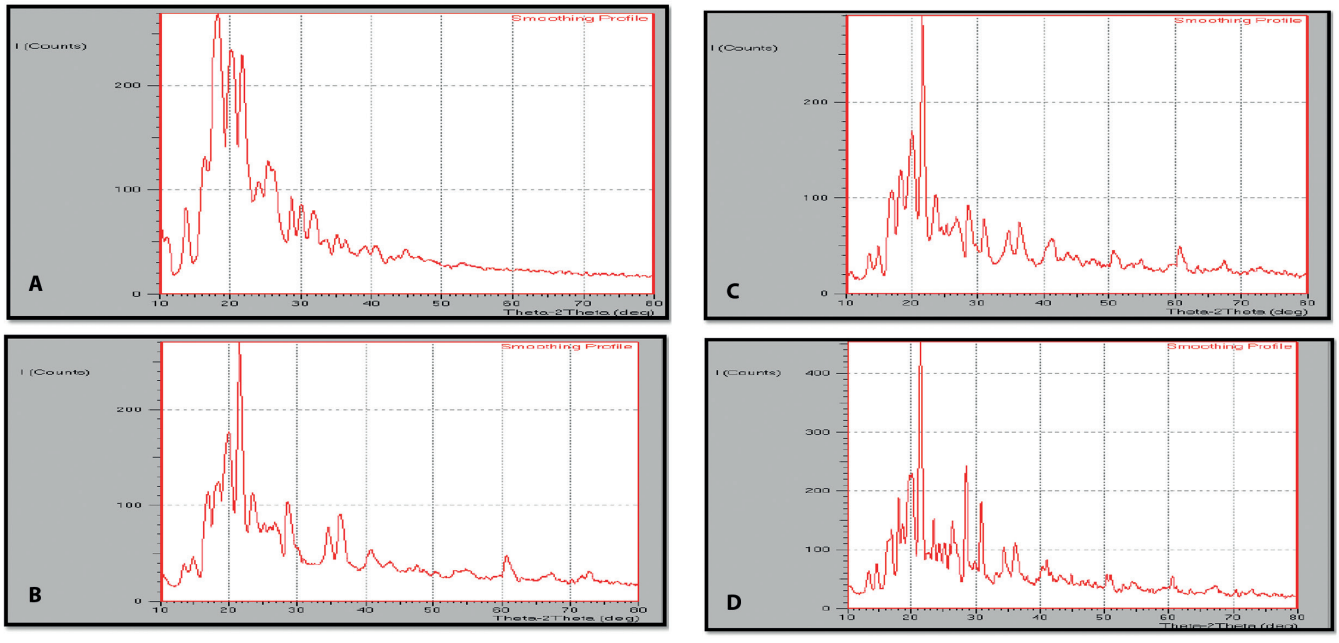

Figure 3. A) X-ray diffraction pattern of ritonavir. B) X-ray diffraction pattern of formulation A-1. C) X-ray diffraction pattern of formulation B-1. D) X-ray diffraction pattern of formulation C-1

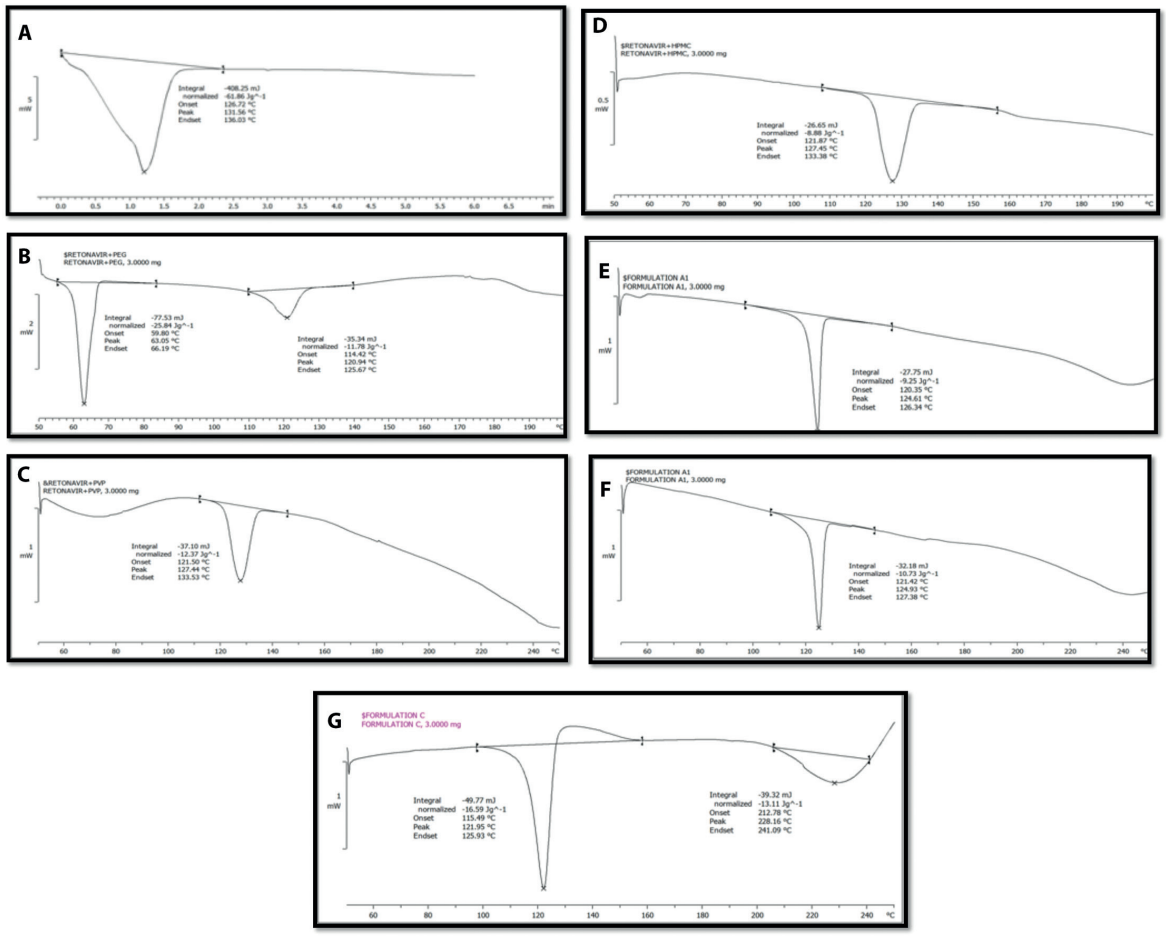

Figure 4. A) Differential scanning calorimetry spectra of ritonavir. B) Differential scanning calorimetry spectra of physical mixture ritonavir + polyethylene glycol-6000. C) Differential scanning calorimetry spectra of physical mixture (ritonavir + polyvinylpyrrolidone K-30). D) Differential scanning calorimetry spectra of physical mixture (ritonavir + hydroxypropylmethylcellulose K-15). E) Differential scanning calorimetry spectra of formulation A-1. F) Differential scanning calorimetry spectra of formulation B-1. G) Differential scanning calorimetry spectra of formulation C-1

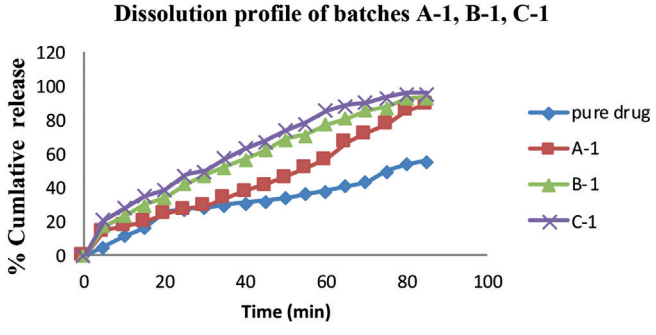

Figure 5. Dissolution profile of agglomerates and pure drug

showed enlarged size with signs of porosity, XRD proved crystallinity, and DSC showed thermal evaluation. The altered size and shape of CCA indicated modified crystal habit, which could be responsible for the dramatic improvement in flowability, solubility, and dissolution properties of ritonavir. CCA of ritonavir is an alternative and effective approach for improvement in the physicochemical and micromeritic properties of ritonavir.

ACKNOWLEDGEMENTS

The authors are thankful to Emcure Pvt. Ltd (Pune) for providing gift sample of ritonavir and also to the Principal and Management of Dadasaheb Balpande College of Pharmacy, Nagpur for providing the research facility.

Conflict of Interest: No conflict of interest was declared by the authors.

REFERENCES

1. Xin Ding, Tuikka M. Halogen bonding in crystal engineering. Recent Adv crystallography. 2012:143-168.
2. Blagden N, de Matas M, Gavan PT, York P. Crystal engineering of active pharmaceutical ingredient to improve solubility and dissolution rates. Adv Drug Del Rev. 2007;59:617-630.
3. Chaturvedi A, Sharma PK, Bansal M. A review on recent advancement in crystallo-co-agglomeration. Adv Bio Res. 2011;5:273-281.
4. Paradkar AR, Pawar AP, Jadhav NR. Crystallo-co-agglomeration: A Novel Particle Engineering Technique. Asian J Pharm. 2010;4:4-10.
5. Garala K, Patel J, Patel A, Raval M, Dharamsi A. Influence of excipients and processing conditions on the development of agglomerates of

racecadotril by crystallo-co-agglomeration. Int J Pharm Investig. 2012;2:189-200.

6. Genikal B, Rajendra A. Formulation of crystallo-co-agglomerates of naproxen; study of effect of polymers on drug release. Int J Pharm. 2013;5:852-864.
7. Jolly CM, Lekshmi P, Constantine I, Bijin EN, Valsalakumari J, Pramod K. Crystallo-co-agglomeration: an innovative technique for size enlargement and improved flow properties of powders. J Mater Sci. 2013;1:1-14.
8. Thenge RR. Crystal Modification of Aceclofenac by Spherical Crystallization to Improve Solubility Dissolution Rate and Micromeritic Properties. J Pharm Res. 2012;5:974-977.
9. Hardik KP, Sangvi K. A review on spherical agglomeration for improvement of micromeritic properties and solubility. Int J Pharm. 2013;3:570-579.
10. Shashank A, Pakash GS, Sanjav J. Particle design of meloxicam-disintegrant agglomerates for fast dissoluation and direct compression crystallo-co-agglomeration technique. Int J Pharm Sci. 2012;1:289-297.
11. Palermo PJ. In Handbook of Modern Pharmaceutical Analysis. In: Ahuja S, Scypinski S, eds. Academic Press, San Deigo. USA; 2001:243-244.
12. Tapas A, Kawtikwar P, Sakarkar D. An improvement of micromeritic properties and dissolution behaviours of carvedilol spherical agglomerates crystallized in presence of Inutec SP1. Turk J Pharm Sci. 2012;9:101-112.

Turk J Pharm Sci 2018;15(3):256-262
DOI: 10.4274/tjps.92400

ORIGINAL ARTICLE

Biopharmaceutical Process of Diclofenac Multi-particulate Systems for Chronotherapy of Rheumatoid Arthritis

Romatoid Artritin Kronoterapisinde Diklofenak Çok Birimli Sistemlerin Biyofarmasötik Süreci

Sowjanya BATTU[1], Prasanna Raju YALAVARTHI[2]*, Subba REDDY GV[3], Saradha RADHAKRISHNAN[1], Ram Mohan Reddy THUMMALURU[1], Abbulu KONDE[1]

[1]CMR College of Pharmacy, Department of Pharmaceutics, Hyderabad, India
[2]Sri Padmavathi School of Pharmacy, Division of Pharmaceutics, Tirupati, India
[3]JNTUA College of Engineering, Department of Chemistry, Pulivendula, India

ABSTRACT

Objectives: Diclofenac exhibits limited solubility, low bioabsorption and gastric toxicity. The objective of the study was to address the above limitations and to design a multi-particulate formulation for the chronotherapy of RA.

Materials and Methods: Solid dispersions of DC with SSG and GG were prepared. Uniform-sized (~400 µm) non-pareil seeds were coated with solid dispersions to produce immediate-release pellets (DMP-1 and DMP-2) and controlled-release pellets (DMP-3 and DMP-4). The resultant controlled-release pellets were further layered with methacrylate polymers to obtain pulsatile-release pellets (DMPP). Solubility, FTIR, DSC, micrometrics, SEM, drug content, drug release, pharmacokinetics, and stability studies were performed for DMPP.

Results: The solubility of DC was improved by 164-folds due to the presence of hydrophilic carriers in the solid dispersions. No chemical and physical interactions were noticed in FTIR spectra and also in thermograms. A fluidized bed processor facilitated the production of high-quality, circular, and regular pellets with an angle of repose less than 19.5 degrees and DC content between 95.18% and 98.87%. The maximum drug was released from DMPP at the end of 12 hours. DMP-1 and DMP-2 pellets had 2 hr of drug release and pulsatile, controlled-release pellets had a 6 hr lag phase followed by 12 hr controlled release. Both DMP-1 and DMP-2–immediate showed first-order release followed by Hixson-Crowell kinetics, whereas DMPP pellets followed zero-order release with Higuchi's kinetics. The maximum concentration of DC in plasma was 400.8 ng/mL at 5 hr for DMP-2 and 381.1 ng/mL at 14 hr for DMPP-5. The solubility of DC was increased with the application of solid dispersion and in turn increased the pharmacokinetics. The pellets were plausibly stable over a period of 90 days.

Conclusion: Thus, multi-particulate pulsatile systems of DC were as effective as chronotherapeutics in the treatment of circadian rhythm-based ailments such as RA.

Key words: Chronomodulation, circadian, fluidized bed, hydrophilic carrier, NSAID, Wurster process

ÖZ

Amaç: Diklofenak sınırlı çözünürlük, düşük biyoabsorpsiyon ve gastrik toksisite gösterir. Çalışmanın amacı, yukarıdaki kısıtlamaları ele almak ve RA'nın kronoterapisi için çok birimli bir formülasyon tasarlamaktır.

Gereç ve Yöntemler: DC, SSG ve GG ile katı dispersiyonları hazırlandı. Aynı boyutlu (~400 µm) nonpareil çekirdekler, hemen salım yapan pelletler (DMP-1 ve DMP-2) ve kontrollü salımlı pelletler (DMP-3 ve DMP-4) üretmek için katı dispersiyonlarla kaplandı. Elde edilen kontrollü salım pelletleri, pulsatil salım pelletleri (DMPP) elde etmek için metakrilat polimerleri ile daha da katmanlı hale getirildi. DMPP için çözünürlük, FTIR, DSC, mikrometrik, SEM, etkin madde içeriği, etkin madde salımı, farmakokinetik ve stabilite çalışmaları yapıldı.

Bulgular: DC'nin çözünürlüğü, katı dispersiyonlardaki hidrofilik taşıyıcıların varlığına bağlı olarak 164 kat arttı. FTIR spektrumunda ve termogramlarda kimyasal ve fiziksel etkileşimler gözlemlenmedi. Akışkanlaştıran yataklı işlemci, 19.5 dereceden daha az bir akış açısı ve %95.18 ile %98.87 arasında DC içeriği olan yüksek kaliteli, yuvarlak ve düzenli pelletlerin üretimini kolaylaştırdı. Maksimum etkin madde 12 saat sonunda DMPP'den salındı.

*Correspondence: E-mail: kanishka9002@gmail.com, Phone: +917661976616 ORCID-ID: orcid.org/0000-0001-7859-0475
Received: 05.07.2017, Accepted: 24.08.2017

DMP-1 ve DMP-2 pelletleri 2 saatlik pulsatil etkin madde salımına sahipti ve kontrollü salımlı pelletler 6 saat gecikme fazının ardından 12 saat kontrollü salıma sahipti. Hem DMP-1 hem de DMP-2-hemen birinci dereceden salım ve ardından Hixson-Crowell kinetiğini gösterirken, DMPP pelletleri ardından Higuchi kinetikle sıfır derece salım gösterdi. Plazmada maksimum DC konsantrasyonu DMP-2 için 5 saatte 400.8 ng/mL ve DMPP-5 için 14 saatte 381.1 ng/mL olmuştur. DC'nin çözünürlüğü katı dispersiyonun uygulanmasıyla arttırılmış ve bunun sonucunda farmakokinetik özellikler artmıştır. Pelletler, 90 günlük bir süre zarfında makul derecede kararlıdır.

Sonuç: Bu nedenle, DC'nin çok birimli pulsatil sistemleri, RA gibi sirkadiyen ritim temelli hastalıkların tedavisinde kronoterapötikler kadar etkiliydi.

Anahtar kelimeler: Kronomodülasyon, sirkadiyen, akışkanlaştıran yatak, hidrofilik taşıyıcı, NSAID, Wurster süreci

INTRODUCTION

Rheumatoid arthritis (RA) is a chronic progressive autoimmune disorder that affects the dense innervation in the joint capsule and synovium, resulting in peripheral inflammation. Chronic inflammation and pain in the fingers, wrists, elbows, shoulders, knees, feet, and ankles occur in RA.[1-3] At a conference in Paris in 2010, "pain modifying analgesic drugs"[4] were proposed for the management of RA. The clinical treatment options for RA are non-steroidal anti-inflammatory drugs (NSAIDs), opioid analgesics, tricyclic antidepressants, corticosteroids, anticonvulsants, topical agents, and serotonin norepinephrine reuptake inhibitors.[5] However, each category of drug holds its own limitations. Disease-modifying antirheumatic drugs (DMARDs) are currently recommended for the treatment of arthritis. Triple-therapy with other drugs such as methotrexate, sulfasalazine, and hydroxychloroquine is the flourishing combination with DMARDs. High dosing, long-term use of the above mentioned medications develops gastric mucosal damage, tolerance, and accumulation of drug metabolites in the kidney, liver, and causes nephro- and hepatotoxicity.[6]

NSAIDs are the most commonly prescribed therapeutic agents in the management of RA, as with other causes of pain. Among the notable NSAIDs, diclofenac (DC), a fenamic acid derivative, is usually prescribed due its potentiality against pain and inflammation in patients with RA. DC is believed to inhibit the synthesis of substance P, a pro-inflammatory neuropeptide, and nociceptive prostaglandins in synovial tissue as well as in blood, and thus it is useful in the treatment of RA.[7] DC, an insoluble Biopharmaceutics Classification System (BCS) class II drug, has a $t_{½}$ of 2 hr and low bioavailability.[8] Nevertheless, the conventional oral medication of DC results with severe gastric mucosal damage and other adverse effects of NSAIDs.[9] A dose form that releases drug according to time (circadian rhythm) would be a promising system because the severity of joint pain, surrounding muscle stiffness, and fatigue in patients with RA is related with the circadian rhythm and is mostly observed in the early hours. Nowadays, Pulsatile® and Diffucap® systems are gaining much research interest in the chronotherapy of circadian rhythm-based ailments so as to release the drug after a predetermined lag phase. Multi-particulate formulations are composed of immediate- and controlled-release particulates and are superior because they present diverse drug delivery patterns in a circadian fashion.[10,11]

DC, a regular medication used in the management of RA, was chosen as the model drug in this study.[12] The aim was to develop multi-particulate systems of DC- containing immediate- and pulsatile-controlled release pellets using non-pareil sugar seeds to avoid gastric mucosal damage and enable pulsatile release in the small intestine.

EXPERIMENTAL

Materials

DC and non-pareil seeds were donated by M/s. Lee Pharma, Visakhapatnam, India. Guar gum (GG), sodium starch glycolate (SSG), eudragit RS100 and eudragit L100 were purchased from S.D. Fine Chem., Mumbai, India. All other chemicals and reagents used in the study were of analytical grade.

Preparation of solid dispersions of DC

Solid dispersions of DC were prepared using GG and SSG in 1:1 and 1:2 weight ratios as mentioned in Table 1. The ingredients were kneaded thoroughly in a glass mortar for about 20 min until a uniform mass was formed. The resultant mass was screened through #80 mesh and kept in a vacuum desiccator for further evaluation and formulation of pellets.[13]

Solubility study

An excess of solid dispersion was taken into calibrated glass vials containing 10 mL of 0.1 N HCl, pH 6.8 and 7.4 phosphate buffer solutions. The resultant solutions were equilibrated at 37°C for 72 hr using a rotary shaker. After equilibration, the solutions were filtered through a 0.45-µm nylon filter and assayed using an ultraviolet (UV)-visible spectrophotometer *(Analytical Technologies, T 70)* at 276 nm.[14]

Step 1: Preparation of multi-particulate pellets

A known quantity (a batch) of non-pareil seeds were coated with DC:SSG and DC: GG solid dispersions in 1:1 and 1:2 proportions. This results in the production of immediate- and controlled-release pellets.

Non-pareil seeds coating with solid dispersion using the solution-layering technique

About 150 g of non-pareil seeds (sugar spheres) were transferred into the vertical chamber of a fluidized bed processor *(GPCG 1.1. Glatt, D-Binzen)* (Wurster process). A solution-layering process was initiated with an inlet temperature of 45-50°C by layering the solid dispersions (300 g) of step 1, on pellets using spray guns, atomized at 2-4.5 bar, and operated at a 60-120 g/min spray rate until the bed was wet and tacky. The process was continued for 45 min to produce the desired size of immediate-

Table 1. Composition of diclofenac immediate- and controlled-release pellets

Solid dispersion composition	DMP-1	DMP-2	DMP-3	DMP-4
DC:SSG	1:1	1:2	-	-
DC:GG	-	-	1:1	1:2

DC: Diclofenac, SSG: Sodium starch glycolate, GG: Guar gum

release pellets (DMP-1 and DMP-2) and controlled-release pellets (DMP-3 and DMP-4). The pellets obtained were sifted through #14 and #18 sieves and the controlled-release pellets retained over #18 were selected for step 2.[15]

Step 2: Preparation of pulsatile controlled-release pellets

In this step, DMP-3 and DMP-4 pellets (controlled-release pellets) were coated with solutions of eudragit RS100 and eudragit L100 prepared in the solvent mixture of triethylamine (plasticizer) and isopropyl alcohol. The eudragit compositions of are presented in Table 2. The process parameters employed in this step were similar to that of step 1. Step 2 resulted in the formation of pulsatile-release pellets (DMPP-1 to DMPP-5). Pulsatile pellets sifted and retained over #20 mesh were selected for further characterization and evaluation studies.[16,17]

Attenuated total resonance-Fourier-transform infrared (ATR-FTIR) spectroscopy

The chemical compatibility of DC and polymer mixtures was examined using an ATR-FTIR spectrometer (Agilent CARY 630 ATR-FTIR). The sample to be tested was placed on a diamond ATR crystal and analyzed by means of Agilent resolutions pro software. Each spectrum was checked with 32 single average scans at 4 cm^{-1} resolution in the 400-4000 cm^{-1} absorption region.

Differential scanning calorimetry (DSC)

Thermal analysis of DC and polymer mixtures was performed using a DSC *(Shimadzu DSC-50)* to check the physical compatibility. During each scan, about 1 to 2 mg of the sample was positioned in sealed aluminum sample pans at a rate of 10°C/min under a nitrogen atmosphere between 25°C and 350°C. An empty aluminum pan was used as reference.

Scanning electron microscopy (SEM)

The surface morphology and cross-section of the prepared pellets was determined using a SEM (Jeol, JSM-1600, Tokyo, Japan). The pellets were coated with fine gold in a 10 mA ion current for 5 min under 0.1 Torr pressure using an ion sputter and laden on studs for examination.

Drug content

A batch of pellets was transferred into a calibrated volumetric flask and dissolved in 10 mL of methanol by ultra-sonication for 10 sec. The volume of the preparation was made up to 100 mL with the same, filtered, and assayed.

Table 2. Composition of diclofenac pulsatile pellets

Formulation	Coating composition (%)	
	Eudragit L100	Eudragit RS100
DMPP-1	100	-
DMPP-2	-	100
DMPP-3	50	50
DMPP-4	60	40
DMPP-5	40	60

Entrapment efficiency and drug loading

A batch of pellets (DMP-1 to 4 and DMPP-1 to 5) equivalent to 100 mg of DC were transferred into a standard Vensil® flask containing 100 mL of phosphate buffer (pH 6.8) and stored overnight. The sample solution was filtered through a 0.44-µm nylon filter to remove undissolved portions of pellets and analyzed at 276 nm. Average of three estimations was considered for each batch of pellets formulated in the study. The entrapment efficiency and drug loading of pellets were calculated from equations (1) and (2):[18,19]

$$\% \text{ Entrapment efficiency} = \frac{\text{Actual drug loading}}{\text{Theoretical drug loading}} \times 100 \quad (1)$$

$$\% \text{ Drug loading} = \frac{\text{Mass of drug in pellets}}{\text{Mass of pellets}} \times 100 \quad (2)$$

In vitro dissolution study

Pellets of DMP-1 to DMP-4 and DMPP-1 to DMPP-5 equivalent to 100 mg of drug were subjected to *in vitro* drug release studies using USP type I dissolution test apparatus at 37°C and 50 rpm in 0.1 N HCl, pH 6.8 and pH 7.4 as dissolution media for the first 2 hr, the next 3 hr, followed by the next 13 hr, respectively. Five-milliliter aliquots were withdrawn at various time intervals by maintaining sink conditions, filtered, and analyzed. The study was repeated for six independent observations and the results were built into diverse kinetic models.

In vivo study

Male rabbits aged 10-14 weeks weighing 2-3 kg were chosen for the study. The animals were housed under 12-12–hr light-dark cycles and fed with standard diet and water. The study process was approved by the Institutional Animal Ethics Committee (CPCSEA/1657/IAEC/CMRCP/PhD-15/43). Twelve rabbits were divided into three equal groups (group 1, group 2, and group 3) and were depilated on the dorsal surface of the ear pinna. Animals were fasted for 24 hr before the study. The dose of the drug to be administered was calculated based on the rabbit's body weight using the formula:

$$\text{Rabbit dose} = \frac{\text{Total Dose (in humans) X 0.07 (for 1.5 kg rabbit)}}{1.5}$$

Groups 1, 2, and 3 were administered DC, DMP2, and DMPP-5 samples, respectively. Blood samples of about 1 mL were collected into heparinized Eppendorf tubes at regular time intervals. The samples were shaken thoroughly, centrifuged at 1500 rpm, and plasma was collected. A previously developed and validated high-performance liquid chromatography (HPLC) method was employed[20] to determine the plasma drug concentrations as a function of time. The C18 (250 mm × 4.6 mm, 5 µm) column, a mixture of acetonitrile and methanol (70:30, v/v) as the mobile phase, and UV detector (276 nm) were adopted and Empower software version-2 was used to assay the DC concentrations in plasma against DC as an internal standard. Samples of about 20 µL were injected into the HPLC

system (Waters, 2695) after filtering the plasma through a 0.2 µm membrane filter.

Statistical Analysis

The mean concentrations of DC in plasma samples as a function of time were calculated. The pharmacokinetic parameters such as $t_{1/2}$, K_e and V_d were characterized and compared statistically using analysis of variance (ANOVA) and the Tukey-Krammer test was applied for the columns comparison. P <0.05 was considered a statistically significant correlation.

Stability study

Accelerated stability testing of pellets was conducted at 25±2˚C/60±5% relative humidity (RH) and 40±2˚C/75±5% RH conditions as per the International Council for Harmonisation of Technical Requirements for Registration of Pharmaceuticals for Human Use guidelines for a period of 120 days. The pellets were then tested for their flow properties, drug content, and *in vitro* drug release.[21,22]

RESULTS

Pulsatile drug delivery as multi-particulate systems have been demonstrated to be successful technologies to overcome limitations such as low solubility and less bioabsorption faced by BCS class II and IV drugs as single-unit drug delivery systems. This solubility study resulted with increased solubility of DC by 164-fold because solid dispersion was employed along with hydrophilic polymers. The resultant amorphous solid dispersions of DC displayed good micrometrics.

The FTIR spectra (Figure 1) of DC confirmed the existence of peaks at 3317, 1677, 1120, and 745 cm^{-1} due to NH stretching, C=O stretching, C-O bending, and C-Cl bending as characteristic functional groups of DC. Similar functional groups indicating peaks were observed without significant shifting of DC in the DMPP-5 mixture. As shown in Figure 2, DSC thermograms displayed endothermic peaks of DC at 276˚C and DMPP-5 at 275˚C, respectively.

The SEM image (Figure 3) of pellets demonstrated smooth, well separated, spherical, and uniformly-distributed, micron-sized particles with 400-500 µm range. The pellets (both types), prepared using the Wurster process, displayed substantial entrapment efficiencies and drug-loading capabilities as mentioned in Table 3.

In vitro drug release profiles of the DC pellets are depicted in Figure 4 and 5. SSG, a hydrophilic carrier composed DMP-1 and DMP-2 pellets, demonstrated burst drug release as 94.2% and 99.5% at the end of the second hour. The controlled-release pellets, DMP-3 and BMP-4, had 98.9% and 99.1% at end of the tenth hour due to the composition of hydrocolloidal polymer GG. The pulsatile-release pellets, DMPP-1-DMPP-5, showed

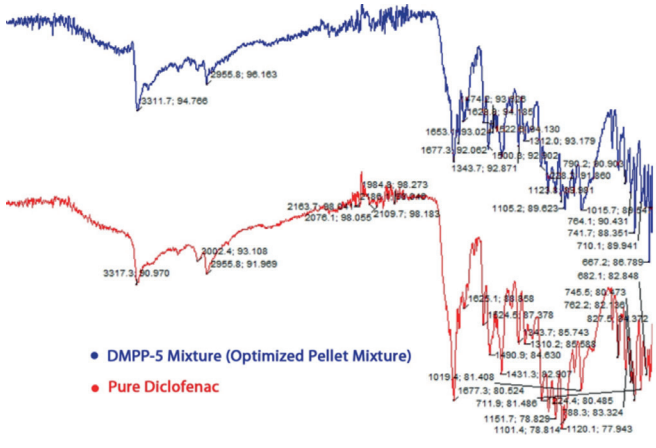

Figure 1. Fourier-transform infrared spectra of diclofenac and DMPP-5 pellet mixture

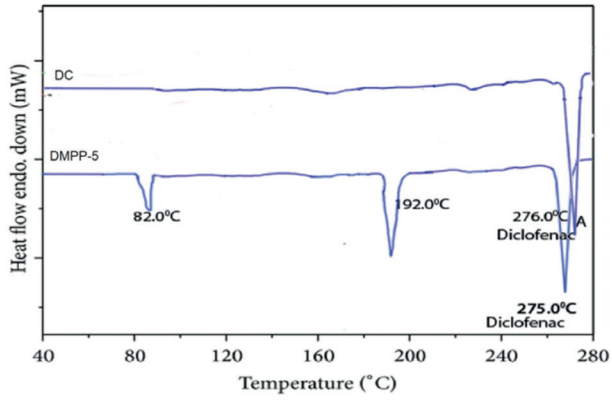

Figure 2. Thermograms of diclofenac and DMPP-5 pellet mixture

DC: Diclofenac

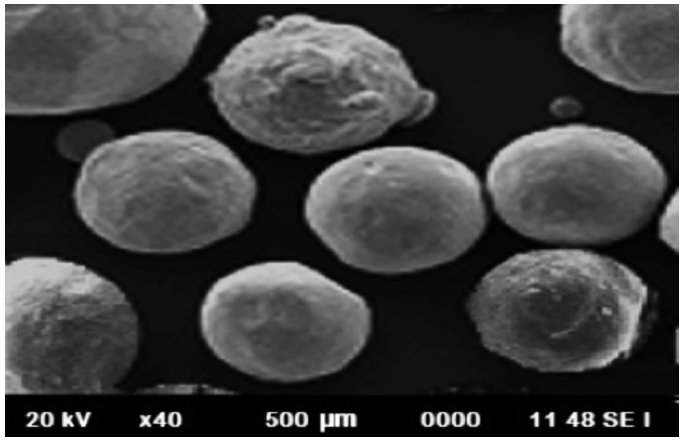

Figure 3. Scanning electron microscopy image of DMPP-5 pellets

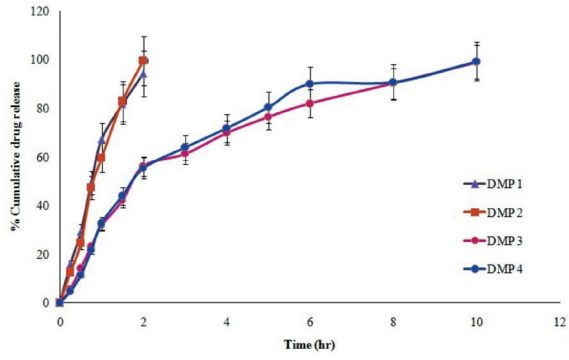

Figure 4. Percent drug release of DMP-1 to DMP-4 pellets

96.1%, 96.3%, 97.4%, 99.1%, and 99.5%, respectively, at the end of the 18th hour (with a 6-hr lag phase). The release of DC from immediate-release pellets followed first-order release with Hixson-Crowell cube root model kinetics, whereas pulsatile-release pellets followed zero-order with the Higuchi kinetic model.

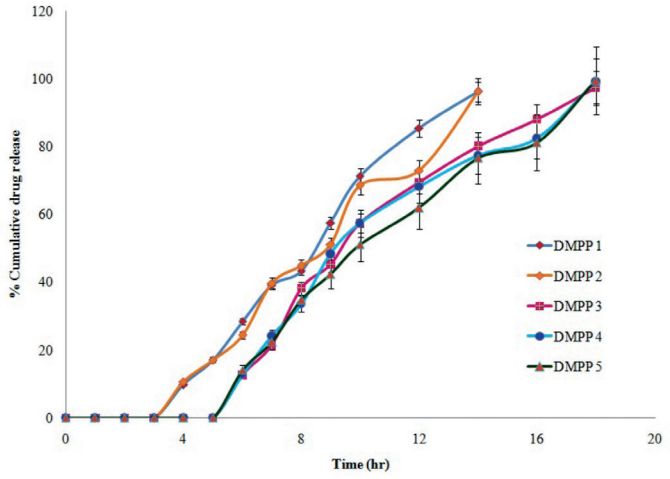

Figure 5. Percent drug release from pulsatile-release pellets (DMPP-1 to DMPP-5)

Table 3. Entrapment efficiency and drug loading properties

Formulation	Entrapment efficiency (%)	Drug loading (%)
DMP-1	96.0±0.10	68.0±0.10
DMP-2	98.3±0.09	70.0±0.14
DMP-3	97.9±0.20	69.9±0.11
DMP-4	98.2±0.15	70.1±0.12
DMPP-1	97.6±0.12	69.7±0.21
DMPP-2	97.4±0.30	69.5±0.15
DMPP-3	97.5±0.13	69.6±0.12
DMPP-4	97.6±0.09	69.7±0.23
DMPP-5	98.9±0.11	70.6±0.16

Values are expressed as mean±SD, n=3

The developed HPLC method eluted the DC peak with a retention time of 2.34 min as shown in Figure 6. The limit of detection and limit of quantification for the HPLC method was found to be 3 and 9 ng/mL, respectively. Upon assaying the plasma samples using this validated HPLC method, the plasma kinetics as function of time were demonstrated in Figure 7. The pharmacokinetics of the DMP-2 pellets such as $t_{1/2}$, K_e and V_d were found to be increased by 2.03, 1.733, and 1.55-fold, respectively. Bioavailability parameters viz., C_{max}, t_{max} and AUC were increased by 1.9, 1.72, and 1.25 times, respectively, when compared with DC. In the case of pulsatile pellets, the DMPP-5 formulation had 5.78, 4.1, and 1.82-fold increase in

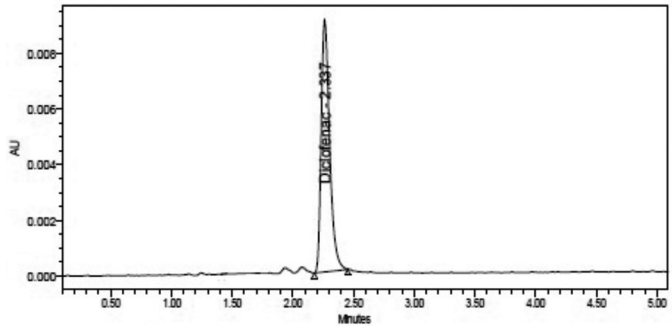

Figure 6. Chromatogram of diclofenac

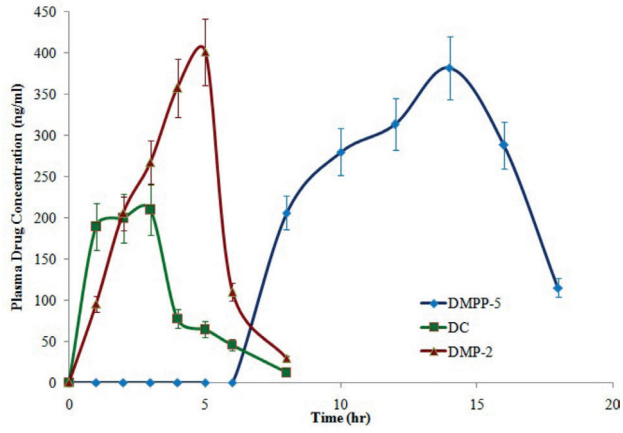

Figure 7. Plasma drug concentration-time profile

DC: Diclofenac

Table 4. *In vivo* pharmacokinetic parameters (mean±SEM)

Pharmacokinetic parameters	DC	DMP-2	DMPP-5	Test of significance
C_{max} (ng/mL)	209.8±106.5	400.8±125	381.1±106	S
T_{max} (hr)	2.9±2.2	5.0±2.9	14.0±3.1	S
$t_{½}$ (hr)	2.0±1.9	4.06±1.1	11.56±2.9	S
K_{el} (hr^{-1})	0.983±0.017	1.7042±0.069	4.0306±1.54	S
V_d (L/hr)	8.9±1.1	13.8±7.1	16.25±6.2	S
AUC_{0-8} (ng/hr/mL^{-1})	1724±123.8	2165±169.9	-	S
AUC_{0-18} (ng/hr/mL^{-1})	2973±138.2	-	3897±111.5	S

S: Significant, SEM: Scanning electron microscopy, DC: Diclofenac

pharmacokinetics and about a 1.82, 4.82, and 1.31-times increase in bioavailability parameters, respectively, as given in Table 4.

The physicochemical properties for all pellets were intact over a period of 90 days due to the eudragit coatings. There were no changes in the evaluation parameters of the pellets even after exposure to various temperature and RH conditions.

DISCUSSION

The kneading technique employed in the formulation facilitated the entanglement of particles to the molecular level as polymeric networks and therefore enhanced solubility of DC was achieved with solid dispersions. Moreover, the solid dispersions of DC showed amorphous geometry with excellent micrometric properties.

SSG and GG have become well established as carriers in the recent past and were shown to be compatible with DC moiety as evidenced in the FTIR spectra. There were no chemical bonds established between DC and carriers other than hydrogen bonding, which was evidenced in the wave numbers of the FTIR spectrum. Thus, the spectra showed no chemical interactions between DC and the carriers selected in the study. The same was attributed in thermograms of DMPP pellets because a minor shift in the endothermic peak of DC was identified in DMPP-5's thermogram as a characteristic interaction between drug and the selected carriers.

The defined surface morphology of the pellets was possible only due to the accurate layering of DC on sugar spheres. The dimensions of pellets were linearly increased with the composition of eudragit as coating solutions and the same result was seen in SEM images. Pulsatile pellets were relatively larger than immediate-release pellets because they had undergone two steps of coating and also had a methacrylate polymer coating. The Wurster process using fluidization was successful in producing the non-agglomerated, free-flowing and moderately high DC content (95.18-98.87%) pellets. The pellets with good entrapment efficiency and drug loading were selected for coating with eudragits so as to produce pulsatalie drug release pellets.

Eudragit RS100, a polymer of enteric grade and a cationic polymer with low permeability, provides additional sustaining activity of drug release along with the gelling properties of GG. Eudragit L100, which is an anionic polymer with high permeability, helps in maintaining the lag phase for about 6 hr. DMPP pellets were composed of a swellable polymer, GG, and enteric polymers (Eudragit L100 and Eudragit RS100). Optimized pulsatile release of DC was achieved with desired lag phase from DMPP pellets owing to typical composition of hydrocolloidal GG and pH dependent eudragits.

Enhanced oral absorption of DC was resulted with multi-particulates. Quick onset of action from DMP-2 formulation was displayed due to presence of SSG, a hydrophilic carrier and same was evidenced in the HPLC data of plasma DC concentrations. Micron-size pellets of immediate-release contributed to the loading dose, and the pulsatile pellets contributed to the maintenance dose of drug in rabbits. The contribution of GG, a polycolloidal polymer, resulted with controlled release of DC from DMPP to reach a maximum concentration in plasma. The desired lag phase of 6 hr was achieved with a typical composition of anionic and cationic methacrylate polymers (Eudragits) at 40:60 ratios. Increased bioabsorption and pharmacokinetics of DC by multi-particulate pulsatile formulation were evident and hence it was attributed to reach adequate concentrations of DC at the synovium to reduce the inflammation. Administration of DMP-2 and DMPP-5 pellets as multi-particulate formulations of DC could produce both immediate- and controlled-release profiles of DC at a predetermined time in the small intestine so as to cater for the requirements of chronotherapy of RA. The physical stability of the pellets was due to the application of superior technology (fluidized coating) and methods (solution layering) in the study.

CONCLUSIONS

Solid dispersions were prepared using different hydrophilic polysaccharides and methacrylate polymers to address the solubility issues of DC. A novel solution layering technique was employed in association with a fluidized bed processor to obtain typically micron-sized, smooth-surfaced and spheronized pellets of the immediate-release and controlled--release category. Further, controlled-release pellets were coated with enteric polymers to produce a 6-hr lag phase in drug release. Promised *in vitro* drug release profiles were achieved by pulsatile technology-based multi-particulates of DC to cater for the needs of chronotherapy of circadian rhythm-based chronic diseases such as RA. Thus, the suitability of applied technologies in the design of multi-particulate drug delivery systems in chronotherapy of RA using DC was convincingly proved using *in vitro* evaluations. The outcomes of the *in vitro* study were further fortified by *in vivo* studies using rabbits. While characterizing the plasma drug concentrations using sensitive and precise HPLC methodology, plasma-drug parameters such as $t_{½}$, and K_e were proved as suitable chronopharmacokinetic parameters. The characteristics and parameters of bioavailability also contributed to this chronomodulated delivery of DC. It was concluded that, the design of spheronized pulsatile pellets of DC is useful in the chronotherapy of RA, but scale-up techniques are required for commercial viability.

ACKNOWLEDGEMENTS

The authors are thankful to M/s. Lee Pharma, Visakhapatnam for gratis of DC.

Conflict of Interest: No conflict of interest was declared by the authors.

Financial Disclosure: The research received no specific grant from any funding agency in public, commercial or not-for-profit sectors.

REFERENCES

1. Cheng HY, Penninger JM. DREAMing about arthritic pain. Ann Rheum Dis. 2004;63(Suppl 2):72-75.

2. Huskisson EC, Hart FD. Pain threshold and arthritis. Br Med J. 1972;4:193-195.
3. Konttinen YT, Honkanen VE, Grönblad M, Keinonen M, Santavirta N, Santavirta S. The relation of extraarticular tenderness to inflammatory joint disease and personality in patients with rheumatoid arthritis. J Rheumatol. 1992;19:851-855.
4. Castillo BA, El Sallab RA, Scott JT. Physical activity, cystic erosions, and osteoporosis in rheumatoid arthritis. Ann Rheum Dis. 1965;24:522-527.
5. Van Laar M, Pergolizzi JV Jr, Mellinghoff HU, Merchante IM, Nalamachu S, O'Brien J, Perrot S, Raffa RB. Pain treatment in arthritis-related pain: beyond NSAIDs. Open Rheumatol J. 2012;6:320-330.
6. Perrot S. Should we switch from analgesics to the concept of "pain-modifying analgesic drugs (PMADS)" in osteoarthritis and rheumatic chronic pain conditions. Pain. 2009;146:229-230.
7. Peesa JP, Yalavarthi PR, Rasheed A, Mandava VBR. A perspective review on role of novel NSAID prodrugs in the management of acute inflammation. J Acu Dis. 2016;5:364-381.
8. Sweetman SC. Martindale: The complete drug reference, Royal Pharmaceutical Society, (36th ed). London; 2009:44.
9. Nandakishore R, Yalavarthi PR, Kiran YR, Rajapranathi M. Selective cyclooxygenase inhibitors: current status. Curr Drug Discov Technol. 2014;11:127-132.
10. Sharma PR, Lewis SA. Design and *in vitro/in vivo* evaluation of extended release matrix tablets of nateglinide. J Young Pharm. 2013;5:167-172.
11. Vadlamudi HC, Raju YP, Asuntha G, Nair R, Murthy KV, Vulava J. Assessment of hupu gum for its carrier property in the design and evaluation of solid mixtures of poorly water soluble drug - rofecoxib. Curr Drug Deliv. 2014;11:62-71.
12. Kroenke K, Krebs EE, Blair MJ. Pharmacotherapy of chronic pain: a synthesis of recommendations from systematic reviews. Gen Hos Psych. 2009;31:206-219.
13. Prasannaraju Y, Chowdary VH, Jayasri V, Asuntha G, Kumar NK, Murthy KV, Nair R. Bioavailability and pharmacokinetic studies of rofecoxib solid dispersion. Curr Drug Deliv. 2013;10:701-705.
14. Ahuja N, Katare OP, Singh B. Studies on dissolution enhancement and mathematical modeling of drug release of poorly water-soluble carriers. Eur J Pharm Biopharm. 2007;65:26-38.
15. Politis SN, Rekkas DM. Pelletization processes for pharmaceutical applications: a patent review. Recent Pat Drug Deliv Formul. 2011;5:61-78.
16. Gowda DV, Aravindram AS, Venkatesh MP, Khan MS. Development and evaluation of clozapin pellets for controlled release. Int J Res Ayur Pharm. 2012;3:611-618.
17. Raval MK, Ramani RV, Sheth NR. Formulation and evaluation of sustained release enteric-coated pellets of budesonide for intestinal delivery. Int J Pharm Investig. 2013;3:203-211.
18. Bhattacharya SS, Banerjee S, Ghosh AK, Chattopadhyay P, Verma A, Ghosh A. A RP-HPLC method for quantification of diclofenac sodium released from biological macromolecules. Int J Biol Macromol. 2013;58:354-359.
19. Nagpal M, Maheshwari D, Rakha P, Dureja H, Goyal S, Dhingra G. Formulation, development and evaluation of alginate microspheres of Ibuprofen. J Young Pharm. 2012;4:13-16.
20. Lu Y, Sturek M, Park K. Microparticles produced by the hydrogel template method for sustained drug delivery. Int J Pharm. 2014;461:258-269.
21. Nanda Kishore R, Yalavarthi PR, Vadlamudi HC, Vandana KR, Rasheed A, Sushma M. Solid self microemulsification of Atorvastatin using hydrophilic carriers: a design. Drug Dev Ind Pharm. 2015;41:1213-1222.
22. Vadlamudi HC, Yalavarthi PR, Mandava Venkata BRM, Thanniru J, Vandana KR, Sundaresan CR. Potential of microemulsified entacapone drug delivery systems in the management of acute Parkinson's disease. J Acu Dis. 2016;5:315-325.

Turk J Pharm Sci 2018;15(3):263-270
DOI: 10.4274/tjps.79553

ORIGINAL ARTICLE

Development of the Composition and Manufacturing Technology of a New Combined Drug: Lavaflam

Yeni Kombine Bir İlacın, Lavaflam, Bileşimi ve Üretim Teknolojisinin Geliştirilmesi

Tanya IVKO[1]*, Milena ASLANIAN[3], Larisa BOBRYTSKA[3], Natalia POPOVA[3], Olena NAZAROVA[2], Natalia BEREZNYAKOVA[3], Tamara GERMANYUK[1]

[1]National Pirogov Memorial Medical University, Vinnytsya, Ukraine
[2]State Enterprise State Scientific Center for Drugs and Medical Products, Kharkov, Ukraine
[3]National University of Pharmacy, Kharkov, Ukraine

ABSTRACT

Objectives: Treatment of diseaes of the biliary system is one of the urgent problems of modern medicine.

Materials and Methods: An original pharmaceutical drug "Lavaflam" in the form of combined tablets, which includes a composition of herbal components flamin (0.05 g) and lavender oil (0.02 g), was proposed for the complex treatment of diseases of the biliary system. Flamin is phytomedicine from the immortelle flowers [*Helichrysum arenarium* (L.) Moench, Asteraceae], which contains a complex of active substances from the flavonoids group (salipurposide, isosalipurposide, kaempferol, luteolin). It is applied as a choleretic and an anti-inflammatory agent in cholecystitis, cholangitis, and biliary dyskinesia. Tablets were prepared by pressing for separate granulation technology.

Results: The lavender oil granulate was prepared using the solid phase method, and β-cyclodextrin was used as an excipient substance. The flamin granulate was prepared by mixing with the spherical-shaped filler mannitol PARTECK M 200. On the basis of previous studies, the excipients of the designed composition tablet "Lavaflam" were β-cyclodextrin (0.27 g), mannitol PARTECK M 200 (0.20 g), croscarmellose sodium (0.03 g), potato starch (0.022 g), PEG 6000 (0.002 g), and magnesium stearate (0.006 g). The assay of the main components of lavender oil with the references linalol and linalyl acetate was performed using gas chromatography. The assay of the total flavonoids of flamin was performed using spectrophotometry with isosalipurposide as the reference.

Conclusion: The new phytomedicine tablets "Lavaflam" meet European Pharmacopoeia requirements on the following parameters: appearance, geometric size, average weight, disintegration, friability, resistance of tablets to crushing, and quantification.

Key words: Lavender oil, flamin, tablets Lavaflam

ÖZ

Amaç: Biliyer sistem hastalıklarının tedavisi, modern tıbbın acil problemlerinden biridir.

Gereç ve Yöntemler: Biliyer sistem hastalıklarının karmaşık tedavisi için, bitkisel bileşenler flamin (0.05 g) ve lavanta yağından (0.02 g) oluşan bir bileşimi içeren kombine tablet formundaki formdaki orijinal farmasötik ilaç "Lavaflam" önerilmiştir. Flamin, flavonoidler grubundan (salipurposid, isosalipurposide, kaempferol, luteolin) aktif maddelerden oluşan bir kompleks içeren, ölmez çiçeklerden [*Helichrysum arenarium* (L.) Moench, Asteraceae] elde edilen bitkisel kaynaklı ilaçtır. Kolesistit, kolanjit ve biliyer diskinezide koloretik ve anti-inflamatuvar ajan olarak uygulanır. Tabletler, ayrı granülasyon teknolojisi için preslenerek hazırlandı.

Bulgular: Lavanta yağı granülesi katı faz metodu kullanılarak hazırlandı ve β-siklodekstrin yardımcı madde olarak kullanıldı. Flamin granülesi küresel şekilli dolgu maddesi mannitol PARTECK M 200 ile karıştırılarak hazırlandı. Önceki çalışmalara dayanarak, tasarlanan "Lavaflam" tablet bileşiminin eksipiyanları, β-siklodekstrin (0.27 g), mannitol PARTECK M 200 (0.20 g), kroskarmeloz sodyum (0.03 g), patates nişastası (0.022 g), PEG 6000 (0.002 g) ve magnezyum stearat (0.006 g) idi. Lavanta yağının ana bileşenlerinin analizi linalol ve linalil asetat referansları ile, gaz kromatografisi kullanılarak gerçekleştirildi. Flaminin toplam flavonoidlerinin analizi, referans olarak isosalipurposid ile spektrofotometri kullanılarak gerçekleştirildi.

Sonuç: Yeni bitkisel kaynaklı tabletler "Lavaflam", Avrupa Farmakopesi gereksinimlerini aşağıdaki parametrelerle karşılamaktadır: görünüm, geometrik boyut, ortalama ağırlık, dağılma, ufalanabilirlik, tabletlerin kırılmaya karşı direnci ve miktar tayini.

Anahtar kelimeler: Lavanta yağı, flamin, Lavaflam tabletleri

*Correspondence: **E-mail:** ivkot1981@gmail.com, **Phone:** +380982640560 **ORCID-ID:** orcid.org/0000-0003-2873-1473
Received: 21.07.2017, **Accepted:** 07.09.2017

INTRODUCTION

Treatment of diseases of the biliary system is one of the urgent problems of modern medicine.[1-4] Diseases of the liver and biliary tract are very common, occurring in 10-20% of the population of developed countries. According to statistics, in Ukraine, the number of such patients is constantly increasing.[5] Currently, combined drugs are the leading pharmacotherapeutic agents, including those for the treatment of diseases of the biliary system, which require complex treatment. The choice of drug combination allows to expand the range of action of the drug and the complex influence on the disease, enhance the activity of every ingredient, as well improve tolerability and reduce adverse effects.[6,7]

Modern herbal medicines are widely used in the complex treatment of various diseases, including in the biliary system. They are characterized by high efficiency, low toxicity, and the possibility of long-term use without the risk of adverse effects.[5,8] Complex treatment of biliary disease is the reason for the creation of drugs of herbal origin, because herbal remedies usually possess many pharmacologic effects and have low levels of adverse effects. Nowadays, immortelle-containing drugs are widely used, which are well-known in the Ukraine and some countries of the former Soviet Union. One of them is flamin, which has choleretic action, but also has established hepatoprotective, antimicrobial, and antiviral properties. This is why it is possible to broaden the variety of action by combining flamin with lavender oil. Adding lavender oil to flamin increases the peristalsis of biliary tract and improves the detoxication function of the liver.[8-11] Pre-clinical *in vivo* research was conducted under the direction of Prof. Drogovoz in the department of pharmacology of National University of Pharmacy, Kharkov, Ukraine, and the indicated effects were confirmed.[9] The aim of the research was to develop an original drug composition and technology in the form of tablets that included a combination of herbal substances, flamin and lavender oil.

MATERIALS AND METHODS

The objects of research were medicinal substances of herbal origin flamin (0.05 g), lavender oil (0.02 g), as well as excipient substances and tablets named "Lavaflam". Lavaflam is new drug in the form of tablets, consisting of flamin, lavender oil, and excipients: β-cyclodextrin (0.27 g), mannitol PARTECK M 200 (0.20 g), croscarmellose sodium (0.03 g), potato starch (0.022 g), polyethylene glycol (PEG) 6000 (0.002 g), magnesium stearate (0.006 g). To achieve this goal, it was necessary to analyze the biologically active compounds of flamin and lavender oil, their stability in tablets, as well to choose excipients and to perform pharmacotechnological analysis of them. Flamin (Pharmaceutical company "Zdorovye", Kharkov, Ukraine) is a yellow or brownish-yellow powder with a weak specific smell, easily soluble in 96% alcohol, and practically insoluble in water and chloroform.[12] Flamin is obtained from the immortelle flowers [*Helichrysum arenarium* (L.) Moench, Asteraceae] by extraction of 50% ethanol followed by purification.[13,14] It contains flavonoid glycosides and aglycones (salipurposide, isosalipurposide, kaempferol, luteolin, naringenin, apigenin and others), essential oils, organic acids, polysaccharides, and other biologically active substances of different groups.[13-15] The antimicrobial and antiviral activity of flamin and other drugs from immortelle flowers has been established.[6,10,13,14,16-21] Analysis of total flavonoids were conducted using spectrophotometry with the reference isosalipurposide-standard (specific absorption index).[7,13,14,16]

Assay of total flavonoids in flamin

The test solution. About 0.60 g (accurately weighed) powdered tablets was placed in a 100 mL volumetric flask, 70 mL of 96% ethanol was added, and allowed to stand in an ultrasonic bath for 5 minutes, diluted to 100 mL with the same solvents, stirred, and filtered through a paper filter "blue ribbon", and the first 15 mL of filtrate was discarded. Two millilitres of the resulting solution was diluted with 96% alcohol to a volume of 50.0 mL and stirred. The absorbance of the test solution was measured using a spectrophotometer (ultraviolet visible HP 8453, Hewlett Packard, USA) at a wavelength 315 nm in a cuvette with 10 mm thickness, using 96% alcohol as a compensation solution.

The total flavonoid expressed as isosalipurposide (X_1, %) in a single tablet was calculated using Equation 1:

$$X_1 = \frac{Ax100x50xb}{E^{1\%}_{1sm}\ xmx2x100} = \frac{Ax25xb}{E^{1\%}_{1sm}xm} \quad \text{(Equation 1)}$$

Where: A - the absorbance of the test solution at λ=315 nm;

$E^{1\%}_{1sm}$ isosalipurposide's specific absorption (96% alcohol) at λ= 315 nm is 260;

m: mass of the drug sample, in grams;

b: the average weight of the tablets, in milligrams.

Amount of total flavonoids expressed as isosalipurposide should be 31.0-39.0 mg of the nominal content.

Lavender oil was obtained from the flower of *Lavandula angustifolia Mill*, Lamiaceae. Lavender oil (Pharmaceutical company "Zdorovye", Kharkov, Ukraine) is a transparent, colorless or pale yellow liquid with a specific fragrance.[22,23] The analysis of lavender oil was conducted according to the requirements of the European Pharmacopoeia and Ukrainian State Pharmacopeia, which regulate the content of the following main components in lavender oil: limonene: less than 1.0%; 3-octanone: 0.1-2.5%; camphor: less than 1.2%; linalool: 20.0-45.0%; linalyl acetate: 25.0-46.0%; terpinene-4-ol: 0.1-6.0%; lavandulyl acetate: more than 0.2%; lavandulol: more than 0.1%; and α-terpineol: less than 2.0%. From the above normalization, the main components of lavender oil are linalol and linalyl acetate. Analysis of these terpenoids was performed using gas chromatography (GC) with internal normalization. A method for the assay of lavender oil in a combined pharmaceutical preparation "Lavaflam" were developed using a gas chromatograph Agilent 7890 (USA) with a flame ionization

detector. Lavender oil was used (1 mg/mL) as the standard sample solution. The calculation was performed for the amount of linalool and linalyl acetate (11).

Methods of analysis of lavender oil in "Lavaflam" tablets

The test solution. About 0.75 g (accurately weighed) of 20 powdered tablets was placed in a 25 mL volumetric flask, 15 mL of methanol was added, allowed to stand in an ultrasonic bath for 10 minutes, and the volume was diluted with the same solvent and thoroughly mixed. The resulting suspension was filtered through a paper filter "blue tape", discarding the first 5 mL of filtrate. The solution used was freshly prepared. Reference solution. About 0.5 g (accurately weighed) of lavender oil was placed in 50-mL volumetric flask, diluted with 50 mL methanol and thoroughly mixed. Five millilitres of this solution was placed in a 50 mL volumetric flask, diluted with methanol, and thoroughly mixed. The solution used was freshly prepared. One microliter of test solution and reference solution were chromatographed using a GC with a flame ionization detector.

Lavender oil content (X_2) in grams per tablet was calculated using Equation 2:

$$X_2 = \frac{\sum S_i \times m_o \times 5 \times 25 \times \mathrm{b}}{\sum S_o \times m \times 50 \times 50} = \frac{\sum S_i \times m_o \times \mathrm{b}}{\sum S_o \times m \times 20}, \quad \text{(Equation 2)}$$

where: ΣS_i-average value of the sum of areas of peaks of linalol and linalyl acetate, calculated from the chromatogram of the test solution;

ΣS_o-average sum of the areas of peaks of linalol and linalyl acetate, calculated from the chromatogram of the reference solution;

b-the average tablet weight calculated for 20 tablets (g);

m_o: mass of lavender oil (g);

m: mass of sample preparation (g).

Normalization lavender oil content is set within 90%-110% of the nominal content.

Pharmaco-technological studies have been carried out for development of the composition of excipients.[24] The bulk density, tap density, flowability, the angle of repose, compressibility, friability, and resistance of the tablets to crushing were determined on the "Pharma test" devices (Germany), and the disintegration on apparatus from "Erweka" (Germany). Flowability was evaluated using the Carr index and Hausner's index.[25,26]

Pharmacologic and technological properties of powders and granulates

Determination of the bulk density

The bulk density is the weight of a unit volume of a powder loosely placed into a measuring cylinder. It depends on the density of a substance, the particle size and shape, and its compatibility.

One hundred grams of the substance being examined is introduced to a dry cylinder without compacting.

The bulk density is calculated in g per mL using the formula m/V_0.

Determination of the density

The cylinder is fixed in its holder. Ten, 500, and 1250 taps are performed and the corresponding volumes V_{10}, V_{500} and V_{1250} are read to the nearest milliliter. The tap density is calculated in g per mL using the formula m/V_f, in which V_f is the final tapped volume.

Determination of flowability

Flowability characterizes the ability of a material to pour out from the container (a feeding funnel) under its own weight. Flowability was determined by outlet velocity of the fixed quantity of the material (100 g) pouring out from a metal funnel with strictly geometric parameters and by the angle of repose. The flowability is expressed in seconds, related to 100 g of the sample.

Determination of angle of repose

The indirect characteristic of flowability is the angle of repose. Powdery materials form a conical hill on a horizontal plane after being poured out from a funnel. The angle between the incline and the base of this hill is called the angle of repose, and is expressed in degrees. It was determined with a goniometer or measured in another way. The angle of repose changes over a wide range from 25-35° for well flowing materials and up to 60-70° for poorly flowing ones.

Determination of Carr index and Hausner's index

The Carr index and Hausner index are used to describe the flowability of a powder. According to Carr, an excellent flowability is between a Carr index of 5% to 15%; a Carr index of above 25% normally shows poor flowability.

$$\text{Carr Index} = \frac{(\text{ptap} - \text{pbulk})}{\text{ptap}} \times 100\%$$

With a Hausner index of 1.0 to 1.1, a powder is considered as free flowing, greater than 1.1 to 1.25, a powder is classified as medium flowing, if greater than 1.25 to 1.4, a powder is classified as difficult to flow, and higher than 1.4 is considered to be very difficult to flow.

$$\text{Haunser Index} = \frac{\text{ptap}}{\text{pbulk}}$$

Determination of compressibility

To determine compressibility, a sample of the powder was compressed (0.3-0.5 g) within a matrix of 9 or 11 mm in diameter, respectively, on a hydraulic press at pressure 120 MPa. Compressibility can also be also evaluated by the hardness of the obtained tablet.

Used excipients

To obtain tablets, lavender oil was converted to the solid state. Lavender oil granulate was prepared using the solid phase method, β-cyclodextrin was used as an excipient substance. Cyclodextrins are used in pharmaceutical technology in order to

build complex systems with a variety of active pharmaceutical ingredients, thereby largely improving their bioavailability and solubility, and increase chemical and physical stability. Cyclodextrin complexes are used to mask the unpleasant taste of active substances and converting liquid substances into solids.[27-30] Granulak 70 ("Meggle Excipients", Germany) is a crystalline form of lactose, it consists of fine particles with sharp edges and has cohesion properties that can be useful in the process of granulation. The following substances were used as fillers: tabletoza 70, microcrystalline cellulose (MCC) 102, di-calcium phosphate (for direct compression), mannitol PARTECK M 200 (for direct compression), and saccharose compressible grade B. Disintegrants were used to improve the disintegration.[30,31] According to the literature[30], as a disintegrants, it is better to use starch in combination with other substances with disintegrating action. In the powdering step, various combinations of the potato starch with the following excipients were used as the disintegrant: sodium croscarmellose, sodium starch glycolate and crospovidone. Lubricants were used to prevent adhesion, improve flowability and plasticity of the granulate for tableting. For this purpose, magnesium stearate in combination with PEG 6000 was used in the dusting granulate stage.

Preparation of granulate

Preparation of granulate A

β-cyclodextrin was mixed with water (30-40%) for 3-5 minutes in a laboratory mixer until a paste was formed. Lavender oil was added to the resulting paste with stirring for 5-10 min. The resulting mass was dried in a tray dryer at room temperature for 48 hours, stirring periodically. After drying, the mass was granulated through a sieve (holes diameter 1.0 mm) to obtain a homogeneous granulate (granulate A).

Preparation of granulate B

Considering the obtained results of flowability values, it is advisable to use 0.2 g PARTECK M 200 mannitol filler for powder flamin. Due to its the spherical shape, mannitol PARTECK M 200 is evenly distributed between the particles of flamin powder, while improving the flowability and uniformity of the resulting granulate mass. When mixed, flamin with mannitol PARTECK M 200 was then granulated through a sieve (holes diameter 1.0 mm) obtaining granules B.

Quality control tests of tablets

Determination of tablet friability

A drum type friabilator was used to determine abrasion of tablets. Tablets were dedusted and weighed with an accuracy of 0.001 g, then placed in a drum, covered with a lid, and the device was allowed to run for 4 minutes, with 100 revolutions. The tablets were dedusted, and if they had no chips and cracks their mass was determined with an accuracy of 0.001 g. The abrasion of the tablets in percentages was calculated using the following formula:

$$U = \frac{m_1 - m_2}{m_1} \times 100\%$$

Where,

m_1: mass of tablet before friability,

m_2: mass of tablet after friability.

The loss in mass of the tested tablets should be not more than 1% of the total mass of the tested tablets.

Determination resistance of tablets to crushing

This test is intended to determine, under defined conditions, the resistance to crushing of tablets measured by the force needed to disrupt them by crushing. The apparatus consists of 2 jaws facing each other, one moves towards the other. The tablet was placed between the jaws taking into account, where applicable, the shape, the break-mark and the inscription; for each measurement, the tablet was oriented in the same way with respect to the direction of application of the force. Measurements of 10 tablets were performed.

The load that caused the destruction of the tablets is a measure of strength. The obtained strength value is measured in Newtons.

Determination of tablets disintegration

This test is used to determine whether tablets disintegrate within the prescribed time when placed in a liquid (water). One dosage unit is placed in each of the 6 tubes of the basket. Operate the apparatus using the specified medium adjusted at 37±2°C as the immersion liquid. At the end of the specified time, the basket is lifted from the liquid and the dosage units are observed: all of the dosage units should have disintegrated completely. A tablet should be broken up within not more than 15 min.

Determination of the average weight of tablets

Twenty tablets are weighed separately with an accuracy of 0.001 g and their average mass is calculated. The deviation of the average mass of tablets from the mass specified in the "composition" section should not exceed ±5%. This work is technological and did not require approval from the ethics committee.

Statistical analysis

All analyses were carried out in triplicate. The results of research were analyzed using Excel 2007 and STATISTICA 6.0 using the average of all samples and are reported as mean±standard deviation.

RESULTS AND DISCUSSION

According to the literature, it is known[30] that the concentration of β-cyclodextrin affects the stability of essential oils during storage. To determine the optimal concentration of β-cyclodextrin granules with lavender oil, samples were prepared with different amounts of β-cyclodextrin: 0.15 g, 0.20 g, 0.25 g, 0.27 g, and 0.30 g. Stability during storage for 5 weeks was determined by the analysis of the concentration of lavender oil. The main components of lavender oil are linalool and linalyl acetate. Analysis of the lavender oil's components was conducted using GC. Lavender oil and granulak 70 was

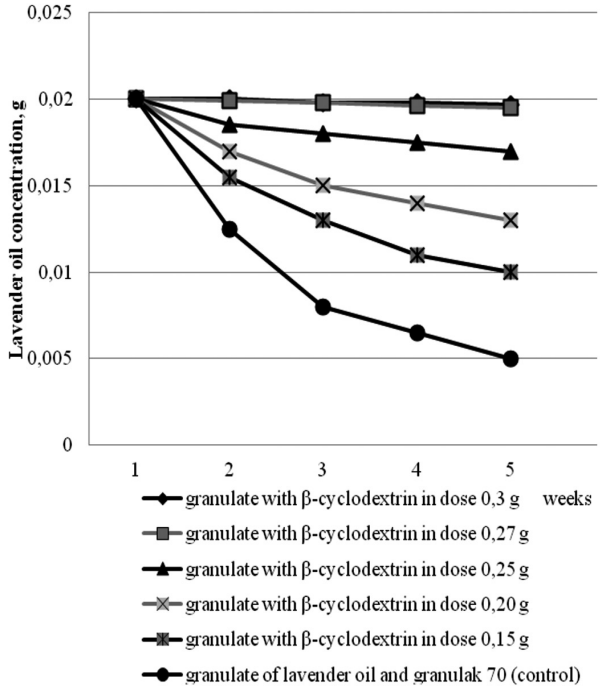

Figure 1. Effect of β-cyclodextrin concentration on the stability lavender oil during storage

Table 1. Pharmaco-technological properties of flamin

Pharmaco-technological properties	Units	Result
Bulk density	g/mL	0.35±0.01
Tap density	g/mL	0.62±0.01
Flowability	sec/100 g of sample	107.10±1.30
Angle of repose	degree	65±1.0
Compressibility	N	75.0±1.0
Carr index	%	43.0±1.0
Hausner index	-	1.77±0.01

used as a control (without β-cyclodextrin) to compare the stability of granules. The effect of β-cyclodextrin concentration on lavender oil stability during storage is shown in Figure 1. β-cyclodextrin has a stabilizing effect on lavender oil during storage. The granulate, which contains β-cyclodextrin in a dose 0.30 g and 0.27 g of lavender oil, was not changed and a constant value was 0.02 g for 5 weeks. The granulate with granulak 70 (without β-cyclodextrin), lavender oil concentration after 2 weeks' storage decreased almost 2 times. Thus on the basis of the research, we have chosen the concentration of β-cyclodextrin in a granulate with lavender oil, 0.27 g, which allows to maintain stability during storage for 5 weeks. The results of the stability studies of the lavender oil granulate with β-cyclodextrin in an amount of 0.27 g at different temperatures (20±5˚C) and (40±5˚C) are shown in Figure 2. As a result of this study, it was found that lavender oil concentration is stable for 12 months at a temperature of 20±5˚C, and the lavender oil concentration in the granulate gradually decreases at a temperature of 40±5˚C after 3 months storage. These results allow us to determine the temperature at which lavender oil will remain stable during storage. It has been found that the lavender oil is almost completely evaporated after 12 days in research of the stability of a powdered mixture of lavender oil and β-cyclodextrin (obtained without the hydration process) at 20±5˚C. Consequently the complex is formed only in the presence of water. The obtained results confirm the formation of the complex due to the process of hydration and optimal concentration of β-cyclodextrin. β-cyclodextrin molecules have the form of a truncated cone that is hollow inside. In the presence of water, the inner cavity gets hydrophobic properties because of glycoside molecules and it plays the role of a "master". This arrangement allows placing "guest molecules" of lavender oil inside the cavity, thus stabilizing it. Microscopic observations showed that there were no oil inclusions of free lavender oil in the samples-t confirms the formation of the complex. For the development of the composition of the excipients of tablets and a choice of rational technology, the next step of the research was to study the pharmaco-technological properties of flamin (Table 1). The results of technological properties of the substance flamin (Table 1) showed that it had low flowability.

Table 2. Pharmaco-technological properties of excipient

Name of excipient	Solubility	Bulk density, g/mL	Tap density, g/mL	Flowability sec/100 g of sample	Index Karra. %
Tabletosa 70. "Meggle excipients", Germany	Slowly soluble in water	0.53±0.01	0.64±0.01	15.3±0.1	17±1
Microcrystalline cellulose 102. "Mingtai chemical", Taiwan	Practically insoluble in water	0.33±0.01	0.45±0.01	30±0.1	26±1
Di-calcium phosphate. "Budenheim", Germany	Insoluble in water	0.45±0.01	0.71±0.01	9.3±0.1	21±1
Mannitol. PARTECK M 200. "Merck", Germany	Soluble in water	0.43±0.01	0.57±0.01	27±0.1	24±1
Saccharose compressible grade B. "Suedzucker", Germany	Soluble in water	0.65±0.01	0.72±0.01	2.8±0.1	9.7±0.5

This was confirmed by the microfine and complex surface of the powder particles and the high value of the angle of repose. The difference in bulk density and tap density indicates that the powder has caking ability. The Hausner index and Carr index also showed poor flowability values. Compressibility is characterized by model tablet strength after depressurization. Polydisperse particles of flamin powder contribute to the strength of the tablets. The substance has a satisfactory value of flamin compressibility. The greater the compressibility of the powder, the higher strength tablets. Pharmaco-technological research of flamin powder showed that to improve the flowability and the production of tablets it is necessary to use a complex of corresponding excipients to obtain a granular mass.[31] Granulated masses were prepared with fillers (Table 2). Flowability was determined for each granulated mass. The results are shown in Figure 3. The use of excipient substances contributes to the formation of a granular mass with the powder of flamin and improves flowability. As can be seen from Figure 3, for each filler these values are different and depend on the pharmaco-technical properties of each material, which are described in Table 2. Relatively good results were obtained for the granular mass mannitol PARTECK M 200 (30 sec/100 g sample), just below the phosphate di-calcium (33 sec/100 g sample) and sucrose in the pressing variety (35 sec/100 g of sample). The flowability values were poor (unsatisfactory) for the granular mass with tabletoza 70 and MCC 102. The results of the effect of the amount of mannitol PARTECK M 200, di-calcium phosphate, and saccharose pressing grade B on flowability values are shown in Figure 4. Figure 4 shows that increased of amount of fillers improved flowability values, respectively. Adding mannitol PARTECK M 200 in an amount of 0.2 g to the flamin powder improved flowability to a value of 15 sec/100 g sample, which is satisfactory. With further increases in amounts of mannitol PARTECK M 200 in the granulated mass, flowability values were practically unchanged. At the same concentration of fillers for flamin powder, flowability value with di-calcium phosphate was 20 sec/100 g of sample, and for saccharose compressible grade B-25 sec/100 g sample. Considering obtained results of flowability values, it is advisable to use mannitol PARTECK M 200 as a filler in an amount of 0.2 g for flamin powder.

The next step of the research was to combine and mix the granular mass. In a laboratory mixer, lavender oil granulate with β-cyclodextrin in an amount of 0.27 g (granulate A) was combined with flamin granulate (granulate B), stirred, and then the resulting granular mass was screened through a sieve with a 1.0 mm hole diameter. An important indicator of the quality that affects the bioavailability of a drug is disintegration. The disintegration time for the different disintegrating agents was from 10 to 18 minutes depending on the nature of the disintegrants (Figure 5). The disintegration time for the starch, as opposed to a combination of substances, is set higher at 18 minutes. The combination of disintegrating agents has a complex mechanism of action on tablet disintegration due to the effect of wettability, capillarity, and swelling. The result of the experiment revealed that the sodium croscarmellose in combination with potato starch had a substantial effect on the disintegration of the tablet, and ultimately on the disintegration time, which was 10 min. Due to the results of research, the excipients used in the composition of "Lavaflam" tablets were as follows: β-cyclodextrin (0.27 g), mannitol PARTECK

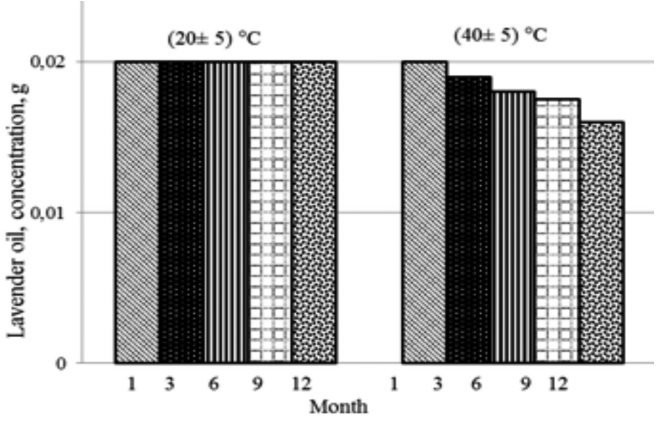

Figure 2. Study of stability lavender oil granulate with β-cyclodextrin at a temperature of (20±5)°C and (40±5)°C

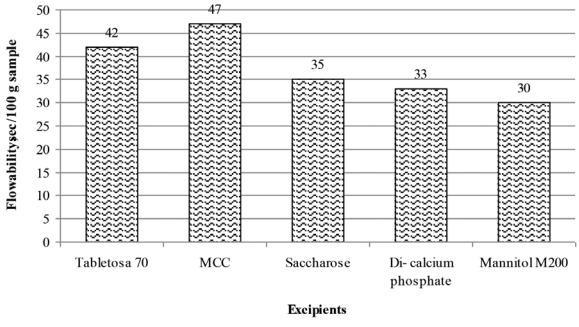

Figure 3. Comparative chart of flowability for various excipients

MCC: Microcrystalline cellulose

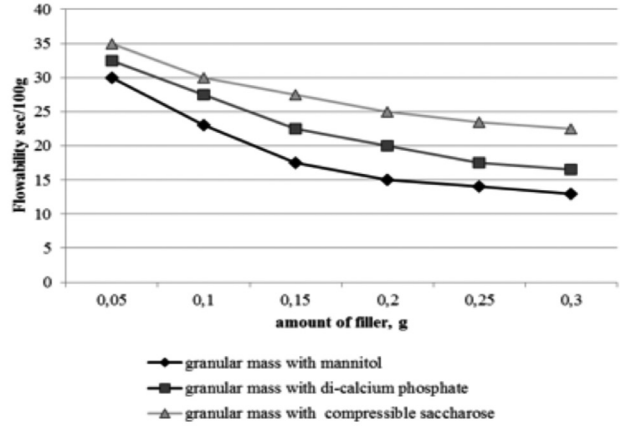

Figure 4. Effect of amount of fillers on flowability

Table 3. Standardization of "Lavaflam" tablets

Indicator	Results	Range measurement	Analysis
1. Appearance	Tablets are yellow with brownish touch, with a specific smell. Shape is flat-cylindrical	Tablets are yellow with brownish touch with a specific smell. Shape is flat-cylindrical	Visual analysis
2. Size	Diameter 12.0±0.3 mm height 4.0±0.5 mm	Diameter 12.0±0.3 mm height 4.0±0.5 mm	Instrumental
3. Average weight	600.0 mg±5.0%	From 570.0 mg up to 630.0 mg (600.0 mg±5%)	Physical
4. Disintegration	7±1 min	Not more than 15 min	Pharmaco-technological
5. Friability	0.7±0.1%	Not more than 1%	Pharmaco-technological
6. Resistance of tablets to crushing	110±10 H	From 50 H	Pharmaco-technological
7. Assay: 7.1. Total flavonoids with the reference into isosalipurposide	35.6 mg	In 1 tablet from 31.0 mg upto 39.0 mg	Spectrophotometry
7.2. Lavender oil	20.2 mg	From 18.0 mg up to 22.0 mg	Gas chromatography

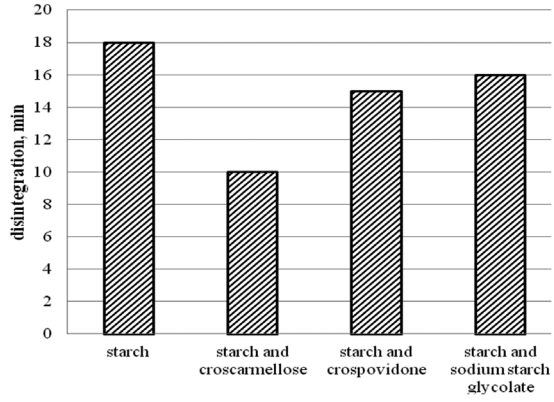

Figure 5. Effect of disintegrants on tablet disintegration

M 200 (0.20 g), croscarmellose sodium (0.03 g), potato starch (0.022 g), PEG 6000 (0.002 g), magnesium stearate (0.006 g). Tablets were prepared using compression with a separate granulation technique, which consisted of the following process steps:

- Preparation of raw materials,
- Preparation of lavender oil granulate with β-cyclodextrin (granulate A),
- Preparation of a granulate with a flamin (granulate B),
- The mixing, sifting and dusting of granulates A and B,
- Tabletting and dedusting,
- Packing of tablets in blisters,
- Packaging blisters in packs,
- Packaging packs into group container.

Standardization of "Lavaflam" tablets was performed based on the following parameters: appearance, geometric size, average weight, disintegration, abrasion resistance, compressive strength, assay (the amount of flavonoids was calculated in recalculation in isosalipurposide, lavender oil - in linalool and linalool acetate). The results are shown in Table 3. The results of research indicated that "Lavaflam" tablets (Table 3) met the European and Ukrainian State Pharmacopoeia requirements (the Ukrainian Pharmacopoeia is harmonized with the European Pharmacopoeia). Specifications for the control of quality of "Lavaflam" tablets have been developed.[11,16]

CONCLUSIONS

The combination phytomedicine "Lavaflam" tablets meet European Pharmacopoeia requirements on the following parameters: appearance, geometric size, average weight, disintegration, friability, resistance of tablets to crushing, and quantification. Lavaflam is planned for manufacture under industrial conditions by the pharmaceutical company "Zdorovya". The introduction of the drug will modernize the current regimens for the treatment of liver and bile duct diseases.

ACKNOWLEDGEMENTS

Authors want to express their gratitude for the idea of "Lavaflam" tablets, continuous support to Prof., Doctor of science Litvinenko V.I. (Kharkov, Ukraine).

Conflict of Interest: No conflict of interest was declared by the authors.

REFERENCES

1. Liang TB, Liu Y, Bai XL, Yu J, Chen W. Sphincter of Oddi laxity: An important factor in hepatolithiasis. World J Gastroenterol. 2010;16:1014-1018.
2. Portincasa P, Wang DQ. Intestinal absorption, hepatic synthesis, and biliary secretion of cholesterol: where are we for cholesterol gallstone formation? Hepatology. 2012;55:1313-1316.
3. Wang DQ, Cohen DE, Carey MC. Biliary lipids and cholesterol gallstone disease. J Lipid Res. 2009;50(Suppl):406-411.

4. Wang DQ, Zhang L, Wang HH. High cholesterol absorption efficiency and rapid biliary secretion of chylomicron remnant cholesterol enhance cholelithogenesis in gallstone-susceptible mice. Biochim Biophys Acta. 2005;1733:90-99.
5. Bobritskaya LA, Arakelyan MA, Popova NV. Marketing research of the market of drugs with the choleretic action. News of pharmacy. 2014;2:63-67.
6. Bobritskaya LA, Ruban HA, Osolodchenko TP, Shcherbak ON, Dmitrievskiy DI. Antibacterial properties of pharmaceutical compositions with ornidazole and flamini. Annals of Mechnikov Institute. 2013;1:27-31.
7. Bobritskaya LA, Popova NV, Ruban EA. Assessment of the quality of capsules with flamin and ornidazole. Pharmacy. 2013;5:20-22.
8. Drogovoz SM, Shtrygol SY, Shchekina EG. Pharmacology to help the student, pharmacist and doctor: Textbook-directory. Kharkov: Tityl; 2013:444-452.
9. Aslanian MA, Bobrytska LO, Nazarova ES. Pharmacological study of hepatoprotective activity of LAVAFLAM tablets, Pharmacy of the XXI century (VII national congress of pharmacists of Ukraine), Kharkiv; 2016:6.
10. Aslanian MA, Bobrytska LO, Osolodchenko TP. Antibacterial properties of pharmaceutical composition of hepatoprotectors. Annals of Mechnikov Institute. 2016;4:102-106.
11. Aslanyan MA, Bobritskaya LA, Nazarova ES, Mirnaya TA, Zborovskaya TV. Development and Validation of a Gas Chromatography Method for Quantitative Determination of Lavendar Oil in Lavaflam Preparation. Pharm Chem J. 2016;50:47-51.
12. Mashkovskij MD. Lekarstvennye sredstva: Posobie dlja vrachej Moscow; Novaja volna; 2000:500-509.
13. Popova NV, Litvinenko VI, The medicinal plants of world flora. Kharkov; 2008:510.
14. Litvinenko VI, Popova NV, Volkovitch OA. Cmins: botanical description, chemical composition, application. Pharmacom. 2001:9-15.
15. Sawilska A, Mielcarek S. The content of flavonoids and polyphenolic acids in inflorescences of Sandy Everlasting [*Helichrysum arenarium* (L.) Moench] from natural stands and plantations. Herba Pol. 2009;55:118-126.
16. Aslanian MA, Bobrytskaya LA, Nazarova ES, Popova NV, Zborovskaya TV. The development of quality control methods of tablets LAVAFLAM. Management, Economy and Quality Assurance in Pharmacy. 2015;5:9-14.
17. Cosar G, Cubukcu B. Antibacterial activity of Helichrysum species growing in Turkey. Fitoterapia. 1990;61:161-164.
18. Rios JL, Recio MC, Villar A. Isolation and identification of the antibacterial compounds from Helichrysum stoechas. J Ethnopharmacol. 1991;33:51-55.
19. Kaij-a-Kamb M, Amoros M, Girre L. Search for new antiviral agents of plant origin. Pharm Acta Helv. 1992;67:130-147.
20. Albayrak S, Aksoy A, Sağdıç O, Hamzaoğlu E. Compositions, antioxidant and antimicrobial activities of Helichrysum (Asteraceae) species collected from Turkey. Food Chem. 2010;119:114-122.
21. Selçuk SS, Birteksöz AS. Flavonoids of Helichrysum chasmolycicum and its antioxidant and antimicrobial activities. S Afr J Bot. 2011;77:170-174.
22. European Pharmacopoeia (8th ed). 8.0, Strasbourg: European Department for Quality of Medicines; 2014:1291-1292.
23. Prusinowska R, Smigielski KB. Composition, Biological Properties and Therapeutic Effects of Lavender (*Lavandula angustifolia* L). Herba Pol. 2014;60:56-66.
24. State Pharmacopoeia of Ukraine, State Enterprise Research Center expert pharmacopoeia, (1st ed). Kharkiv; RIREG; 2001:151-167.
25. Li Q, Rudolph V, Weigl B, Earl A. Interparticle van der Waals force in powder flowability and compactibility. Int J Pharm. 2004;280:77-93.
26. Etti CJ, Yusof YA, Chin NL, Tahir SM. Flowability Properties of Labisia Pumila Herbal Powder. Agriculture and Agricultural Science Procedia. 2014;2:120-127.
27. Buschmann HJ, Schollmeyer E. Applications of cyclodextrins in cosmetic products: A review. J Cosmet Sci. 2002;53:185-191.
28. Challa R, Ahuja A, Ali J, Khar RK. Cyclodextrins in drug delivery: An updated review. AAPS PharmSciTech. 2005;6:329-357.
29. George SJ, Vasudevan DT. Studies on the Preparation, Characterization, and Solubility of 2-HP-β-Cyclodextrin-Meclizine HCl Inclusion Complexes. J Young Pharm. 2012;4:220-227.
30. Georgievskiy VP, Konev FA. Technology and standardization of drugs. Kharkov; Rireg; 1996:539-602.
31. Rowe RC, Sheskey PJ, Cook WG, Quinn ME. Handbook of Pharmaceutical excipients, (7th ed). London; Pharmaceutical Press; 2012:1064.

Turk J Pharm Sci 2018;15(3):271-277
DOI: 10.4274/tjps.43265

ORIGINAL ARTICLE

Development and Full Validation of a Stability-indicating HPLC Method for the Determination of the Anticancer Drug Temozolomide in Pharmaceutical Form

Anti-kanser İlaç Temozolomidin Farmasötik Formundan Miktar Tayini için Ters Faz Sıvı Kromatografisi Yönteminin Geliştirilmesi, Validasyonu ve Stabilite Çalışması

Evin KAPÇAK, Eda Hayriye ŞATANA-KARA*

Gazi University, Faculty of Pharmacy, Department of Analytical Chemistry, Ankara, Turkey

ABSTRACT

Objectives: In the present study, an accurate, precise and simple method has been developed for the determination of TMZ in its pharmaceutical form by using HPLC.

Materials and Methods: An HPLC method with a DAD was validated according to ICH guidelines. A C18 column (150x4.6 mm. i.d., 5 µm particle size) and an aqueous acetate buffer (0.02 M)-acetonitrile (90:10, v/v) (pH 4.5) as a mobile phase were used.

Results: The linear range and LOD value were 5-100 µg/mL and 0.02 µg/mL, respectively. The accuracy of the method was determined using a recovery test and found as 98.8-100.3%. In addition, forced degradation studies of the drug were also performed in bulk drug samples to demonstrate the specificity and stability-indicating. Degradation studies under acidic, basic, oxidative, and thermal degradation conditions were applied.

Conclusion: The proposed method could be applied successfully for the determination and identification of the degradation of the drug.

Key words: Temozolomide, HPLC, validation, determination, degradation

ÖZ

Amaç: Bu çalışmada TMZ'nin farmasötik formundan tayini için doğru, kesin ve basit bir yüksek basınçlı sıvı kromatografi yöntemi geliştirilmiştir.

Gereç ve Yöntemler: DAD dedektörlü HPLC yöntemi ICH kurallarına göre valide edilmiştir. C18 kolon (150x4.6 mm. i.d., 5 µm tanecik boyutu) ve hareketli faz olarak sulu asetat tampon (0.02 M)- asetonitril (90:10, h/h) (pH 4.5) karışımı kullanılmıştır.

Bulgular: Doğrusal aralık ve LOD değerleri sırası ile 5-100 µg/mL and 0.02 µg/mL'dir. Yöntemin doğruluğu geri kazanım yöntemi ile belirlenmiş ve %98.8-100.3 olarak bulunmuştur. Bu çalışmaların yanı sıra bozunma çalışmaları yapılmıştır. Bozunma çalışmaları asidik, bazik, oksidatif ve termal bozunma şartlarında gerçekleştirilmiştir.

Sonuç: Önerilen metod ilacın miktar tayini ve bozunma çalışması için başarı ile uygulanmıştır.

Anahtar kelimeler: Temozolomid, HPLC, validasyon, miktar tayini, bozunma

INTRODUCTION

Temozolomide (TMZ), 4-methyl-5-oxo-2,3,4,6,8-pentazabicyclo [4.3.0]nona-2,7,9-triene-9-carboxamide, is an oral anticancer drug. It belongs to the alkylating agent class and is used for the treatment of brain cancer such as glioblastoma multiforme.[1,2] The antitumor effect of TMZ depends on its ability to alkylate/methylate DNA. This methylation damages DNA and triggers the death of tumor cells. TMZ is a prodrug and an imidazotetrazine derivative of the dacarbazine, 5-(3-dimethyltriazen-1-yl)-imidazo-4-carboxamide (DTIC). TMZ demonstrates better

*Correspondence: E-mail: eda@gazi.edu.tr, Phone: +90 535 389 23 45 ORCID-ID: orcid.org/0000-0003-1002-9045
Received: 25.07.2017, Accepted: 07.09.2017

antitumor activity and a better safety profile in preclinical assessments.[3,4] The antitumor activity of the drug depends on linear triazine, 5-(3-methyltriazen-1-yl)-imidazo-4-carboxamide (MTIC). DTIC is metabolically converted to MTIC in the liver, whereas TMZ is degradated chemically to MTIC at physiologic pH.[5] MTIC shows a cytotoxic effect due to alkylation at the O6 and N7 positions of guanine. After this process, MTIC converts itself to 5(4)-aminoimidazole-4(5)-carboxamide (AIC) (Figure 1).[6,7] In a literature survey, different techniques exist for the analysis of TMZ. Ultraviolet (UV) spectrophotometric methods have been described for the determination of TMZ in pharmaceutical formulations.[8-11] Only two electrochemical studies based on an investigation of the electrochemical behavior of TMZ exist in the literature.[12,13] In addition, chromatography with UV[14-21] and mass spectrometry detection[22-24] were the most common techniques used for the separation and determination of TMZ, its metabolites, and degradation products. The aim of this research was to optimize and develop a simple, rapid, economical, precise and accurate, reproducible, and fully validated high-performance liquid chromatography (HPLC) method with good detection limits for the estimation of TMZ in a pharmaceutical preparation. Forced degradation studies are also presented to show the stability-indicating capacity of the developed HPLC method. The stability tests for the developed method were performed according to International Conference on Harmonization (ICH) guidelines.[25,26]

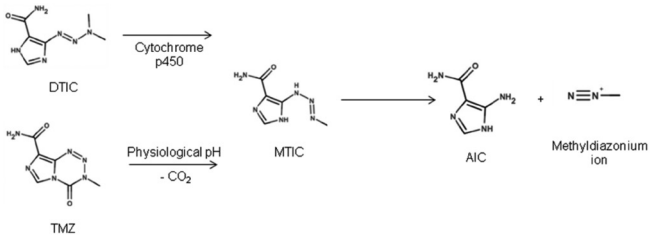

Figure 1. Chemical structures and conversion process of temozolomide

MTIC: 5-(3-methyltriazen-1-yl)-imidazo-4-carboxamide, DTIC: 5-(3-dimethyltriazen-1-yl)-imidazo-4-carboxamide, AIC: 5(4)-aminoimidazole-4(5)-carboxamide, TMZ: Temozolomide

EXPERIMENTAL

Chemical and reagents

TMZ and dose form were purchased from Sigma-Aldrich and local suppliers, respectively. Chromatographic-grade acetonitrile and analytical grade acetic acid, sodium acetate, phosphoric acid, boric acid, HCl, and NaOH were obtained from Merck (Darmstadt, Germany). Double-distilled water with conductivity lower than 0.05 µS/cm was used to prepare the mobile phase solutions. The mobile phase used in HPLC was an aqueous acetate buffer (0.02 M)-acetonitrile (90:10, v/v) (pH 4.5). After mixing, the mobile phase was degassed. For the preparation of the standard TMZ stock solution, 20.0 mg TMZ was accurately weighed and dissolved in mobile phase in a 100 mL volumetric flask and then adjusted to 100.0 mL with the same solution. For stabilization experiments, a similar quantity of TMZ was dissolved in 100 mL deionized water. Standard solutions in the range of 5.0-100.0 µg/mL were prepared using the appropriate dilution of the stock solution. A calibration curve was drawn using the peak area values versus these concentration values at the optimized conditions.

Instrumentation

The HPLC system consisted of a Agilent series 1260 solvent delivery system with an Agilent 1260 diode-array detector (DAD) system. An ACE C18 column (150x4.6 mm. i.d., 5 µm particle size) was used. Mobile phase filtration was performed using an Erich Wiegand GmbH type N 022 AN 18 vacuum pump with all tech 47 mm, 0.45 m filter paper. Bondelin Sonorex RK 100 H was used as a degasser. The typical operating conditions were as follows: flow rate, 0.8 mL/min; operating temperature, 30˚C; injection volume, 30 µL.

Analysis of pharmaceutical form

The average mass of 10 capsules was determined. Capsule contents were accurately weighed. A definite amount of the powder was transferred to a 250 mL volumetric flask and the volume was adjusted to the mark with the mobile phase. The solution was sonicated in an ultrasonicator for 20 min and the solution was filtered. The appropriate volume of the filtrate was diluted with the mobile phase prior to analysis. In order to determine the TMZ content of the capsule, TMZ standard solutions were injected and the calibration curve was obtained as the peak area versus the concentration. The sample solution, 30 µL, was injected, and the detection was at 260 nm. The amount of TMZ in a capsule was determined using the calibration curve.

Degradation studies

Degradation studies were attempted for stress conditions by acidic hydrolysis, alkaline hydrolysis, oxidation, and heat in an oven (at 100˚C), to evaluate the ability of the proposed method to separate TMZ from its degradation product. The peak purity test was performed for TMZ peaks by using a DAD in the stress samples. The optimized method was used to study the forced degradation behavior of TMZ and may also applied in the stability testing of pharmaceuticals. An appropriate blank was injected before analysis of the forced samples.

The reactions were conducted with 20 µg/mL of TMZ. The stress conditions were as follows:

- Acidic hydrolysis: Drug solution in 1 M HCl was exposed at 80˚C for 60 min.

- Alkaline hydrolysis: Drug solution in 1 M NaOH was exposed 80˚C for 60 min.

- Oxidative condition: Drug solutions in 3% H_2O_2 were stored at 80˚C for 60 min.

- Thermal stress: Bulk drugs were subjected to dry heat at 100˚C for 24 hr.

In addition, TMZ is highly unstable in alkaline solutions and relatively stable under acidic pH conditions. Therefore, a TMZ stock solution was also prepared in deionized water to provide

degradation in the working environment and chromatograms were recorded.

There was no need for ethics committee approval for this study.

RESULTS AND DISCUSSION

Optimization of chromatographic conditions

The column, mobile phase composition, pH, flow rate, and column temperature were tested to optimize the separation conditions. In order to evaluate the effect of the column on the separation, C8 and C18 columns were tested. A well-shaped symmetrical peak was obtained with the C18 column. Different buffer solutions have been tested to characterize the drug at different pH values. For this purpose, acetate buffer (pH 3.5-5.5), phosphate buffer (pH 6.0-8.0), borate buffer (pH 9.0), 0.1 M HCl, and 0.1 M NaOH solutions were tried. According to the literature, TMZ is stable in medium at pH <5. In addition, obtained results from absorbance spectra show that highest absorbance value was achieved at pH <5. Hence, pH 4.5 acetate buffer was selected. The mobile phase acetate buffer (0.02 M)-acetonitrile (90:10, v/v) (pH 4.5) was most found suitable for TMZ analysis using DAD detection at 260 nm at 30°C. When methanol was used as an organic phase, the peak of TMZ had a shoulder, and the tailing factor of the peak was more than 2. However, when using acetonitrile, a sharp symmetrical peak was obtained. For the optimization of the organic phase ratio, 10%, 20%, and 30% acetonitrile ratios were tried. When the organic phase ratio was increased above 10%, the retention time was shortened such that the separation in the TMZ peak could not be sufficient and tailing at the peak was observed. When the ratio of acetonitrile was 10%, retention improved and a symmetrical peak was observed. Temperatures between 15°C and 40°C were scanned to examine the effect of temperature. It was observed that temperature affected both the separation and the peak symmetries. Hence, 30°C was selected as the optimized temperature. It was observed that the flow rate had little effect on the resolution but changed the retention time to a great extent. Different flow rates, 0.8 mL/min; 1 mL/min, and 1.3 mL/min were tried and optimum results were obtained at 0.8 mL/min. Optimized chromatographic conditions and a typical LC chromatogram are given in Table 1 and Figure 2a, respectively. After determining the best conditions, a satisfactory chromatographic peak resolution was obtained in a short analysis time. Under the optimized operating conditions, the retention time corresponding to TMZ was 3.5 min, being extremely stable among injections. Using these optimum conditions, shorter analysis times, and higher accuracy and selectivity were obtained. The proposed method was successfully used for the determination of TMZ in its dose form and related data on the specificity for their estimation in the presence of their degradation compounds are reported (Figure 2b). The proposed study was easily used with mixtures of stressed samples with drug degradation. The resolution between the degradation products and the drug peak was satisfactory.

Table 1. Optimized chromatographic conditions

Mobile phase	Acetate buffer (0.02 M)-acetonitrile (90:10, v/v) (pH 4.5)
Column	ACE C18 (150x4.6 mm. i.d., 5 µm particle size)
Flow rate	0.8 mL/min
Injection volume	30 µL
Column temperature	30°C
Detection wavelength	260 nm
Retention time	3.5 min

Validation procedures of the methods

A system suitability test can be defined as a test to specify that a method can generate acceptable accuracy and precision results. According to the USP, system suitability tests were performed prior to analysis.[27] Hence, system suitability for the proposed method was evaluated. For this purpose, test parameters such as capacity factor, theoretical plate number, retention time, symmetry factor, selectivity, and relative standard deviation (RSD) % of the peak area for repetitive injections were calculated. For the method to be valid, at least two of these criteria were required to demonstrate system suitability for the proposed method. The results obtained from system suitability tests were found within acceptable limits and in agreement with the USP requirements. The parameters obtained from the system suitability analysis are presented in Table 2.

Linearity

The linearity of the detector responses for TMZ was determined using peak area versus concentration. The linearity was obtained in the range of 5.0-100 µg/mL at a detection wavelength 260 nm, with a correlation coefficient (r) of 0.9998.

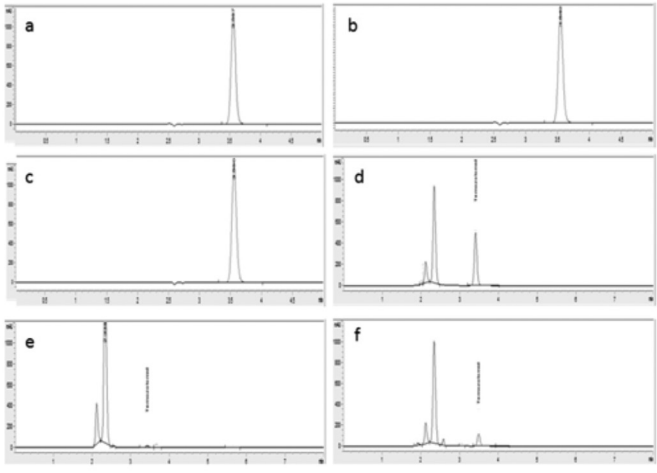

Figure 2. Chromatograms of (a) 20 µg/mL TMZ standard solution and (b) 20 µg/mL TMZ capsule solution. Chromatograms of the stress studies under (c) acidic hydrolysis, (d) alkaline hydrolysis, (e) oxidation and (f) dry heat

TMZ: Temozolomide

The good linearity of the calibration graph and the negligible scatter of experimental points were evident by the values of the correlation coefficient and standard deviation. The analytical features of calibration graph are listed in Table 3.

Limit of detection and limit of quantification

Several approaches are given in the ICH guidelines to determine the limit of detection (LOD) and limit of quantification (LOQ). LOD and LOQ were calculated from the equations of LOD=3.3 s/m and LOQ=10 s/m[28] where s is the standard deviation of responses and m is the slope of the calibration curve (Table 3).

Table 2. System suitability test parameters

Parameters	Calculated values
Theoretical plate number (N)	7964
Capacity factor (k')	1.393
Tailing factor (T)	1.055
Resolution (R_S)	5.05
Symmetry factor	0.99
RSD% of peak area	0.08
Retention time (t_r)	3.5

RSD: Relative standard deviation

Table 3. Regression data of the calibration lines for quantitative determination of temozolomide by high-performance liquid chromatography

Linearity range (µg/mL)	5-100
Slope	52.27
Intercept	22.31
Correlation coefficient	0.9998
SE of slope	0.16
SE of intercept	7.52
LOD (µg/mL)	0.02
LOQ (µg/mL)	0.06

LOD: Limit of detection, LOQ: Limit of quantification

Table 4. The results of intra-day and inter-day precision

Inter-day precision (µg/mL)	(RSD %)*
20.04	0.12
25.05	0.03
30.06	0.04
Intra-day precision (µg/mL)	(RSD %)*
20.04	0.08
25.05	0.11
30.06	0.08

*Each value is the mean of six experiments, RSD: Relative standard deviation

Precision

System repeatability was determined through six replicate applications at three different concentrations (20.04, 25.05, and 30.06 µg/mL) on the same day (intra-day precision) and measurements of the peak area for the active compound. Inter-day precision was assessed by the assay of similar concentration sample sets on three different days. The results summarized in Table 4 indicate a high degree of precision for the proposed method.

Accuracy

In order to find out the accuracy of the proposed method, recovery studies were performed by spiking the sample of a capsule with an appropriate amount of a stock solution of TMZ. Recovery of the method was determined by spiking the marketed sample with 50%, 100%, and 150% standard solutions. As can be seen in Table 5, relatively high recovery values were obtained using the proposed method. These high recovery values proved the accuracy of the developed method.

Robustness

Robustness can be defined as the capacity of a developed method to remain unaffected by analysis parameters. Hence, the results of the organic phase ratio, pH value, temperature, flow rate, and wavelength parameters were evaluated to determine the robustness of the proposed method. The robustness tests were performed at 20 µg/mL of TMZ. The analyzed conditions, obtained results, and RSD% values are shown in Table 6. The results were evaluated statistically using the Friedman test. As seen from the table, the calculated values of all parameters were smaller than the theoretical value, which indicated that minor changes in the system did not lead to significant differences in peak areas. Therefore, it can be said that the developed method was stable and robust.

Forced degradation studies

To present the stability and indicate the capability of the developed HPLC method, forced degradation studies were

Table 5. Results of the assay and the recovery analysis of temozolomide in pharmaceutical dose forms via high-performance liquid chromatography

Labeled claim (mg)	5.00			
Amount found (mg)[a]	5.00±0.004			
RSD (%)	0.30			
Bias (%)	0.00			
Recovery results[b]				
Added (mg)	**Found (mg)***	**Recovery (%)**	**RSD %**	**Bias (%)**
2.5	2.47±0.02	98.90	0.26	1.2
5	5.02±0.15	100.40	0.13	-0.4
7.5	7.47±0.21	99.65	0.55	0.4

[a]Each value is the mean of five experiments, [b]Each value is the mean of three experiments, *Each value is the mean of three experiments, RSD: Relative standard deviation

performed. Degradation studies were performed as mentioned in the experimental section. Degradation experiments were designed using acidic hydrolysis, alkaline hydrolysis, hydrogen peroxide, and dry heat. The stock solutions of the compounds were diluted with HCl, NaOH, and H_2O_2 to 20 µg/mL and left for 1 h. Degradation peaks were separated from the main peaks. When applying drastic conditions, TMZ was stable in acidic media, whereas it was clearly degraded in basic media, and with heat and oxidation. Degradation percentage values were calculated as a ratio of the peak areas of untreated drug solution and treated solutions. The chromatograms are shown in Figure 2c-f and degradation percentages were tabulated after each treatment, as shown in Table 7. In addition, it has been shown in the literature that TMZ chemically degrades to MTIC both *in vivo* and *in vitro* at physiologic pH (pH 6-7).[29] The degradation product, MTIC, is disrupted by the formation of the methyldiazonium ion and AIC as shown in Figure 1. In order to evaluate degradation, the stock TMZ solution was prepared in deionized water and the required dilutions were made with water again (Figure 3a). The pH value of the prepared aqueous stock solution was measured as about 8.5. This value causes degradation of TMZ. As seen from Figure 3, a new peak appeared at 2.2 min. A 6-hour stability test was performed for chromatographic studies. When chromatograms of the diluted solution of deionized water were examined, it was observed that the peak area of TMZ decreased with time and the peak of the unknown species increased without changes in the retention times of both species (Table 8). On the other hand, in the solution in which the diluent was made using the pH 4.5 acetate buffer, there was no change in the values of the TMZ and the unknown species (Figure 3b and Table 8). Compared with the spectra of the TMZ, MTIC, and AIC species obtained from the literature,[30] and the three-dimensional spectrum obtained from the DAD detector, it is suggested that the unknown species belongs to AIC.

Table 6. Statistical comparison of robustness results of high-performance liquid chromatography method

Parameters		Peak area*	RSD %
Organic phase ratio (%)	8	1101.8	0.15
	10	1100.3	0.18
	12	1099.4	0.18
$\chi^2_{r(calculated)}$=1.5			
pH value	4.3	1096.4	0.15
	4.5	1092.2	0.18
	4.7	1094.4	0.18
$\chi^2_{r(calculated)}$=3.1			
Temperature (°C)	27	1101.1	0.07
	30	1100.3	0.12
	33	1101.8	0.09
$\chi^2_{r(calculated)}$=2.6			
Flow rate (mL/min)	0.7	1102.9	0.15
	0.8	1100.2	0.14
	0.9	1099.9	0.17
$\chi^2_{r(calculated)}$=4.2			
Wavelength (nm)	258	1098.1	0.11
	260	1101	0.18
	262	1098.8	0.11
$\chi^2_{r(calculated)}$=2.1			

*Each value is the mean of six experiments, α=0.05, $\chi^2_{r(theoretical)}$=5.99, RSD: Relative standard deviation

Table 7. The results of forced stress conditions of temozolomide

The response of hard stress conditions	Degradation of compound (%)	RSD (%)
HCl (1 M)	-	-
NaOH (1 M)	89	0.12
H_2O_2 (3%)	55	0.08
Heating (100°C)	98	0.21

*Each value is the mean of three experiments, RSD: Relative standard deviation

Application of the HPLC method for the analysis of commercial formulations

In the present work, the application of the developed method for the determination of TMZ in pharmaceutical samples was presented. Evaluation of pharmaceutical formulations was performed by using the calibration curve method. Calibration graphs were constructed by measuring the peak areas obtained at these concentrations under optimized conditions. The proposed methods were applied to the determination of TMZ in its pharmaceutical form Temodal® (Schering-Plough, Belgium), labeled as 5 mg TMZ. This is a simple procedure that can be used without any sample extraction, evaporation, or filtration. No interfering peaks were observed from any of the inactive ingredients of the assayed preparations. The precision and

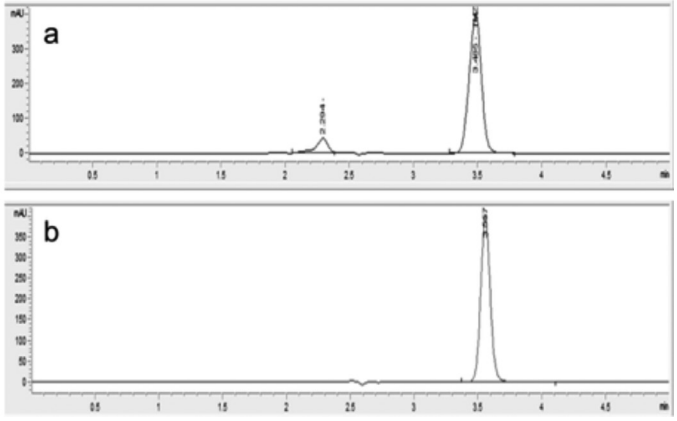

Figure 3. Chromatograms of 20 µg/mL temozolomide standard solutions prepared in (a) deionized water and (b) pH 4.5 acetate buffer

Table 8. Peak areas changes of temozolomide and unknown species

Prepared in deionized water					Prepared in pH 4.5 acetate buffer			
Time (min)	Unknown peak area	Unknown t_R	TMZ peak area	TMZ t_R	Unknown peak area	Unknown t_R	TMZ peak area	TMZ t_R
0	99.1	2.3	1084.6	3.5	19.9	2.3	1126.3	3.7
30	110.6	2.3	1080.3	3.5	20.8	2.3	1123.5	3.7
60	133.1	2.3	1076.0	3.5	20.5	2.3	1125.7	3.7
120	463.7	2.3	905.0	3.5	20.1	2.3	1124.1	3.7
180	1133.8	2.3	729.4	3.5	20.2	2.3	1126.8	3.7
240	1314.4	2.3	358.5	3.5	20.6	2.3	1124.2	3.7
300	1695.0	2.3	314.8	3.5	20.4	2.3	1124.9	3.7
360	1699.0	2.3	311.2	3.5	20.4	2.3	1121.7	3.7

TMZ: Temozolomide

accuracy results showed that the proposed methods could be applied for the determination of TMZ in pharmaceutical formulations without any interference effect of the inactive ingredients. The use of all of the proposed method was verified by means of replicate estimations of pharmaceutical preparations and the results obtained were evaluated statistically (Table 5).

CONCLUSIONS

The stability-indicating HPLC method was fully validated according to ICH guidelines and was presented for the determination of TMZ in capsule formulation, which offers numerous advantages, such as rapidity, use of minimum amounts of organic solvents, simplicity, low cost, ease of operation, and high selectivity. Good recoveries, high reproducibility, and interference-free chromatograms were also achieved. A high percentage of recovery results showed that the proposed methods were free from interferences of commonly used excipients and additives in the formulation.

Conflict of Interest: No conflict of interest was declared by the authors.

REFERENCES

1. Wang Z, Hu P, Tang F, Lian H, Chen X, Zhang Y, He X, Liu W, Xie C. HDAC6 promotes cell proliferation and confers resistance to temozolomide in glioblastoma. Cancer Lett. 2016;379:134-142.
2. Lee SY. Temozolomide resistance in glioblastoma multiforme. Genes & Diseases. 2016;3:198-210.
3. Stevens MF, Hickman JA, Langdon SP, Chubb D, Vickers L, Stone R, Baig G, Goddard C, Gibson NW, Slack JA, Newton C, Lunt E, Fizames C, Lavelle F. Antitumor activity and pharmacokinetics in mice of 8-carbamoyl-3-methyl-imidazo[5,1-d]-1,2,3,5-tetrazin-4(3H)-one (CCRG 81045; M & B 39831), a novel drug with potential as an alternative to dacarbazine. Cancer Res. 1987;47:5846-5852.
4. Tsang LL, Quarterman CP, Gescher A, Slack JA. Comparison of the cytotoxicity in vitro of temozolomide and dacarbazine, prodrugs of 3-methyl-(triazen-1-yl) imidazole-4-carboxamide. Cancer Chemother Pharmacol. 1991;27:342-346.
5. Wei JH, Zhou RH, Peng Y, Liu YC. Studies on the binding properties of temozolomide with DNA. Asian J Chem. 2013;25:2597-2600.
6. Hartley JA, Gibson NW, Kohn KW, Mattes WB. DNA sequence selectivity of guanine-N7 alkylation by three antitumor chloroethylating agents. Cancer Res. 1986;46:1943-1947.
7. Meer L, Janzer RC, Kleihues P, Kolar GF. In vivo metabolism and reaction with DNA of the cytostatic agent, 5-(3,3-dimethyl-1-triazeno)imidazole-4-carboxamide (DTIC). Biochem Pharmacol. 1986;35:3243-3247.
8. Madhu M, Raj NRS, Swathi V, Yasmeen R, Ishaq BM. Development and validation of UV spectroscopic method for the estimation of temozolomide in capsule dosage form. Int J Biol Pharm Res. 2014;5:701-705.
9. Razak A, Omshanthi B, Suresh V, Obulamma P. Development and validation of UV method of temozolomide in bulk and capsule formulation. Int J Biol Pharm Res. 2013;4:1419-1423.
10. Ishaq M, Hindustan AH, Muneer S, Parveen S, Fahmida B. Analytical method development and validation for the estimation of temozolomide in phosphate buffer in pH 2.0 as a solvent by UV spectroscopy. Int Res J Pharm. 2014;5:17-20.
11. Sankar DG, Latha PVM, Kumar BA, Babu PJ. UV spectrophotometric determination of temozolomide and gemcitabine. Asian J Chem. 2007;19:1605-1607.
12. Lopes IC, Oliveira SCB, Brett AMO. Temozolomide chemical degradation to 5-aminoimidazole-4-carboxamide-electrochemical study. J Electroanal Chem. 2013;704:183-189.
13. Ghalkhani M, Fernandes IPG, Oliveira SCB, Shahrokhian S, Shahrokhian S, Oliveira-Brett AM. Electrochemical redox behaviour of temozolomide using a glassy carbon electrode. Electroanalysis. 2010;22:2633-2640.
14. Khan A, Imam SS, Aqil M, Sultana Y, Ali A, Khan K. Design of experiment based validated stability indicating RP-HPLC method of temozolomide in bulk and pharmaceutical dosage forms. Beni-Suef Univ J Appl Sci. 2016;5:402-408.
15. Gilant E, Kaza M, Szlagovska A, Byczak K, Rudzki PJ. Validated HPLC method for determination of temozolomide in human plasma. Acta Pol Pharm. 2012;69:1347-1355.
16. Rao AL, Ramesh GT, Rao JVLNS. RP-HPLC analysis of temozolomide in pharmaceutical dosage forms. Asian J Chem. 2010;22:5067-5071.

17. Shen F, Decosterd LA, Gander M, Leyvraz S, Biollax J, Lejeune F. Determination of temozolomide in human plasma and urine by high-performance liquid chromatography after solid-phase extraction. J Chromatogr B Biomed Appl. 1995;19:291-300.

18. Kim HK, Lin CC, Parker D, Veals J, Lim J, Likhari P, Statkevich P, Marco A, Nomeir AA. High-performance liquid chromatographic determination and stability of 5-(3-methyltriazen-1-yl)-imidazo-4-carboximide, the biologically active product of the antitumor agent temozolomide, in human plasma. J Chromatogr B Biomed Sci Appl. 1997;703:225-233.

19. Pallerla S, Prabhakar B. Bio analytical method development and validation of temozolomide in rat plasma using RP-HPLC method. Int J Pharm Sci Res. 2016;7:1298-1301.

20. Attari Z, Kumar L, Rao CM, Koteshwara KB. Validation of a sensitive and robust reversed phase-HPLC method for determination of temozolomide. Lat Am J Pharm. 2016;35:967-971.

21. Saravanan G, Ravikumar M, Jadhav MJ, Suryanarayana MV, Someswararao N, Acharyulu PVR. A stability indicating LC assay and degradation behaviour of temozolomide drug substances. Chromatographia. 2007;66:291-294.

22. Chowdhury SK, Laudicina D, Blumenkrantz N, Wirth M, Alton KB. An LC:MS:MS method for the quantitation of MTIC (5-(3-N-methyltriazen-1-yl)-imidazole-4-carboxamide), a bioconversion product of Temozolomide, in rat and dog plasma. J Pharm Biomed Anal. 1999;19:659-668.

23. Zhang Y, Sun Y, HE Q, Han J, Shi M, Fang C, Fawcett JP, Yang Y, Gu J. Simultaneous determination of temozolomide acid and its hexyl ester in plasma by LC-MS/MS: application to the first pharmacokinetic study of temozolomide hexyl ester in rats. Anal Methods. 2014;6:8973-8978.

24. Negreira N, Mastroianni N, Lopez de Alda M, Barcelo D. Multianalyte determination of 24 cytostatics and metabolites by liquid chromatography-electrospray-tandem mass spectrometry and study of their stability and optimum storage conditions in aqueous solution. Talanta. 2013;116:290-299.

25. ICH Guideline (Q2A) (R1) Validation of analytical procedures: text and methodology IFPMA, Geneva, 2005.

26. ICH Guideline (Q1AR) Stability testing of new drug substances and products International Conference on harmonization IFPMA, Geneva, 2000.

27. McNally R. The United States Pharmacopoeia, 24th revision, Easton: Taunton; MA; 2000.

28. Swartz ME, Krull IS. Analytical Development and Validation; Marcel Dekker Inc.; New York; 1997.

29. Jedynak L, Puchalska M, Zezula M, Laszcz M, Luniewskib W, Zagrodzka J. Stability of sample solution as a crucial point during HPLC determination of chemical purity of temozolomide drug substance. J Pharm Biomed Anal. 2013;83:19-27.

30. Khalilian MH, Mirzaei S, Taherpour AA. The simulation of UV spectroscopy and electronic analysis of temozolomide and dacarbazine chemical decomposition to their metabolites. J Mol Model. 2016;22:270.

Turk J Pharm Sci 2018;15(3):278-290
DOI: 10.4274/tjps.59454

ORIGINAL ARTICLE

Formulation and Evaluation of Sintered Floating Tablets of Cefpodoxime Proxetil

Sefpodoksim Proksetilin Sinterlenmiş Yüzen Tabletlerinin Formülasyonu ve Değerlendirilmesi

Latha KUKATI*, Kishore CHITTIMALLI, Naseeb Basha SHAIK, Shailaja THOUDOJU

G. Pulla Reddy College of Pharmacy, Department of Pharmaceutics, Hyderabad, India

ABSTRACT

Objectives: To develop sintered floating tablets of CP using locust bean gum as a release-controlling material. CP is an orally- administered, extended-spectrum, semi-synthetic antibiotic of the cephalosporin class.

Materials and Methods: CP has a short elimination half-life, possesses high solubility, chemical, enzymatic stability and absorption profiles in acidic pH, which makes it a suitable candidate for formulation in a gastro-retentive dose form for improved bioavailability. Camphor was used to get the desired floating properties. The prepared CP floating tablets were subjected to sintering, where the cross linkage within the polymeric structure was increased by exposing the tablets to acetone vapors. The advantage with sintering is that prolonged drug release can be attained at low hardness and low concentrations of polymers.

Results: The prepared tablets were evaluated and found to have acceptable physicochemical properties. Formulation S2 containing locust bean gum: drug (0.3:1.0) and camphor (10% w/w), which was exposed to acetone vapors for a period of 6 hrs showed optimum floating properties and a better dissolution profile i.e. 97.3% in 12 hrs. Hence, formulation S2 was considered as the optimized formulation. The *in vitro* release data of the optimized formulation was treated with mathematical equations and the drug release followed zero-order kinetics (0.9599) with an anomalous transport mechanism (0.5331).

Conclusion: Based on the results, it can be concluded that sintered floating matrix tablets of CP containing locust bean provides a better choice for controlled release.

Key words: Cefpodoxime proxetil, controlled material, gastro-retentive floating tablets, sintering technique

ÖZ

Amaç: CP'nin, keçiboynuzu zamkını salım kontrol edici bir materyal olarak kullanımıyla sinterlenmiş yüzen tabletler geliştirmektir. CP, sefalosporin sınıfının oral yolla uygulanan genişletilmiş spektrumlu, yarı sentetik bir antibiyotiğidir.

Gereç ve Yöntemler: CP, kısa bir eliminasyon yarı ömrüne sahiptir, asidik pH'da yüksek çözünürlük, kimyasal, enzimatik stabilite ve absorpsiyon profillerine sahiptir, bu da, biyoyararlanımın iyileştirilmesi için midede kalan dozaj formuna uygun bir aday olmasını sağlar. İstenen yüzme özelliklerini elde etmek için kafur kullanıldı. Hazırlanan CP yüzen tabletler, sinterlemeye tabi tutuldu; burada polimerik yapı içindeki çapraz bağlantı, tabletleri aseton buharlarına maruz bırakarak arttırıldı. Sinterlemenin avantajı, uzun süreli etkin madde salımının düşük sertlikte ve düşük konsantrasyonlarda polimerlerle elde edilebilmesidir.

Bulgular: Hazırlanan tabletler değerlendirildi ve kabul edilebilir fizikokimyasal özelliklere sahip olduğu bulundu. Altı saat süre ile aseton buharlarına maruz bırakılan keçiboynuzu zamkı: etkin madde (0.3:1.0) ve kafur (%10 a/a) içeren formülasyon S2, optimum yüzme özellikleri ve 12 saatte %97.3 gibi daha iyi bir çözünme profili gösterdi. Bunun sonucu olarak formülasyon S2 optimize edilmiş formülasyon olarak kabul edildi. Optimize edilmiş formülasyonun *in vitro* salım verileri, matematiksel denklemlere uygulandı ve etkin madde salımı, anomalous transport mekanizması (0.991) ile sıfır derece kinetiğe (0.9599) uyum gösterdi.

Sonuç: Sonuçlara göre, sefpodoksim proksetilin keçiboynuzu içeren sinterlenmiş yüzen matriks tabletlerinin kontrollü salım için daha iyi bir seçenek sağladığı sonucuna varılabilir.

Anahtar kelimeler: Sefpodoksim proksetil, kontrollü materyal, midede kalan yüzen tabletler, sinterleme tekniği

*Correspondence: **E-mail:** lathakukatil@gmail.com, **Phone:** +9848630966 **ORCID-ID:** orcid.org/0000-0001-7785-2111
Received: 27.07.2017, **Accepted:** 28.09.2017

INTRODUCTION

Gastro-retentive systems swell and are retained in the stomach for a number of hours, while it continuously releases the drug at a controlled rate leading to higher bioavailability, therapeutic efficacy, reduced time intervals for drug administration, and thus improved patient compliance. Hence these gastro-retentive drug delivery systems (GRDDS) are advantageous for drugs absorbed mainly from the upper part of the gastrointestinal (GI) tract (GIT) because they have a narrow absorption window and are unstable in the medium of distal intestinal regions.[1] They are even beneficial in the local therapy of the stomach. Compounding drugs with narrow absorption windows in a GRDDS would enable an extended absorption phase of these drugs.[2] The retention of oral dose forms in the upper GIT causes prolonged contact time of drug with the GI mucosa.

Sintering techniques: Sintering is defined as "the bonding of adjacent particle surfaces in a mass of powder, or in a compact, by the application of heat or by exposing to solvents". The sintering process has been used for the fabrication of sustained-release (SR) matrix tablets for the stabilization and retardation of the drug release.

Sintering means fusion of particles or formulations of welded bonds between particles of a polymer. In other words, sintering increases the cross-linking between particles in the polymer. Sintering can be achieved by physical (thermal)[3] and chemical (solvent casting)[4,5] methods.

Physical method: It includes exposing the dose form to different temperatures, then polymer molecules rearrange at high temperature and result in increased cross- linking in the dose forms.

Thermal sintering: SR oral dose forms are exposed to temperatures above the glass transition point of the polymer, which melts or deforms min amounts of polymer on the surface. These molecules move on the polymer or move into the cross-linked structure of the polymer and become entangled in the three-dimensional structure of the polymer, thereby increasing the complexity, which results in decreased drug release by increased retardation hardness of the dose forms.

Chemical method: This includes exposing the dose form to solvent for different time periods. In this method, polymer molecules undergo partial solubilization in a given solvent and then reoriented to give denser forms with new cross-linking by forming bonds between the polymer molecules. Generally, the cross-linking solvents used are acetone, glutaraldehyde, and formaldehyde.

Solvent casting method: In this method, the prepared tablets are exposed to acetone vapors as a cross-linking agent. CP is available for oral dosing as an ester-prodrug, which keeps it stable and increases the oral absorption and is less likely to produce GI upset, palatability problems, and changes in intestinal flora prior to absorption. In present study, a CP floating drug delivery system was prepared using locust bean gum as a rate-retarding material. The prepared tablets were subjected to sintering using acetone as a cross-linking agent.

MATERIALS AND EXPERIMENTAL WORK

Materials

Cefpodoxime proxetil was received as a gift sample from Micro Labs Pvt. Ltd., Bangalore. Polyvinylpyrrolidone (PVP) K30 was obtained from Burgoyne Burbidges & Co., Mumbai. Magnesium stearate was purchased from SD fine chemicals, Mumbai. Locust bean gum was purchased from Himedia laboratories Pvt. Ltd., which contains galactomannans (plant reserve carbohydrates present in large quantities in the endosperm of the seeds of many leguminosae such as Ceratonia silique). Chemically, they consist of a (1-4)-linked β-D-mannose backbone with (1-6)-linked side chains of α-D-galactose,[6,7] thus being neutral polymers.[8] Citric acid anhydrous was purchased from Universal Laboratories, Mumbai. Camphor was purchased from Sigma-Aldrich Chemicals Pvt. Ltd., Mumbai, and all other chemicals, reagents, and solvents used were of analytical grade.

Experimental work

CP has good stability and solubility in acidic pHs. Tablets were prepared by wet granulation using locust bean gum as a retardant material.

Preformulation studies

Preformulation studies are performed for testing the physical and chemical properties of a drug substance alone and in combination with excipients.

Precompression parameters of powder blends and granules

Required quantities of all the ingredients were subjected to grinding then passed through a no. #60 sieve. The granules were prepared by blending powder with PVP K30 in iso propyl alcohol (IPA) as a granulating agent and the wet mass was screened using a no. #44 sieve, then dried at 40°C in a hot air oven. The powder blend and dried granules were tested for flow properties using the angle of repose, bulk density (BD), tapped density (TD), Carr's index, and Hausner's ratio.[9]

Angle of repose

Angle of repose is the angle between the surface pile of granules and a horizontal plane. A fixed amount of blend was taken and carefully poured through the funnel whose tip was fixed at a height of 2.5 cm above graph paper, which was placed on a horizontal surface. The blend of the powder was poured till the apex of the conical pile just touches the tip of the funnel. The angle of repose is calculated using the following formula.

$$\theta = \text{Tan}^{-1} (h/r) \quad (1)$$

Where, θ = angle of repose, r = radius of the pile, h = height of the pile

BD

BD is defined as the ratio mass of an untapped powder divided by the bulk volume (V) including the inter-particulate void spaces. Apparent BD was determined by pouring the blend into a graduated cylinder. The bulk V and weight of the powder (M) was determined. The BD was calculated using the following formula:

$$BD = M / V \quad (2)$$

TD

A measuring cylinder containing a known mass of blend was tapped for a fixed time (around 100 taps). The minimum volume (V_t) ccupied in the cylinder and the weight (M) of the blend was measured. The TD was calculated using the following formula:

$$TD = M / (V_t) \quad (3)$$

Carr's index

The compressibility index is an indirect measure of BD, size, shape, surface area, moisture content, and cohesiveness of powder. The correlation between compressibility index and powder flow properties is given in the following formula:

$$CI (\%) = TD - BD / TD \times 100 \quad (4)$$

Hausner's ratio

This is an indirect index of ease of powder flow and is measured by the ratio of TD to BD.

$$\text{Hausner's ratio} = TD / BD \quad (5)$$

Drug-excipient compatibility studies

Fourier-trasform infrared (FTIR)

The spectrum analysis of pure drug and physical mixture of drug and different excipients used for the preparation of tablets was studied using FTIR. FTIR spectra were recorded by preparing potassium bromide (KBr) discs using a Shimadzu Corporation (Koyto, Japan). KBr discs were prepared by mixing a few milligrams of sample with KBr and compressed at 10 tons pressure. The resultant disc was mounted in a suitable holder in an IR spectrophotometer and the spectrum was recorded from 4000 cm^{-1} to 500 cm^{-1}. The resultant spectrum was compared for any spectral changes. They were observed for the presence of characteristic peaks for the respective functional group in the compound.

Formulation of cefpodoxime proxetil floating tablets

Dose calculation

Cefpodoxime is available in proxetil salt form. Dose is calculated based on its $t_{1/2}$ and Vd.

$$K^0 r = \text{Rate in} = \text{Rate out} = Ke \times Cd \times V \quad (6)$$

Where $K^0 r$ is the zero-order rate constant for drug release (amount/time), Ke is the first-order rate constant of overall drug elimination (hr^{-1}), Cd is the desired drug level in the body (amount/V), and Vd is the V in which the drug is distributed.

$$K_e = 0.693 / t_{1/2} \quad (7)$$

The $t_{1/2}$ (elimination half-life) of CP is 2.4 hours, thus Ke = 0.693/2.4 = 0.288 hr^{-1}

Cd is 1.4 mg/L, and Vd is 32.3 L, then **$K^0 r = Ke \times Cd \times Vd$** = 0.288 x 1.4 x 32.3 = 13.05 mg/h.

$K^0 r$ was calculated as 13.05 mg/h, so the drug release constant should also have been equal to the elimination constant to maintain the steady-state condition.

Cefpodoxime only has 50% oral absorption in fasting conditions, whereas it is ~75% with food

$K^0 r = 13.05 \times 125/ 100 = 16.32$ mg/h

$$\text{Loading dose (DL)} = Di - K^0 r \, Tp \quad (8)$$

Time to reach the peak drug level (Tp) is 2.5 hours.

$$\text{Maintenance dose (Dm)} = K^0 r \, Td \quad (9)$$

$$\text{Total dose} = DL + Dm \quad (10)$$

Where Td is the total time desired for SR from 1 dose (i.e., 12 hours).

Hence, total dose = (100 – 16.32 x 2.5) + 16.32 x 12 = (100 – 40.8) + 195.28 = 255.04

Since 130 mg of cefpodoxime proxetil is equivalent to 100 mg of cefpodoxime.

= 255.04 x 1.3 = 331.55 mg. Hence the dose used was 330 mg/ tablet.

Preparation of tablets by wet granulation using a sublimating agent

The tablets were prepared through wet granulation using sublimating agent. All the ingredients, locust bean gum and drug were passed through a no. #60 sieve. Granules were prepared using 5% PVP in IPA as a binder solution and passed through a no. #44 sieve. Granules were dried at 40°C for 2 hrs and passed through a no. #30 sieve. Camphor was added according to the respective formula and lubricated with magnesium stearate. Formulations were prepared as given in Table 1 and the final blend was compressed into tablets on a 10-station rotary tablet machine using 11.9 punches. The prepared tablets were sublimated in a hot air oven at 60°C for 3 days. Tablets with a final weight equal to the theoretical weight after complete sublimation were selected for further experimentation (Figure 1).

Evaluation of cefpodoxime proxetil floating tablets

The prepared bilayer tablets were evaluated for various parameters such as weight variation, thickness, density, hardness, friability,[9] drug content, content uniformity, and *in vitro* dissolution studies.[10-12]

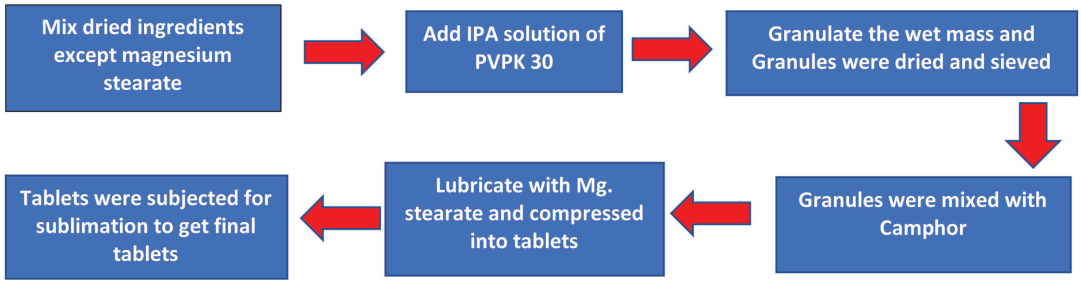

Figure 1. Preparation of cefpodoxime proxetil floating tablets by wet granulation using sublimating agent

Tablet thickness

The thickness in millimeters (mm) was measured individually for 10 pre-weighed tablets by Vernier calipers. The average thickness and standard deviation were reported.

Density of tablets

The density of the sublimated tablets (g/cm^3) was calculated both before and after sublimation from the tablet height, diameter, and mass using the following equation:

$$D = W / [(M/2)^2 \times \Pi \times h] \quad (11)$$

Where W is the mass of a tablet, M is the tablet diameter, Π is the circular constant, and h is the tablet height.

Tablet hardness

Tablet hardness was measured using a Monsanto hardness tester. The average crushing strength of the 5 tablets with known weight and thickness of each was reported.

Friability test

Ten tablets were accurately weighed and placed in the friability test apparatus (Roche friabilator), and rotated at 25 rpm for 4 mins. The tablets were taken, dedusted, and reweighed. The friability was calculated as the percentage weight loss using equation 12. Friability values below 1% are generally acceptable.

$$\% \text{ Friability} = (W_1 - W_2) \times 100 / W_1 \quad (12)$$

Where, W_1 = Initial weight of the tablets, W_2 = Final weight of the tablets.

Weight variation test

To study weight variation, individual weights (W_I) of 20 tablets from each formulation were noted using an electronic balance. Their average weight (W_A) and percentage weight variation was calculated using equation 13.

$$\% \text{ Weight variation} = (W_A - W_I) \times 100 / W_A \quad (13)$$

Drug content

Ten tablets were weighed and taken into a mortar and crushed into a fine powder. An accurately weighed portion of the powder equivalent to 100 mg of CP was transferred to a 100-mL volumetric flask containing methanol. It was shaken mechanically for 1 hr, then filtered using Whatman filter paper.[10] From this filtrate, 1 mL was taken, diluted to 10 mL with 0.1N HCl, and the absorbance was measured against a blank at 264.2 nm using an ultraviolet (UV)-spectrophotometer. The drug content of the floating tablets meets the requirements if the tablet amount lies within the range of 90% to 110%.

Buoyancy/floating test

Tablets were placed into a 100-mL beaker containing 0.1 N HCl and the time between the introduction and the tablet emerging on the surface of the medium is called the "floating lag time". The total duration of time during which the dose form remains buoyant is called the "total floating time (TFT)".

In vitro dissolution studies[10,12]

The tablet was placed in a dissolution test apparatus USP II, containing 900 mL of 0.1 N HCl at a speed of 50 rpm. A 5 mL aliquot was withdrawn every 1 hr up to 12 hrs and replaced with 5 mL of fresh dissolution medium. Each sample was analyzed at 264.2 nm using a double-beam UV spectrophotometer against a reagent blank.

Sintering

According to the compositions given in Table 1, tablets were prepared and subjected to sublimation, then these tablets were subjected to lower as well as higher polymeric concentrations prepared using low hardness and subjected to sintering process.

Procedure: The lower chamber of the dessicator was filled with acetone, closed, and kept aside for saturation. After saturation of the chamber, the compressed tablets were placed over a wire-mesh, which is kept above the lower chamber of the dessicator containing acetone. The dessicator is made airtight by closing the lid with the help of vacuum grease. Tablets of each formulation described in Table 2 were exposed to different durations of sintering (1.5, 3.0, 4.5, 6, 7.5, 9 and 10.5 hrs). Finally, the tablets were dried in an oven at 36°C for 24 hours and then stored in a vacuum desiccator fused with calcium chloride until further use.

Evaluation of sintered tablets

Sintered tablets were subjected to various evaluation tests including hardness, friability, buoyancy studies and *in vitro* dissolution studies. Buoyancy and dissolution studies were performed in 0.1 N HCl.

Kinetic analysis of dissolution data (model dependent method)

The dissolution profiles of optimized formula in 0.1 N HCl were fitted to zero-order, first-order, Higuchi and Korsemeyer-

Table 1. Formulation of floating tablets

Formulation code	Cefpodoxime proxetil (mg)	Locust bean gum (mg)	Camphor (mg)	Magnesium stearate (mg)	PVP (mg)
F1	330	115.5	22.27	5	23.6
F2	330	115.5	44.55	5	24.7
F3	330	115.5	66.82	5	25.8
F4	330	100	21.5	5	22.8
F5	330	100	43	5	25.6
F6	330	100	64.5	5	26.8

PVP: Polyvinylpyrrolidone

Peppas kinetic models. The model with the highest correlation coefficient was considered to be the best fitting one. By these studies the release mechanisms were determined.

Determination of surface morphology of prepared tablets using scanning electron microscopy (SEM)

The effect of the sublimation material (camphor) on the morphology of the prepared tablets was examined using SEM. The main objective of the study was to examine the surface of the prepared tablets during sublimation before and after sintering.

FTIR studies of sintered matrix tablets

FTIR studies were performed for the powdered tablets after sintering. The spectrum obtained was observed for the presence of characteristic peaks and compared with pure drug.

Determination of residual acetone using gas chromatography (GC)

Analytical instrument settings

GC was employed for the determination of acetone in the tablet. The GC used was an Aligent, Model 7890, GC equipped with a flame ionization detector (FID). The analysis was performed under the following chromatographic conditions: Column - WCOT Fused Silica, 30 x 0.32 x 1.8 µm. The temperature of the FID was 220˚C, and the injector temperature was 220˚C. The oven temperature was programmed to 40˚C (for 2 min), followed by an increase of 5˚C/min until 200˚C. The carrier gas was nitrogen with a flow of 1.5 mL/min. The injection of test and standard was performed using a 10-µL Hamilton syringe.

Optimized sintered tablets were crushed and taken to 1000-mL volumetric flask and the V was made up with deionized water. The flask was shaken and kept aside to obtain a clear supernatant. A fixed V of supernatant (0.5 µL) was injected into the chromatographic system and the amount of acetone in the tablets was calculated.

Determination of gastric retention period using X-ray imaging studies

Evaluation of gastric retention of CP sintered floating tablets was performed on rabbits using a radio opaque marker, barium sulfate. X-ray imaging studies are non-invasive method that provides identification or monitoring of total GI residence time without affecting normal gastrointestinal motility.

Dose translation was based on body surface area (BSA). The animal dose should not be extrapolated to a human equivalent dose (HED) based on body weight by simple conversion. The use of BSA normalization is suggested for more appropriate conversion of doses from humans to animals or vice versa. BSA correlates well with most mammalian species by several parameters of biology, including oxygen use, caloric expenditure, basal metabolism, blood V, circulating plasma proteins, and renal function.

The rabbit dose was calculated according to the following equation:

Animal dose (mg/kg)=HED x human Km value/animal Km value (14)

To convert dose in mg/kg=Dose in mg/m^2 x Km value.

Human (human adult of weight 60 kg) Km value 37, animal (rabbit weighing 1.8 kg) Km value 12.

Values based on data from the United Sates Food and Drug Administration draft guidelines.

Animal dose (mg/kg)=5.5 x 37/12 = 5.5 x 3.08=16.94 mg/kg.

Rabbit under study weighed 1.9 kg. So, 16.94 x 1.9=32.1 mg.

Hence the dose for *in vivo* studies taken was 32.1 mg. 25% of drug was replaced with barium sulfate i.e., so 8.025 mg per each tablet. The formulas for *in vivo* gastro retentive (GR) tablets are given in Table 3.

The tablets were prepared on 10-station rotary tablet machine using 4 mm punches. Prepared tablets were sublimated at 60˚C in a hot air oven for 3 days. The sublimated tablet was exposed to acetone for 6 hours for sintering. The tablets were then dried in the hot air oven at 36˚C for 24 hours and then stored in vacuum desiccators.

Table 3. Formula according to animal dose

S. No	Ingredient	Quantity taken (mg)
1	Cefpodoxime proxetil	24
2	Barium sulfate	8
3	Locust bean gum	7.2
4	Camphor	4
5	Magnesium stearate	0.5
6	PVP K30	2.18

PVP: Polyvinylpyrrolidone

Table 2. Formulation of sintered tablets containing camphor

Formulation code	Cefpodoxime proxetil (mg)	Locust bean gum (mg)	Camphor (mg)	Magnesium stearate (mg)	PVP (mg)
S1	330	82.5	41.2	5	22.9
S2	330	100	43	5	23.9
S3	330	115.5	44.5	5	24.75
S4	330	132	46.2	5	25.6

PVP: Polyvinylpyrrolidone

Healthy rabbits of 2.0±0.2 kg were fasted over night and in the following morning, tablet formulation S2, which was adjusted to a rabbit dose with tracing radio opaque agent, was administered through plastic tubing followed by flushing of 25-30 mL of water. During the entire study, the rabbits had free access to water alone. At different time intervals of 0, 1, 2, 4, 6 and 8 hours, the rabbit GI tract was photographed using X-rays in the supine position and observed for the nature and position of the CP floating tablet.

Determination of stability of tablets after sublimation using thin-layer chromatography (TLC)

The stability of CP, which can be determined by exposure to acetone vapors in a desiccator for 9 hours, was evaluated using TLC.

Procedure

Preparation of standard solution: An accurately weighed quantity of 10 mg of CP was transferred to a 10-mL volumetric flask an dissolved in methanol. The V was made up with the same solvent to obtain a concentration of 1 mg/mL.

Mobile phase

Water: Methanol 50:50 v/v composition.

Antimicrobial studies for sintered GR tablets

The microbial assay is based on a comparison of the inhibition of growth of bacteria by measured concentrations of the compound to be examined with that produced by known concentrations of standard preparation of the antibiotic with known activity.

The microbial assay may be conducted by two methods. Method A: Cylinder or cup-plate diffusion and Method B: Turbidimetric or tube assay.

In the present investigation, the cylinder or cup-plate technique was employed.

The following strains of bacteria were used for the study.

1. Gram-positive bacteria - *Bacillus subtilus*
2. Gram-negative bacteria - *Escherichia coli*

Preparation of standard antibiotic solution

The stock solution (1 mg/mL) of antibiotics was prepared by dissolving 10 mg of CP in a volumetric flask containing 10 mL dimethyl sulfoxide (DMSO). From stock solution, 2 mL was taken and further diluted to 10 mL with DMSO to get 10 mg/50 mL.

Preparation of test solutions: The formulation was crushed into powder. Powder weight equivalent to 10 mg of drug was dissolved in 10 mL of DMSO (the drug assay was performed for tablets and equivalent to10 mg was taken). From this solution, further dilutions were made using DMSO to obtain concentrations of 10 µg/50 µL, 5 µg/50 µL, 2.5 µg/50 µL, and 1.25 µg/50 µL.

Accelerated stability studies

Optimized formulation F2 was subjected to stability studies at 40°C±2°C/75%±5% RH and room temperature, and analyzed for its physical characteristics, drug content, and dissolution studies for a period of one month.

This study was approved by the IAEC (ID No: GPRCP / IAEC / 3 / PCE / AE - 3).

RESULTS AND DISCUSSION

Preformulation studies

Drug-excipients compatibility study by FTIR

CP compatibility with excipient was studied using FTIR (Figure 2, Table 4). FTIR results showed that the characteristic functional groups matched those reported in the literature.[13]

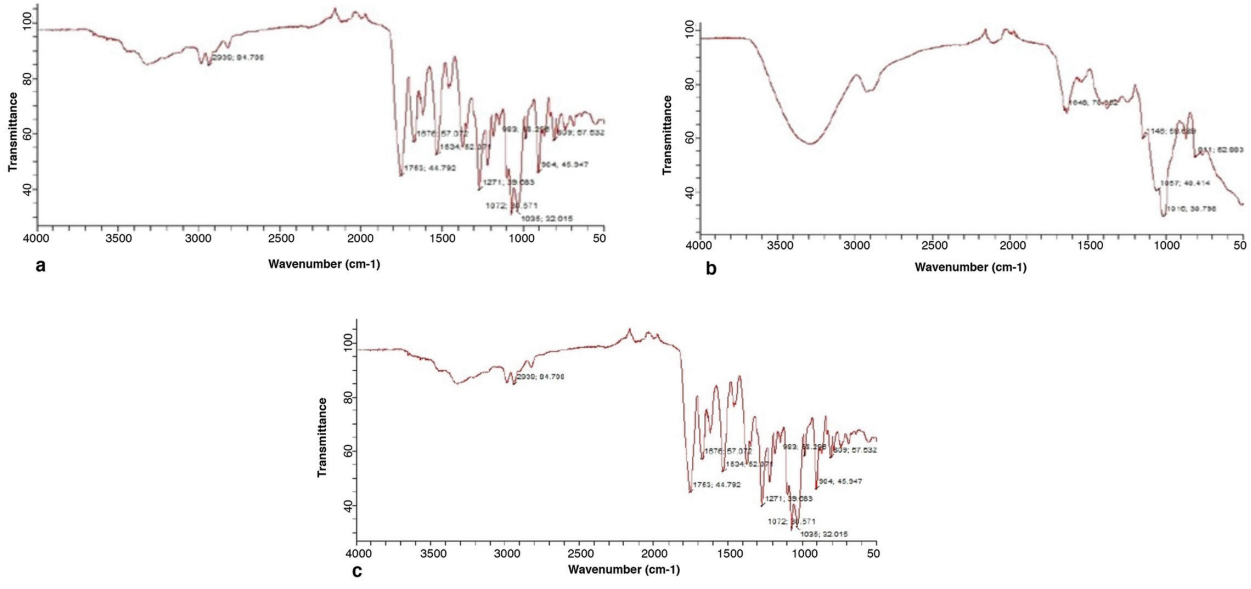

Figure 2. FTIR spectra of (a) cefpodoxime proxetil (b) locust bean gum and (c) physical mixture of cefpodoxime and locust bean gum

It was found that the drug and the other powder blends do not possess the required flow characteristics for direct compression because the angle of repose, Hausner's ratio, and Carr's compressibility index were not within flow property limits as shown in Table 5. Hence, tablets were prepared using the wet granulation method.

The flow property values of the granules of all formulations were found to possess good flow properties and were within the compendial limits of the Indian Pharmacopoeia;[8] the values are shown in Table 6.

Evaluation of CP floating tablets

Prepared floating tablets were evaluated for physiochemical properties.

The physicochemical evaluation of tablets such as weight variation test, friability, hardness, and content uniformity of all the formulations were within compendial standards. The values are as shown in Table 7.

Effect of sublimation of camphor on tablet properties

The floating properties of the GR tablets and effects of sublimation on thickness, density, and crush strength (hardness) are summarized in Table 8.

The crush strength of the tablets decreased after sublimation. As the camphor content in the tablet increased from 5% to 15% w/w, the crush strength of the GR tablet decreased, and the densities of the tablets also decreased.[14] When more than 40 mg of camphor was added to the GR tablet formulations, the density of the tablets was less than 1.00 g/cm^3. In all formulations, the thickness and porosity of tablets slightly increased after sublimation, which resulted in the tablets having a density less than 1 gm/cm^3. Thus, the tablets floated on the dissolution media due to air in the porous tablets without any lag time.[15]

Buoyancy/floating test

In the sublimation method, camphor was used at different concentrations and floating properties were studied (Table 9).

Table 4. Interpretation of cefpodoxime proxetil FTIR scan

S. No	Region in cm^{-1}	Type of vibration	Functional group present
1	3396.41, 3230.54	N-H stretching	Primary amine
2	1676	N-H bending	Aromatic primary amine
3	1274	C-N	Amine
4	3066.61	Aromatic C-H stretch	Aromatic
5	1638	C=N	--
6	809	C-S-C stretching	--
7	1753	C=O	Lactam

FTIR: Fourier-transform infrared

Table 5. Precompression parameters of the powder blends

Ingredients	Angle of repose (θ)	Hausner's ratio*	Carr's index (%)
Drug	53.3±0.54	1.40±0.09	29.67±0.2
Drug + locust bean gum	44.92±0.13	1.32±0.04	22.46±0.15
Drug + LG + camphor	50±0.49	1.46±0.02	24.1±0.17

Values are expressed as mean±SD, *n=3

Table 6. Precompression parameters of the granules

Formulation code	Angle of repose (θ)*	Bulk density (g/cm^3)*	Tapped density (g/cm^3)*	Hausner's ratio*	Carr's index (%)*
F1	26.76±0.76	0.310±0.013	0.392±0.01	1.23±0.09	16.84±0.14
F2	26.26±1.0	0.344±0.01	0.432±0.013	1.137±0.011	17.06±0.84
F3	26.34±0.82	0.361±0.01	0.346±0.012	1.228±0.010	19.39±0.78
F4	26.26±0.69	0.368±0.01	0.458±0.016	1.234±0.00	17.87±0.82
F5	27.54±0.81	0.346±0.01	0.428±0.00	1.226±0.04	20.19±0.34
F6	22.47±0.84	0.322±0.00	0.421±0.00	1.395±0.06	21.72±0.52

Values are expressed as mean±SD, *n=3

Camphor, upon sublimation, resulted in a slight increase in thickness and also increased porosity, which finally resulted in the tablets having density less than 1 gm/cm^3. Tablets so formed floated on dissolution media without any lag time.

Formulations containing 15% camphor showed floating properties with no lag time, but cracks developed in the tablets after 9 to 10 hours, as a result chipping was observed on tablet surface. Hence, formulations F2 and F5 were found to have optimum floating properties (Figure 3).

The formulations with a lag time of less than 30 mins and TFT of greater 12 hours were selected and subjected to dissolution studies for optimization.

Figure 3. Floating ability (without lag time) of cefpodoxime proxetil tablets containing camphor

In vitro drug dissolution testing of floating tablets

Based on the floating study results, formulations F2 and F5 were selected and subjected to dissolution studies for further optimization.

Among the different formulations subjected to dissolution studies, formulation F2 (containing a 0.35 ratio of locust bean gum with respect to drug and camphor 10%) showed a comparatively better dissolution profile of 95.8% for 12 hours (Figure 4). Based on the results of floating studies (no lag time) and dissolution studies, formulation F2 was selected and subjected to sintering.[16]

Effect of camphor concentration on in vitro release of CP

Different formulations from F1 to F6 were studies with increased amounts of camphor, which led to the decreased density of the resultant GR tablets after sublimation.

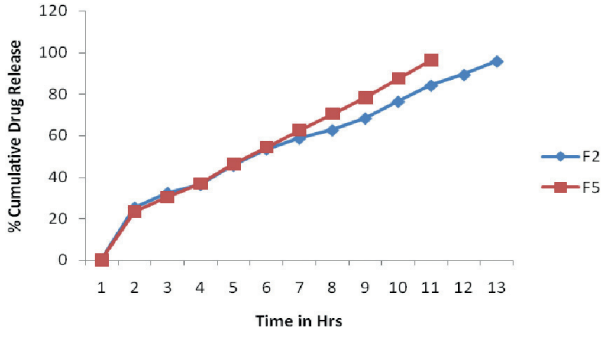

Figure 4. Dissolution profiles of formulations F2 and F5

Table 7. Physiochemical evaluations of tablets containing camphor

Formulation code	Drug content (%)[a]	Weight variation (%)[b]	Friability[a]
F1	96.4±0.20	3.03±0.30	0.62±0.01
F2	97.1±0.23	4.02±0.60	0.55±0.06
F3	96.8±0.64	4.1±0.30	0.71±0.01
F4	99.4±0.77	3.9±0.50	0.77±0.01
F5	95.3±0.40	3.7±0.22	0.71±0.04
F6	97.6±0.96	2.8±0.70	0.69±0.02

Values are expressed as mean±SD, [a]: n=10, [b]: n=20

Table 8. Comparison of physical parameters before and after sublimation

Formulation code	Before sublimation			After sublimation		
	Thickness (mm)[a]	Density (g/cm^3)[a]	Hardness (kg/cm^2)[a]	Thickness (mm)[a]	Density (g/cm^3)[a]	Hardness (kg/cm^2)[a]
F1	4.6±0.01	1.10±0.00	7.1±0.01	4.8±0.00	1.02±0.01	6.2±0.01
F2	4.8±0.00	1.03±0.01	6.9±0.35	5.1±0.67	0.873±0.00	6.1±0.00
F3	5.0±0.08	1.08±0.01	7.3±0.28	5.3±0.00	0.84±0.06	5.8±0.30
F4	4.5±0.12	1.12±0.03	7.1±0.01	4.7±0.01	1.01±0.21	6.0±0.30
F5	4.7±0.80	1.03±0.22	7.0±0.00	5.1±0.16	0.84±0.01	6.1±0.01
F6	4.9±0.07	1.05±0.21	7.2±0.01	5.3±0.18	0.82±0.09	5.7±0.45

Values are expressed as mean±SD, [a]: n=5

Drug release kinetics: Model-dependent method

The release kinetics for the different formulations was calculated using Microsoft Office Excel, 2007. The release data were analyzed by fitting the drug release profiles of all the formulations into zero-order release, first-order release, Higuchi and Korsmeyer-Peppas models.

From the results of model-dependent kinetic analyses of the dissolution profiles of the formulations F2 and F5, it was found that the release of drug from these formulations followed zero-order kinetics and the mechanism of release was found to be anomalous transport from r^2 and n values, as shown in Table 10.

Sintering technique

The prepared floating tablets were exposed to acetone vapors for sintering. Based on the results in the floating test and *in vitro* dissolution studies, formulation F2 (0.35 ratio polymer to drug) was found to be better when compared with the other formulation. Hence, the 0.35 ratio was selected.

Drug retardation was increased with long exposure times to acetone vapors in formulation S1. This may be due to the cross-linking of polymer as well as the process of sintering. After further exposure to acetone i.e., for 9 hours and 10.5 hours, there was no significant difference in drug release due to saturation of the cross-linking on the tablet surface.

From the dissolution studies of formulations S1 to S3 (Figure 5, 6, and 7), it can be concluded that S2 had better sustained drug release (97.3%, in 12 hours) on exposure to acetone for 6 hours; therefore, it was selected as the optimized formulation.

Table 9. Floating lag time and floating time of formulation containing camphor

Formulation code	Floating lag time	Floating time (hrs)
F1	Not floating	-
F2	Floating with no lag time	>12
F3	Floating with no lag time	<10
F4	Not floating	-
F5	Floating with no lag time	>12
F6	Floating with no lag time	<10

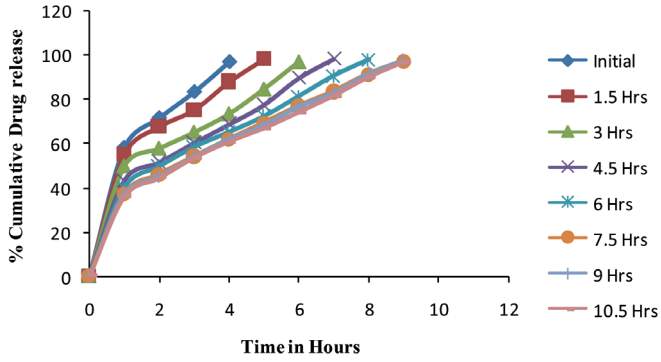

Figure 5. Dissolution profiles of formulation S1

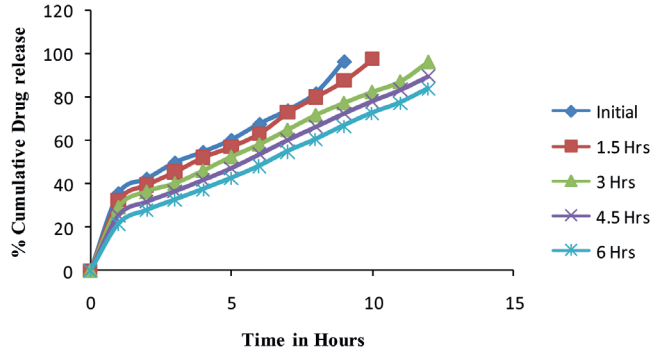

Figure 6. Dissolution profiles of formulation S2

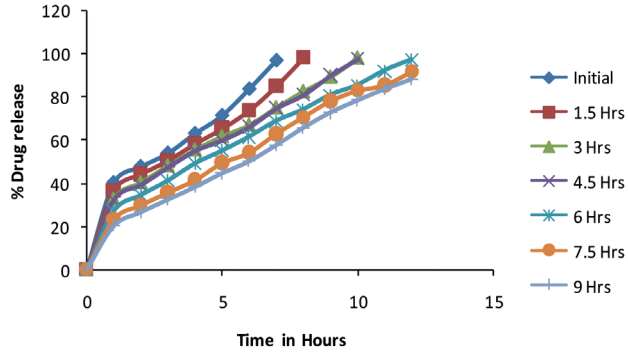

Figure 7. The dissolution profiles of formulation S3

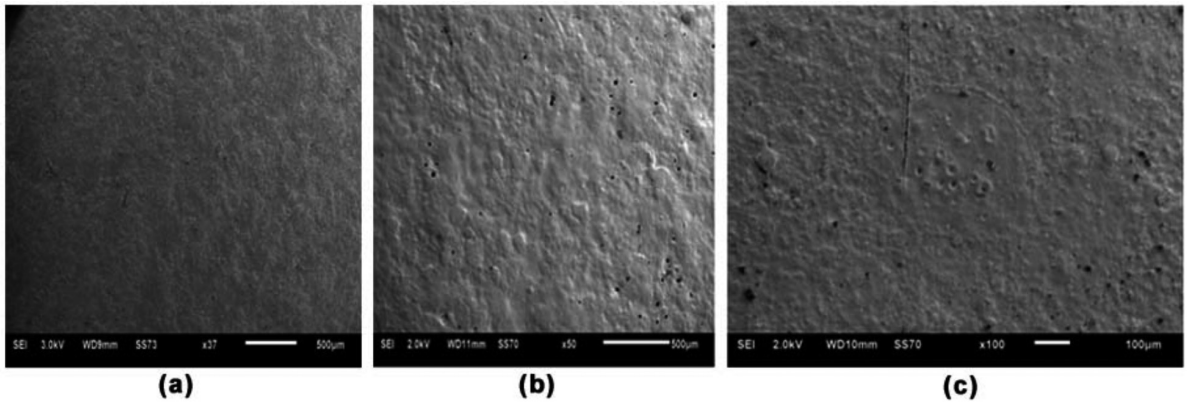

Figure 8. Surface morphology of the tablet (a) before sublimation (b) after sublimation (c) after sintering

The optimized S2 formulation was physically evaluated for hardness and friability before and after sintering (Tables 11, 12).

SEM

Figure 8a, 8b shows the morphology of S2 before and after sublimation, respectively, as viewed under SEM,[13] Figure 8c shows the morphology of S2 after sintering.

The morphology of the tablet composites after sublimation is highly porous, which affects the density and floating properties of tablets. It was observed that the pore cavity on the tablets and also porosity (to some extent) was reduced after sintering. The reason attributed to the decrease in porosity was the redistribution of polymer during sintering. The polymer undergoes partial solubility in acetone vapors, which results in the redistribution of polymer molecules on the tablet surface and also into the pores formed due to sublimation.

FTIR studies

The prepared tablets were subjected to FTIR studies both after sublimation and after sintering to conform the drug stability in final formulation (Figure 9).

From the results of FTIR, it was found that the functional peaks of the drug were retained after being subjected to sublimation and sintering. This implies that the drug was stable and also compatible with other excipients throughout the process.

Determination of residual camphor and acetone using GC

GC was employed to estimate the amount of residual acetone in the optimized tablets. The retention time of acetone was found as 9 mins and 30 seconds. The regression equation for the standard curve constructed by taking known concentrations (µg/mL) of acetone was found as y=1605x-177.

The chromatogram of acetone (known concentration i.e., 10 µg/mL) is shown in Figure 10, non-sintered tablets (not exposed

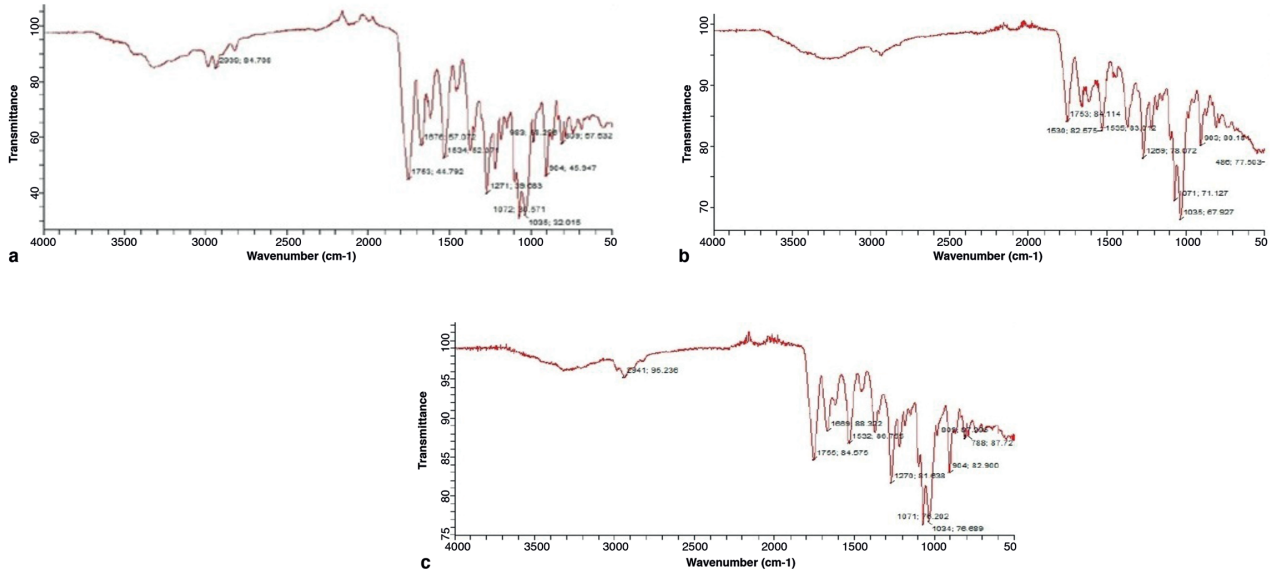

Figure 9. FTIR spectra of (a) pure cefpodoxime proxetil (b) after sublimation (c) after sintering

Table 10. Model-dependent kinetic analysis for the dissolution profile of different formulation

Formulation	Zero- order	First- order	Higuchi	Korsmeyer-Peppas		Release mechanism
	R^2	R^2	R^2	R^2	n	
F2	0.9842	0.8396	0.9628	0.9748	0.6348	Anomalous transport
F5	0.9691	0.8766	0.9783	0.9744	0.5549	Anomalous transport

Table 11. Comparison of different physical parameters before and after sublimation

Formulation	Drug content[a]	Before sintering			After sintering		
		Thickness (mm)[a]	Density (g/cm^3)[a]	Hardness (kg/cm^2)[a]	Thickness (mm)[a]	Density (g/cm^3)[a]	Hardness (kg/cm^2)[a]
S1	97.2±0.7	4.6±0.01	1.02±0.01	5.7±0.01	4.9±0.46	0.85±0.01	4.9±0.07
S2	96.4±0.6	4.7±0.00	1.03±0.66	5.7±0.00	5.1±0.01	0.83±0.01	5.0±0.50
S3	97.1±0.6	4.8±0.24	1.03±0.07	5.8±0.58	5.1±0.09	0.84±0.05	5.1±0.11

Values are expressed as mean±SD, [a]: n=5

to acetone vapors) in Figure 11, and the optimized tablet (tablet exposed to 6 hours of acetone) in Figure 12.

Based on results of GC, the residual concentration of acetone in the optimized tablet was found to be within the limits of generally recognized as safe (Table 13). It can be concluded that the tablets prepared by chemical sintering using acetone are safe and this method can be used as alternate technique in the preparation of matrix tablets.

In vivo buoyancy study

An in vivo buoyancy study was performed on a healthy rabbit. The animal dose was calculated using dose translation based on BSA. Figure 13 depicts the position and nature of the tablets at different time intervals after oral administration.

From the obtained results, it was observed that the floating tablets formulated with CP and locust bean gum remained in the gastric region even after 8 hours of administration, indicating good retention of the tablets in the stomach region.[17,18]

TLC

TLC was performed to check the stability of CP when exposed to acetone vapors, by comparing the R_f values of test with pure or standard CP.

From the TLC, no colored spot other than the principal spot of CP was observed in the chromatogram, which also showed a similar Rf value to that of the standard (0.67) (Figure 14). This indicated that CP did not degrade even after exposure to acetone vapors.

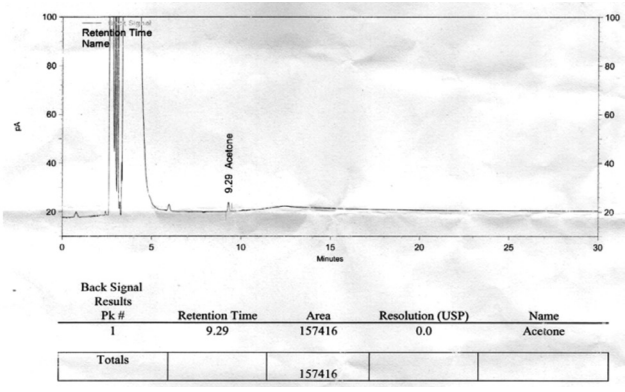

Figure 10. Chromatogram showing peak area for standard acetone concentration (10 µg/mL)

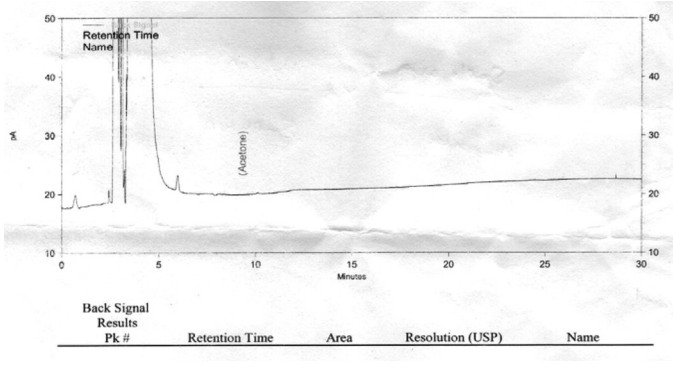

Figure 11. Chromatogram of unsintered tablets

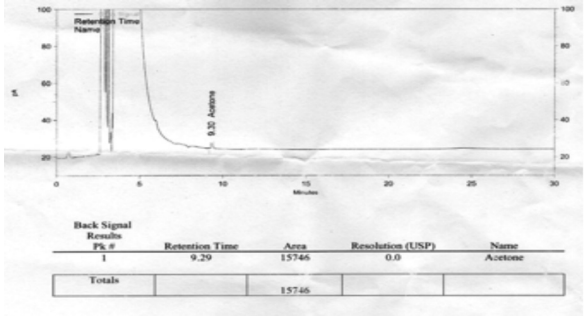

Figure 12. Chromatogram of sintered tablets i.e. 6-hour exposure to acetone vapors

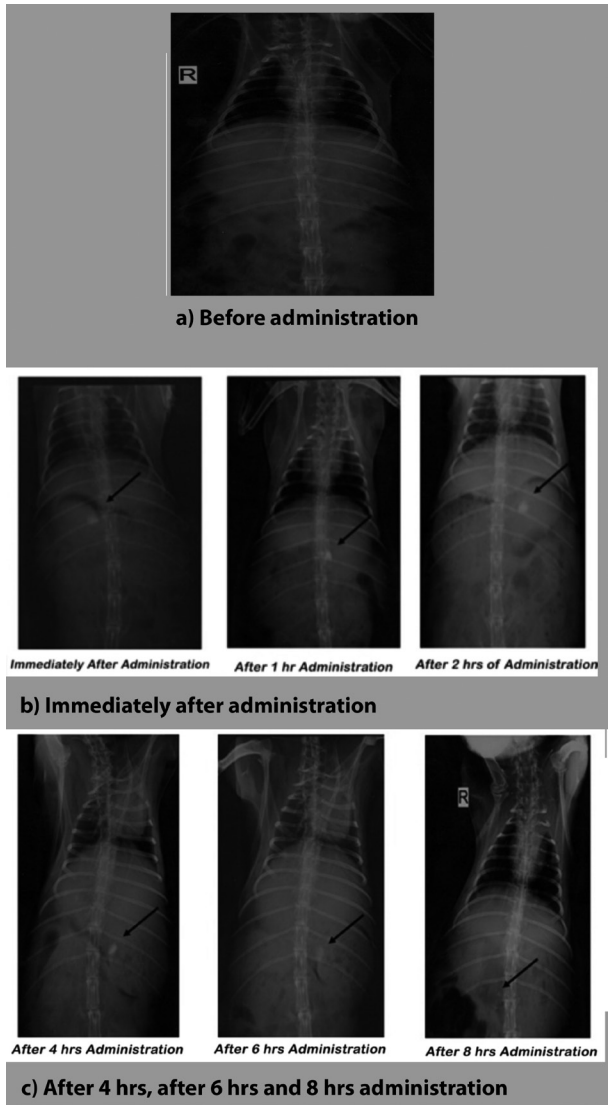

Figure 13. a,b,c) X-rays of GIT of rabbit at different time intervals after administration of floating tablet

Anti-microbial studies

The anti-microbial activity of the final formulation tested. Zone of inhibition studies were performed using the test drug solution and a standard (pure) antibiotic solution. Figure 15 shows the zone of inhibition of the test and standard solutions and the diameter of the zones obtained. The zone diameters are reported in Table 14.

From the microbiologic studies, similar zones of inhibition were shown for both pure drug as well as sintered matrix tablets. Therefore, it can be concluded that CP in the final formulation retained its antibacterial activity.

Stability studies

The optimized formulation was subjected to stability studies and the results are given in Table 15 and in Figure 16.

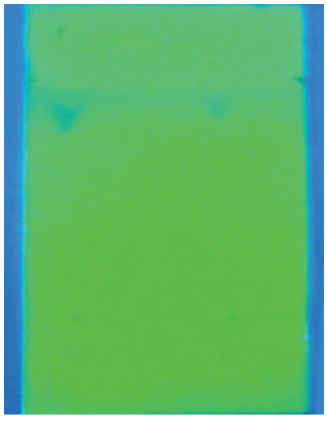

Figure 14. Chromatogram showing pure drug spot and test drug spot

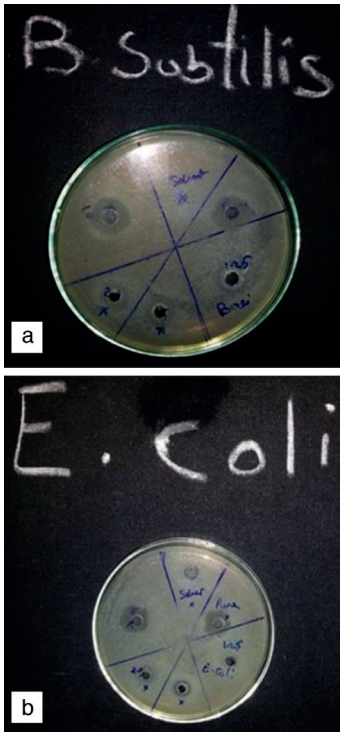

Figure 15. Composition of zone of inhibition between test and standard antibiotic solutions on (a) *Bacillus subtilis* (b) *Escherichia coli*

During the accelerated stability studies, optimized tablets were stable with insignificant changes in floating lag time, floating time, drug content, and *in vitro* drug release characteristics.

CONCLUSIONS

In conclusion, formulation S2, which was prepared using locust bean gum as a rate control polymer at the ratio of 0.3:1.0 (locust bean gum:drug), showed better floating properties <14 min and dissolution profile with 95.0% for 12 hrs compared to other formulations such as S1 and S3. Formulation S2 can be considered as the final optimized formulation for a sintered, floating gastro-retentive matrix tablet of CP to increase gastric residence time and thereby improve its bioavailability.

Table 12. Comparative physical evaluation of optimized formulation S2 both before and after sintering

Parameters	Before sintering	After sintering
Hardness (kg/cm^2)[a]	5.0±0.02	6.4±0.23
Friability[a]	0.7%±0.01	0.5%±0.22

Values are expressed as mean±SD, [a]: n=5

Table 13. Different concentrations of acetone with its corresponding peak area

Preparations	Peak area	Concentration (µg/mL)
Standard acetone solution	157416	10
Optimized formulation	15746	0.9

Table 14. Comparison of zones of inhibition between test and standard antibiotic solutions

Antibiotic solution	*Escherichia coli*	*Bacillus subtilis*
Standard antibiotic solution (10 µg/ 50 µL)	16	17
Test antibiotic solutions (10 µg/ 50 µL)	15	18
Test antibiotic solutions (5 µg/ 50 µL)	10	11

Note: Values of zone of inhibition in mm, diameter of bore: 8 mm, zone of inhibition is average of duplicate

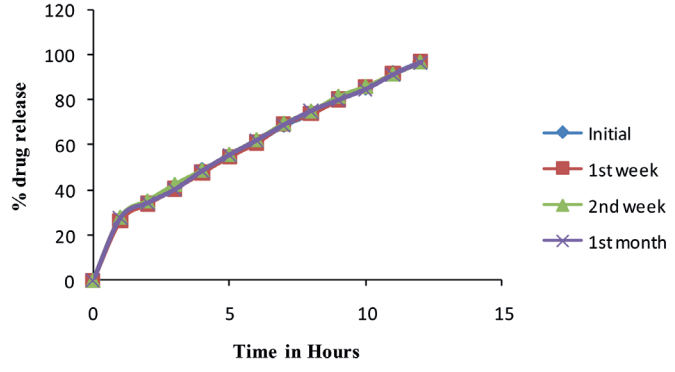

Figure 16. Percentage drug release of optimized formulation during accelerated stability studies

Table 15. Physicochemical properties of optimized formulation during stability studies

Parameters	Time in weeks			
	0 (initial)	1st week	2nd week	1st month
Floating lag time	No lag time	No lag time	No lag time	No lag time
Floating time	>12 hours	>12 hours	>12 hours	>12 hours
Drug content[a] (%)	98.3±0.38	97.6±0.69	96.5±1.06	97.5±0.73
Thickness (mm)[a]	5.1±0.01	5.1±0.01	5.0±0.01	5.1±0.01
Density (g/cm^3)[a]	0.83±0.01	0.829±0.01	0.83±0.01	0.83±0.01
Hardness (kg/cm^2)[a]	5.0±0.50	5.1±0.50	5.0±0.50	5.0±0.50

Values are expressed as mean±SD, [a]: n=5

Conflict of Interest: No conflict of interest was declared by the authors.

REFERENCES

1. Chavanpatil M, Jain P, Chaudhari S, Shear R, Vavia P. Development of sustained release gastroretentive drug delivery system for ofloxacin: *In vitro* and *in vivo* evaluation. Int J Pharm. 2005;304:178-184.
2. Uhumwhangho MU, Ramana Murty KV. Release characteristics of diltiazem hydrochloride wax-matrix granules-Thermal sintering effect. J App Sci Environ Manage. 2011;15:365-370.
3. Sameer shafi, Chowdary KA, Nagoba S, Sachin A. Formulation and evaluation of sintered matrix tablets of diltiazem hydrochloride. Int J App Sci. 2011;3:16-19.
4. Srinivas RB, Prasanna RY, Srinivas L, Seshasayana A. Design and evaluation of Eudragit RL100 sintered matrix tablets. Indian J Pharm Sci. 2012;66:202-207.
5. Laurienzo P. Marine polysaccharides in pharmaceutical applications: An overview. Mar Drugs. 2010;8:2435-2465.
6. Rinaudo M. Main properties and current applications of some polysaccharides as biomaterials. Polym Int. 2008;57:397-430.
7. Beneke C, Viljoen AM, Hamman JH. Polymeric plant-derived excipients in drug delivery. Molecules. 2009;14:2602-2620.
8. Indian Pharmacopeia published by Indian Pharmacopeia Commission. Ghaziabad; 2010;2:751-754.
9. Siddalinga Swamy MS, Kumar Shety AS, Anil Kumar SM. UV-visible spectrophotometric methods for the estimation of cefpodoxime proxetil in bulk drug and pharmaceutical dosage form. International Journal of Pharm Tech Research. 2012;4:750-756.
10. Rao KS, Vairagkar RR, Udgirkar DB, Patil PS, Biradar KV. Gastro-Retentive Floating Matrix Tablets of Cefpodoxime Proxetil. J App Pharm Sci. 2011;1:190-194
11. United States Pharmacopeia 24 and National Formulary 19 by United States Pharmacopeial convention, INC. 2000;2:1941-1945.
12. Alonso-Sande M, Teijeiro-Osorio D, Remuñán-López C, Alonso MJ. Glucomannan, a promising polysaccharide for biopharmaceutical purposes. Eur J Pharm Biopharm. 2009;72:453-462.
13. Khan F, Kataram R, Ramteke S. Enhancement of bioavailability of cefpodoxime proxetil using different polymeric microparticles; AAPS PharmSciTech. 2010;11:1368-1375.
14. Ishak RA. Buoyancy-generating agents for stomach-specific drug delivery: An overview with special emphasis on floating behavior. J Pharm Pharm Sci. 2015;18:77-100.
15. Oh TO, Kim JY, Ha JM, Chi SC, Rhee YS, Park CW, Park ES. Preparation of highly porous gastroretentive metformin tablets using a sublimation method. Eur J Pharm Biopharm. 2013;83:460-467.
16. Rao BS, Seshasayana A, Himasankar K, Raju YP, Murthy KR. Design and evaluation of ethylene vinyl acetate sintered matrix tablets. Ind J Pharm Sci. 2003;65:496-502.
17. Patil SH, Talele GS. Formulation development and *in vitro* and *in vivo* evaluation of gastroretentive floating drug delivery system of Lafutidine. Asian Journal of Pharmaceutics. 2013;7:68-74.
18. Gnanaprakash K, Shekhar KBc, Chetty CMS. Floating tablets of Ranitidine HCl with natural polymer: An approach for gastric treatment. Int J Pharm Health Sci. 2010;1:109-115.

Turk J Pharm Sci 2018;15(3):291-297
DOI: 10.4274/tjps.55707

ORIGINAL ARTICLE

Antimicrobial Activities of New Indole Derivatives Containing 1,2,4-Triazole, 1,3,4-Thiadiazole and Carbothioamide

1,2,4-Triazol, 1,3,4-Tiyadiazol ve Karbotiyoamit İçeren Yeni İndol Türevlerinin Antimikrobiyal Aktiviteleri

Hanif SHIRINZADEH[1]*, Sibel SÜZEN[2], Nurten ALTANLAR[3], Andrew D. WESTWELL[4]

[1]Erzincan University, Faculty of Pharmacy, Department of Pharmaceutical Chemistry, Erzincan, Turkey
[2]Ankara University, Faculty of Pharmacy, Department of Pharmaceutical Chemistry, Ankara, Turkey
[3]Ankara University, Faculty of Pharmacy, Department of Pharmaceutical Microbiology, Ankara, Turkey
[4]Cardiff University, Faculty of Pharmacy, Department of Pharmaceutical Chemistry, Cardiff, United Kingdom

ABSTRACT

Objectives: In new antimicrobial drug development studies, indole and its derivatives create an important class of compounds. In addition, azoles and their derivatives were recognized to be associated with a variety of biologic activities such as antibacterial and antifungal. In this study antimicrobial activities of some indole derivatives mainly substituted with 1,2,4-triazole, 1,3,4-thiadiazole and hydrazinecarbothioamide were investigated to evaluate their efficacy.

Materials and Methods: The efficacy of new compounds was evaluated using 2-fold serial dilutions against *Staphylococcus aureus*, MRSA, *Escherichia coli, Bacillus subtilis, Candida albicans*, and *Candida krusei*.

Results: The MIC was determined for test compounds and for the reference standards sultamicillin, ampicillin, fluconazole, and ciprofloxacin.

Conclusion: The compounds possessed a broad spectrum of activity having MIC values of 3.125-50 µg/mL against the tested microorganisms. This study provides valuable evidence that the indole-triazole derivative compound 3d holds significant promise as a novel antibacterial and antifungal lead compound.

Key words: Indole, 1, 2, 4-triazole, 1, 3, 4-thiadiazole, MRSA, *C. krusei*

ÖZ

Amaç: Yeni antibakteriyel ilaç geliştirilme çalışmalarında indol ve türevleri önemli bir bileşik sınıfı oluşturmaktadır. Ayrıca azoller ve türevlerinin antibakteriyel ve antifungal gibi biyolojik aktivite gösterdikleri dikkat çekmektedir. Bu çalışmada 1,2,4-triazol, 1,3,4-tiyadiazol ve hidrazinkarbotiyoamid ile sübstitüe edilmiş indol türevi yeni bileşiklerin, antimikrobiyal etkinlikleri araştırılarak değerlendirilmiştir.

Gereç ve Yöntemler: Yeni bileşiklerin antimikrobiyal etkinlikleri, 2-kat seri dilüsyon yöntemi kullanılarak, *Staphylococcus aureus*, MRSA, *Escherichia coli, Bacillus subtilis, Candida albicans* ve *Candida krusei*'ye karşı araştırılarak değerlendirilmiştir.

Bulgular: Yeni sentezlenen bileşiklerin MİK, sultamisilin, ampisilin, flukonazol ve siprofloksasin gibi standart referans bileşiklere karşı belirlenmiştir.

Sonuç: Bileşikler test edilen mikroorganizmalara karşı 3.125-50 µg/mL gibi geniş spektrum aralığında MİK değerleri göstermişlerdir. Bu çalışmada değerli veriler elde edilmiş ve indol-triazol türevi olan 3d bileşiği antibakteriyel ve antifungal lider bileşik olarak ileri çalışmalar için gelecek vaad etmektedir.

Anahtar kelimeler: İndol, 1, 2, 4-triazol, 1, 3, 4-tiyadiazol, MRSA, *C. krusei*

***Correspondence: E-mail:** hanif.shirinzade@gmail.com, **Phone:** +904462245344 **ORCID-ID:** orcid.org/0000-0001-9663-9199
Received: 03.08.2017, **Accepted:** 19.10.2017

INTRODUCTION

Antimicrobial resistance is often used as a definition for drug resistance, which occurs when microorganisms such as bacteria, viruses, fungi, and parasites withstand a drug that was intended to cure the infection.[1,2] Multidrug-resistant strains of Methicillin-resistant *Staphylococcus aureus* (MRSA) cause some serious infections such as pneumonia, endocarditis, and skin and soft tissue infections within intensive care units.[3,4] Recent studies confirmed that indole derivatives have promising antimicrobial activity against various microorganisms including MRSA.[5] Studies showed that one of the main contributors to *Staphylococcus aureus* antibiotic resistance is the *NorA* efflux pump.[6,7] *NorA* is able to export a variety of structurally unrelated drugs, such as fluoroquinolones, ethidium bromide, cetrimide, benzalkonium chloride, tetraphenylphosphonium bromide, and acriflavine.[8] Indoles are one of the reported classes of *NorA* inhibitors,[9] for example, 5-nitro-2-phenylindole, which characterizes a promising lead structure able to produce a 4-fold increase in *S. aureus* susceptibility to ciprofloxacin.[10] Tert-butyl (2-(3-hydroxyureido)-2-(1H-indol-3-yl)ethyl) carbamate, which is not toxic to human cells, was also found to be an active indolic *NorA* inhibitor.[11]

Azole-containing compounds such as fluconazole, ketoconazole, and itraconazole are the most widely used antifungal agents in the clinic.[12,13] Despite all the claims, many studies have demonstrated the ineffectiveness of fluconazole against *Candida krusei*,[14,15] which has been recognized as a potentially multidrug-resistant fungal pathogen.[16] Consequently, it is essential to develop new active compounds against fungal pathogens including *C. krusei*. Multidrug-resistant infection strains are diseases of emerging healthcare concern and have demanded the attention of researchers. Synthesis and antifungal activity of indole-linked triazole derivatives[17] showed that almost all indole derivatives showed excellent antifungal activities against *Candida albicans* and *C. krusei* with low minimum inhibitory concentration (MIC) values.[18] Antimicrobial activity studies of some 1,2,4-triazole and 1,3,4-thiadiazole derivatives indicated good antimicrobial activity.[19,20] In addition, it is well known that imidazoles and triazoles (azoles) make up the largest group of agents against mycosis infections.[21] Indole derivatives were found to be particularly effective and suitable for further developments in antimicrobial drug development studies.[22]

This study is part of an ongoing project in the search for novel antimicrobial drug candidates, especially against MRSA and *C. krusei.* New indole derivatives substituted with triazole, thiadiazole, and carbothioamide were tested against *S. aureus*, MRSA, *Escherichia coli*, *Bacillus subtilis*, *C. albicans* and *C. krusei* using the 2-fold serial dilution technique. The MIC was determined for the test compounds and for the reference standards sultamicillin, ampicillin, fluconazole, and ciprofloxacin.

MATERIALS AND METHODS

Chemistry

The synthesis and spectroscopic characterization of 31 indole derivatives (Table 1) were published in our earlier study.[23] The reaction of indole 3-acetylhydrazine with isothiocyanates in ethanol under reflux gave the corresponding hydrazinecarbothioamides (**1a-h**). Treatment of **1a-h** under acidic conditions with full region chemical control gives the corresponding 2-aminothiadiazoles (**2a-h**). Conversely, treatment of **1a-h** under basic conditions (aq. NaOH) with heating produced 3-thiotriazoles (**3a-h**). Triazoles (**3a-h**) could be further alkylated under basic conditions to yield substituted triazoles (**4a-g)**.

Microbiology

Antibacterial and antifungal activity tests were conducted against standard strains. The American Type Culture Collection (ATCC) strains of the microorganisms used in this study were obtained from the culture collection of the Refik Saydam Health Institution of Health Ministry, Ankara, and maintained at the Microbiology Department of the Faculty of Pharmacy of Ankara University. Mueller-Hinton broth (MHB) (Difco), Mueller-Hinton agar (MHA) (Oxoid), Sabouraud Dextrose agar (SDA) (Difco), and Sabouraud Dextrose broth (SDB) (Difco), were used for growing and diluting the microorganism suspensions. The following reference strains were used for testing antimicrobial activity: Gram-positive bacteria: *S. aureus* ATCC 25923, *MRSA* ATCC 43300, *B. subtilis* ATCC 6633. Gram-negative bacteria: *E. coli* ATCC 25922, Yeast: *C. albicans* ATCC 10231 and *C. krusei ATCC 6258.*

Antibacterial and antifungal activity assay

The bacterial strains were maintained on MHA medium for 24 h at 37°C and fungi were maintained on SDA for 48 h at 25°C. Overnight cultures were prepared by inoculating approximately 2 mL MHB with 2-3 colonies of each organism taken from MHA. Inocula were prepared by diluting overnight cultures into 0.9% sterile saline solution until the visible turbidity was equal to 0.5 Mcfarland standard having approximately 10^8 CFU/mL for bacteria and 10^7 CFU/mL for yeasts. The tube dilution technique was used for the determination of the MICs.[24,25] Indole derivatives were investigated to evaluate their efficacy against multi-drug-resistant microbial infections by using the 2-fold serial dilution technique against *S. aureus*, MRSA*, E. coli, B. subtilis*, *C. albicans* and *C. krusei*.

The synthesized compounds and standards were dissolved in 12.5% DMSO at concentrations of 200 µg/mL. Further dilutions of the compounds and standard drugs in the test medium were prepared at the following quantities of 400, 200, 100, 50, 25, 12.5, 6.25, 3.12, 1.56 and 0.78 µg/mL concentrations with MHB and SDB. A set of tubes containing only inoculated broth was used as controls.

After incubation for 24 h at 37°C for the antibacterial assay and for 48 h at 25°C for the antifungal assay, the last tube with no growth of microorganism and/or yeast was recorded to represent the MIC (expressed in µg/mL). The MIC was determined for test compounds and for the reference standards sultamicillin, ampicillin, fluconazole, and ciprofloxacin. Every experiment in the antibacterial and antifungal assays was performed in duplicate.

There was no need for ethics committee approval because the study was conducted *in vitro*.

Table 1. Chemical structures of new indole-based MLT analogues

	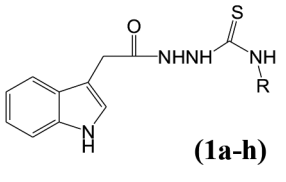 (1a-h)		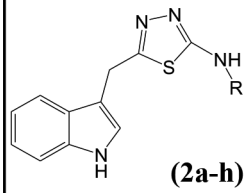 (2a-h)		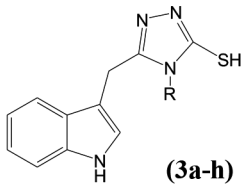 (3a-h)		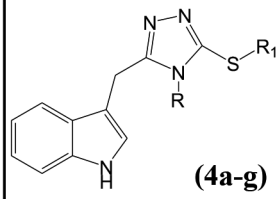 (4a-g)	
	R		R		R		R	R_1
1a	CH_3-CH_2-	**2a**	CH_3-CH_2-	**3a**	CH_3-CH_2-	**4a**	CH_3-CH_2-	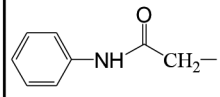
1b	CH_3-CH_2-CH_2-	**2b**	CH_3-CH_2-CH_2-	**3b**	CH_3-CH_2-CH_2-	**4b**	CH_3-CH_2-CH_2-	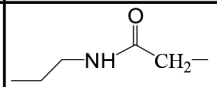
1c	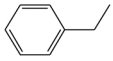	**2c**	H	**3c**	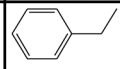	**4c**	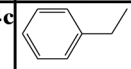	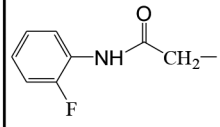
1d	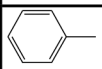	**2d**	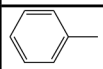	**3d**	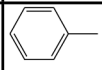	**4d**	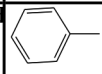	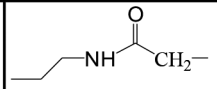
1e	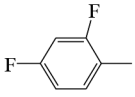	**2e**	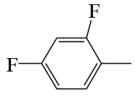	**3e**	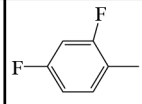	**4e**	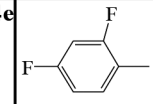	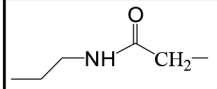
1f	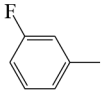	**2f**	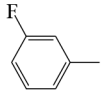	**3f**	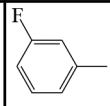	**4f**	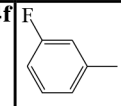	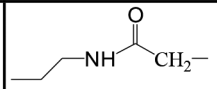
1g	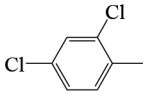	**2g**	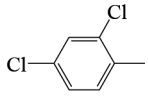	**3g**	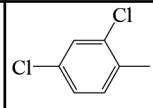	**4g**	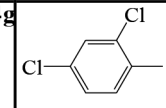	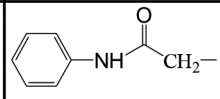
1h	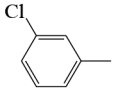	**2h**	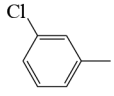	**3h**	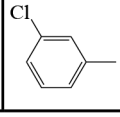			

MLT: Melatonin

RESULTS AND DISCUSSION

Antimicrobial activity was investigated by finding the MICs of the indole derivatives against *S. aureus*, MRSA, *E. coli*, *B. subtilis*, *C. albicans* and *C. krusei* strains and comparing with ampicillin, sultamicillin, ciproflaxacin and fluconazole as standard drugs. The MIC values of the compounds and standard drugs are given in Table 2. The MIC values were within the range of 3.125-50 µg/mL. Most of the compounds showed significant antibacterial activity against *S. aureus*, MRSA, *E. coli*, and *B. subtilis*. In addition, the compounds demonstrated a good level of antifungal activity, particularly against *C. krusei*, even more effective than the standard drug fluconazole.

The antibacterial activity of all tested compounds demonstrated acceptable antibacterial effects. Compounds 1c, 1h, 3h, and 4c showed moderate activity against *S. aureus* compared with ampicillin, sultamicillin, ciprofloxacin; the most effective compounds were 2h (indole-thiadiazole) and 3d (indole-triazole) with an MIC value of 6.25 µg/mL (Figure 1a).

Figure 1b shows the antibacterial effects of the tested compounds against MRSA strains. The activities of compounds

Table 2. MIC values (μg/mL) of tested indole derivatives

1a-h	*S. aureus*	MRSA	*E. coli*	*B. subtilis*	*C. albicans*	*C. krusei*	2a-h	*S. aureus*	MRSA	*E. coli*	*B. subtilis*	*C. albicans*	*C. krusei*
1a	25	25	25	50	6.25	3.125	2a	25	25	25	25	6.25	3.125
1b	25	12.5	25	25	3.125	3.125	2b	25	6.25	25	25	3.125	3.125
1c	12.5	25	25	25	12.5	6.25	2c	25	3.125	25	3.125	3.125	3.125
1d	25	6.25	25	25	6.25	3.125	2d	25	25	25	25	3.125	3.125
1e	50	50	25	25	6.25	6.25	2e	50	50	25	25	6.25	6.25
1f	50	12.5	25	50	25	12.5	2f	25	25	25	25	12.5	12.5
1g	25	25	25	25	12.5	12.5	2g	50	25	25	25	12.5	12.5
1h	12.5	6.25	25	25	12.5	6.25	2h	6.25	6.25	50	6.25	12.5	6.25
3a-h	***S. aureus***	**MRSA**	***E. coli***	***B. subtilis***	***C. albicans***	***C. krusei***	**4a-g**	***S. aureus***	**MRSA**	***E. coli***	***B. subtilis***	***C. albicans***	***C. krusei***
3a	50	25	25	25	12.5	3.125	4a	25	25	25	12.5	12.5	3.125
3b	25	12.5	25	25	3.125	3.125	4b	50	50	25	50	12.5	6.25
3c	25	50	25	3.125	3.125	3.125	4c	12.5	25	25	25	12.5	6.25
3d	6.25	3.125	50	25	3.125	3.125	4d	50	50	25	50	12.5	3.125
3e	50	25	25	25	6.25	3.125	4e	50	50	25	50	6.25	3.125
3f	25	25	25	25	12.5	12.5	4f	50	50	25	50	12.5	3.125
3g	25	12.5	25	50	6.25	3.125	4g	25	25	25	25	12.5	3.125
3h	12.5	6.25	25	12.5	6.25	3.125	-	-	-	-	-	-	-

Reference standards	***S. aureus***	**MRSA**	***E. coli***	***B. subtilis***	***C. albicans***	***C. krusei***
Sultamicillin	0.39	25	25	0.78	-	-
Ampicillin	0.78	50	50	50	-	-
Fluconazole	-	-	-	-	1.56	64
Ciprofloxacin	0.78	6.25	0.19	0.09	-	-

1d, 1h, 2b, 2h, and 3h were found to be at the same level as ciprofloxacin, and compounds 2c (indole-thiadiazole) and 3d (indole-triazole) demonstrated excellent activity against MRSA, being more effective than ciprofloxacin. The other tested compounds were found to have the same activity value or were more active than ampicillin and sultamicillin.

None of the tested indole derivatives were more active than ciprofloxacin, which has an MIC value of 0.09 μg/mL against *E. coli*. However, most of the synthesized compounds demonstrated the same or lower MIC values compared with ampicillin and sultamicillin (Figure 2a). Finally, the effects of the tested indole derivatives against *B. subtilis* strains (Figure 2b) showed that the most effective compounds were 2c (indole-thiadiazole) and 3c (indole-triazole) with an MIC value of 3.125 μg/mL. Although the tested compounds were not as active as ciprofloxacin and sultamicillin, they were much more active than ampicillin.

The MIC values of the tested indole derivatives indicated that nearly all them showed excellent antifungal activities against *C. krusei* and moderate activities against *C. albicans* compared with the standard drug fluconazole. Figure 3a shows the MIC values of the indole compounds against *C. albicans* compared with fluconazole. The most effective compounds were 1b, 2b-d, and 3b-d, with MIC values of 3.125 μg/mL. Although the activity results against *C. albicans* were not very satisfactory, the results of antifungal activity against *C. krusei* strains were quite promising. All the tested compounds were found several times more effective than fluconazole. As seen in Figure 3b, most of the effective compounds 1a, 1b, 1d/2a-d/3a-d, 3h, and 4a, 4d-g

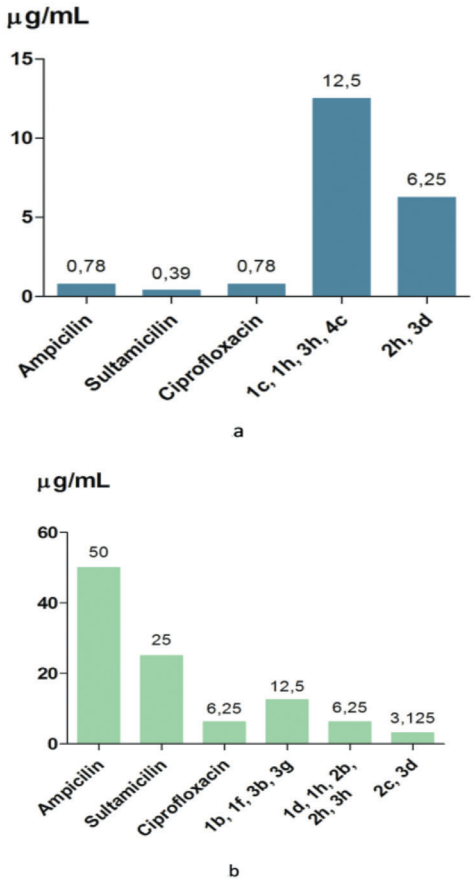

Figure 1. a) The MIC value of synthesized compounds against *S. aureus* compared with ampicillin, sultamicillin, ciprofloxacin. b) The MIC value of synthesized compounds against MRSA compared with ampicillin, sultamicillin, and ciprofloxacin

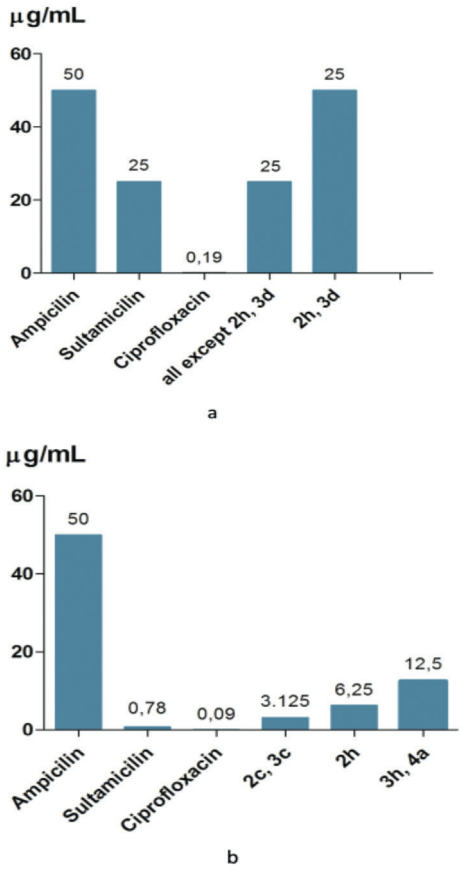

Figure 2. a) The MIC value of synthesized compounds against *E. coli* compared with ampicillin, sultamicillin, ciprofloxacin. b) The MIC value of synthesized compounds against *B. subtilis* compared with ampicillin, sultamicillin, ciprofloxacin

had MIC values of 3.125 µg/mL, whereas fluconazole has an MIC value of 64 µg/mL. The results were in accordance with those found by Na, 2010.[17] The most potent antifungal activity against *C. krusei* was obtained with halogenated indole derivatives.

CONCLUSIONS

According to the activity results, all of synthesized compounds demonstrated significant antibacterial and antifungal effects, and the antifungal effects of compounds 3a-h are promising for development into new, more effective lead compounds against *C. krusei*. Roughly 17% of *Candida* isolates exhibit resistance against azoles, and most probably, the extensive use of fluconazole is the main reason for this resistance. *C. krusei* is one of the species that shows actual resistance to fluconazole.[16,26] Therefore, the search for new and more effective anti-fungal agents against *C. krusei* seems ever more important.[27] Azole compounds prevent the synthesis of ergosterol by inhibiting the cytochrome P-450-dependent enzyme lanosterol 14α-demethylase. Triazoles have a broad range of applications in the treatment of fungal infections because of their good affinity for fungal cytochrome P-450 enzymes.[28] It is reasonable to assume that the synthesized indole-triazole derivatives (3a-h, 4a-g) have the same mechanism of action.

Compounds 2c (indole-thiadiazole) and 3d (indole-triazole) demonstrated excellent activity against MRSA at a much higher level than ciprofloxacin. It was observed that compounds 1h, 2h and 3h had MIC values of 6.25 µg/mL, which is the same as for ciprofloxacin. All these compounds have a *m*-chlorophenyl group as a substituent. This shows that both the indole ring and the side chains are important for activity. Singh stated that chloro substituents for triazolylindole derivatives were beneficial as well as hydroxy and methoxy substitution for activity.[29]

Most of the tested indole derivatives were found to be highly active against *C. krusei*. Between the tested indoles, the most active compounds were found in the indole-triazole group, followed by the indole-thiadiazole group. These results suggest that the tested indole derivatives are eligible for development as candidates, especially compound 3d, which is a promising lead compound mainly against MRSA and *C. krusei*. However, further research needs to be performed to determine the specific mode of action and approve indole derivatives as antimicrobial agents.

The common use of antifungal molecules combined with insufficient treatment are responsible for promoting these microorganisms' resistance to drugs used in treatment. The antibacterial and antifungal activity results were thought to

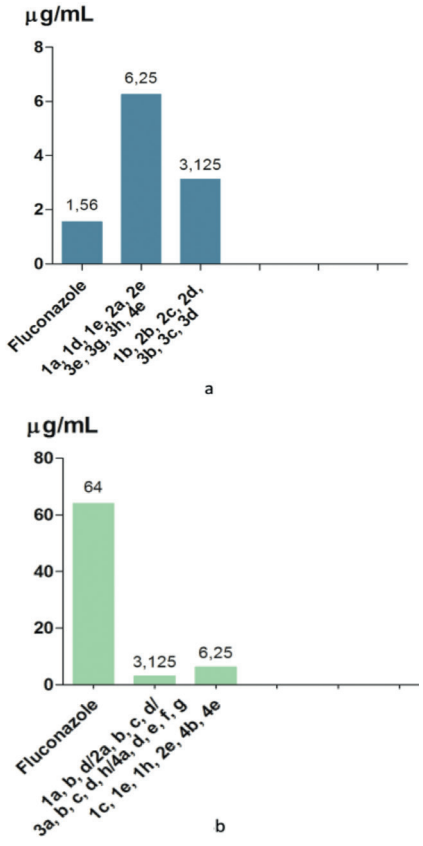

Figure 3. a) The MIC value of synthesized compounds against *C. albicans* compared with fluconazole. b) The MIC value of synthesized compounds against *C. krusei* compared with fluconazole

be exerted through a target because the introduction of the substituent groups on the indole caused differences in the activity. Therefore, modifications of these compounds should continue to be investigated.

ACKNOWLEDGEMENTS

The chemical synthesis part of this work was supported by the Scientific and Technological Research Council of Turkey (TUBİTAK) Research and Development Grant 112S599.

Conflict of Interest: No conflict of interest was declared by the authors.

REFERENCES

1. Cerniglia CE, Pineiro SA, Kotarski SF. An update discussion on the current assessment of the safety of veterinary antimicrobial drug residues in food with regard to their impact on the human intestinal microbiome. Drug Test Anal. 2016;8:539-548.
2. Hahn AW, Jain R, Spach DH. New Approaches to antibiotic use and review of recently approved antimicrobial agents. Med Clin North Am. 2016;100:911-926.
3. Liu C, Bayer A, Cosgrove SE, Daum RS, Fridkin SK, Gorwitz RJ, Kaplan SL, Karchmer AW, Levine DP, Murray BE, J Rybak M, Talan DA, Chambers HF. Clinical practice guidelines by the infectious diseases society of America for the treatment of methicillin-resistant *Staphylococcus aureus* infections in adults and children. Clin Infect Dis. 2011;52:18-55.
4. Kaku N, Morinaga Y, Takeda K, Kosai K, Uno N, Hasegawa H, Miyazaki T, Izumikawa K, Mukae H, Yanagihara K. Antimicrobial and immunomodulatory effects of tedizolid against methicillin-resistant *Staphylococcus aureus* in a murine model of hematogenous pulmonary infection. Int J Med Microbiol. 2016;306:421-428.
5. Al-Qawasmeh RA, Huesca M, Nedunuri V, Peralta R, Wright J, Lee Y, Young A. Potent antimicrobial activity of 3-(4,5-diaryl-1H-imidazol-2-yl)-1H-indole derivatives against methicillin-resistant *Staphylococcus aureus*. Bioorg Med Chem Lett. 2010;20:3518-3520.
6. Lepri S, Buonerba F, Goracci L, Velilla I, Ruzziconi R, Schindler BD, Seo SM, Kaatz, GW, Cruciani G. Indole based weapons to fight antibiotic resistance: a structure-activity relationship study. J Med Chem. 2016;59:867-891.
7. Costa SS, Viveiros M, Amaral L, Couto I. Multidrug Efflux Pumps in *Staphylococcus aureus*: an Update. Open Microbiol J. 2013;7:59-71.
8. Deng X, Sun F, Ji Q, Liang H, Missiakas D, Lan L, He C. Expression of multidrug resistance efflux pump gene NorA is iron responsive in *Staphylococcus aureus*. J Bacteriol. 2012;194:1753-1762.
9. Markham PN, Westhaus E, Klyachko K, Johnson ME, Neyfakh AA. Multiple novel inhibitors of the NorA multidrug transporter of *Staphylococcus aureus*. Antimicrob Agents Chemother. 1999;43:2404-2408.
10. Ambrus JI, Kelso MJ, Bremner JB, Ball AR, Casadei G, Lewis K. Structure-activity relationships of 2-aryl-1h-indole inhibitors of the nora efflux pump in *Staphylococcus aureus*. Bioorg Med Chem Lett. 2008;18:4294-4297.
11. Hequet A, Burchak ON, Jeanty M, Guinchard X, Le Pihive E, Maigre L, Bouhours P, Schneider D, Maurin M, Paris JM, Denis JN, Jolivalt C. 1-(1H-Indol-3-yl)ethanamine derivatives as potent *Staphylococcus aureus* NorA efflux pump Inhibitors. Chem Med Chem. 2014;9:1534-1545.
12. Fridkin SK, Jarvis WR. Epidemiology of nosocomial fungal infections. Clin Microbiol Rev. 1996;9:499-511.
13. Che X, Sheng C, Wang W, Cao Y, Xu Y, Ji H, Dong G, Miao Z, Yao J, Zhang W. New azoles with potent antifungal activity: design, synthesis and molecular docking. Eur J Med Chem. 2009;44:4218-4226.
14. Samaranayake YH, Samaranayake LP. *Candida krusei*: biology, epidemiology, pathogenicity and clinical manifestations of an emerging pathogen. J Med Microbiol. 1994;41:295-310.
15. Deorukhkar SC, Saini S. Echinocandin susceptibility profile of fluconazole resistant *Candida* species isolated from blood stream infections. Infect Disord Drug Targets. 2016;16:63-68.
16. Pfaller MA, Diekema DJ, Gibbs DL, Newell VA, Nagy E, Dobiasova S, Rinaldi M, Barton R, Veselov A. Global Antifungal Surveillance Group. *Candida krusei*, a Multidrug-Resistant Opportunistic Fungal Pathogen: Geographic and Temporal Trends from the ARTEMIS DISK Antifungal Surveillance Program, 2001 to 2005. J Clin Microbiol. 2008;46:515-521.
17. Na YM. Synthesis and activity of novel indole linked triazole derivatives as antifungal agents. Bull Korean Chem Soc. 2010;31:3467-3470.
18. Ryu CK, Lee JY, Park RE, Ma MY, Nho JH. Synthesis and antifungal activity of 1H-indole-4,7-diones. Bioorg Med Chem Lett. 2007;17:127-131.
19. Chen H, Li Z, Han Y. Synthesis and fungicidal activity against rhizoctoniasolani of 2-alkyl (alkylthio)-5-pyrazolyl-1,3,4-oxadiazoles (thiadiazoles). J Agric Food Chem. 2000;48:5312-5315.

20. Ahmed S, Zayed MF, El-Messery SM, Al-Agamy MH, Abdel-Rahman HM. Design, synthesis, antimicrobial evaluation and molecular modeling study of 1,2,4-Triazole-based 4-Thiazolidinones. Molecules. 2016:21.

21. Odds FC, Brown AJ, Gow NA. Antifungal agents: mechanisms of action. Trends Microbiol. 2003;11:272-279.

22. Varvaresou A, Tsantili-Kakoulidou A, Siatra-Papastaikoudi T, Tiligada E. Synthesis and biological evaluation of indole containing derivatives of thiosemicarbazide and their cyclic 1,2,4-triazole and 1,3,4- thiadiazole analogs. Arzneimittelforschung. 2000;50:48-54.

23. Shirinzadeh H, Ince E, Westwell AD, Gurer-Orhan H, Suzen S. Novel indole-based melatonin analogues substituted with triazole, thiadiazole and carbothioamides: studies on their antioxidant, chemopreventive and cytotoxic activities. J Enzyme Inhib Med Chem. 2016;31:1312-1321.

24. Clinical and Laboratory Institute. Methods for dilution antimicrobial susceptibility tests for bacteria that grow aerobically, Approved Standard. in: CLSI Publication M07-A10, Twelfth ed. CLSI; Wayne, PA, USA; 2009.

25. Clinical and Laboratory Standards Institute (CLSI), Reference method for broth dilution antifungal susceptbility testing of yeasts; Approved Standart. Third ed. CLSI document M27-A3. Wayne, PA, USA; 2008.

26. Kanafani ZA, Perfect JR. Antimicrobial resistance: to antifungal agents: mechanisms and clinical impact. Clin Infect Dis. 2008;46:120-128.

27. Gill K, Kumar S, Xess I, Dey S. Novel synthetic anti-fungal tripeptide effective against *Candida krusei*. Indian J Med Microbiol. 2015;33:110-116.

28. Asami T, Mizutani M, Shimada Y, Goda H, Kitahata N, Sekimata K, Han SY, Fujioka S, Takatsuto S, Sakata K, Yoshida S. Triadimefon, a fungicidal triazole-type P450 inhibitor, induces brassinosteroid deficiency-like phenotypes in plants and binds to DWF4 protein in the brassinosteroid biosynthesis pathway. Biochem J. 2003;369:71-76.

29. Singh I. Synthesis and evaluation of some newly triazolylindole derivatives for antifungal activity. Int Res J Pharm. 2014;5:891-895.

Turk J Pharm Sci 2018;15(3):298-303
DOI: 10.4274/tjps.38258

ORIGINAL ARTICLE

Simultaneous Determination of Arbutin and Hydroquinone in Different Herbal Slimming Products Using Gas Chromatography-mass Spectrometry

Arbutin ve Hidrokinonun Farklı Bitkisel Zayıflama Ürünlerinde Gaz Kromatografisi-Kütle Spektrometresi ile Eşzamanlı Belirlenmesi

Benan DURSUNOĞLU[1], Hafize YUCA[1], Zühal GÜVENALP[1]*, Sefa GÖZCÜ[2], Bilal YILMAZ[3]

[1]Atatürk University, Faculty of Pharmacy, Department of Pharmacognosy, Erzurum, Turkey
[2]Erzincan University, Faculty of Pharmacy, Department of Pharmacognosy, Erzincan, Turkey
[3]Atatürk University, Faculty of Pharmacy, Department of Analytical Chemistry, Erzurum, Turkey

ABSTRACT

Objectives: The aim of our study was to develop a simple, precise, sensitive and specific method for the simultaneous determination of arbutin and hydroquinone in different herbal slimming products using GC-MS.

Materials and Methods: The methanol and aqueous extracts of nine herbal slimming products in Turkey were evaluated for analysis of arbutin and hydroquinone using GC-MS method.

Results: The retention times of arbutin and hydroquinone were found as 11.32 and 5.44 min, respectively. The linear ranges in this method were 5-500 ng/mL for arbutin and hydroquinone, respectively. The intra- and inter-day precisions, expressed as the relative standard deviation, were less than 1.94 and 2.73%, determined from quality control samples for arbutin and hydroquinone, and accuracy was within 1.13 and 2.56% in terms of relative error, respectively. The limit of detection and quantification were 0.555 and 1.665 ng/mL for arbutin, and 0.031 and 0.093 ng/mL for hydroquinone, respectively.

Conclusion: The developed method can be used for routine quality control analysis of arbutin and hydroquinone in different herbal slimming products.

Key words: Arbutin, hydroquinone, GC-MS, herbal slimming products, *Calluna vulgaris*

ÖZ

Amaç: Bu çalışmanın amacı, farklı bitkisel zayıflama ürünlerinde arbutin ve hidrokinonun GC-MS yöntemiyle, eşzamanlı olarak belirlenmesi için basit, hassas ve spesifik bir yöntem geliştirmektir.

Gereç ve Yöntemler: Türkiye'de bulunan dokuz bitkisel zayıflama ürününün sulu ve metanolik ekstreleri, arbutin ve hidrokinon analizi için GC-MS yöntemi ile değerlendirilmiştir.

Bulgular: Arbutin ve hidrokinon için alıkonma zamanları sırasıyla 11.32 ve 5.44 dakika olarak bulunmuştur. Geliştirilen yöntemin doğrusallık aralığı arbutin ve hidrokinon için 5-500 ng/mL'dir. Kalite kontrol numunelerinden belirlenen ve bağıl standart sapma olarak ifade edilen gün-içi ve günler-arası kesinlik, arbutin ve hidrokinon için sırasıyla %1.94 ve %2.73'ten düşüktür. Bağıl hataya göre doğruluk değerleri arbutin ve hidrokinon için sırasıyla %1.13 ve %2.56 arasındadır. Gözlenebilme ve miktar tayin sınırı arbutin için sırasıyla 0.555 ve 1.665 ng/mL, hidrokinon için 0.031 ve 0.093 ng/mL'dir.

Sonuç: Geliştirilen yöntem, farklı bitkisel zayıflama ürünlerinde arbutin ve hidrokinonun rutin kalite kontrol analizleri için kullanılabilir.

Anahtar kelimeler: Arbutin, hidrokinon, GC-MS, bitkisel zayıflama ürünleri, *Calluna vulgaris*

*Correspondence: E-mail: guvenalp@atauni.edu.tr, Phone: +90 505 521 20 43 ORCID-ID: orcid.org/0000-0002-8803-8147
Received: 09.08.2017, Accepted: 02.11.2017

INTRODUCTION

Arbutin (4-hydroxyphenyl-β-D-glucopyranoside) is a phenolic glucoside that is found mainly in the Ericaceae and Saxifragaceae families.[1] It is an inhibitor of tyrosinase, which is the essential enzyme for melanin formation. Melanin is important for the protection of skin from harmful ultraviolet (UV)-A and UVB radiation. Arbutin is disinfectant in genitourinary diseases and has anti-inflammatory, antioxidant, and antitumor effects. It is used in urinary therapeutics, skin-whitening, and depigmenting cosmetics.[1-3]

Hydroquinone is 1,4-dihydroxybenzene and a metabolite of arbutin.[4] It has antibacterial, astringent, disinfectant, and antioxidant effects. It is used for the treatment of hyperpigmentation and is a component of topical pharmaceutical agents.[1,5]

Calluna vulgaris (C. vulgaris) (L.) Hull (heather) is a perennial shrub that is a member of the Ericaceae family. It is distributed throughout most of Europe, Russia, Asia Minor, and the Atlantic coast of North America.[6,7] Secondary metabolites of *C. vulgaris* are flavonoids, tannins, proanthocyanidins, caffeic acid derivatives, phenols, triterpenes, steroids and hydroquinone glycosides (arbutin). The infusion of aerial parts of *C. vulgaris* is traditionally used in Turkey as a urinary tract disenfectant, diuretic, and antidiaretic.[8] *C. vulgaris* has diuretic, antimicrobial, antirheumatic, antioxidant, antibacterial, and monoamine oxidase-A inhibitory effects[7,9-11] and is presented in herbal slimming teas due to its diuretic and digestive effects.

Obesity is a serious disease that can be due to genetic and environmental reasons, defined as abnormal or excessive fat accumulation that may impair health by the World Health Organization. In addition to the various synthetic medicines used in obesity treatment, there is an increasing trend towards herbal products in this field.[12] The effectiveness of herbal slimming products and their adherence to standards is a matter of debate. Thus, the quality control analysis of these products is important for public health. Arbutin and hydroquinone are among the effective components in herbal slimming products containing *C. vulgaris*.

Several analytical methods have been reported for the determination of arbutin and/or hydroquinone including high-performance liquid chromatography (HPLC), gas chromatography-mass spectrometry (GC-MS), capillary zone electrophoresis, and densitometry.[5,13-22]

However, no method has been used to quantify the presence of arbutin and hydroquinone simultaneously from different herbal slimming products. Therefore, analytical methods for their separation and simultaneous quantification are required for quality control purpose. Hence, in the present research, a simple, rapid, precise and accurate GC-MS method was developed and validated using International Conference on Harmonization Guidelines for the simultaneous determination and quantification of arbutin and hydroquinone form different herbal slimming products.[23]

MATERIALS AND METHODS

Chemicals

Methanol (France), arbutin (England) and hydroquinone (Switzerland) were purchased from Sigma-Aldrich. Acetonitrile and N-methyl-N-(trimethylsilyl) (TMS) trifluoroacetamide (MSTFA) were obtained from Sigma (St. Louis, MO, USA).

Plant material and pharmaceutics

Nine herbal slimming products containing *C. vulgaris* were acquired from the internet and different pharmacies in Turkey. The herbal slimming products from 1 to 7 were tea mixtures, product 8 was a slimming tea capsule, product 9 was *C. vulgaris* tea.

Extraction of the herbal slimming products

Ten grams of each product were extracted with distilled water and methanol (100 mLx2) separately at 40˚C for 30 min. The extracts were filtered. Then, the aqueous extracts were cooled at -80˚C and lyophilized. Methanol was evaporated to dryness and the methanol extracts were obtained.

Derivatization process

Arbutin, hydroquinone, and contained extracts were derivatized using MSTFA to increase the performance of the gas chromatographic separation. The hydroxy (-OH) groups were converted to the corresponding silyl (-O-TMS) groups. After establishing the optimum reaction conditions, the compounds were analyzed.

GC-MS conditions

Chromatographic analysis was performed on an Agilent 7820A GC system equipped with a 5977 series mass selective detector, 7673 series autosampler, and Agilent chemstation (Agilent Technologies, Palo Alto, CA). An HP-5 MS column with 0.25-µm film thickness (30 m x 0.25 mm I.D., USA) was used for separation. Splitless injection was used and the carrier gas was helium at a flow rate of 1.0 mL/min. The injector volume was 1 mL. The MS detector parameters were transfer line temperature 230˚C, solvent delay 3 min and electron energy 70 eV. The GC temperature gradient program was as follows: the initial temperature was 100˚C, held for 2 min, which was increased to 220˚C at a rate of 30˚C/min, held for 1 min, and finally to 300˚C at a rate of 20˚C/min and held for 2.0 min. The MS detector parameters were: transfer line temperature 280˚C; solvent delay 3 min; electron energy 70 eV; the MS was run in electron impact mode with selected ion monitoring (SIM) for quantitative analysis (m/z 254 for arbutin, m/z 239 for hydroquinone).

Standards and quality control samples

Stock solutions of arbutin and hydroquinone were prepared by dissolving the accurately weighed reference compounds in acetonitrile to give a final concentration of 100 µg/mL of both. The solution was then serially diluted with chloroform to achieve standard working solutions at concentrations of 5, 10, 25, 50, 100, 250 and 500 ng/mL for arbutin and hydroquinone, respectively. Structural formula and derivatization of arbutin and hydroquinone are shown in Figure 1.

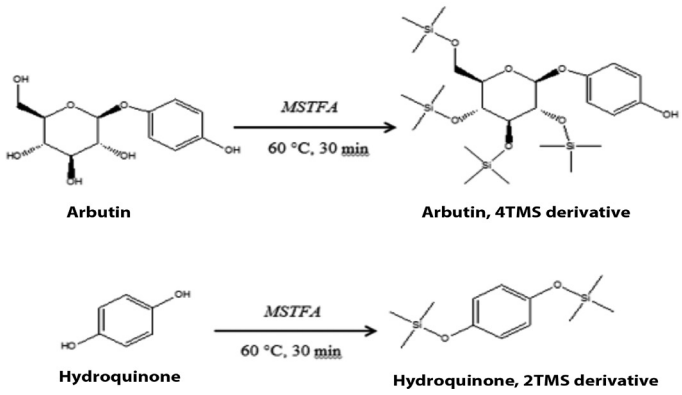

Figure 1. Structural formula and derivatization mechanism of arbutin and hydroquinone

All solutions were stored at 4˚C and were brought to room temperature before use. Quality control solutions were prepared by adding aliquots of standard working solution of final concentrations of 7.5, 75 and 375 ng/mL for arbutin and hydroquinone, respectively.

There were no experimental animal or clinical studies in our study. Thus, we did not need ethics committee approval for the study.

RESULTS

Method development and optimization

Arbutin and hydroquinone are polar molecules so a capillary column coated with 5% phenyl and 95% dimethylpolysiloxane were used for separation. During GC-MS method development, the injection port and detector temperatures were set to 250˚C and 290˚C, respectively. Different temperature programs were investigated to give an optimum temperature program as follows; initial temperature was 100˚C, held for 2 min, increased to 220˚C at 30˚C/min, held for 1 min, and finally to 300˚C at 20˚C/min with a final hold of 2.0 min. The injector volume was 1 mL in splitless mode.

MSTFA is an effective TMS donor. MSTFA reacts to replace labile hydrogens on a wide range of polar compounds with a TMS group and is used to prepare volatile and thermally stable derivatives for GC-MS.[24]

The effects of time and temperature on the reaction were investigated. Therefore, arbutin and hydroquinone were dissolved in acetonitrile. 50 µL of MSTFA solution was added to 50 µL of 200 ng/mL arbutin and hydroquinone solution and reacted at room temperature, 50 and 75˚C for 5, 15, 30 and 45 min. The resulting samples were quantitated using the GC-MS system. The optimized conditions for derivatization were 50˚C and 30 min.

Then, dry residue of the herbal slimming products was dissolved in 100 µL of a mixture of acetonitrile and MSTFA (50:50, v/v). The mixture was vigorously shaken and then delayed at 50˚C for 30 min. A 1-µL sample was injected into the GC-MS system.

Method validation

To evaluate the validation of the present method, parameters such as selectivity, linearity, precision, accuracy, limit of detection (LOD), and limit of quantification (LOQ) were investigated according to ICH validation guidelines.

Selectivity

The selectivity of the GC-MS method was investigated by observing interferences between arbutin and hydroquinone. For GC-MS, the electron impact mode with SIM was used for quantitative analysis (m/z 254 for arbutin and m/z 239 for hydroquinone). The mass spectra of the arbutin and hydroquinone are shown in Figure 2.

The retention times of arbutin and hydroquinone in GC-MS method were approximately 11.32 and 5.44 min with good peak shape (Figure 3).

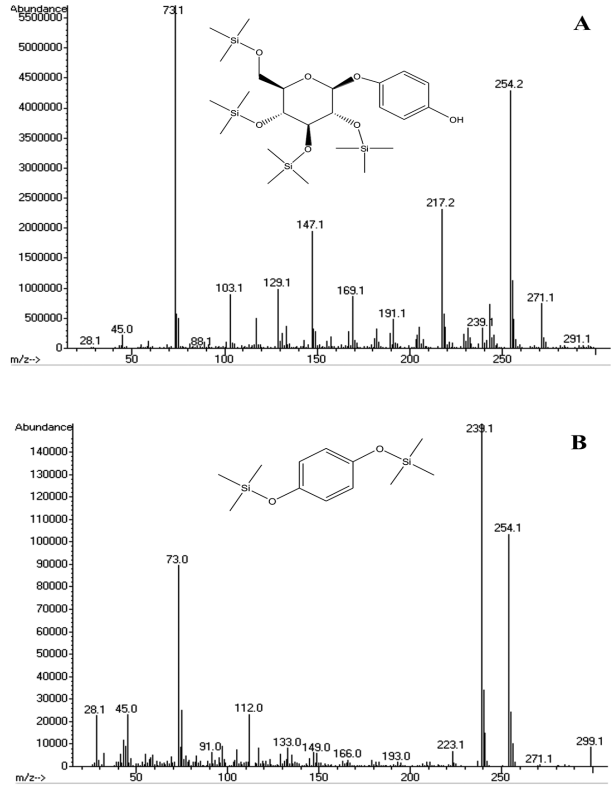

Figure 2. Mass spectrometry spectra of arbutin (A) and hydroquinone (B)

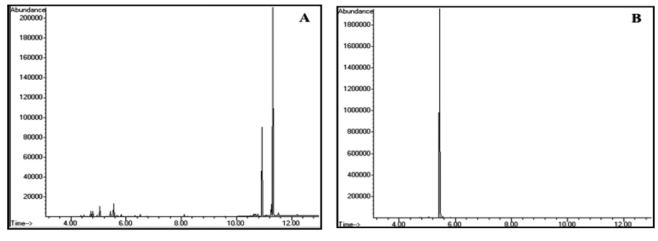

Figure 3. Gas chromatography-mass spectrometry chromatograms of arbutin (A) and hydroquinone (B) (500 ng/mL)

Linearity

Linearity was determined for arbutin and hydroquinone in the range of 5-500 ng/mL. The calibration curves constructed were evaluated using their correlation coefficients. The calibration equations from three replicate experiments demonstrated the linearity of the method. Standard deviations of the slope and intercept for the calibration curves are given in Table 1.

Table 1. Features of the calibration curves of arbutin and hydroquinone

Parameters	Arbutin	Hydroquinone
Linearity (ng/mL)	5-500	5-500
Regression equation[a]	y=1215.7x+810.48	y=1195.4x+4902
Correlation coefficent	0.9933	0.9915
Standard deviation of correlation coefficent	$5.0x10^{-3}$	$2.9x10^{-3}$
Limit of detection (ng/mL)	0.555	0.031
Limit of quantification (ng/mL)	1.665	0.093

[a]Based on three calibration curves, y: peak-height, x: arbutin and hydroquinone concentration

Precision and accuracy

The precision of the GC-MS method was determined through repeatability (intra-day) and intermediate precision (inter-day). Repeatability was evaluated by analyzing quality control samples six times per day, at three different concentrations, which were quality control samples. The intermediate precision was evaluated by analyzing the same samples once daily for three days. The relative standard deviation (RSD) of the predicted concentrations from the regression equation was taken as precision. The accuracy of this analytic method was assessed as the percentage relative error. For all the concentrations studied, intra- and inter-day RSD values were ≤2.73% and for all concentrations of arbutin and hydroquinone the relative errors were ≤2.56%.

LOD and LOQ

The LOD is the lowest amount of arbutin and hydroquinone in a sample that can be detected but not necessarily quantitated as an exact value. The LOQ is the lowest amount of arbutin and hydroquinone that can be quantitatively determined with suitable precision. The LOD and LOQ of the developed method were determined by injecting progressively lower concentrations of the standard solution under the chromatographic conditions. The lowest concentrations assayed where the signal/noise ratio was at least 10:1 was regarded as the LOQ. The LOD was

Table 2. Application of arbutin and hydroquinone in different herbal slimming products (1.0 mg/mL)

Sample name (1 mg/mL)		Arbutin (ng/mL)	% Concentration	Hydroquinone (ng/mL)	% Concentration
1	Aqueous extract	n.d.	-	8.4867	0.0008
	Methanol extract	20.0256	0.0020	15.4885	0.0015
2	Aqueous extract	n.d.	-	8.6724	0.0008
	Methanol extract	33.9755	0.0034	26.2841	0.0026
3	Aqueous extract	n.d.	-	7.2009	0.0007
	Methanol extract	63.4331	0.0063	18.0860	0.0018
4	Aqueous extract	n.d.	-	9.2036	0.0009
	Methanol extract	2.7145	0.0002	23.9543	0.0024
5	Aqueous extract	n.d.	-	7.6376	0.0007
	Methanol extract	34.4716	0.0034	41.1235	0.0041
6	Aqueous extract	n.d.	-	7.7472	0.0007
	Methanol extract	36.2843	0.0036	16.9257	0.0017
7	Aqueous extract	n.d.	-	8.1354	0.0008
	Methanol extract	18.8898	0.0019	16.3477	0.0016
8	Aqueous extract	n.d.	-	7.4452	0.0007
	Methanol extract	n.d.	-	25.7495	0.0026
9	Aqueous extract	60.6236	0.0060	15.7178	0.0016
	Methanol extract	35.2968	0.0035	11.6379	0.0012

n.d.: not determined

defined as a signal/noise ratio of 3:1. The results are shown in Table 1.

Application of method

The developed GC-MS method was used for the simultaneous determination of arbutin and hydroquinone from different herbal slimming products. The sample working solutions (1 µL) were injected and the height of both arbutin and hydroquinone peaks were measured. From the calibration curve, the amounts of arbutin and hydroquinone in different herbal slimming products were calculated. The retention time of arbutin and hydroquinone in sample solutions were 11.32 and 5.44 min, respectively (Figure 4). The mean amounts and percent values of arbutin and hydroquinone found in different herbal slimming products are presented in Table 2.

DISCUSSION

Comparison of methods

Today, GC-MS is a powerful technique for highly specific and quantitative measurements of low levels of analytes in samples. As compared with HPLC, high-resolution capillary GC has been less frequently used.[25]

During the development of the method, it became evident that arbutin and hydroquinone were very sensitive to matrix effects during the derivatization process in different herbal slimming products. Sample preparation techniques such as extraction and derivatization were used in order to minimize matrix suppression effects.

GC-MS sensitivity is not enough for the determination of arbutin and hydroquinone in different herbal slimming products. For this reason, MSTFA was chosen as a chromagenic derivatization reagent. In this study, the purpose of the derivatization reaction is to raise the sensitivity, thus the possibility of working at low concentrations was able to be realized.

A literature survey revealed that some of the related methods have been reviewed. A GC-MS method was reported for separating and determining arbutin and hydroquinone from strawberry tree leaf extracts.[4] In a reported method, the calibration curve of GC-MS method was linear for arbutin and hydroquinone in the range 0.5-200 µg/mL. Intra- and inter-day precision, expressed as the RSD were less than 5.0%, and accuracy (relative error) was better than 3.80%. In statistical comparison ($p<0.05$) with the other method in the literature, the proposed method indicated high accuracy, precision, and sensitivity.[4] The minimum determinable concentration wss 9 ng/mL. The present method has the following advantage over the reported method. The LOQ of the reported method was 29 ng/mL, whereas the the LOQ of the present method was 0.093 ng/mL.

When this method is applied to different herbal slimming product samples, its sensitivity was found to be adequate for analysis studies. The present method has the following advantages over the reported method. The sensitivity was evaluated using the LOQ, which was determined as 0.093 ng/mL. This method is as good as or superior to that reported in the other papers.[4,16,19,20]

Calibration curves of arbutin and hydroquinone were linear over the concentration range of 5-500 ng/mL for the study, which is as good as or superior to that reported in other papers.[15-20]

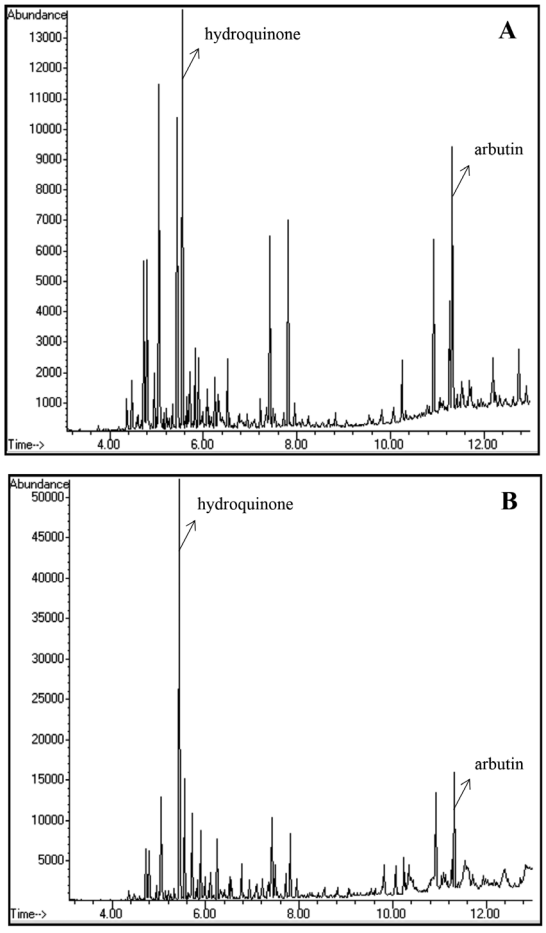

Figure 4. Typical chromatograms of methanol (A) and aqueous (B) extracts of product 9 (1.0 mg/mL)

CONCLUSIONS

In the present work, a new, simple and sensitive GC-MS method was developed for the simultaneous quantitation of arbutin and hydroquinone in whole plant powder of different herbal slimming products. The method was validated to track the active principles in the complex mixture of herbal ingredients. The method can be extended for the marker-based standardization of other herbal products containing arbutin and hydroquinone. The method was found to be simple, precise, accurate, specific and sensitive and can be used for routine quality control of herbal raw materials and for the quantification of these compounds in plant materials.

ACKNOWLEDGEMENTS

Benan Dursunoğlu would like to acknowledge the scholarship during her postgraduate program provided by the Turkish Scientific and Technical Research Council (TUBİTAK).

Conflict of Interest: No conflict of interest was declared by the authors.

REFERENCES

1. Migas P, Baranowska MK. The significance of arbutin and its derivatives in therapy and cosmetics. Phytochem Lett. 2015;13:35-40.
2. Thongchai W, Liawruangrath B, Liawruangrath S. Arbutin determination in medicinal plants and creams. Int J Cosmet Sci. 2009;31:87-96.
3. Pop C, Vlase L, Tamas M. Natural resources containing arbutin. Determination of arbutin in the leaves of *Bergenia crassifolia* (L.) Fritsch. acclimated in Romania. Not Bot Hort Agrobot Cluj. 2009;37:129-132.
4. Jurica K, Karaconji IB, Segan S, Opsenica DM, Kremer D. Quantitative analysis of arbutin and hydroquinone in strawberry tree (*Arbutus unedo* L., Ericaceae) leaves by gas chromatography-mass spectrometry. Arh Hig Rada Toksikol. 2015;66:197-202.
5. Jeon JS, Kim BH, Lee SH, Kwon HJ, Bae HJ, Kim SK, Park JA, Shim JH, Abd El-Aty AM, Shin HC. Simultaneous determination of arbutin and its decomposed product hydroquinone in whitening creams using high-performance liquid chromatography with photodiode array detection: Effect of temperature and pH on decomposition. Int J Cosmet Sci. 2015;37:567-573.
6. Monschein M, Neira JI, Kunert O, Bucar F. Phytochemistry of heather (*Calluna vulgaris* (L.) Hull) and its altitudinal alteration. Phytochem Rev. 2010;9:205-215.
7. Gruenwald J, Brendler T, Jaenicke C. PDR for Herbal Medicines (2nd ed). New Jersey; Medical Economics Company; 2007:383-384.
8. Baytop T. Türkiye'de Bitkiler ile Tedavi: Geçmişte ve Bugün (2nd ed). İstanbul; Nobel Tıp Kitabevleri; 1999:208.
9. Drozdz P, Sentkowska A, Pyrzynska K. Biophenols and antioxidant activity in wild and cultivated heather. Nat Prod Res. 2017;31:1181-1184.
10. Vucic DM, Petkovic MR, Rodic-Grabovac BB, Stefanovic OD, Vasic SM, Comic LR. *In vitro* activity of heather [*Calluna vulgaris* (L.) Hull] extracts on selected urinary tract pathogens. Bosn J Basic Med Sci. 2014;14:234-238.
11. Saaby L, Rasmussen HB, Jager AK. MAO-A inhibitory activity of quercetin from *Calluna vulgaris* (L.) Hull J Ethnopharmacol. 2009;121:178-181.
12. Çayır A, Atak N, Köse SK. Beslenme ve diyet kliniğine başvuranlarda obezite durumu ve etkili faktörlerin belirlenmesi. Ank Üni Tıp Fak Mecm. 2011;64:13-19.
13. Gimeno P, Maggio AF, Bancilhon M, Lassu N, Gornes H, Brenier C, Lempereur L. HPLC-UV method for the identification and screening of hydroquinone, ethers of hydroquinone and corticosteroids possibly used as skin-whitening agents in illicit cosmetic products. J Chromatogr Sci. 2016;54:343-352.
14. Wittig J, Wittemer S, Veit M. Validated method for the determination of hydroquinone in human urine by high-performance liquid chromatography-coulometric-array detection. J Chromatogr B Biomed Sci Appl. 2001;761:125-132.
15. Chang ML, Chang CM. Simultaneous HPLC determination of hydrophilic *withening* agents in cosmetic products. J Pharm Biomed Anal. 2003;33:617-626.
16. Thongchai W, Liawruangrath B, Liawruangrath S. High-performance liquid chromatographic determination of arbutin in skin-whitening creams and medicinal plant extracts. J Cosmet Sci. 2007;58:35-44.
17. Kittipongpatana N, Chaiwan A, Pusod U, Kittipongpatana OS. High-performance liquid chromatographic method for separation and quantitative analysis of arbutin in plant tissue cultures. CMU J Nat Sci. 2007;6:65-74.
18. Parejo I, Viladomat F, Bastida J, Codina C. A single extraction step in the quantitative analysis of arbutin in bearberry (*Arctostaphylos uva-ursi*) leaves by high-performance liquid chromatography. Phytochem Anal. 2001;12:336-339.
19. Rychlinska I, Nowak S. Quantitative determination of arbutin and hydroquinone in different plant materials by HPLC. Not Bot Horti Agrobo. 2012;40:109-113.
20. Lamien-Meda A, Lukas B, Schmiderer C, Franz CH, Novak J. Validation of a quantitative assay of arbutin using gas chromatography in *Origanum majorana* and *Arctostaphylos uva-ursi* extracts. Phytochem Anal. 2009;20:416-420.
21. Glöckl I, Blaschke G, Veit M. Validated methods for direct determination of hydroquinone glucuronide and sulfate in human urine after oral intake of bearberry leaf extract by capillary zone electrophoresis. J Chromatogr B Biomed Sci Appl. 2001;761:261-266.
22. Pyka A, Bober K, Stolarczyk A. Densitometric determination of arbutin in cowberry leaves (*Vaccinium vitis idaea*). Acta Pol Pharm. 2007;64:395-400.
23. ICH Steering Committee. International Conference on Harmonisation (ICH) of Technical Requirements for Registration of Pharmaceuticals for Human Use: Harmonised Tripartite Guideline on Validation of Analytical Procedures: Methodology, Recommended for Adoption at Step 4 of the ICH. Switzerland; IFPMA; 1996:1-17.
24. Donike M. N-Methyl-N-trimethylsilyl-trifluoracetamid, ein neues Silylierungsmittel aus der Reihe der silylierten Amide. J Chromatogr. 1969;42:103-104.
25. Yilmaz B, Arslan S, Akba V. Gas chromatography-mass spectrometry method for determination of metoprolol in the patients with hypertension. Talanta. 2009;80:346-351.

Turk J Pharm Sci 2018;15(3):304-308
DOI: 10.4274/tjps.64935

ORIGINAL ARTICLE

Design, Synthesis and Evaluation of the Biological Activities of Some New Carbohydrazide and Urea Derivatives

Bazı Yeni Karbohidrazit ve Üre Türevlerinin Tasarımı, Sentezi ve Biyolojik Aktivitelerinin Değerlendirilmesi

Fatih TOK[1], Recep İLHAN[2], Selin GÜNAL[2], Petek BALLAR-KIRMIZIBAYRAK[2], Bedia KOÇYİĞİT-KAYMAKÇIOĞLU[1]*

[1]Marmara University, Faculty of Pharmacy, Department of Pharmaceutical Chemistry, İstanbul, Turkey
[2]Ege University, Faculty of Pharmacy, Department of Biochemistry, İzmir, Turkey

ABSTRACT

Objectives: Urea and carbohydrazide derivatives are important compounds exhibiting cytotoxic activities. In this study, a series of new urea and carbohydrazide derivatives containing an pyridine ring were synthesized and evaluated for cytotoxic activity.

Materials and Methods: The proposed structures of the synthesized compounds were confirmed using elemental analysis, IR, and ^{1}H-NMR spectroscopic techniques. The cytotoxic potencies of synthesized compounds were determined using a 3-(4,5-dimethylthiazol-2-yl)-2,5-diphenyltetrazolium bromide assay (MTT) on *BRCA* mutant-carrying HCC1937 and Capan-1 cell lines, as well as on MCF7, HeLa, and MRC5 cells.

Results: 3a, 3b, 3c and 3d showed cytotoxic activity against all cancer cell lines.

Conclusion: Our data indicate that compounds 3a-d are more selective to cancer cells compared with nontumoral fibroblasts; however, these compounds are not more potent on HR defective cells with *BRCA* mutants.

Key words: Carbohydrazide, urea, cytotoxic activity

ÖZ

Amaç: Üre ve karbohidrazit türevleri önemli sitotoksik etkinlik gösteren bileşiklerdir. Bu çalışmada, bir yeni seri piridin halkası taşıyan üre ve karbohidrazit türevleri sentezlenmiş ve sitotoksik etkileri araştırılmıştır.

Gereç ve Yöntemler: Sentezlenen bileşiklerin önerilen yapıları elemental analiz, IR, ^{1}H-NMR spektroskopik yöntemleriyle doğrulanmıştır. Sentezlenen bileşiklerin sitotoksik etki güçleri, 3-(4,5-dimetiltiyazol-2-il)-2,5-difeniltetrazolyum bromür (MTT) kullanılarak *BRCA* mutasyonu taşıyan HCC1937 ve Capan-1 hücre hatları olan MCF7, HeLa ve MRC5 hücreleri üzerinde tespit edilmiştir.

Bulgular: 3a, 3b, 3c ve 3d tüm kanser hücre hatlarına karşı sitotoksik etki göstermiştir.

Sonuç: Verilerimiz, 3a-d bileşiklerinin kanser hücrelerinde tümöral olmayan fibroblastlarla kıyaslandığında daha seçici olduğunu, ancak bu bileşiklerin *BRCA1* mutant homolog rekombinasyonal (HR) DNA onarımı hatalı hücrelerde ise daha fazla etkili olmadığını göstermektedir.

Anahtar kelimeler: Karbohidrazit, üre, sitotoksik aktivite

INTRODUCTION

Cancer is one of the major causes of death worldwide. The development of identification and treatment are important for cancer treatment. However, effective and selective treatment methods are insufficient against some types of cancer. Scientists continue their studies to find effective molecules for cancer treatment.[1,2] Compounds bearing nitrogen, sulfur, and oxygen play a significant role by forming hydrogen bonds with DNA.[3] Therefore heterocyclic compounds such as pyridine and pyrimidine showed anticancer,[4] antibacterial,[5] antifungal,[6] analgesic, and anti-inflammatory activity.[7]

Sorafenib, which carries a pyridine ring and urea group was confirmed by the United States Food and Drug Administration for the treatment of renal cell carcinoma in 2005. Sorafenib, which

*Correspondence: E-mail: bkaymakcioglu@marmara.edu.tr, Phone: +90 532 507 94 60 ORCID-ID: orcid.org/0000-0003-0817-8236
Received: 22.08.2017, Accepted: 21.09.2017

has a broad spectrum for anticancer therapy, inhibits some kinases such as vascular endothelial and platelet-derived growth factor. Therefore, sorafenib could be used with numerous types of cancer. Chemical structures of compounds were envisioned consisting of three parts: pyridyl moiety, a linker, and urea functional group as a pharmacophore (Scheme 1).[8]

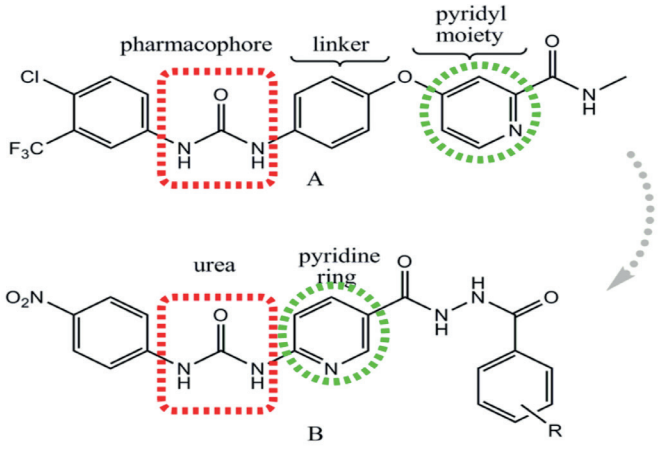

Scheme 1. The similarity of synthesized compounds (A) and sorafenib (B)

Wang et al.[9] studied new benzimidazole-2-urea derivatives that decrease the proliferation of some cancer cells (HeLa, K562, HepG2) and reported that these molecules could be used as tubulin inhibitors. In another study, Fortin et al.[10] discovered that compounds containing urea derivatives had greater antiproliferative activity than amide groups from their structure activity relationship. De et al.[11] synthesized N'-(2-(4-substitute)cyclopropanecarbonyl)isonicotinohydrazide-containing carbohydrazide and a pyridine ring and evaluated their cytotoxic activity against A549, PC3, and U373 cells.

Pyridine is an important ring system with numerous biologic activities. For example, Kurumurthy et al.[12] selected pyridine derivatives to achieve cytotoxic activity against THP1, U937, HL60 and B16-F10 cells.

Using results obtained in the literature and pharmacophore analysis (Scheme 1), target molecules carrying urea and carbohydrazide derivatives were synthesized from methyl 6-aminopyridine-3-carboxylate and evaluated their cytotoxic activity against cancer cells (HCC1937, Capan1, MCF-7, HeLa and MRC5).

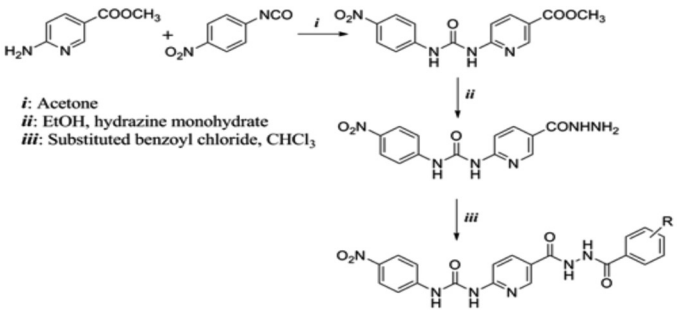

Scheme 2. The synthesis route of the compounds

MATERIALS AND METHODS

Chemistry

All chemicals reagents and solvents were obtained from Sigma-Aldrich (St. Louis, MO, USA), and Merck (Darmstadt, Germany). The homogeneity and purity of the compounds were checked using thin-layer chromatography (TLC), performed on commercially available silica gel (Kieselgel 60, F254) coated aluminum sheets (Merck) by using petroleum ether:ethyl acetate (10:90 v/v) as the solvent system. Visualization on TLC was performed using ultraviolet light (λ=254 nm) and an iodine indicator. Melting points (MP) were determined using a Schmelzpunktbestimmer SMP II. IR spectra were recorded with a Shimadzu FTIR-8400S (Japan). ^{1}H-NMR spectra were recorded on a Bruker Avance 400 MHz (USA) in DMSO-d_6 using tetramethylsilane (TMS) as the internal reference. Chemical shifts (δ) were expressed in parts per million relative to TMS and the following abbreviations were used to describe the peak patterns when appropriate: s, (singlet); d, (doublet); t, (triplet); m, (multiplet). Elemental analysis (C, H and N) was performed on a CHNS-Thermo Scientific Flash 2000 (Waltham, MA USA).

Synthesis of urea derivatives

Methyl 6-aminopyridine-3-carboxylate was dissolved in acetone at 80°C. Then, a solution of the corresponding equimolar isocyanate in dry acetone was added as two parts, every 30 minutes. The reaction mixture was refluxed for 6 hours. The reaction was finalized by checking with TLC and left overnight. The precipitate was filtered off, dried, and purified with acetone.[13]

Methyl 6-(3-(4-nitrophenyl)ureido)nicotinate (1)

Yellow solid; Yield: 70%; MP: 237-239°C; IR (ν_{max} cm^{-1}): 3365, 3211 (N-H), 3080 (=C-H stretching), 2983, 2843 (C-H), 1708 (urea C=O), 1604, 1562, 1506, 1491, 1411 (C=C, NO_2, N-H bending, C-N), 1273 (C-O), 839 (=C-H). ^{1}H-NMR (DMSO-d_6/TMS, 400 MHz, δ in ppm): 3.83 (s, 3H, -OCH_3), 7.69-8.84 (m, 7H, Ar-H), 9.99 (s, 1H, NH), 10.73 (s, 1H, NH). For $C_{14}H_{12}N_4O_5$ (M.W.: 316.27 g/mol) calculated (%): C:53.17, H:3.82, N:17.71. Found: C:54.46, H:3.66, N:17.95.

Synthesis of the hydrazide derivatives

Methyl 6-(3-(4-nitrophenyl)ureido)nicotinate was dissolved in ethanol on a magnetic stirrer. Then, hydrazine monohydrate (1 mL) was added. The reaction mixture was refluxed for 6 hours. The mixture was filtered and washed with methanol.[14]

1-(5-(Hydrazinecarbonyl)pyridin-2-yl)-3-(4-nitrophenyl)urea (2)

Yellow solid; Yield: 65%; MP: 274-275°C; IR (ν_{max} cm^{-1}): 3338, 3221 (N-H), 3078 (=C-H stretching), 1712 (C=O urea), 1678 (C=O hydrazide), 1620 (C=N), 1562, 1510, 1491, 1431 (C=C, NO_2, N-H, C-N), 815 (=C-H). ^{1}H-NMR (DMSO-d_6/TMS, 400 MHz, δ in ppm): 4.48 (s, 2H, NH_2), 7.71-8.87 (m, 7H, Ar-H), 9.93 (s, 1H, NH), 10.04 (s, 1H, NH), 10.78 (s, 1H, NH). $C_{13}H_{12}N_6O_4$ (M.W.: 316.27 g/mol) calculated (%): C:49.37, H:3.82, N:26.57. Found: C:51.05, H:3.97, N:25.25.

Synthesis of the carbohydrazide derivatives

To a solution of hydrazide (1 mmol) (2) and triethylamine (2 mmol) in dry CH_2Cl_2 (5 mL), a solution of previously prepared benzoyl chloride (1 mmol) was added dropwise at room temperature. The reaction mixture was stirred on a magnetic stirrer for 3 hours. The precipitate was then washed with distilled water and filtered. The purity of compounds was checked with TLC.[15]

1-(5-(2-(4-Fluorobenzoyl)hydrazinecarbonyl)pyridin-2-yl)-3-(4-nitrophenyl)urea (3a)

Yellow solid; Yield: 70%; MP: 257-259°C; IR (ν_{max} cm^{-1}): 3304, 3207, 3122 (N-H), 3080 (=C-H stretching), 1712 (C=O), 1612, 1562, 1508, 1492 (C=C, NO_2, N-H, C-N), 842 (=C-H). ^{1}H-NMR (DMSO-d_6/TMS, 400 MHz, δ in ppm): 7.67-8.84 (m, 11H, Ar-H), 9.69 (s, 1H, NH), 10.04 (s, 1H, NH), 10.84 (s, 2H, NH). $C_{20}H_{15}FN_6O_5$ (M.W.: 438.37 g/mol) calculated (%): C:54.80, H:3.45, N:19.17. Found: C:55.24, H:3.22, N:18.65.

1-(5-(2-(4-Chlorobenzoyl)hydrazinecarbonyl)pyridin-2-yl)-3-(4-nitrophenyl)urea (3b)

Yellow solid; Yield: 75%; MP: 202-203°C; IR (ν_{max} cm^{-1}): 3304, 3207, 3122 (N-H), 3080 (=C-H stretching), 1712 (C=O), 1612, 1562, 1508, 1492, 1431 (C=C, NO_2, N-H, C-N), 842 (=C-H). ^{1}H-NMR (DMSO-d_6/TMS, 400 MHz, δ in ppm): 7.71-8.85 (m, 11H, Ar-H), 9.98 (s, 2H, NH), 10.73 (s, 2H, NH). $C_{20}H_{15}ClN_6O_5$ (M.W.: 454.82 g/mol) calculated (%): C:52.81, H:3.32, N:18.48. Found: C:52.75, H:3.48, N:18.44.

1-(5-(2-(4-Nitrobenzoyl)hydrazinecarbonyl)pyridin-2-yl)-3-(4-nitrophenyl)urea (3c)

Yellow solid; Yield: 80%; MP: 273-275°C; IR (ν_{max} cm^{-1}): 3215, 3124 (N-H), 3082 (=C-H stretching), 1714 (C=O), 1612, 1564, 1510, 1492 (C=C, NO_2, N-H, C-N), 846 (=C-H). ^{1}H-NMR (DMSO-d_6/TMS, 400 MHz, δ in ppm): 7.68-8.85 (m, 11H, Ar-H), 9.62 (s, 1H, NH), 10.00 (s, 1H, NH), 10.74 (s, 2H, NH). $C_{20}H_{15}N_7O_7$ (M.W.: 465.38 g/mol) calculated (%): C:51.62, H:3.25, N:21.07. Found: C:52.33, H:3.12, N:20.66.

1-(5-(2-(2,6-Dichlorobenzoyl)hydrazinecarbonyl)pyridin-2-yl)-3-(4-nitrophenyl)urea (3d)

Yellow solid; Yield: 70%; MP: 258-260°C; IR (ν_{max} cm^{-1}): 3369, 3215, 3122 (N-H), 3084 (=C-H), 1712 (C=O), 1612, 1566, 1492, 1481 (C=C, NO_2, N-H, C-N), 1031 (C-Cl), 844 (=C-H). ^{1}H-NMR (DMSO-d_6/TMS, 400 MHz, δ in ppm): 7.78-8.68 (m, 10H, Ar-H), 9.43 (s, 1H, NH), 10.00 (s, 1H, NH), 10.75 (s, 2H, NH). $C_{20}H_{14}Cl_2N_6O_5$ (M.W.: 489.27 g/mol) calculated (%): C:49.10, H:2.88, N:17.18. Found: C:50.35, H:2.97, N:16.85.

1-(5-(2-(4-Methylbenzoyl)hydrazinecarbonyl)pyridin-2-yl)-3-(4-nitrophenyl)urea (3e)

Yellow solid; Yield: 65%; MP: 275-277°C; IR (ν_{max} cm^{-1}): 3369, 3205, 3122 (N-H), 3049 (=C-H stretching), 2987 (C-H), 1712 (C=O), 1610, 1562, 1508, 1492, 1431 (C=C, NO_2, N-H, C-N), 844 (=C-H). ^{1}H-NMR (DMSO-d_6/TMS, 400 MHz, δ in ppm): 2.39 (s, 3H, -CH_3), 7.47-8.81 (m, 11H, Ar-H), 9.45 (s, 1H, NH), 10.06 (s, 1H, NH), 10.77 (s, 2H, NH). $C_{21}H_{18}N_6O_5$ (M.W.: 434.41 g/mol) calculated (%): C:58.06, H:4.98, N:19.15. Found: C:57.23, H:5.05, N:18.56.

1-(5-(2-(4-Bromobenzoyl)hydrazinecarbonyl)pyridin-2-yl)-3-(4-nitrophenyl)urea (3f)

Yellow solid; Yield: 75%; MP: 240-241°C; IR (ν_{max} cm^{-1}): 3207, 3122 (N-H), 3082 (=C-H stretching), 1712 (C=O), 1610, 1562, 1508, 1491, 1431 (C=C, NO_2, N-H, C-N), 844 (=C-H). ^{1}H-NMR (DMSO-d_6/TMS, 400 MHz, δ in ppm): 7.45-8.81 (m, 11H, Ar-H), 9.36 (s, 1H, NH), 10.20 (s, 1H, NH), 10.84 (s, 2H, NH). $C_{20}H_{15}BrN_6O_5$ (M.W.: 499.27 g/mol) calculated (%): C:48.11, H:3.03, N:16.83 Found: C:47.48, H:3.25, N:16.92.

1-(4-nitrophenyl)-3-(5-(2-(4-(trifluoromethyl)benzoyl) hydrazinecarbonyl)pyridin-2-yl)urea (3g)

Yellow solid; Yield: 70%; MP: 299-300°C; IR (ν_{max} cm^{-1}): 3333, 3271, 3213 (N-H), 3080 (=C-H stretching), 1712 (C=O), 1680 (C=O hydrazide), 1614 (C=N), 1564, 1489, 1431, 1411 (C=C, NO_2, N-H, C-N), 1261 (C-F), 890 (=C-H). ^{1}H-NMR (DMSO-d_6/TMS, 400 MHz, δ in ppm): 7.64-8.84 (m, 11H, Ar-H), 9.75 (s, 1H, NH), 9.97 (s, 1H, NH), 10.72 (s, 2H, NH). $C_{21}H_{15}F_3N_6O_5$ (M.W.: 488.38 g/mol) calculated (%): C:51.65, H:3.10, N:17.21 Found: C:51.48, H:3.25, N:16.92.

1-(5-(2-(4-methoxybenzoyl)hydrazinecarbonyl)pyridin-2-yl)-3-(4-nitrophenyl)urea (3h)

Yellow solid; Yield: 75%; MP: 222-223°C; IR (ν_{max} cm^{-1}): 3275, 3171, 3117 (N-H), 3080 (=C-H stretching), 2978 (C-H asymmetric stretching), 2841 (C-H symmetric stretching), 1703 (C=O), 1662 (C=O hydrazide), 1633 (C=N), 1537, 1506, 1499, 1471 (C=C, NO_2, N-H, C-N), 1327 (C-O), 824 (=C-H). ^{1}H-NMR (DMSO-d_6/TMS, 400 MHz, δ in ppm): 3.84 (s, 3H, OCH_3), 7.05-8.84 (m, 11H, Ar-H), 9.79 (2s, 1H, NH), 10.45 (2s, 1H, NH), 10.72 (s, 2H, NH). $C_{21}H_{18}N_6O_6$ (M.W.: 450.40 g/mol) calculated (%): C:56.00, H:4.03, N:18.66 Found: C:56.48, H:3.25, N:18.92.

1-(5-(2-benzoylhydrazinecarbonyl)pyridin-2-yl)-3-(4-nitrophenyl)urea (3i)

Yellow solid; Yield: 70%; MP: 203-204°C; IR (ν_{max} cm^{-1}): 3271, 3213, 3124 (N-H), 3045 (=C-H stretching), 1712 (C=O), 1666 (C=O hydrazide), 1641 (C=N), 1602, 1562, 1506, 1489, 1431 (C=C, NO_2, N-H, C-N), 846 (=C-H). ^{1}H-NMR (DMSO-d_6/TMS, 400 MHz, δ in ppm): 7.45-8.84 (m, 11H, Ar-H), 9.80 (2s, 1H, NH), 10.68 (2s, 1H, NH), 11.48 (s, 2H, NH). $C_{20}H_{16}N_6O_5$ (M.W.: 420.38 g/mol) calculated (%): C:57,14 H:3.84, N:19.99 Found: C:57.48, H:3.65, N:19.92.

1-(4-nitrophenyl)-3-(5-(2-(4-(trifluoromethylthio)benzoyl) hydrazinecarbonyl)pyridin-2-yl)urea (3j)

Yellow solid; Yield: 65%; MP: 277-278°C; IR (ν_{max} cm^{-1}): 3333, 3221 (N-H), 3080 (=C-H stretching), 1714 (C=O urea), 1680 (C=O hydrazide), 1641 (C=N), 1564, 1510, 1492 (C=C, NO_2, N-H, C-N), 844 (=C-H). ^{1}H-NMR (DMSO-d_6/TMS, 400 MHz, δ in ppm): 7.63-8.83 (m, 11H, Ar-H), 9.79 (2s, 1H, NH), 9.97 (s, 1H, NH), 10.72 (s, 2H, NH). $C_{21}H_{15}F_3N_6O_5S$ (M.W.: 520.44 g/mol) calculated (%): C:48.46, H:2.91, N:16.15 Found: C:48.76, H:3.05, N:16.92.

Biology

Cell culture

A human pancreatic adenocarcinoma Capan1 cell line, human cervix carcinoma HeLa cell line, human lung fibroblasts MRC5

cell line, human breast adenocarcinoma MCF7 and HCC1937 cell line were obtained from American Type Culture Collection (Bethesda), and maintained as exponentially growing monolayers by culturing according to the supplier's instructions in a humidifier incubator at 37°C supplied with 5% CO_2. All cell culture reagents were purchased from Biological Industries (Israel).

Cytotoxicity test

The cytotoxic potencies of the test compounds were determined using a WST1 Cell Protliferation Assay (Roche) according to the manufacturer's instructions. All tested compounds were dissolved in DMSO. Cells were seeded into a 96-well plate at a density of 5000 cells/well for HeLa, MCF7 and HCC1937, 7500 cells/well for Capan1 and 10,000 cells per well for MRC5. The next day, cells were treated with compounds with the final concentrations of 1, 2, 5, 10, 25 µM and incubated for 48 hours at conventional cell culture conditions. DMSO was used a negative solvent control, and doxorubicin was included in the study as a positive cytotoxic control compound. The ratio of surviving cells after compound treatment was determined using a colorimetric WST-1 assay (Roche) as indicated in the protocol provided by manufacturer. The absorbance was measured using a Varioscan microplate reader (Thermo) at 450 nm with a 620-nm reference filter. To determine the IC_{50} values, a sigmoid-dose response curve was fitted to the data using nonlinear regression on GraphPad Prism 5 software.

This study did not need ethics committee approval because *in vitro* methods were used for biologic activity processes.

RESULTS AND DISCUSSION

The synthetic route to the target compounds is outlined in Scheme 2. The structures of the compounds (1, 2, 3a-j) were confirmed using IR, ^{1}H-NMR, and elemental analysis. IR spectra of the compounds (1, 2, 3a-j) afforded N-H stretching (3115-3369) bands. IR spectra of all compounds (1, 2, 3a-j) were described C-H stretching (3045-3082), urea and carbohydrazide C=O stretching (1662-1714) bands, aromatic rings C=C stretching and NO_2 stretching (1411-1604) bands. The NH protons of carbohydrazide and urea groups resonated as two different singlet peak at 9.36-11.48 ppm. The aromatic protons displayed a multiplet at 7.05-8.85 ppm. The elemental analysis of compounds was in agreement with the proposed structures of the compounds.

It is known that some PARP inhibitors are highly-selective promising agents against cancer cells with homologous recombination (HR) DNA repair pathway deficiencies such as those harboring mutations on tumor suppressors *BRCA1* or *BRCA2* via generation of chromatid breaks, cell cycle arrest and apoptosis.[16,17] Therefore, we included HCC1937 and Capan1, which are defective in *BRCA1* and *BRCA2*, respectively. We aimed to compare the cytotoxicity of the compounds on these cell lines with their activities on HR-proficient cancer cell lines (HeLa and MCF7) and also a non-tumoral MRC5 fibroblast cell line.

When the substitution pattern at the phenyl ring was determined, the effect of electron donor and electron acceptor groups on activity was considered. Therefore, methyl, methoxy, and halogens such as F, Cl, Br were selected as electron donors and a nitro group was selected as an electron acceptor. Our data suggest that only 3a having fluoro, 3b having chloro, 3c having nitro and 3d having 2,6 dichloro substituents had cytotoxic activities at the tested concentrations. The IC_{50} values of these compounds are given in Table 1. Compounds 3e-j showed less cytotoxic activity on all cancer cells compared with 3a-d. However, our results suggest that the compounds possessed no selectivity toward HR defective Capan1 and HCC1937 cells harboring *BRCA* mutations compared with MCF7 and HeLa cells with intact HR pathways.

CONCLUSIONS

In the present paper, we reported the synthesis of some new urea and carbohydrazide derivatives from methyl 6-aminopyridine-

Table 1. Cytotoxic activity of compounds

			IC_{50} (µM)		
Compounds	**HCC1937**	**Capan1**	**MCF7**	**HeLa**	**MRC5**
3a	7.6±0.09	7.4±0.62	7.3±0.86	6.6±0.53	15.4±1.42
3b	8.9±0.07	8.4±0.26	9.2±0.49	11.7±1.02	19.6±1.06
3c	10.4±0.6	9.3±0.79	9.6±0.56	9.8±1.86	18.3±1.54
3d	7.8±0.82	7.3±0.75	7.5±0.13	7.9±1.68	17.4±1.12
3e	>25	>25	>25	>25	>25
3f	>25	>25	>25	>25	>25
3g	>25	>25	>25	>25	>25
3h	>25	>25	>25	>25	>25
3i	>25	>25	>25	>25	>25
3j	>25	>25	>25	>25	>25
Doxorubicin	1.05±0.07	0.98±0.08	1.13±0.12	0.73±0.13	7.2±1.37

3-carboxylate. The synthesized compounds were evaluated for their cytotoxic activity. Our data indicate that 3a-d are more selective to cancer cells compared with nontumoral fibroblasts; however, these compounds are not more potent on HR defective cells with *BRCA* mutants.

ACKNOWLEDGEMENTS

This study was supported by TÜBİTAK 215S112 and Marmara University Scientific Research Commission (project number: SAG-C-DRP-100616-0260).

Conflict of Interest: No conflict of interest was declared by the authors.

REFERENCES

1. Nepali K, Sharma S, Sharma M, Bedi PM, Dhar KL. Rational approaches, design strategies, structure activity relationship and mechanistic insights for anticancer hybrids. Eur J Med Chem. 2014;77:422-487.
2. Liu Z, Wang Y, Lin H, Zuo D, Wang L, Zhao Y, Gong P. Design, synthesis and biological evaluation of novel thieno[3,2-d]pyrimidine derivatives containing diaryl urea moiety as potent antitumor agents. Eur J Med Chem. 2014;85:215-227.
3. Horowitz S, Trievel RC. Carbon-oxygen hydrogen bonding in biological structure and function. J Biol Chem. 2012;287:41576-41582.
4. He H, Wang X, Shi L, Yin W, Yang Z, He H, Liang Y. Synthesis, antitumor activity and mechanism of action of novel 1,3-thiazole derivatives containing hydrazide-hydrazone and carboxamide moiety. Bioorg Med Chem Lett. 2016;26:3263-3270.
5. Morjan RY, Mkadmh AM, Beadham I, Elmanama AA, Mattar MR, Raftery J, Pritchard RG, Awadallah AM, Gardiner JM. Antibacterial activities of novel nicotinic acid hydrazides and their conversion into N-acetyl-1,3,4-oxadiazoles. Bioorg Med Chem Lett. 2014;24:5796-5800.
6. Altıntop MD, Özdemir A, Turan-Zitouni G, Ilgın S, Atlı Ö, İşcan G, Kaplancıklı ZA. Synthesis and biological evaluation of some hydrazone derivatives as new anticandidal and anticancer agents. Eur J Med Chem. 2012;58:299-307.
7. Salgin-Gökşen U, Gökhan-Kelekçi N, Göktaş O, Köysal Y, Kiliç E, Işik S, Aktay G, Ozalp M. 1-Acylthiosemicarbazides, 1,2,4-triazole-5(4H)-thiones, 1,3,4-thiadiazoles and hydrazones containing 5-methyl-2-benzoxazolinones: Synthesis, analgesic-anti-inflammatory and antimicrobial activities. Bioorg Med Chem. 2007;15:5738-5751.
8. Chen JN, Wang XF, Li T, Wu DW, Fu XB, Zhang GJ, Shen XC, Wang HS. Design, synthesis and biological evaluation of novel quinazolinyl-diaryl urea derivatives as potential anticancer agents. Eur J Med Chem. 2015;107:12-25.
9. Wang W, Kong D, Cheng H, Tan L, Zhang Z, Zhuang X, Long H, Zhou Y, Xu Y, Yang X, Ding K. New benzimidazole-2-urea derivatives as tubulin inhibitors. Bioorg Med Chem Lett. 2014;24:4250-4253.
10. Fortin S, Moreau E, Lacroix J, Cote MF, Petitclerc E, Gaudreault R. Synthesis, antiproliferative activity evaluation and structure-activity relationships of novel aromatic urea and amide analogues of N-phenyl-N'-(2-chloroethyl)ureas. Eur J Med Chem. 2010;45:2928-2937.
11. De P, Baltas M, Lamoral-Theys D, Bruyere C, Kiss R, Bedos-Belval F, Saffon N. Synthesis and anticancer activity evaluation of 2-(4-alkoxyphenyl)cyclopropyl hydrazides and triazolo phthalazines. Bioorg Med Chem. 2010;18:2537-2548.
12. Kurumurthy C, Veeraswamy B, Sambasiva Rao P, Santhosh Kumar G, Shanthan Rao P, Loka Reddy V, Venkateswara Rao J, Narsaiah B. Synthesis of novel 1,2,3-triazole tagged pyrazolo[3,4-b]pyridine derivatives and their cytotoxic activity. Bioorg Med Chem Lett. 2014;24:746-749.
13. Ghorab MM, Alqasoumi SI, Abdel-Kader MS, Alsaid MS. Utility of L-Norephedrine in the semisynthesis of novel thiourea and thiazolidine derivatives as a new class of anticancer agents. Acta Pol Pharm. 2014;71:615-623.
14. Jha KK, Samad A, Kumar Y, Shaharyar M, Khosa RL, Jain J, Kumar V, Singh P. Design, synthesis and biological evaluation of 1,3,4-oxadiazole derivatives. Eur J Med Chem. 2010;45:4963-4967.
15. Lu C, Tang K, Li Y, Li P, Lin Z, Yin D, Chen X, Huang H. Design, synthesis and evaluation of novel diaryl urea derivatives as potential antitumor agents. Eur J Med Chem. 2014;77:351-360.
16. Bryant HE, Schultz N, Thomas HD, Parker KM, Flower D, Lopez E, Kyle S, Meuth M, Curtin NJ, Helleday T. Specific killing of BRCA2-deficient tumours with inhibitors of poly(ADP-ribose) polymerase. Nature. 2005;434:913-917.
17. Farmer H, McCabe N, Lord CJ, Tutt AN, Johnson DA, Richardson TB, Santarosa M, Dillon KJ, Hickson I, Knights C, Martin NM, Jackson SP, Smith GC, Ashworth A. Targeting the DNA repair defect in BRCA mutant cells as a therapeutic strategy. Nature. 2005;434:917-921.

Turk J Pharm Sci 2018;15(3):309-318
DOI: 10.4274/tjps.29200

ORIGINAL ARTICLE

Design, Formulation and *In Vitro* Evaluation of Sustained-release Tablet Formulations of Levosulpiride

Levosulpirid Sürekli Salım Tablet Formülasyonlarının Tasarımı, Formülasyonu ve *İn Vitro* Değerlendirilmesi

Muhammad SAMIE[1]*, Sajid BASHIR[2], Jabbar ABBAS[3], Samiullah KHAN[1], Nargis AMAN[1], Habibullah JAN[4], Naveed MUHAMMAD[4]

[1]COMSATS Institute of Information Technology, Department of Pharmacy, Abbottabad, Pakistan
[2]Sargodha University, Faculty of Pharmacy, Sargodha, Pakistan
[3]People's University of Medical and Health Sciences for Women, Institute of Pharmaceutical Sciences, Shaheed Benazir Abad, Pakistan
[4]Abdul Wali Khan University Mardan, Department of Pharmacy, Mardan, Pakistan

ABSTRACT

Objectives: Levosulpiride is a widely used gastroprokinetic agent in the treatment of various gastric disorders; however, its short half-life and increased dosage frequency leads to non-compliance and possible adverse effects. The prime objective of the current study was to develop a sustained-release formulation of Levosulpiride incorporating bioresorbable cellulose derivatives.

Materials and Methods: Sustained-release formulations of Levosulpiride were prepared through direct compression using various cellulose derivatives such as CMC sodium, HPC, and HPMC in different polymer-to-drug weight ratios as release-modifying polymers. The powder blends and compressed tablets were then subjected to pre-compressional and post-compressional evaluation, as well as FTIR analysis. *In vitro* release studies were performed for all formulations of the model drug in buffer solution of pH 6.8 at a wave length of 214 nm by a UV-visible light spectrophotometer.

Results: The FTIR results confirmed that the interaction between components was physical, and from the different kinetic models data, the release profile was best expressed by the Higuchi model because the results showed high linearity. The results also showed formulation F9 to be the ideal one among the developed formulations, exhibiting sustained- release behavior.

Conclusion: Levosulpiride sustained-release matrices were prepared successfully using CMC sodium, HPC, and HPMC as the release-retarding polymer/carrier.

Key words: Levosulpiride, sustained release tablets, dissolution, compliance, polymers

ÖZ

Amaç: Levosulpirid, çeşitli gastrik bozuklukların tedavisinde yaygın olarak kullanılan bir gastroprokinetik ajandır; bununla birlikte, kısa yarı ömrü ve artan dozlama sıklığı, uyumsuzluk ve olası yan etkilere yol açar. Bu çalışmanın asıl amacı, biyolojik olarak resorbe olabilen selüloz türevlerini içeren Levosulpiridin sürekli salımlı bir formülasyonunu geliştirmektir.

Gereç ve Yöntemler: Levosulpiridinin sürekli salım formülasyonları, salım modifiye eden polimerler olarak CMC sodyum, HPC ve HPMC gibi çeşitli selüloz türevlerinin farklı polimer-etkin madde ağırlık oranlarında kullanımıyla direkt basım yoluyla hazırlandı. Daha sonra, toz karışımları ve basılmış tabletler basım öncesi ve basım sonrası değerlendirmeye ve aynı zamanda FTIR analizlerine tabi tutuldu. UV/görünür ışık spektrofotometresi ile 214 nm dalga boyunda pH 6.8 tampon çözeltisinde model etkin maddenin tüm formülasyonları için *in vitro* salım çalışmaları gerçekleştirildi.

Bulgular: FTIR sonuçları, bileşenler arasındaki etkileşimin fiziksel olduğunu ve farklı kinetik model verilerinden, salım profilinin Higuchi modeline en iyi şekilde uyum gösterdiğini doğruladı, çünkü sonuçlar yüksek doğrusallık gösterdi. Sonuçlar ayrıca, geliştirilmiş sürekli salım formülasyonları arasında F9 formülasyonunun ideal olduğunu gösterdi.

Sonuç: Salım geciktirici polimer/taşıyıcı olarak CMC sodyum, HPC ve HPMC kullanılarak levosulpirid sürekli salımlı matrisler, başarıyla hazırlandı.

Anahtar kelimeler: Levosulpirid, sürekli salım tabletleri, çözünme, uyum, polimerler

*Correspondence: E-mail: sami.jadoon.83@gmail.com, Phone: +923339402306 ORCID-ID: orcid.org/0000-0002-0017-2692
Received: 28.08.2017, Accepted: 02.11.2017

INTRODUCTION

The oral route of drug administration is the most acceptable and frequently used route because of the convenience of self-administration, ease of manufacturing, and high-degree of dose accuracy.[1] Dosage forms are designed by exploiting the unique features of the gastro-intestinal tract (GIT) as the drug has to pass from the walls of GIT before getting access to the systemic circulation.[2] The pharmaceutical industry is focusing on the establishment of novel drug delivery systems rather than investigating and developing new drug entities due to the increased investigational cost of new drugs.[3] Over the past several decades, controlled-release technology has rapidly emerged as a drug delivery system that offers novel approaches for the delivery of bioactive compounds into systemic circulation at a predetermined rate, which significantly improves drug bioavailability and clinical outcomes with decreased toxicity. Sustained-release (SR) dose forms are designed in such a way that the rate of drug release from the tablet matrix occurs in a controlled manner over an extended period of time maintaining a constant plasma drug level thus improving patient compliance and effective clinical outcomes.[4] A constant therapeutic drug level is maintained throughout the dosing intervals, which often prolongs the onset of pharmacologic action.[5]

The development of sustained drug delivery systems is a challenging task in terms of providing a constant drug release profile retaining the dosage form in the stomach or upper small intestine until all the drug is completely released in the desired time.[6] An ideal oral drug delivery system will steadily release a measurable and reproducible amount of drug over an extended period of time.[7] Several mechanisms are involved in the release of drugs from controlled-release formulations such as dissolution- controlled release systems and diffusion-controlled release systems. In dissolution- controlled systems, dissolution is the rate-controlling step. The drug is embedded in slowly dissolving or erodible matrix or by coating it with slowly dissolving substances, whereas in diffusion-controlled release systems, the release rate of drug is dependent on its diffusion through an inert water insoluble membrane barrier. In matrix-diffusion controlled devices, the therapeutic agent is dispersed in an insoluble matrix of rigid non-swellable hydrophobic materials or a swellable (soluble) hydrophilic substance. Among different strategies to prolong the drug action, matrix tablet formulations have gained immense popularity because they have the advantage of simple processing and low-cost fabrication.[8] Matrix tablets are cost effective, easy to prepare, and exhibit predictable release behavior.

Polymers are becoming increasingly important in the field of drug delivery. They owe their unique properties to their size, three-dimensional shape, and asymmetry. Polymers occur naturally (biopolymers) as well as synthesized in the laboratory on a large scale. Advances in polymer science have led to the development of several novel drug delivery systems.[9] The chemical reactivity of polymers depends to a large extent on the way the monomer units are put together. Polymers can be used in film coatings to mask the unpleasant taste of a drug, to enhance drug stability, and to modify drug-release characteristics. Discovery of polymers with ideal properties still provides new avenues in pharmaceutical research.

Studies have shown that the rate and extent of drug release depends on the type and level of the excipient/polymer used. Many polymers have been used in the formulation of matrix-based SR drug delivery systems. Water-soluble polymers are being widely used in the designing of matrix systems in order to provide sustained drug delivery because of their excellent drug-retarding ability, low cost, and broad regulatory acceptance.[10,11] Hydrophilic polymers are usually not affected by variations in pH; therefore, they release the drug at a constant rate from oral dose forms. However, in the case of water-soluble drugs, the use of hydrophilic polymers alone for prolonging drug release is restricted because of the leakage of dissolved drug from the hydrophilic gel network through diffusion, hence a blend of hydrophilic and hydrophobic polymers is recommended for such drugs.[12] Among the cellulose ether derivatives, hydroxypropyl methyl cellulose (HPMC) has been widely investigated for its drug-releasing effect as compared with methyl cellulose and hydroxypropyl cellulose (HPC).[13]

Carboxy methyl cellulose (CMC) sodium, is described by the United States Pharmacopeia (USP) as the sodium salt of poly carboxy methyl ether of cellulose. CMC or cellulose gum, often used as a sodium salt, is a derivative of cellulose (a beta-glucopyranose polymer) with carboxy methyl groups (-CH_2-COOH) attached to the hydroxyl groups of the glucopyranose backbone. It occurs as white, odorless, granular powder with the molecular formula [$C_6 H_7 O_2 (OH)_2 CH_2 COONa$] n. Figure 1 indicates the chemical structure of CMC sodium. A number of grades of CMC sodium are available such as Accelerate. Grades are typically classified as being of low, medium or high viscosity.

HPMC, also known as hypromellose, is propylene glycol ether of methyl cellulose. It is a semi synthetic, inert, visco-elastic polymer used as an ophthalmic lubricant, as well as an excipient and controlled-delivery component in oral medicaments. HPMC is the most important hydrophilic carrier material used in the preparation of oral controlled drug delivery systems because of its non-toxic nature, ease of compression and accommodation to high level of drug loading.[14] Figure 2 represents the chemical structure of HPMC.

HPC is a derivative of cellulose, soluble in both water and organic solvents. It has the property to retain water by forming a film that prevents water loss and exhibits greater drug retarding properties than hydroxyethyl cellulose. The drug release from HPC matrices is controlled primarily by diffusion through pores and channels in the structure.[15] HPC is generally used as an

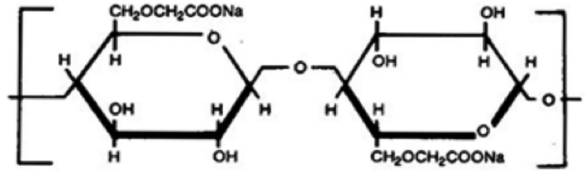

Figure 1. The chemical structure of carboxy methyl cellulose sodium

emulsifier, thickening agent, and film-former in tablet coatings because of its surface properties, but it lacks the property to form gel because it forms open helical coils. Figure 3 indicates the chemical structure of HPC.

Medicinal products of the prokinetics class are found to be effective in the treatment of all clinical forms of dyspepsia.[16] Levosulpiride, as a gastroprokinetic agent, has shown promising results in the treatment of various gastric disorders such as functional dyspepsia and non-erosive reflux disorder.[17] Chemically, it is a synthetic benzamide derivative with a strong inhibitory effect on dopaminergic D_2 receptors both in the central nervous system and in the GIT.[18] Studies have shown Levosulpiride to be effective in the treatment of various diseases such as dyspepsia (functional or organic), diabetic gastroparesis, reflux esophagitis, iatrogenic emesis induced by drugs such as chemotherapy, calcitonin, and anesthetics, as well as non-iatrogenic nausea and vomiting.[19] It also acts as a moderate agonist at the serotonergic 5-HT_4 receptor and to a lesser extent on 5-HT_3 receptors.[20,21] The serotonergic (5-HT_4) component of Levosulpiride may enhance its therapeutic efficacy in gastrointestinal disorders.[22] This property, together with antagonism at D2 receptors, may contribute to its gastrointestinal prokinetic effect.[17] In a randomized, double-blind trial, it was found that Levosulpiride had a similar effect to cisapride in the treatment of dysmotility-like functional dyspepsia.[23] The drug is given mostly at the dosage of 25-50 mg three times a day because of its short half-life, which leads to poor treatment adherence by patients and adverse drug effects. Figure 4 represents the structure of Levosulpiride.

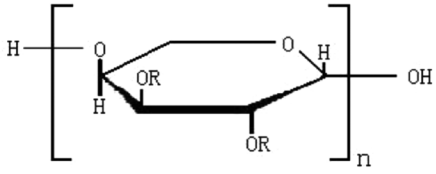

Figure 2. The Chemical structure of hydroxypropyl methyl cellulose

The aim of the current work was an attempt to develop SR matrix tablets of Levosulpiride for improved patient compliance and better therapeutic effects of various polymers with different polymeric compositions. Various physical tests were performed for the formulated tablets such as weight variation, and thickness, hardness, and friability tests. The tablets were evaluated for uniformity of active ingredients by performing a pharmaceutical assay. The release of the model drug from the developed matrix tablets was performed in USP phosphate buffer of pH 6.8. The mechanism of drug release was studied by subjecting drug release data to various kinetic models.

MATERIALS AND METHODS

Chemicals

For the preparation of matrix tablets of various polymeric compositions, methocel E-5 (HPMC), HPC, and CMC sodium were used as polymers, respectively. Microcrystalline cellulose PH-200 was used as a bulking agent for the tablets. Talcum and magnesium stearate were used as lubricants, respectively. De-ionized water and 0.1 N NaOH solution were used as solvents. Potassium dihydrogen phosphate, sodium chloride, and all other chemicals used were of analytical grade.

Preparation of the matrix tablets

Levosulpiride tablets were formulated and evaluated at Aims Pharmaceuticals (pvt) Ltd. Kahuta triangle industrial area, Islamabad, Pakistan, where all the tablet manufacturing equipment and testing instruments were available. Table 1 indicates the composition of all matrix formulations of the model drug (Levosulpiride). To formulate the tablets, the model drug, polymers, and excipients (except glidants and lubricants) were first passed individually from mesh #16 and then mixed

Table 1. Formulation Sheet of Levosulpiride sustained-release tablets

Formulation	Drug (Levosulpiride) (%)	Polymers		MCC (%)	Talc (%)	Mg stearate (%)
		Name	(%)			
F1	12.5	HPMC (K100LV)	50	35	1.25	1.25
F2	12.5	HPMC (K100LV)	65	20	1.25	1.25
F3	12.5	HPMC (K100LV)	75	10	1.25	1.25
F4	12.5	HPC (K100M)	50	35	1.25	1.25
F5	12.5	HPC (K100M)	65	20	1.25	1.25
F6	12.5	HPC (K100M)	75	10	1.25	1.25
F7	12.5	CMC sodium	50	35	1.25	1.25
F8	12.5	CMC sodium	65	20	1.25	1.25
F9	12.5	CMC sodium	75	10	1.25	1.25

MCC: Microcrystalline cellulose, HPMC: Hydroxypropyl methyl cellulose, HPC: Hydroxypropyl cellulose, CMC: Carboxy methyl cellulose, Mg: Magnesium

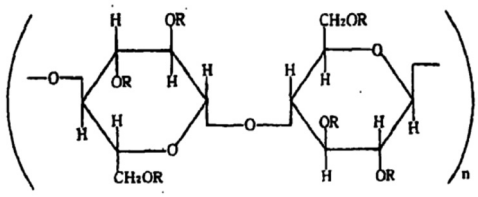

Figure 3. The chemical structure of hydroxypropyl cellulose

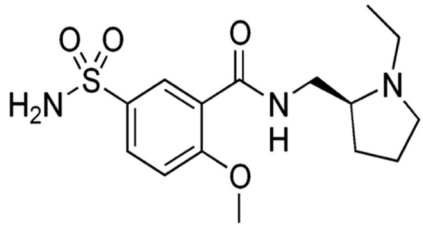

Figure 4. The chemical structure of Levosulpiride

for 15 min. The contents were mixed for a further 5 min after the addition of lubricants and glidants. The bulk was then compressed into tablets using a ZP-17 tablet compression machine (Shanghai Tianfeng, China). Before subjecting the bulk to the various physical tests, the micrometric properties of the powders were determined. The prepared formulations of the model drug were then evaluated for the various physical parameters.

Characterization

Micrometric properties of powders

Powder flow plays an important role in the manufacturing of a fine tablet. The flow properties of the powder blends were evaluated by determining the bulk density, tapped density, and angle of repose.

Bulk density

To measure the bulk density, a pre-sieved powder blend was carefully poured into a dry graduated cylinder without compaction and the weight and volume were measured. The unit of bulk density is g/mL and is given by

$$D_b = \frac{M}{V_0}$$

Where M represents the mass of powder and V_0 represents the bulk volume of the powder.

Tapped density

Tapped density was calculated by pouring a known mass of powder blend in a graduated cylinder placed on a mechanical tapping apparatus. The compact volume of the powder after tapping was measured. Tapped density is also expressed as g/mL and is given by

$$D_t = \frac{M}{V_t}$$

Where M represents the mass of powder and V_t is the tapped volume of the powder.

Angle of repose

The funnel method was adopted to measure the angle of repose. The powder was allowed to drop from the funnel to form a cone to a maximum height. The diameter of the heap (D) and height of the heap (h) was measured and the angle of repose (θ), which was calculated using the following formula:

$$\text{Tan}\theta = \frac{h}{r}$$

$$\theta = \text{Tan}^{-1}\left(\frac{h}{r}\right)$$

Where, h is the height in cm, r is the radius, and θ is the angle of repose.

Weight variation

The weight variation of tablets was calculated as per the method described in the B.P using an electronic balance (Sartorius). The individual weights were then compared with the average weight for the determination of weight variation.

Hardness or crushing strength of tablets

The hardness test represents the structural integrity and the point at which the tablet breaks during storage, transportation, and handling before use. Moreover, the hardness of the tablet also affects the disintegration time. The hardness was measured using a digital hardness tester.

Thickness of tablets

Variation in tablet thickness may cause problems during counting and packaging. The thickness of tablets was determined using Vernier calipers.

Friability of tablets

Tablets from each formulation were selected randomly and weighed. The pre-weighed tablets were then placed in the plastic chamber of Roche friabilator. The friabilator allows the tablets to face a combined effect of abrasion and shock in a plastic chamber revolving at 25 rpm. After four min (100 revolutions), the tablets were removed, de-dusted, and weighed again. The following formula was used to calculate the friability of the tablets:

$$\frac{W_1 - W_2}{W_1} X100$$

Where W_1 is the initial weight of the tablets and W_2 is the final weight.

Content uniformity of tablets

The tablets were also evaluated for the content uniformity by randomly selecting a specific number of tablets from each formulation and weighed on a suitable tare container. The tablets were then powdered using a pestle and mortar and a solution of Levosulpiride was prepared in a 100-mL volumetric flask by dissolving the powder equivalent to 25

mg of Levosulpiride in 0.1 N NaOH. Further dilutions were made and the absorbance of the resultant solutions was measured against the standard at a wavelength of 214 nm using a UV-visible spectrophotometer.

Calculations

$$\%\text{Assay} = \frac{A_1}{A_2} X100$$

Where:

A_1 = Absorbance of sample

A_2 = Absorbance of working standard

In vitro drug release studies

A dissolution test was performed using dissolution test apparatus USP type II (Pharma test Germany) in phosphate buffer solution (pH 6.8) for all nine formulations of Levosulpiride. For this purpose, 900 mL of buffer solution was placed in each vessel of the dissolution test apparatus and the solution was allowed to reach a temperature of 37°C. A single tablet of Levosulpiride was placed in each vessel of the dissolution test apparatus and the apparatus was operated at a rate of 50 rpm. Five milliliters of the sample were collected from each vessel after defined intervals and was filtered and diluted with the dissolution medium. After each sampling, fresh dissolution medium was added to the vessels in order to maintain the volume of the dissolution medium.[24] The absorbance of the samples and standard were then measured using a UV-visible spectrophotometer.

Fourier-transform infrared (FTIR) spectroscopy

The structure and intermolecular interactions between components of the tablets were investigated using FTIR spectroscopy. The FTIR spectra of the tablets and individual components were recorded using a Thermo-Fischer Scientific Nicolet 6700 FTIR spectrometer at 8 cm^{-1} resolution averaging 256 scans. The spectra were collected over the 4000-400 cm^{-1} range.

Drug release kinetics

To evaluate the kinetics and *in vitro* drug release data, different mathematical models were used including the zero order rate equation, which describes the system where the drug release rate is independent of its concentration:[25]

$$Q = kt \quad (1)$$

Where Q is amount of undissolved drug at time t, K is the zero order rate constant, and t is time.

The first order rate equation describes the system where the drug release rate is dependent on its concentration:[26]

$$LogC = LogC_0 - kt / 2.303 \quad (2)$$

Where C_0 is the initial concentration of drug and K is the first order constant.

The Higuchi model is an invaluable framework that has been used to develop a number of drug delivery systems. A direct relationship between the amount of drug released from a matrix system and square root of time is established using the Higuchi model.[27] It is expressed in equational form as follows:

$$Q = KV\ t \quad (3)$$

Where Q represents the percent of drug released in time; K is Higuchi's constant and t is the time.

The Hixson-Crowell cube root law describes drug release from systems where there is a change in surface area and diameter of particles or tablets.[28] The mathematical expression of this model is shown below:

$$Q_0^{1/3} - Q_t^{1/3} = K_{HC}\ t \quad (4)$$

Q_0 is the initial amount of the drug in tablet, Q_t is the amount of drug released in time (t), and K_{HC} is the Hixson-Crowell rate constant.

A simple relationship to describe the release behavior of a drug from hydrophilic matrix systems was developed by Korsmeyer-Peppas, which is mathematically expressed as follows:

$$M_t / M_\alpha = K_{kp} t^n \quad (5)$$

Where M_t / M_α is the fraction of drug released in time (t), K_{kp} is the rate constant incorporating the properties of macromolecular polymeric system and drug, and n is the release exponent used to characterize the transport mechanism.[29] The n value is used to describe various release mechanisms for cylindrical-shaped devices as shown in Table 2.

Table 2. Diffusion exponent and solute release mechanism for various systems

Diffusion exponent	Solute diffusion mechanism
0.45	Fickian diffusion
0.45<n<0.89	Anomalous (non-Fickian) diffusion
0.89	Case-II transport
n>0.89	Super case-II transport

RESULTS AND DISCUSSION

Flow properties of powders

The particle size of powders was found to be in the range of 760-890 µm, which resulted in free-flow properties of the powders. The data given in Table 3 show that the angle of repose for all formulation was <30 degrees, which clearly depicts that the granules had excellent flow characteristics.

Weight variation

The standard weight of Levosulpiride tablet was selected as 200 mg and the standard limit for weight variation was set as ± 5%. Twenty tablets from each formulation were selected and individual tablet weights were calculated. The results shown in Table 4 indicate that all results were within the specified range, which was also studied previously by Abdel-Rahman et al.[30]

Hardness of tablets

It is better considered that the hardness of uncoated tablets should not be less than 5 kg/cm^2. A minimum of 6 tablets should

be tested for hardness. Ten tablets from each formulation were selected and their hardness was calculated. According to Table 4, the average hardness of the tablets of all formulations was within the specified range, as previously described by Vueba et al.[13]

Thickness of tablets

Ten tablets from each formulation were taken and average thickness values were calculated. The usual thickness range of tablets weighing up to 250 mg is 3-4 mm. According to the results indicated in Table 4, the average thicknesses of the tablets of all formulations were within the specified limits.

Friability of tablets

The friability of tablets should be less than 1%. Twenty tablets from each formulation were selected at random and their percent friability was calculated. According to the results shown in Table 4, all results were within the specified limits.

Table 3. Evaluation of powder flow for Levosulpiride sustained-release tablets

S. no	Formulation	Angle of repose	Bulk density (g/mL)	Tapped density (g/mL)
1	F1	29.01±0.18	0.700±0.02	0.830±0.001
2	F2	28.76±0.09	0.730±0.05	0.850±0.003
3	F3	28.13±0.18	0.718±0.01	0.865±0.002
4	F4	29.22±0.18	0.747±0.04	0.889±0.006
5	F5	25.01±0.18	0.710±0.02	0.836±0.001
6	F6	24.76±0.09	0.735±0.05	0.854±0.003
7	F7	29.13±0.18	0.713±0.01	0.869±0.002
8	F8	28.22±0.18	0.765±0.04	0.881±0.006
9	F9	27.01±0.18	0.701±0.02	0.840±0.001

All data are reported as mean±SD, n=3 per experiment

Content uniformity of tablets

Twenty tablets from each formulation were selected randomly. Table 4 represents the content uniformity of each formulation and it is evident that each formulation was within the official limits i.e., 95-105%.

In vitro drug release studies

To study the *in vitro* drug release behavior from the polymer matrix in simulated intestinal medium, dissolution studies were conducted for all formulations. The dissolution test was performed using USP type II dissolution apparatus. The tablets were placed in 900 mL of phosphate buffer solution maintained at 37±1°C and the apparatus was operated at 50 rpm for 8 hrs. To study the effect of the polymer on drug release, the polymer-drug ratio was altered. Formulations F1, F2, and F3 contained HPMC, F4, F5, and F6 contained HPC, and F7, F8, and F9 contained CMC sodium in an increasing order of polymer drug ratio. The percentage of drug release from the matrix tablets as shown in Table 5, which indicates that the drug release from the formulations reduced as the polymer ratio increased, irrespective of the type of polymer used. The data also show that Levosulpiride release from the matrix tablet was sustained over an extended period of time at pH 6.8 and the sequence of retarding the drug release was found as CMC sodium > HPC > HPMC. Among the three polymers, CMC sodium proved to be the best retarding material and formulation 9 was found to be the best one. Figure 5, 6, 7 indicates the individual *in vitro* drug release profile of all the developed matrix tablet samples. Figure 8 represents the cumulative percentage release of all the formulations.

FTIR spectroscopy

The FTIR spectra of pure Levosulpiride, CMC sodium, and their blends are given in Figure 9, 10, and 11, respectively. The FTIR spectrum of Levosulpiride demonstrates sharp transmittance bands for (C-H) at 2810 cm^{-1}, which also appears in the final spectrum. The characteristic (–OH/–NH) bands in Levosulpiride at 3124 cm^{-1} and 3367 cm^{-1} also shifted to short and broader peaks, which depicts the involvement of these groups in interfacial H-bonding between the components.

Table 4. Evaluation of Levosulpiride sustained-release tablets

Formulation	Average weight (mg)	Average hardness (kg)	Average thickness (mm)	Friability (%)	Assay (%)
F1	205	6.5	3.40	0.52	97
F2	201	6.4	3.56	0.74	101
F3	200	6.3	3.60	0.46	102
F4	198.9	6.2	3.90	0.28	95
F5	202	7.0	3.80	0.19	98
F6	199.6	6.9	3.80	0.48	102
F7	199	6.8	3.62	0.67	97
F8	202	7.0	3.62	0.43	103
F9	200	6.9	3.62	0.22	98

All data are reported as mean±SD, n=3 per experiment

The other important contributions from Levosulpiride are the presence of an amide I band corresponding to (C=O) vibration of the acetyl group at ~1623 cm^{-1} and (C–N) stretching vibration at ~1060 cm^{-1}, which can also be seen in CMC sodium. FTIR spectroscopy revealed that no chemical interaction occurred between the components.

Drug release kinetics

Using zero order, first order kinetic models, the Higuchi, Hixon–Crowell, and Korsmeyer–Peppas models, drug-release kinetics were investigated. The values of drug-release constant (k) and regression coefficient (r) were obtained.

To examine the drug release mechanism, the data obtained from all nine formulations was fitted into the various kinetic models. The results obtained from the kinetic models are presented cumulatively in Table 6. It is evident from the data that the formulations released the drug according to Higuchi's pattern. The "n" value for all formulations was found to be greater than 0.5, which according to the Peppas model, approximates the non-Fickian diffusion mechanism, as shown in Table 6.

Figures 12, 13, 14 show the graphs for the Higuchi model for formulations 07-09.

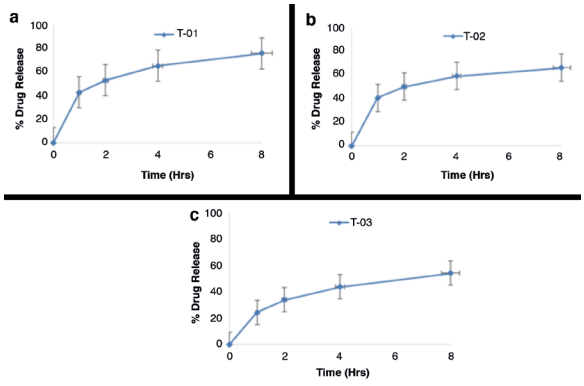

Figure 5. *In vitro* drug release profile of formulations a) T-01 b) T-02 c) T-03 after 8 hours in phosphate buffer solution of pH 6.8 at 37°C

CONCLUSIONS

SR tablets of Levosulpiride were prepared successfully using polymers such as HPMC, HPC, and CMC sodium in varying concentrations. The particle size and drift behavior of the granules were found to be in accordance with the official standards. Direct compression method was selected on the basis of Good compressibility index of the granules. The physical properties of compressed tablets like thickness, hardness, weight variation and friability were in compliance with the official limits. Free-flowing powder facilitates the formation of tablets with ideal properties. The drug release was primarily controlled by the type and concentration of polymers and a slight change in polymer concentration resulted in altered drug release. On the basis of these results, it can be concluded that the drug release could be further prolonged if the polymers are used in combination because of their possible interaction and subsequent cross-linking. The kinetic model that best fits to the release data was found as the Higuchi's equation, followed by zero order with non-Fickian behavior over an 8-hr period. The objective of the study was met through the formulation of a novel SR formulation of Levosulpiride, which will help to

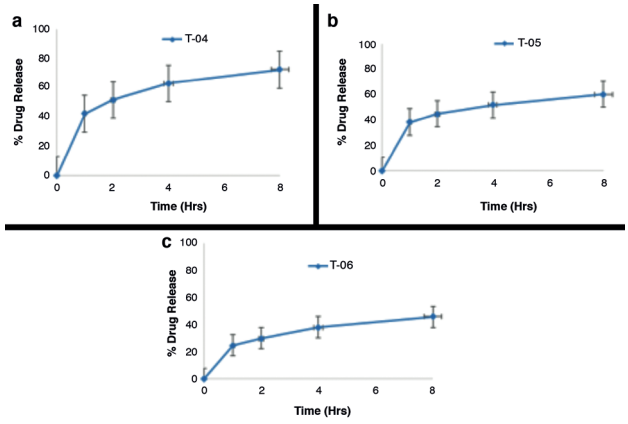

Figure 6. *In vitro* drug release profile of formulations a) T-04 b) T-05 c) T-06 after 8 hours in phosphate buffer solution of pH 6.8 at 37°C

Table 5. *In vitro* drug release data from compressed matrix tablets of Levosulpiride

S. No	Formulation	Percentage release of Levosulpiride			
		1st hour	2nd hour	4th hour	8th hour
1	F1	43.22%	53.52%	65.96%	76.44%
2	F2	41.02%	50.27%	59.39%	66.68%
3	F3	24.64%	34.18%	44.14%	54.40%
4	F4	42.28%	57.61%	62.98%	72.55%
5	F5	38.26%	44.81%	51.91%	60.41%
6	F6	24.53%	29.79%	37.90%	45.82%
7	F7	37.48%	47.81%	59.90%	69.42%
8	F8	26.95%	36.93%	46.56%	56.95%
9	F9	13.18%	21.99%	29.71%	39.66%

All data are reported as mean±SD, n=3 per experiment

Table 6. Data showing *in vitro* release kinetics of various formulations of Levosulpiride in buffer pH 6.8

Formulation	Zero-order		First-order		Higuchi		Hixon-Crowel		Korsmeyer-Peppas		Result
	R^2	K	R^2	K	R^2	K	R^2	K	R^2	n	
F1	0.680	7.705	0.865	-0.160	0.976	18.04	0.887	0.097	0.993	0.864	AM
F2	0.620	6.512	0.764	-0.116	0.989	13.74	0.859	0.078	0.994	0.881	AM
F3	0.782	5.817	0.875	-0.088	0.981	16.01	0.884	0.115	0.991	0.871	AM
F4	0.664	7.237	0.834	-0.140	0.976	16.43	0.889	0.091	0.994	0.881	AM
F5	0.620	5.815	0.748	-0.095	0.991	11.94	0.927	0.074	0.990	0.876	AM
F6	0.729	4.703	0.748	-0.095	0.992	11.72	0.927	0.091	0.993	0.864	AM
F7	0.699	7.105	0.849	-0.131	0.969	17.31	0.872	0.100	0.990	0.881	AM
F8	0.761	6.005	0.864	-0.093	0.979	16.03	0.882	0.110	0.991	0.871	AM
F9	0.870	4.491	0.918	-0.058	0.998	14.09	0.872	0.134	0.993	0.881	AM

AM: Anomalous

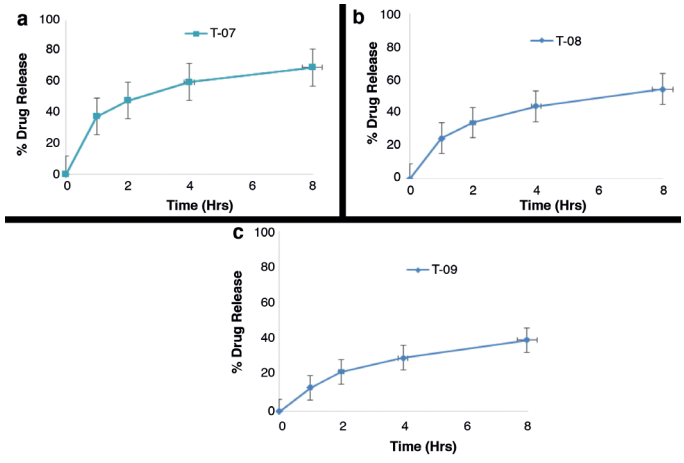

Figure 7. *In vitro* drug release profile of formulations a) T-07 b) T-08 c) T-09 after 8 hours in phosphate buffer solution of pH 6.8 at 37°C

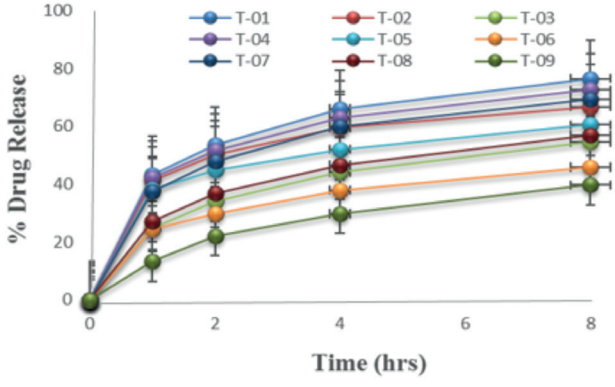

Figure 8. *In vitro* drug release profile of Levosulpiride sustained-release tablets of all the prepared 09 samples after 8 hrs in phosphate buffer solution of pH 6.8 at 37°C

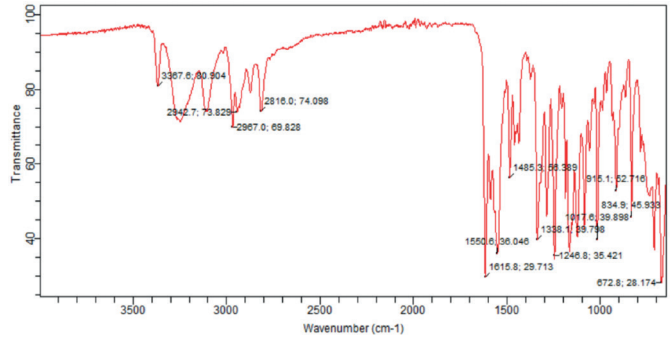

Figure 9. Fourier-transform infrared-spectrum of pure Levosulpiride

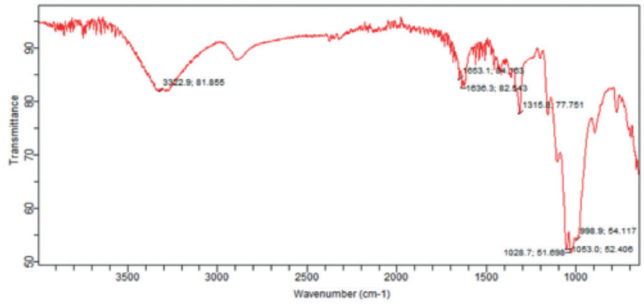

Figure 10. Fourier-transform infrared spectrum of carboxy methyl cellulose sodium

reduce dosing frequency, plasma drug level fluctuations, dose-related adverse effects and improve patient compliance. These prepared tablets can be evaluated in the future for their stability studies and *in vivo* behavior and to develop an *in vitro-in vivo* correlation.

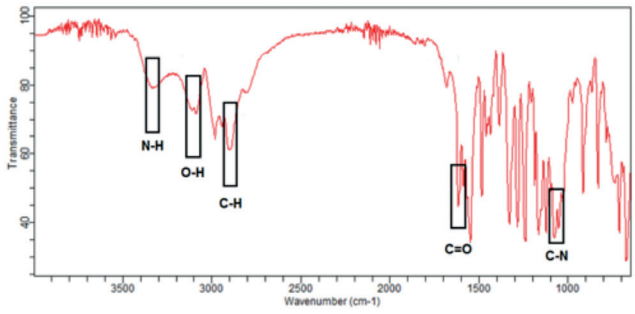

Figure 11. Fourier-transform infrared spectra of Levosulpiride and carboxy methyl cellulose sodium

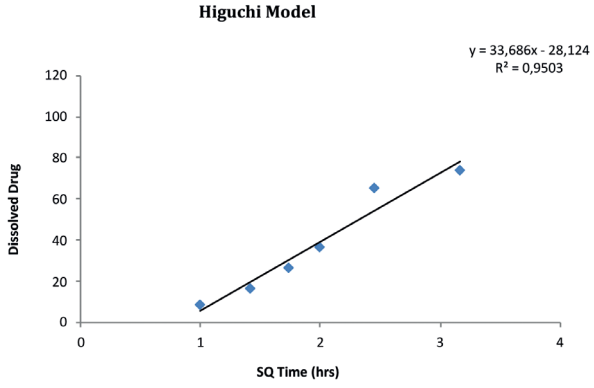

Figure 12. Graph of Higuchi model for formulation T-07

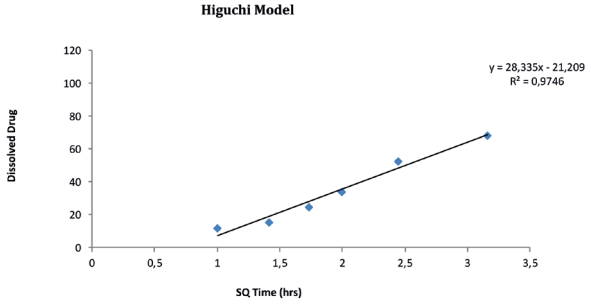

Figure 13. Graph of Higuchi model for formulation T-08

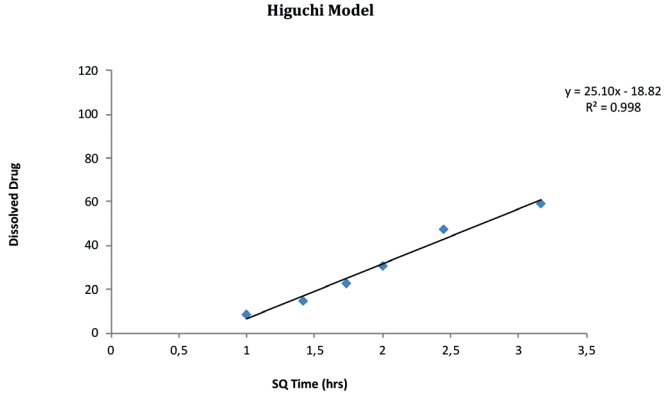

Figure 14. Graph of Higuchi model for formulation T-09

ACKNOWLEDGEMENTS

We thanks Aims Pharmaceuticals (pvt) Ltd. Kahuta triangle Industrial Area Islamabad, Pakistan for providing us the tablet manufacturing and testing facilities.

Conflict of Interest: No conflict of interest was declared by the authors.

REFERENCES

1. Gilhotra RM, Ikram M, Srivastava S, Gilhotra N. A clinical perspective on mucoadhesive buccal drug delivery systems. J Biomed Res. 2014;28:81-97.
2. Aulton ME, Taylor K. The Design and Manufacture of Medicines. Aulton's Pharmaceutics (4th ed). Churchill Livingstone; New York; 2013:894.
3. Hughes JP, Rees S, Kalindjian SB, Philpott KL. Principles of early drug discovery. Br J Pharmacol. 2011;162:1239-1249.
4. Nokhodchi A, Raja S, Patel P, Asare-Addo K. The role of oral controlled release matrix tablets in drug delivery systems. Bioimpacts. 2012;2:175-187.
5. Tanaka N, Imai K, Okimoto K, Ueda S, Tokunaga Y, Ohike A, Ibuki R, Higaki K, Kimura T. Development of novel sustained-release system, disintegration-controlled matrix tablet (DCMT) with solid dispersion granules of nilvadipine. J Control Release. 2005;108:386-395.
6. Prajapati ST, Patel LD, Patel DM. Gastric floating matrix tablets: design and optimization using combination of polymers. Acta Pharm. 2008;58:221-229.
7. Sastry SV, Khan MA. Aqueous based polymeric dispersion: Plackett--Burman design for screening of formulation variables of atenolol gastrointestinal therapeutic system. Pharm Acta Helv. 1998;73:105-112.
8. Reddy KR, Mutalik S, Reddy S. Once-daily sustained-release matrix tablets of nicorandil: formulation and in vitro evaluation. AAPS PharmSciTech. 2003;4:61.
9. Florence A, Attwood D. Physicochemical principles of pharmacy: In manufacture, formulation and clinical use (6th ed). Pharmaceutical Press; 2016:296-297.
10. Salsa T, Veiga F, Pina ME. Oral Controlled-release Dosage Forms. I. Cellulose Ether Polymers in Hydrophilic Matrices. Drug Dev Ind Pharm. 1997;23:929-938.
11. Guo JH, Skinner GW, Harcum WW, Barnum PE. Pharmaceutical applications of naturally occurring water-soluble polymers. Pharm Sci Technolo Today. 1998;1:254-261.
12. Liu J, Zhang F, McGinity JW. Properties of lipophilic matrix tablets containing phenylpropanolamine hydrochloride prepared by hot-melt extrusion. Eur J Pharm Biopharm. 2001;52:181-190.
13. Vueba ML, Batista de Carvalho LA, Veiga F, Sousa JJ, Pina ME. Influence of cellulose ether polymers on ketoprofen release from hydrophilic matrix tablets. Eur J Pharm Biopharm. 2004;58:51-59.
14. Colombo P. Swelling-controlled release in hydrogel matrices for oral route. Adv Drug Deliv Rev. 1993;11:37-57.
15. Sinha Roy D, Rohera BD. Comparative evaluation of rate of hydration and matrix erosion of HEC and HPC and study of drug release from their matrices. Eur J Pharm Sci. 2002;16:193-199.
16. Maev IV, Samsonov AA, Karmanova EA, Ivanchenko EA. The use of prokinetics for the correction of motor and tonic digestive disorders. Klin Med (Mosk). 2009;87:49-53.

17. Lozano R, Concha MP, Montealegre A, de Leon L, Villalba JO, Esteban HL, Cromeyer M, García JR, Brossa A, Lluberes G, Sandí EI, Quirós HB. Effectiveness and safety of levosulpiride in the treatment of dysmotility-like functional dyspepsia. Ther Clin Risk Manag. 2007;3:149-155.

18. Rossi F, Forgione A. Pharmacotoxicological aspects of levosulpiride. Pharmacol Res. 1995;31:81-94.

19. Distrutti E, Fiorucci S, Hauer SK, Pensi MO, Vanasia M, Morelli A. Effect of acute and chronic levosulpiride administration on gastric tone and perception in functional dyspepsia. Aliment Pharmacol Ther. 2002;16:613-622.

20. Serra J. Levosulpiride in the management of functional dyspepsia and delayed gastric emptying. Gastroenterol Hepatol. 2010;33:586-590.

21. Karamanolis G, Tack J. Promotility medications--now and in the future. Dig Dis. 2006;24:297-307.

22. Tonini M, Cipollina L, Poluzzi E, Crema F, Corazza GR, De Ponti F. Review article: clinical implications of enteric and central D2 receptor blockade by antidopaminergic gastrointestinal prokinetics. Aliment Pharmacol Ther. 2004;19:379-390.

23. Herbert MK, Holzer P. Standardized concept for the treatment of gastrointestinal dysmotility in critically ill patients--current status and future options. Clin Nutr. 2008;27:25-41.

24. Nagarsenker MS, Garad SD, Ramprakash G. Design, optimization and evaluation of domperidone coevaporates. J Control Release. 2000;63:31-39.

25. Xu G, Sunada H. Influence of formulation change on drug release kinetics from hydroxypropylmethylcellulose matrix tablets. Chem Pharm Bull (Tokyo). 1995;43:483-487.

26. Bourne DWA. Pharmacokinetics. In: Banker GS, Rhodes CT, eds. Modern Pharmaceutics (4th ed). Marcel Dekker Inc; New York; 2002:67.

27. Higuchi T. Mechanism of sustained action medication. Theoretical analysis of rate of release of solid drugs dispersed in solid matrices. J Pharm Sci. 1963;52:1145-1149.

28. Hixson AW, Crowell JH. Dependence of Reaction Velocity upon surface and Agitation. Ind Eng Chem. 1931;23:923-931.

29. Siepmann J, Peppas NA. Modeling of drug release from delivery systems based on hydroxypropyl methylcellulose (HPMC). Adv Drug Deliv Rev. 2001;48:139-157.

30. Abdel-Rahman SI, Mahrous GM, El-Badry M. Preparation and comparative evaluation of sustained release metoclopramide hydrochloride matrix tablets. Saudi Pharm J. 2009;17:283-288.

Turk J Pharm Sci 2018;15(3):319-327
DOI: 10.4274/tjps.33042

ORIGINAL ARTICLE

Formulation and Optimization of Gentamicin Hydrogel Infused with Tetracarpidium Conophorum Extract via a Central Composite Design for Topical Delivery

Gentamisin Hidrojelinin Tetrakarpidium Conophorum Ekstraktı ile Aşılanarak Formülasyonu ve Optimizasyonu

Margaret Okonawan ILOMUANYA[1]*, Nosakhare Andrew AMENAGHAWON[2], Joy ODIMEGWU[3], Omotunde Olufunke OKUBANJO[1], Chinelo AGHAIZU[1], Adeyinka OLUWATOBILOBA[1], Thomas AKIMIEN[1], Tolulope AJAYI[1]

[1]University of Lagos, Faculty of Pharmacy, Department of Pharmaceutics and Pharmaceutical Technology, Lagos, Nigeria
[2]University of Benin, Faculty of Engineering, Department of Chemical Engineering, Edo State, Nigeria
[3]University of Lagos, Faculty of Pharmacy, Department of Pharmacognosy, Lagos, Nigeria

ABSTRACT

Objectives: Response surface methodology coupled with statistically designed experiments has been found to be very useful in optimising multivariable processes. The aim of this study was to evaluate the influence of two independent variables, a ratio of permeation enhancers/antioxidants (transcutol and ethanolic extract of tetracarpidium conophorum EETC) and stirring rate, on the flux and permeation of gentamicin hydrogel.

Materials and Methods: A modification of free radical initial polymerization was used to formulate the gentamicin hydrogel. A 32 factorial CCD was then used to investigate the effect of independent variables of the permeation enhancer transcutol: EETC (X1), stirring speed (X2) via 14 formulation batches, which were evaluated for dependent variables flux (Y1) and amount of drug permeated after 12 hours (Y2) *ex vivo*.

Results: The results of ANOVA performed to determine the fit of the models revealed that the models were statistically significant ($p<0.05$) and did not show lack of fit ($R2>0.80$). The regression equation generated for flux was $Y1=19.35 - 25.82X1 - 0.044X2 + 0.0097X1X2 + 11.86X21$ and for cumulative permeation of gentamicin in 12 hours $Y2=315.50 - 189.67X1 + 0.28X2 - 1.29X1X2 + 123.55X21$. The validity of the statistical models used for predicting flux and drug permeation was confirmed by conducting three confirmation experimental runs at the identified optimum conditions. The results showed that there was no significant difference between the experimental results and those predicted by the statistical models.

Conclusion: The excellent correlation between the predicted and measured values shows the validity of statistical models ($R2=0.95$). An antioxidant and permeation enhancer has been used for the first time to investigate the influence on dependent variables. Optimization of gentamicin hydrogel using central composite statistical design is valid for the prediction of drug permeation and flux using variables in formulation.

Key words: Hydrogels, polymer, *Tetracarpidium conophorum*, response surface methodology, gentamicin

ÖZ

Amaç: İstatistiksel olarak tasarlanmış deneyler ile birleştirilmiş cevap yüzey metodolojisinin, çok değişkenli proseslerin optimize edilmesinde çok yararlı olduğu bulunmuştur. Bu çalışmanın amacı, iki bağımsız değişkenin, permeasyon arttırıcı/antioksidanların (transkutol ve tetrakarpidium conophorum EETC'nin etanolik ekstresi) ve karıştırma hızının, gentamisin hidrojelinin akışı ve permeasyonu üzerindeki etkisini değerlendirmektir.

Gereç ve Yöntemler: Gentamisin hidrojelini formüle etmek için serbest radikal başlangıç polimerizasyonunun modifikasyonu kullanıldı. Daha sonra, permeasyon arttırıcı transkutol: EETC (X1), karıştırma hızı (X2) bağımsız değişkenlerinin etkisini araştırmak için, bağımlı değişkenler, akış (Y1) ve 12 saat *ex vivo* permeasyondan sonra elde edilen ilaç miktarı (Y2), için değerlendirilen, 14 formülasyon grubuyla, 32 faktöriyel merkez CCD kullanılmıştır.

*Correspondence: E-mail: milomuanya@unilag.edu.ng, Phone: +2348033295077 ORCID-ID: orcid.org/0000-0001-8819-1937
Received: 05.09.2017, Accepted: 19.10.2017

Bulgular: Modellerin uyumunu belirlemek için yapılan ANOVA sonuçları, modellerin istatistiksel olarak anlamlı olduğunu ($p<0.05$) ve uyumsuzluk göstermediğini ortaya koymuştur ($R2>0.80$). Akış için oluşturulan regresyon denklemi Y1=19.35 - 25.82X1 - 0.044X2 + 0.0097X1X2 + 11.86X21 idi ve 12 saatte gentamisinin kümülatif permeasyonu Y2=315.50 - 189.67X1 + 0.28X2 - 1.29X1X2 + 123.55X21 idi. Akış ve etkin madde permeasyonunu tahmin etmek için kullanılan istatistiksel modellerin geçerliliği, belirlenen optimum şartlarda üç doğrulama deneysel çalışması ile onaylanmıştır. Sonuçlar, deney sonuçları ile istatistiksel modeller tarafından tahmin edilenler arasında anlamlı bir fark olmadığını göstermiştir.

Sonuç: Öngörülen ve ölçülen değerler arasındaki mükemmel korelasyon istatistiksel modellerin geçerliliğini göstermektedir ($R2=0.95$). Bağımlı değişkenler üzerindeki etkiyi araştırmak için ilk kez bir antioksidan ve geçirgenlik arttırıcı kullanılmıştır. Gentamisin hidrojelinin istatistiksel merkez esaslı kompozit tasarım kullanılarak optimizasyonu, formülasyondaki değişkenleri kullanarak etkin madde permesyonu ve akışın tahmin edilmesi için geçerlidir.

Anahtar kelimeler: Hidrojeller, polimer, *Tetracarpidium conophorum*, cevap yüzey metodolojisi, gentamisin

INTRODUCTION

Gentamicin is a water-soluble aminoglycoside antibiotic derived from *Micromonospora purpurea*, and actinomycete. It is used for the treatment of infections caused by susceptible strains of *Pseudomonas aeruginosa*, *Proteus* species (indole-positive and indole-negative), *Escherischia coli*, *Klebsiella-Enterobactor-Serratia* species, *Citrobacter* species, and *Staphylococcus* species (coagulase-positive and coagulase-negative). When required for topical administration, it is usually formulated as creams as well as ointments, which possess various disadvantages in terms of reduced stability, erratic drug release, and decreased skin permeability when compared with hydrogels.[1]

The water holding capacity and permeability are the most important characteristic features of a hydrogel.[2] Biocompatibility is the third most important characteristic required by a hydrogel because it calls for compatibility of the gel with human natural tissue without causing any toxicity upon its degradation.[2] In addition to the above characteristics, the soft and rubbery nature of hydrogels minimises irritation to surrounding tissue. Their highly porous structure, which can easily be tuned by controlling the density of the cross-links in the gel matrix and the affinity of the hydrogels for the aqueous environment in which they are swollen,[3] is also an advantage. The porosity of hydrogels also permits loading of drugs into the gel matrix and subsequent drug release at a rate that is dependent on the diffusion coefficient of the small molecule or macromolecule through the gel network.[3]

Tetracarpidium conophorum, commonly called the African walnut plant, whose ethanolic extract would make up the second component of the formulation of study, is a perennial climbing shrub 10 to 20 feet high, found growing wild in forest zones of sub-Sahara Africa, including Nigeria. Studies have shown that the African walnut possess some beneficial antibacterial,[4] antioxidant,[4,5] and immune-stimulating properties. It is commonly used in Nigerian folkloric medicine for the treatment of bacterial infections and ailments caused by oxidative stress.[6] Photochemical screening of ethanolic extracts of *Tetracarpidium conophorum* showed presence of alkaloids, saponins, glycosides, flavonoids, and tannins in studies by Ezealisiji et al.[6] The antibacterial properties of this plant extract can be attributed to the presence of these secondary metabolites. By incorporating these extracts into a three-dimensional polymer network formed by hydrophilic polymer chains via either physical or chemical bonds, hydrogels will be used to form a novel drug delivery system comprising components that will work synergistically to facilitate wound healing.[7]

In the development of a topical dose form, an important issue was to design an optimized pharmaceutical formulation with an appropriate penetration rate within a short time period with minimum trials. Traditional experiments require more effort, time, and materials when a complex formulation needs to be developed. Recently, response surface methodology (RSM) via central composite design (CCD) coupled with statistically designed experiments has been found to be very useful in optimising multivariable processes and it has been successfully applied to the optimisation of many bioprocesses.[8-11] Based on the principle of design of experiments, the methodology encompasses the use of various types of experimental designs, generation of polynomial equations, and mapping of the response over the experimental domain.

In this investigation, we explored the utility of RSM via CCD for the optimization of topical gentamicin hydrogel production using a two variable CCDs via free radical initial polymerization of the alkyl acrylate polymer. The developed optimised formulation was evaluated for performance-related *in vitro* drug release and *ex vivo* permeation study. Physicochemical characterization of the gel was conducted via rheologic studies, drug content evaluation, Fourier-transform infrared spectroscopy (FTIR), and the mechanism of release was evaluated via varying kinetic models.

EXPERIMENTAL

Chemical and reagents

Gentamicin sulphate (BP grade) was obtained as a gift from Drugfield Pharmaceuticals Limited (Ogun State, Nigeria), Carbopol Ultrez 21® was obtained as a gift from Metchem Limited (Mumbai India/Lubrizol Corporation, USA), Carbopol 940® (Lubrizol Corporation, USA), propylene glycol, triethanolamine (TEA) (Merck Germany), Transcutol® was obtained as a gift from Gattefosse (Cedex, France), O-Phthalaldehyde OPA from Fluka (Steiheim Germany). N-acetyl cysteine (NaC) sodium hydroxide was from Sigma Aldrich (St. Louis, USA). All other chemical and reagents were of analytical grade.

Extraction of ethanolic extract of Tetracarpidium conophorum (EETC)

The plant was collected from farms in Nkwere Local Government Area, Imo state, Nigeria, and identified by Mr Oyebanji O.O of

the Department of Botany, University of Lagos, Lagos, Nigeria. A voucher specimen assigned reference number LUH6972 was deposited in the institutional herbarium for reference.

The methanolic extract of the leaves was obtained using a method by Amaeze et al.,[5] 2011. The plants were air dried for 14 days and the leaves were separated and ground using a Retsch rotor mill ZM 200. Two hundred grams of the finely ground leaves of *T. conophorum* were weighed and placed in a container with 2 litres of ethanol and allowed to macerate for 24 hrs, and then filtered. The extraction was performed three times and the combined filtrate was centrifuged at 3000 rpm using a Sorvall ST 8 centrifuge. The EETC obtained was freeze dried, transferred into a glass vial, and kept in a desiccator at 20˚C until analysis.

Preparation of gentamicin-loaded acrylate copolymer based hydrogels

Gentamicin sulphate (0.1% w/w) was dissolved in aliquots of purified water and propylene glycol was titrated in drops into the mixture. The permeation enhancer Transcutol:EETC (antioxidant extract) in varying ratios 2% v/v and 10% v/v propylene glycol were incorporated into the aqueous phase of the formulation. At 25˚C, the gel phase was prepared by dispersing the alkyl acrylate cross-polymers Carbopol® Ultrez 21 (1.5% w/v) in purified water using a mechanical stirrer at a predetermined stirring rate. The pH was adjusted with the cross-linking agent TEA to a pH of 5.5. Both the aqueous fraction and the gel fraction were then mixed at a varying stirring rates to form the polymeric hydrogel. The hydrogels were stored in sealed glass containers for further analysis.

FTIR

Gentamicin, EETC, and Carbopol Ultez 21® compatibility was evaluated using FTIR. Physical mixtures of gentamicin, the polymers (Carbopol Ultrez 21) and excipients (1:1) were separately mixed with three parts of potassium bromide and compressed to form pellets with a hydraulic press at 10 tons' pressure. The FTIR absorption spectra of all samples were recorded in the range of 400-4000/cm using the potassium bromide disc method with FTIR spectroscopy (Bruker, South Africa). The optimized hydrogel formulation was also analysed via FTIR. The physical appearance of the samples and the appearance (or disappearance) of peaks in the spectra were observed to access any possible physical or chemical interactions.

Experimental design

A two-variable, CCD was used for the formulation of the gentamicin hydrogels. The independent variables tested included the Transcutol:EETC ratio and stirring speed. These variables were varied over five levels and replicated six times at the centre point to result in a total of fourteen experimental runs. The ranges of the independent variables are shown in Table 1. Two responses, namely flux (µg/cm^2/hr) and the amount of drug permeated after 12 hours (µg/cm^2) were chosen for optimisation using RSM. The experimental observations were analysed using Design Expert® 7.0.0 software (Stat-ease, Inc. Minneapolis, USA). The coded and actual values of the independent variables were calculated using Equation (1).

$$X_i = \frac{X_i - X_0}{\Delta X_i} \quad (1)$$

Where x_i and X_i are the coded and actual values of the independent variable, respectively. X_o is the actual value of the independent variable at the centre point and ΔX_i is the step change in the actual value of the independent variable. The experimental data was fitted according to Equation (2) as a second-order polynomial equation including the main effects and interaction effects of each variable. One-way analysis of variance (ANOVA) and response surface plots were generated using Design Expert and the optimised value of the independent variables for optimum response was determined using numerical optimisation.

$$Y_i = b0 + \sum b_i X_j + \sum b_{ij} X_i X_i + \sum b_{ii} X^2_i + e_i \quad (2)$$

where Y_i is the dependent variable or predicted response, X_i and X_j are the independent variables, b_o is offset term, b_i and b_{ij} are the single and interaction effect coefficients, and e_i is the error term.

Physical evaluation of hydrogel formulation

The hydrogels were physically examined for colour, homogeneity, and consistency.

pH evaluation

The pH of the hydrogels was recorded using a pH meter (Ashford, UK), ensuring that the electrode was in contact with the formulated hydrogel for 45 seconds to allow for equilibration. Experiments were performed in triplicate.

Rheologic studies

The viscosities of the varying formulations were determined at 25˚C at varying rpm with the aid of a cone and plate viscometer with spindle-4, (Brookfield Engineering Laboratories, DV-E Digital viscometer ID:12020N15).

Drug content determination

One gram of hydrogel was dissolved in 10 mL of water, centrifuged at 500 rpm for 45 mins, and filtered using a 0.5-µm millipore filter. Using a 1:50 dilution, the concentration of gentamicin was obtained using a ultraviolet (UV)/visible spectrophotometer (UV-Vis 2600 Shimadzu Analytical and measuring instruments) after derivatisation using O-Phthalaldehyde reagent with Kowalczuk's method.[12] Phthalaldehyde reagent was formulated prior to use by dissolving 20 mg of O-Phthalaldehyde in 1.0

Table 1. Experimental range of independent variables for a two factor CCD

Independent variables	Symbols	Coded and actual levels				
		-1.414	-1	0	1	1.41
Transcutol:EETC (-)	X_1	1/3	3/7	2/3	0.902	1
Stirring speed (rpm)	X_2	60	77.57	120	162.43	180

EETC: Ethanolic extract of *Tetracarpidium conophorum,* CCD: Central composite design

mL of methanol to 1.5 mL of a 10% NaC and diluting to 10 mL with 0.2 mL^{-1} solution of borate buffer (pH 10). Gentamicin, an aminoglycoside antibiotic, does not absorb UV light due to its weak chromophore, hence the need for derivatisation. The phthalaldehyde reagent was stored in amber-coloured bottles and kept in a dark cupboard prior to use. The reaction of the amine group in the aminoglycoside with the O-Phthalaldehyde in the presence of NaC yields a fluorescent isoindole which is measured at 332 nm absorbance.[12] This method is superior to that used by Nnamani et al.,[1] where mercaptoethanol, emits a characteristic unpleasant odour during the derivatization process.

Preparation of wistar rat abdominal skin

The hair of ether anesthetized Wistar rats weighing between 150-200 g was carefully removed with electric clippers, and the full thickness of skin was removed from the abdominal region. The epidermis was prepared surgically using a heat separation technique,[13] which involved soaking the entire abdominal skin in water at 60˚C for 45 s, followed by careful removal of the epidermis. The epidermis was washed three times with water and used for *ex vivo* permeability studies.

Ex vivo permeation studies

Permeation studies were performed using skin obtained from the rats (skin thickness 0.45-0.8 mm) mounted on modified Franz diffusion cells with a diffusion area of 3.71 cm^2. The receptor compartment contained 30 mL phosphate buffer (pH of 7.4 at 37.1˚C±0.2˚C). One gram of each hydrogel formulation was applied on the skin surface in the donor compartment area with the stratum corneum facing downwards. An aliquot of 1 mL was withdrawn at predetermined time intervals and replaced with an equal volume of fresh media. The samples were analysed using a UV/visible spectrophotometer (UV-Vis 2600 Shimadzu Analytical and measuring instruments) after derivatisation using O-Phthalaldehyde reagent. Absorbance was measured at 332 nm. All experiments were performed in triplicate.

Cumulative amounts of permeated drug (µg/cm^2) was plotted against time in hours and drug (µg/cm^2/hr) at steady state was calculated by dividing the slope of the linear portion of the curve by the area of the exposed skin surface (3.71 cm^2). The permeation coefficient was deduced by dividing the flux by initial drug load as shown in Equations 3 and 4:

$$PEc = \delta Q (A\ \delta t)^{-1} / Co \quad (3)$$

$$PEc = Jss / Co\ (cm/hr) \quad (4)$$

where PEc is the permeation coefficient (cm/hr^{-1}); Co is the initial drug concentration in the drug compartment: Jss represents the steady state flux (µg/cm^2/hr), where Q indicates the quantity of substances crossing the rat skin, A is the area of the rat skin exposed, and t is the time of exposure in hours.

The optimised gentamicin hydrogel derived from statistical analysis was then compared with a marketed gentamicin formulation via *ex vivo* permeation studies and the data obtained were evaluated using ANOVA followed by Tukeys test at $p<0.05$.

Ex vivo permeation kinetics of drug release

The mechanism of drug release from the hydrogels was analysed by fitting the release data to various release kinetic models. The zero-order (Ko), first order (Kf), and Korsemeyer-Peppas model was used to determine the model with the best fit.[1,11]

Accelerated stability testing

The International Council for Harmonisation of Technical Requirements for Pharmaceuticals for Human Use (ICH) guidelines (40˚C/75% RH) were followed in the accelerated stability testing of the optimised hydrogel formulation. The hydrogels were packed in amber-coloured jars and kept in a stability chamber with a set temperature and relative humidity. The formulations were subjected to accelerated stability testing at both room temperature and at 40˚C and parameters were recorded on day 0, 10, 15, 30, and 90. The formulations were evaluated for pH, assay, gel index (GI), and percentage of drug released at 12 hours.

The study was approved by the College of Medicine, University of Lagos Health Research Ethics Committee (CMULHREC number: CMUL/HREC/04/17/117, 15.04.2015).

Statistical analysis

The data were expressed mean standard deviation (±SD) using ANOVA (±SD). Significant differences ($p<0.05$) of mean values were determined using the Tukey test.

RESULTS

FTIR spectroscopy

The individual spectra and the physical mixture spectra were recorded and analysed. The finger print region and absorbance values relating to the relevant bioactive functional groups of the individual spectra analysed and the physical mixtures showed an absence of interaction between gentamicin, carbopol, and Transcutol and EETC as shown in Figure 1. Absorbance patterns corresponding in position and relative intensity to those in the FTIR spectra of the individual components were observed with no significant change in FTIR spectra after introduction of the polymers and the permeation enhancers, thus indicating a lack of physical or chemical interaction, as shown in Figure 1.

Some major bands/peaks on the spectra were 3089.75 cm^{-1} O-H stretching, 1706.88 cm^{-1} carboxyl group, which is characteristic of the principal absorption peaks of Carbopol®. Gentamicin was characterized by principal peaks at 610.22 cm^{-1} and 1100-1400 cm^{-1}. The spectral data of EETC confirmed the presence of functional groups such as hydroxyl, an ester group and an aldehyde group among others 2920.21 cm^{-1} - –C-H stretching depicting alkenes and aryl groups, 1730.32 cm^{-1} - aldehyde/ ketone –C=C- stretching at 1440 cm^{-1}. For the compatibility study, the FTIR spectra were compared and there was no disappearance or major shift of important peaks in the physical mixtures of Carbopol®, EETC, and Transcutol spectra.

Gel characterization

All formulations had a pale greenish colour and a good gel-like consistency. The hydrogels formulated using the CCD had

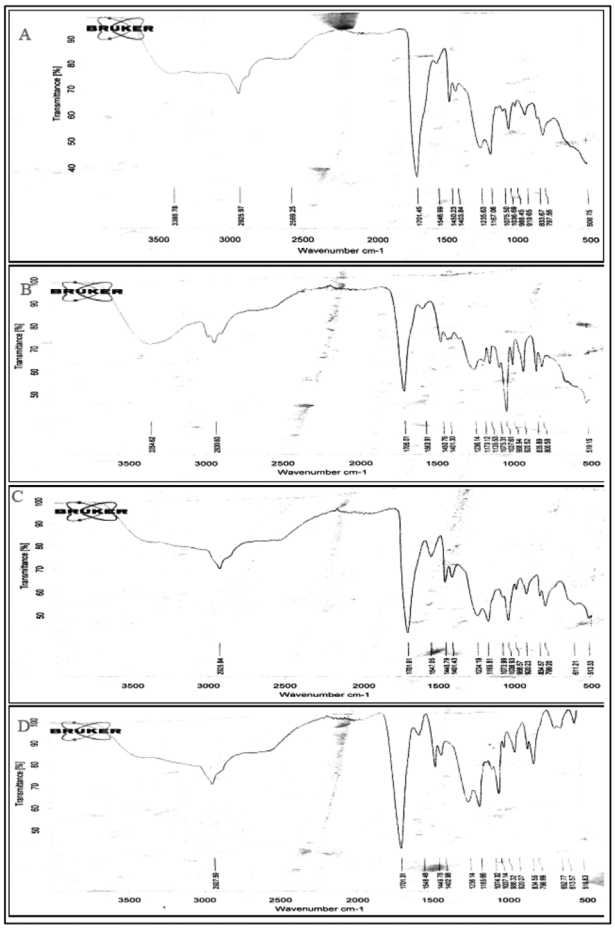

Figure 1. Fourier-transform infrared spectroscopy peaks of A) Gentamicin and the physical mixtures of Carbopol® (B) Physical mixtures of Carbopol® and EETC, (C) Physical mixtures of Carbopol® and EETC:Transcutol (D) Hydrogel formulation containing Carbopol®, EETC Transcutol and all other excipients

drug content variation form 94.5%-102.9% had excellent *ex vivo* permeation profiles, GeH 11 had 258.06 µg/cm^2±0.43 of gentamicin permeated at eight hours in as seen in Figure 2. The pH of all the 14 hydrogel formulations ranged of 5.50-5.95 after neutralization with TEA as shown in Table 2. This pH range is important for use on the surface of wounds to facilitate wound healing at an acidic pH.[1,3]

Rheologic measurements

Spindle 4 was used for the viscometric characterisation of the hydrogels. Characterisation was performed at 20-60 rpm, which is the working range for this spindle. As the shear rate increased there was a corresponding decrease in the viscosity of the gels. This was evaluated exponentially using the Power Law as shown in Equation 3.

$$T = K D^n \quad (5)$$

where T is shear stress, K is GI or consistency index, D is shear rate, and n is fow index. Gel indices computed ranged from 1.02 to 2.11 as shown in Table 2.

Statistical modelling and analysis

Analysis of the experimental data using the Design Expert software revealed that the quadratic model was suitable for describing the formulation of the hydrogels. The final statistical models for predicting the flux and the amount of drug permeated after 12 hours are given in Equations 6 and 7.

$$Y=19.35-25.82X_1 -0.044X_2 +0.0097X_1X_2 +11.86X_1^2 \quad (6)$$

$$Y=31.50-189.67X_1 -0.28X_2 +1.29X_1X_2 +123.55X_1^2 \quad (7)$$

The values of the responses as predicted by Equations 4 and 5 are presented in Table 3 alongside the experimental data for comparison. The results of ANOVA conducted to determine the fit of the statistical models for flux and drug permeation are presented in Tables 3, 4, and 5.

Table 2. Observed responses in the central composite design for gentamicin hydrogels

Hydrogel formulation	pH	Assay (%)	PEc (cm/hr)	Gel index	Kinetic modelling		
					Zero-order (Ko)	First-order (Kf)	Higuchi model (Kh)
GeH 1	5.67±0.05	98.65±0.11	1.77	1.02	0.912	0.567	0.943
GeH 2	5.69±0.04	98.73±0.28	1.91	1.76	0.893	0.329	0.954
GeH 3	5.78±0.32	99.43±0.78	1.72	1.89	0.903	0.510	0.964
GeH 4	5.51±0.09	101.02±0.21	1.85	1.76	0.911	0.622	0.932
GeH 5	5.86±0.03	98.82±0.88	1.70	1.65	0.954	0.476	0.954
GeH 6	5.54±0.48	99.72±0.01	1.69	1.97	0.963	0.619	0.922
GeH 7	5.88±0.11	100.07±0.29	1.73	1.56	0.945	0.409	0.973
GeH 8	5.89±0.77	98.99±0.89	1.71	2.00	0.953	0.743	0.917
GeH 9	5.61±0.37	98.62±0.67	1.77	1.97	0.944	0.599	0.972
GeH 10	5.92±0.11	99.89±0.32	1.78	1.56	0.891	0.421	0.954
GeH 11	5.93±0.07	100.33±0.06	1.93	2.11	0.932	0.511	0.911
GeH 12	5.55±0.32	101.77±0.03	1.72	1.99	0.894	0.613	0.919
GeH 13	5.63±0.04	102.31±0.15	1.73	1.34	0.843	0.412	0.963
GeH 14	5.78±0.12	100.99±0.45	1.72	1.69	0.909	0.592	0.951

Tables 3, 4, 5, and 6 show the results of ANOVA conducted to determine the fit of the statistical models representing the flux and drug permeation after twelve hours. Tables 3 and 4 show that the models for flux and drug permeation were statistically significant with very low p values of 0.0001 and 0.0019, respectively. The single-effect model terms representing the effect of Transcutol:EETC ratio and stirring speed for both models (Equations 5 and 6) were significant indicating changes in the values of these variables could affect the flux and drug permeation.

Table 5 shows that the models for flux and drug permeation had high R^2 values of 0.90 and 0.82, respectively. The R^2 value indicates the degree to which a model is able to predict a response. The closer the R^2 value is to unity, the better the model can predict the response.[14,15] The high R^2 values obtained for both models show that there was significant fit between the observed and predicted values of flux and drug permeation. Table 5 also shows that the SD of the observations was relatively small compared with the mean values of flux and drug permeation showing that there was very little dispersion about the mean for the data predicted by both models. The experimental runs were performed with high reliability and precision as seen from the relatively low values of coefficient of variation obtained for flux and drug permeation (8.75 and 12.27, respectively).[16] The adequate precision values of both models were greater than four. This shows that the models had adequate signals and thus could be used to navigate the design space.[17]

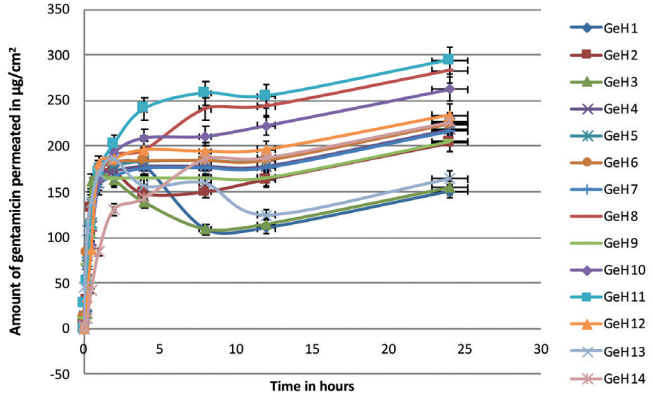

Figure 2. *Ex vivo* permeation profile of the varying gentamicin hydrogel formulations GeH 1-GeH 14

Effect of independent variables on hydrogel formulation

Figures 3 and 4 are response surface plots showing the effect of Transcutol:EETC ratio and stirring speed on the flux and

Table 4. ANOVA results for model representing flux

Sources	Sum of squares	df	Mean squares	F value	p value
Model	59.92	4	14.98	20.71	0.0001
X_1	35.41	1	35.41	48.94	<0.0001
X_2	21.18	1	21.18	29.28	0.0004
X_1X_2	0.038	1	0.038	0.053	0.8238
X_1^2	3.29	1	3.29	4.55	0.0617

ANOVA: Analysis of variance

Table 3. Experimental design matrix for gentamicin hydrogel formulation

Run	Factors				Responses			
	Coded values		Actual values		Flux (µg/cm²/hr)		Drug permeation (µg/cm²)	
	X_1	X_2	X_1	X_2	Actual	Predicted	Actual	Predicted
GeH 1	1	1	0.902	162.43	6.91	6.37	124.43	102.10
GeH 2	1	-1	0.902	77.57	9.25	9.43	186.93	176.70
GeH 3	-1.414	0	1/3	120.00	12.75	13.64	222.4	249.07
GeH 4	-1	-1	3/7	77.57	14.24	13.83	254.8	235.96
GeH 5	0	0	2/3	120.00	9.8	9.34	178.02	175.02
GeH 6	0	-1.414	2/3	60.00	11.21	11.64	196.26	209.49
GeH 7	0	0	2/3	120.00	8.57	9.34	163.78	175.02
GeH 8	1.414	0	1	120.00	7.63	7.69	114.21	128.71
GeH 9	0	1.414	2/3	180.00	5.59	7.03	110.21	140.55
GeH 10	0	0	2/3	120.00	9.71	9.34	184.98	175.02
GeH 11	-1	1	3/7	162.43	11.51	10.38	243.99	213.06
GeH 12	0	0	2/3	120.00	9.98	9.34	183.99	175.02
GeH 13	0	0	2/3	120.00	9.82	9.34	176.43	175.02
GeH 14	0	0	2/3	120.00	9.05	9.34	165.34	175.02

Table 5. ANOVA results for model representing drug permeation

Sources	Sum of squares	df	Mean squares	F value	p value
Model	20265.19	4	5066.30	10.50	0.0019
X_1	14486.89	1	14486.89	30.02	0.0004
X_2	4753.28	1	4753.28	9.85	0.0120
X_1X_2	667.96	1	667.96	1.38	0.2695
X_1^2	357.05	1	357.05	0.74	0.4120

ANOVA: Analysis of variance

drug permeation of the hydrogels, respectively. Lower levels of stirring speed and transcutol:EETC ratio enhanced the flux of the formulated hydrogel as shown in Figure 3. This is evidenced by the fact that the flux increased with a reduction in stirring speed. This observation was recorded at all values of Transcutol:EETC ratio investigated. A similar trend was also observed for the Transcutol:EETC ratio for all values of stirring speed investigated.

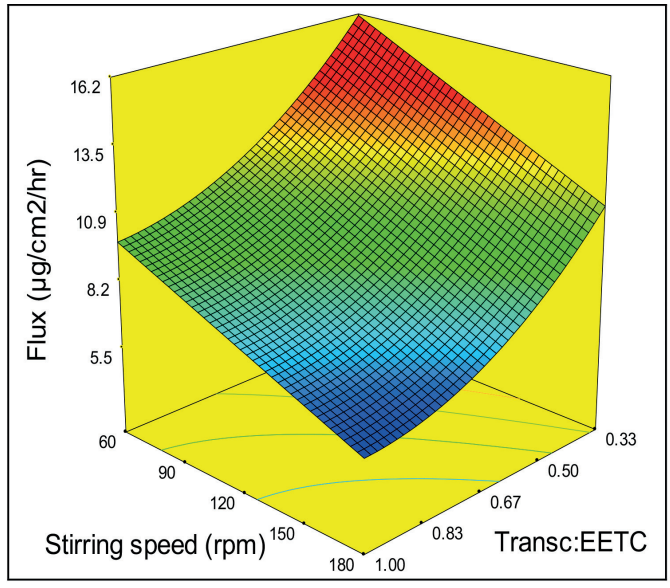

Figure 3. Effect of Transcutol:EETC ratio and stirring speed on flux

DISCUSSION

Gentamicin is freely soluble in water (hydrophilic) and much of the drug was present in the aqueous phase of the formulations, loosely attached at or near the particle surface, because the more hydrophilic the substance, the weaker the interaction with particle surface, and eventually the compound could be localized in the surfactant layer.[1] When more drug particles at the periphery of the particle surface eventually encounter the polymeric cross-linked gel-matrices, stabilization would occur.[18,19] Maximisation of skin uptake and delivery of a drug that is hydrophilic such as gentamicin in a hydrogel would thus be affected by increased stirring speeds above 60-77 rpm. Figure 4 shows that the drug permeation after twelve hours reduced with an increase in stirring speed. This trend was, however, more significant at a higher ratio of Transcutol to EETC compared with when the lower ratio was used. An increase of stirring speed above this point will ensure decreased porosity of the polymeric system increasing entrapment of the Transcutol:EETC within the hydrophilic matrix due to excessively intense agitation during formulation. This may consequently result in decreased release rates as seen in Figure 2 and 4, inadvertently negatively influencing permeation of gentamicin through the skin as seen in Figure 4.[1] A burst effect as result of increase stirring speed may also account for the decreased drug permeation with an increase in stirring speed as the drug is freed from the polymeric matrices and as such cannot be transported through the biologic membrane using transcutol:EETC. This effect will account for why there is a reduced flux at higher stirring speeds, as shown in Table 3, where the experimental values were closely correlated with the predicted responses.

EETC has been studied for toxicity and biocompatibility and has been seen to be nontoxic to and biocompatible with mammalian cell lines, thus informing its use in this formulation

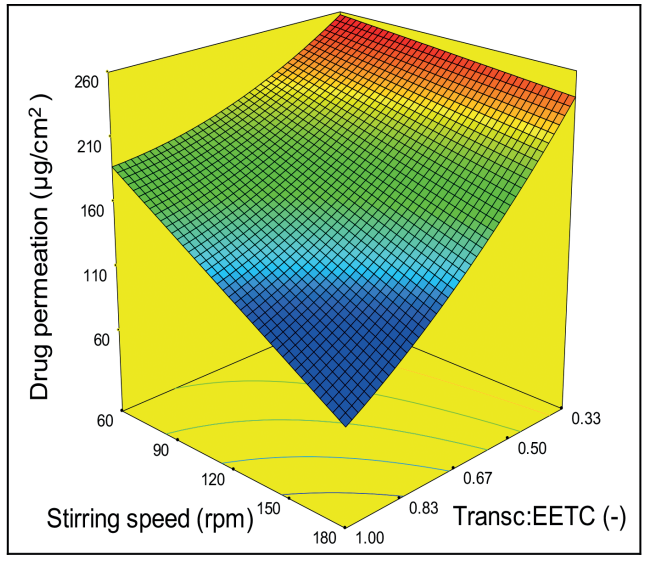

Figure 4. Effect of Transcutol:EETC ratio and stirring speed on drug permeation after 12 hours

development.[4-6] EETC is very high in antioxidants, which lower inflammatory markers and facilitate wound healing by promoting fibroblast migration. This combination of EETC with transcutol (2-(2-Ethoxyethoxy)ethanol), a chemical permeation enhancer, synergistically causes diffusional resistance of the stratum corneum, thereby increasing migration of gentamicin through the skin via increased solubility in the stratum corneum. Transcutol:EETC at high concentrations facilitates interaction with stratum corneum lipids to increase fluid into the skin producing increased flux, Pec, and ultimately drug permeation. There was an inverse relationship between the drug permeation after twelve hours and the transcutol:EETC ratio. This ensures that increased permeation occurs in the first

12 hours of hydrogel application. The flux obtained ranging from 9.05 to 14.42 μg/cm²/hr (accounting for release at the linear portion of the gentamicin permeation curve in Figure 1, which represents the first 4 hours of drug release and permeation) showed that GeH 4 with flux 14.42 μg/cm²/hr had the highest flux, which reflects increased permeation at an optimal stirring speed. This trend was observed both at high as well as at low values of stirring speed. However, the correlation between the drug permeation and transcutol:EETC ratio was more significant at high values of stirring speed due to the increased porosity of the hydrogel matrix. The mechanism of release predominantly observed was the Higuchi model, thus relating that the initial drug concentration in the hydrogel matrix was much higher than drug solubility with drug diffusion taking place in one dimension with edge effect being negligible, this accounts for increased release through pores in the matrix hydrogel system.

Optimisation of hydrogel formulation

Numerical optimization was performed to maximize the flux and drug permeation using the Design Expert software. The optimum conditions were chosen from the results obtained from the software possessing the highest desirability. These conditions are summarized in Table 6. The implication of these results is that the maximum flux and drug permeation can only be obtained if the independent variables are fixed at the values shown in Table 7. Accelerated stability testing of the optimized formulation showed that no variation in pH, assay, gel index, percentage of drug released at 12 hours was observed, as shown in Table 8.

Table 6. Statistical information for ANOVA

Parameter	Response	
	Flux	Drug permeation
R-squared	0.90	0.82
Mean	9.72	178.98
Standard deviation	0.85	21.97
C.V %	8.75	12.27
Adeq. precision	14.68	11.20

ANOVA: Analysis of variance

Table 7. Summary of optimum conditions for the formulation of hydrogels

Variables	Optimum value
Stirring speed (rpm)	60
Transcutol:EETC ratio (-)	1/3
Flux (μg/cm²/hr)	16.1
Drug permeation after 12 hours (μg/cm²)	258

EETC: Ethanolic extract of *Tetracarpidium conophorum*

Validation of statistical models

The validity of the statistical models used for predicting flux and drug permeation was confirmed by conducting three confirmation experimental runs at the identified optimum conditions (Table 6). The results showed that there was no significant difference between the experimental results and those predicted by the statistical models. The excellent correlation between the predicted and measured values shows the validity of the statistical models. Figure 5 shows the percentage of drug released from the optimised formulation in comparison with a marketed formulation. The *ex vivo* permeation study showed an improved release rate was obtained compared with the marketed topical formulation with 100% release occuring at 12 hours with a significant effect ($p<0.05$) compared with the marketed brand, which had 90% release at the same time point. This result is in consonance with the optimum value of drug permeation given in Table 7. Flux was obtained as 16.9 μg/cm²/hr compared with 9.98 μg/cm²/hr for the marketed formulation, and the amount of drug permeated after 12 hours was 260 μg/

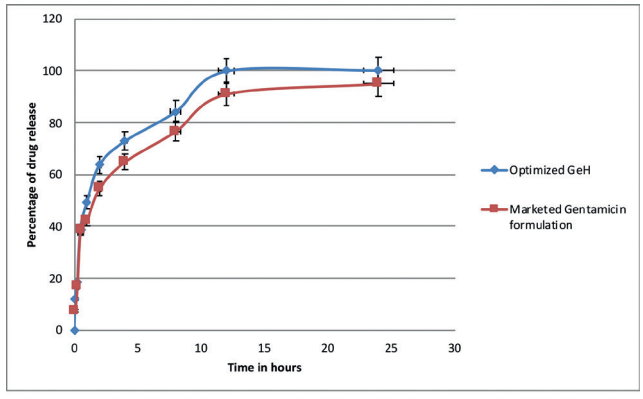

Figure 5 Comparison of percentage of gentamicin release from the optimised hydrogel fromulation and marketed gentamicin topical formulation against time in hours

Table 8. Accelerated stability testing on the optimized (GeH) gentamicin hydrogel at 40°C/75% RH ($p \leq 0.05$)

Duration	pH	Assay (%)	Gel index	Flux	Drug permeation after 12 hours (μg/cm²)	Appearance and homogeneity
Day 0	5.77±0.05	99.65±0.11	1.93±0.02	15.93±0.22	254.03±1.01	Satisfactory
Day 10	5.79±0.04	99.73±0.28	1.96±0.03	15.83±0.74	251.72±2.11	Satisfactory
Day 15	5.78±0.32	99.43±0.78	1.99±0.01	16.09±0.32	253.32±0.93	Satisfactory
Day 30	5.78±0.07	100.02±0.21	1.96±0.01	15.99±0.18	250.11±1.02	Satisfactory
Day 90	5.76±0.03	99.98±0.03	1.93±0.04	15.93±0.07	254.2±0.97	Satisfactory

cm^2 compared with 176 µg/cm^2 for the marketed formulation. The results are in consonance with the optimized values given in Table 7 from CCD with the solubilizing effect of the permeation enhancer/antioxidant ratio ensuring optimal flux and transdermal permeation within 12 hours at 60 rpm. All the gel formulations were stable at room temperature and under stressed conditions, as shown in Table 8, after accelerated stability testing.

CONCLUSIONS

Optimisation of gentamicin hydrogel using central composite statistical design is valid for the prediction of drug permeation and flux using variables in formulation preparation i.e. stirring speed and permeation enhancer:antioxidant ratio, thus showing their interaction with each other. The contour plots aided in the prediction of the value of transcutol:EETC and stirring speed, which would provide an optimized gentamicin hydrogel with optimal and drug permeation after 12 hours. The evaluation of therapeutic efficacy in an animal model is recommended for further studies.

ACKNOWLEDGEMENTS

The authors would like to thank Drugfield Pharmaceuticals Limited (Ogun State, Nigeria) for the gift of Gentamicin sulphate, Metchem Limited (Mumbai India) for the gift of Carbopol® Ultrez 21 and Gattefosse (Cedex, France) for the gift of Transcutol®.

Conflict of Interest: No conflict of interest was declared by the authors.

REFERENCES

1. Nnamani PO, Kenechukwu FC, Anugwolu CL, Attama AA. Evaluation of hydrogels based on Poloxamer 407 and polyacrylic acids for enhanced topical activity of gentamicin against susceptible infections. Tropical Journal of Pharmaceutical Research. 2014;13:1385-1391.
2. Gulrez SKH, Al-Assaf S, Phillips GO. Hydrogels: Methods of preparation, characterization and applications A. Carpi (Ed), Progress in molecular and environmental bioengineering - From analysis and modeling to technology applications, InTech Publisher; Rijeka, Croatia; 2011:117-150.
3. Goindi S, Narula M, Kalra A. Microemulsion-based topical hydrogels of tenoxicam for treatment of arthritis. AAPS PharmSciTech. 2016;17:597-666.
4. Ajaiyeoba EO, Fadare DA. Antimicrobial potential of extracts and fractions of the African walnut-*Tetracarpidium conophorum*. Afr J Biotechnol. 2006;5:2322-2325.
5. Amaeze OU, Ayoola GA, Sofidiya MO, Adepoju-Bello AA, Adegoke AO, Coker HA. Evaluation of antioxidant activity of *Tetracarpidium conophorum* (Müll. Arg) Hutch & Dalziel Leaves. Oxid Med Cell Longev. 2011;2011:976701.
6. Ezealisiji KM, Omotosho AE, Udoh R, Agbo MO. Wound healing activity of N-hexane and methanol extracts of *Tetracarpidium conophorum* (Mull. Arg) Hutch. (African walnut) in wistar rats. Malaysian Journal of Pharmaceutical Sciences. 2014;12:79-88.
7. Hasatsri S, Yamdech R, Chanvorachote P, Aramwit P. Physical and biological assessments of the innovative bilayered wound dressing made of silk and gelatin for clinical applications. J Biomater Appl. 2015;29:1304-1313.
8. Amenaghawon NA, Osemwengie SO, Omoregbe O, Asogwa UJ. Application of experimental design method for the optimisation of xanthan gum production from pineapple peels using Xanthomonas campestris via submerged fermentation. Nigerian Journal of Technology. 2015;34:491-498.
9. Gopinadh R, Ayyanna C, Ramakrishna CH, Narayana SKV, Ravi VK, Jagadhi R. Optimization of Chemical Parameters for the Production of Citric acid using Box-Behnken Design. J Bioprocess Biotech. 2015;5:1-6.
10. Thongdumyu P, Intrasungkha N, Thong SO. Optimization of ethanol production from food waste hydrolysate by co-culture of Zymomonas mobilis and Candida shehatae under non-sterile condition. Afr J Biotechnol. 2014;13:866-873.
11. Ilomuanya M, Billa N, Uboh C, Ifudu N, Ciallella J, Igwilo C. Formulation and characterization of activated charcoal and metronidazole layered tablets and evaluation of the *in vivo* performance of metronidazole - Activated charcoal formulation in Sprague Dawley® rat model infected with *Escherichia coli* O157:H7. International Journal of Pharmaceutical Sciences and Research 2017;8:45-59.
12. Kowalczuk D, Pietras R, Paw B, Czerkies A. Applying liquid chromatography with fluorescence detection to determine Gentamicin Polish J of Environ Stud. 2010;19:587-591.
13. Gannu R, Yamsani VV, Yamsani MR. Enhancement potential of Aloe vera on permeation of drugs with diverse lipophilicites across rat abdominal skin. Curr Trends Pharm Biotechnol. 2008;2:548-554.
14. Gethin G. The significance of surface pH in chronic wound Wounds UK; 2007;3:51-53
15. Amenaghawon NA, Osarumwense JO, Oti EO. Experimental design method for the production of bonded particleboards with optimum mechanical properties using sawdust. Journal of Civil, Construction and Environmental Engineering. 2016;14:73-82.
16. Montgomery DC. Design and Analysis of Experiments. 6. ed. New York; John Wiley & Sons, Inc; 2005.
17. Cao G, Ren N, Wang A, Lee DJ, Guo W, Liu B, Feng Y, Zhao Q. Acid hydrolysis of corn stover for biohydrogen production using Thermoanaerobacterium thermosaccharolyticum W16. International Journal of Hydrogen Energy. 2009;34:7182-7188.
18. Lu Z, Fassihi R. Influence of colloidal silicon dioxide on gel strength, robustness, and adhesive properties of diclofenac gel formulation for topical application. AAPS PharmSciTech. 2015;16:636-644.
19. Gannu R, Yamsani VV, Yamsani SK, Palem CR, Yamsani MR. Optimization of hydrogels for transdermal delivery of lisinopril by Box-Behnken statistical design AAPS PharmSciTech. 2009;10:505-514.

Turk J Pharm Sci 2018;15(3):328-332
DOI: 10.4274/tjps.03371

ORIGINAL ARTICLE

The Effect of Sumatriptan in Ischemic Conditions in the Rat Heart

Sumatriptanın Sıçan Kalbinde İskemik Koşullardaki Etkisi

Hande Özge ALTUNKAYNAK-ÇAMCA, Müge TECDER-ÜNAL, Meral TUNCER*

Başkent University, Faculty of Medicine, Department of Pharmacology, Ankara, Turkey

ABSTRACT

Objectives: The aim of this study was to investigate the effect of SUM on IR-induced injury in rat heart and its effect on IPC-induced protection.

Materials and Methods: The rats were randomly divided into four groups: IR, SUM-IR, IPC, and SUM-IPC. The mean arterial blood pressure and heart rate were recorded to calculate PRP. Standard limb lead 2 ECG were recorded to evaluate arrhythmia parameters.

Results: The PRP values in the SUM-IPC group were significantly lower than in the SUM-IR group at the beginning of reperfusion ($p<0.05$). The incidence of VT in the IPC, SUM-IR, and SUM-IPC groups was significantly lower than in the IR group ($p<0.05$). VF was only observed in the IR group.

Conclusion: SUM protects the heart against IR injury but is not as protective as IPC alone. Although SUM diminishes IPC-induced protection against VT, the preventive effect of SUM against VF may be predictive for cardioprotection in ischemic conditions.

Key words: Sumatriptan, heart, ischemia and reperfusion, ischemic preconditioning, arrhythmia

ÖZ

Amaç: Bu çalışmanın amacı, SUM'un, IR'nin sıçanlarda neden olduğu kardiyak hasar ve IPC'nin oluşturduğu koruyuculuk üzerine etkisini incelemektir.

Gereç ve Yöntemler: Sıçanlar rastgele olarak; IR, SUM-IR, IPC ve SUM-IPC gruplarına bölündü. Ortalama arteriyel kan basıncı ve kalp atım hızı, basınç hız ürününü (PRP) hesaplamak için kaydedildi. Aritmi parametrelerini değerlendirmek için standart EKG'ler kaydedildi.

Bulgular: SUM-IPC grubundaki PRP değerleri, SUM-IR grubundakilerden reperfüzyon başlangıcında anlamlı olarak daha düşüktü ($p<0.05$). IPC, SUM-IR ve SUM-IPC gruplarındaki VT insidansı, IR grubundakinden anlamlı olarak daha düşüktü ($p<0.05$). VF sadece IR grubunda gözlendi.

Sonuç: IPC'nin koruyucu etkisi kadar olmasa da, sumatriptan'ın kalbi IR hasarına karşı koruduğu gözlenmiştir. SUM VT'ye karşı IPC'nin oluşturduğu koruyuculuğu kısmen azaltsa da, VF'ye karşı önleyici etkisi iskemik koşullarda kalp için koruyucu olabilir.

Anahtar kelimeler: Sumatriptan, kalp, iskemi ve reperfüzyon, iskemik ön koşullama, aritmi

INTRODUCTION

5-hydroxytryptamine (5-HT; serotonin) has physiologic and pathophysiologic importance due to its effects on the periphery and the central nervous system.[1] In this regard, regulation of the cardiovascular system by 5-HT could result in complex effects such as hypotension/hypertension, vasodilatation/vasoconstriction, and bradycardia/tachycardia, primarily depending on which 5-HT receptors are involved.[2] Sumatriptan (SUM), a 5-$HT_{1B/1D}$ receptor agonist, was the prototype of triptans used for the acute treatment of acute migraine attacks.[3,4] Its therapeutic effect is closely linked with vasoconstriction of cranial blood vessels by the drug.[5] Although SUM is generally well tolerated in the acute treatment of migraine attacks, some chest symptoms (i.e. chest pressure, tightness, and pain) mimicking angina pectoris and even myocardial infarction and fatal arrhythmia have been reported after the use of SUM.[3,4,6-8] This could be related to the extracranial contractile effects of SUM including coronary vasoconstriction both *in vivo* and *in vitro*.[9,10] This effect is thought to be predominantly mediated by the agonistic activity of SUM at 5-HT_{1B} receptors.[6] Myocardial ischemia occurs when coronary blood supply to the myocardium is reduced (low-flow or no-flow ischemia), or relative to increased tissue demand (demand ischemia).[11] Reperfusion, that is, the re-

*Correspondence: E-mail: mtuncer@baskent.edu.tr, Phone: +90 312 246 66 83 ORCID-ID: orcid.org/0000-0003-3360-5092
Received: 07.09.2017, Accepted: 02.11.2017

admission of oxygen and metabolic substrates together with washout of ischemic metabolites is necessary for the viability of ischemic myocardium. However, reperfusion could also have deleterious effects on ischemic myocardium, the process termed as "reperfusion injury".[11] Therefore, protection from cardiac ischemia/reperfusion (IR) injury including arrhythmias, myocardial infarction, and contractile dysfunction has been the focus of intense research. Such a cardioprotective intervention is known as ischemic preconditioning (IPC), which applies brief non-lethal IR cycles before sustained ischemia of myocardium.[11]

Previous works suggested that the pressure rate product (PRP) could be an indirect index of myocardial oxygen consumption.[12,13] It has been demonstrated that the tachycardia induced by positive inotropic agents including digitalis glycosides and ouabain enhanced myocardial oxygen consumption.[14] As myocardial oxygen consumption increases, the heart rate (HR) is increased, and finally it negatively affects the cardiac function.[14]

There are some previous findings showing that SUM can induce an exacerbation of regional myocardial ischemia injury concomitant with a reduction in coronary blood flow.[9] To the best of our knowledge, no studies have evaluated the effect of SUM on IPC-induced protection. Therefore, we aimed to investigate the effects of SUM in ischemic conditions in rats subjected to IR.

MATERIALS AND METHODS

Animals

The study was approved by Başkent University Ethics Committee for Experimental Research on Animals (project no: DA11/11, protocol number: 2011/21, date: 21.03.2011). Twenty male Wistar albino rats (250-350 g) were used in this study. The rats were housed in cages at room temperature 21±1°C, under 12/12-hour light/dark cycles and were allowed access to standard laboratory diet and tap water ad libitum.

Surgical procedures

The rats were anesthetized using a ketamine/xylazine mixture (60/10 mg/kg, i.p.). The body temperature of the rats was measured using a rectal probe and maintained at 37±1°C with a lamp. Tracheotomy was performed to the anesthetized rats for mechanical ventilation through an animal ventilator (Rodent Ventilator 7025 UgoBasile, Italy, 5 mL/100 g, 34 pulse/min room air). A standard limb lead 2 electrocardiogram (ECG) and HR were continuously monitored and recorded throughout the experiments, using an ECG (100B; Biopac. System Inc., US) and a computerized data acquisition system. The right jugular vein and left carotid artery were cannulated for administration of SUM (3 mg/kg, i.v., bolus injection) and mean arterial pressure monitoring, respectively. The mean arterial blood pressure (MABP) and body temperature were also continuously monitored and recorded throughout the experiment using the same data acquisition system. Before the IR induction procedures, a left thoracotomy was performed through the fourth and fifth intercostal space, the pericardium was incised, and the heart was gently exteriorized. Afterwards, ischemia was induced by occlusion of the left anterior descending artery, close to its origin. Successful occlusion and ischemia were confirmed by a pronounced decrease in arterial pressure and ECG alteration. At the end of the study, the rats were sacrificed with a high-dose anesthetic.

Experimental protocols

The dose of SUM (3 mg/kg) was selected based on previously published studies.[15,16]

The rats were randomly divided into the groups as follows (n=5/group): IR group: following a stabilization period of 30 min, the rats were subjected to 10 min of ischemia followed by 10 min of reperfusion (Figure 1).

SUM-IR group: following a stabilization period of 10 min, a bolus SUM injection (3 mg/kg) was administered. 20 min after the SUM injection, the rats were subjected to 10 min of ischemia followed by 10 min of reperfusion (Figure 1).

IPC group: Following a stabilization period of 10-min, IPC was applied by 2 cycles of 5-min ischemia/5-min reperfusion.[17] Afterwards, the rats were subjected to 10 min of ischemia followed by 10 min of reperfusion (Figure 1).

SUM-IPC group: Following a stabilization period of 10 min, a bolus SUM injection (3 mg/kg) was performed and immediately after IPC was applied by 2 cycles of 5-min ischemia/5-min reperfusion. Afterwards, the rats were subjected to 10 min of ischemia followed by 10 min of reperfusion (Figure 1).

Measured and calculated parameters

Hemodynamic variables (MABP, HR) were monitored and recorded to calculate rate pressure product (PRP= MABP x HR / 1000) as an indirect index of myocardial oxygen consumption.[12,13] PRP was calculated after the surgical procedure (baseline), before and at the end of ischemia, at the beginning and end of the reperfusion.

The arrhythmia parameters were also evaluated from the ECG recordings of the rats in accordance with the Lambeth

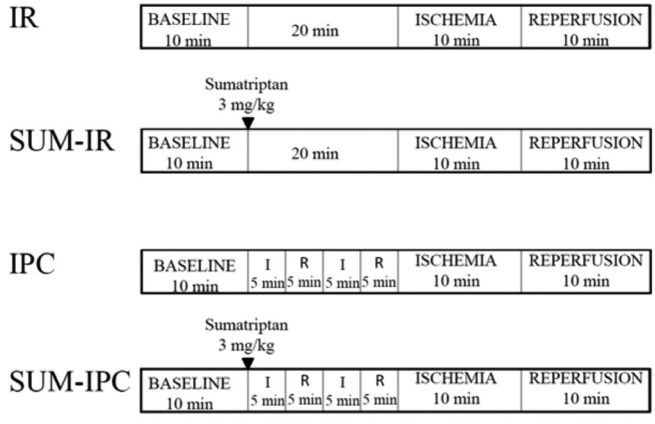

Figure 1. Schematic diagram illustrating experimental protocol

IR: Ischemia/reperfusion, SUM: Sumatriptan, IPC: Ischemic preconditioning, I: Ischemia, R: Reperfusion

conventions at the end of the experimental protocols.[18] The incidence of ventricular tachycardia (VT) and ventricular fibrillation (VF) were determined in each group.

Statistical analysis

Data are expressed as mean ± standard error and the percentage of the incidence. Data of PRP were analyzed using one-way analysis of variance followed by the Bonferroni post-hoc test (for selected columns). Incidence of arrhythmia was evaluated using Fisher's exact test. All analyses were conducted using the GraphPad Prism (version 5.00 for Windows, GraphPad Software, San Diego California USA). P values of <0.05 were considered statistically significant.

Drugs

SUM succinate (GlaxoSmithKline, Turkey) was dissolved in saline.

RESULTS

PRP values, calculated for myocardial oxygen consumption, during experimental protocols are shown in Figures 2A-E. PRP values at both baseline and before the ischemia did not significantly differ between the groups. However, the PRP value in the SUM-IPC group was significantly lower than that of the SUM-IR group at the beginning of the reperfusion (Figure 2D, $p<0.05$). Although there was a tendency for a decrease in the PRP value of the SUM-IPC group when compared with the IPC group, the difference was not significant at the end of the reperfusion (Figure 2E).

SUM produced a significant reduction in the incidence of VT in the SUM-IR and SUM-IPC groups (40%). In the IPC group, the incidence of VT was significantly lower than in the SUM-IPC group (10% and 40%, respectively, $p<0.05$) (Figure 3A).

VF was only observed in the IR group and the incidence was 80%. The administration of SUM both in the SUM-IR and in the SUM-IPC groups inhibited VF, similar to the IPC group alone (Figure 3B).

DISCUSSION

We investigated the effect of SUM in myocardial ischemic conditions in anesthetized rats. Our findings showed that SUM was cardioprotective against IR injury, but not as protective as IPC alone. The administration of SUM before IPC resulted in the reduction of myocardial oxygen consumption as shown by decreased PRP at the beginning of reperfusion. Despite that, it provided no additional protection from VT induced by IPC. In addition, administration of SUM alone to the rats subjected to IR in the SUM-IR group produced a reduction in the incidence of VT compared with the IR group. Among these groups, VF was only observed in the IR group. It appears that SUM is effective in preventing VF, similar to that of IPC.

IPC has been shown to decrease ischemia-induced arrhythmia in normal hearts.[19] Consistent with these findings, we demonstrated that IPC conferred a marked reduction in arrhythmogenesis as shown by the reduction in the incidence of VT and prevention of VF. Similarly, administration of SUM alone to the rats subjected to IR decreased the incidence of

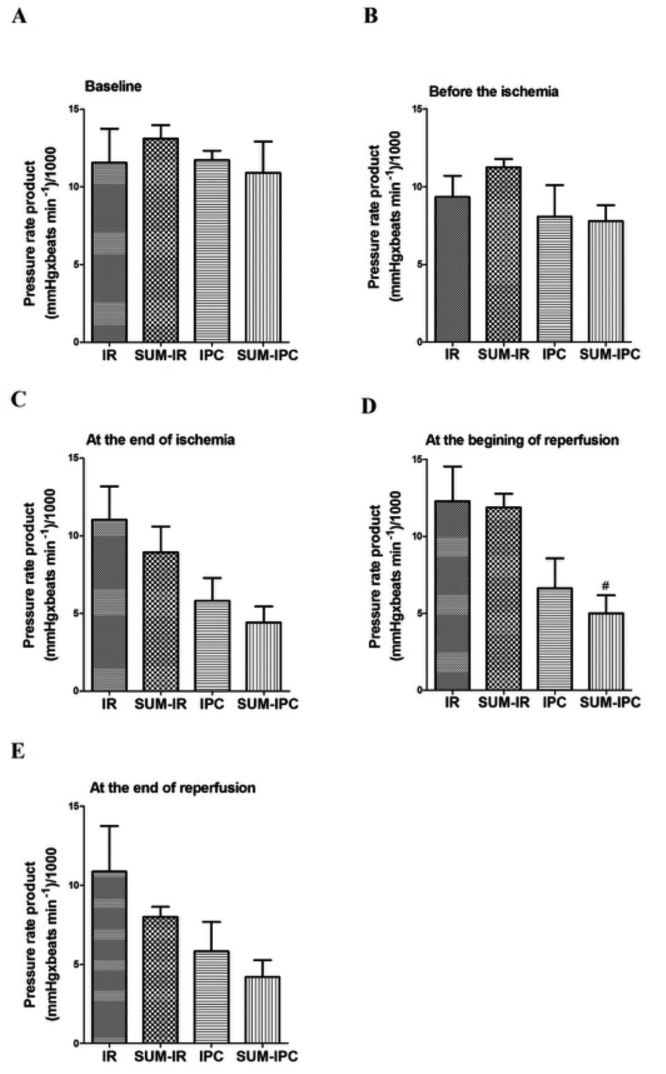

Figure 2. PRP values for baseline (A), before the ischemia (B), at the end of ischemia (C), at the beginning of the reperfusion (D) and at the end of reperfusion (E) in IR, SUM-IR, IPC and SUM-IPC groups

IR: Ischemia/reperfusion, SUM: Sumatriptan, IPC: Ischemic preconditioning, #$p<0.05$ vs SUM-IR

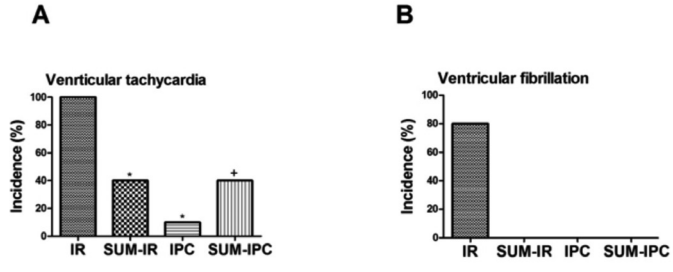

Figure 3. The incidence of ventricular tachycardia and ventricular fibrillation in IR, SUM-IR, IPC and SUM-IPC groups

IR: Ischemia-reperfusion, SUM: Sumatriptan, IPC: Ischemic preconditioning, *$p<0.05$ vs IR, +$p<0.05$ vs IPC

VT. However, it diminished IPC-induced protection against VT when applied before IPC. Interestingly, at the beginning of reperfusion, the myocardial oxygen consumption in the SUM-IPC group was lower than in the SUM-IR group. However, it provide no additional protection against VT in the SUM-IPC group.

Taken together, one might think that SUM could interfere with the common mechanisms of IPC. On the other hand, it may also mimic the IPC by leading to coronary vasoconstriction. Support for this conclusion comes from a number of studies in which SUM-induced contractions of coronary arteries have been shown both *in vivo* and *in vitro*.[9,10] Therefore, SUM might interfere with the common mechanisms of IPC. The majority of *in vivo* human angiographic and positron emission tomography studies with SUM reported very slight to no coronary artery constriction or reduction in myocardial perfusion with no association with ECG changes or anginal symptoms.[20-23] However, it was noticed that even modest epicardial coronary constriction could be sufficient to provoke an ischemic event in patients with coronary artery disease.[23] It has also been reported that SUM provoked coronary vasospasm in patients with variant angina but not in control subjects, suggesting the coronary constrictory effect of SUM may be more notable in patients with ischemic heart disease.[24] For this reason, SUM should be used with caution in these kinds of patients. Additionally the physicians must be aware when they prescribe sumatriptan for migraine attacks in patients with any cardiovascular symptoms.

Some mechanisms of IPC are associated with the release of substances such as adenosine, bradykinin, endothelin, and endorphins.[25] Some alternative protective mechanisms independent from signal transduction cascades mediated by antioxidant and anti-inflammatory mechanisms are also involved in IPC-induced protection.[25] Additionally, IPC exerts protection through a reduction of myocardial energy demand during ischemia.[26] In the present study, we demonstrated that myocardial oxygen consumption was decreased both in the IPC and SUM-IPC groups. Furthermore, the myocardial oxygen consumption in the SUM-IPC group was significantly lower than SUM-IR at the beginning of reperfusion. Despite that, the protective effect against VT was similar in both groups, but less than in the IPC group. Taken together, these findings exclude the possibility that neither IPC nor SUM protects the heart against VT by altering oxygen consumption of the myocardium. It could be thought that mechanism other than the decrease in oxygen consumption might contribute to this protection.

In our study, the duration of ischemia was sufficient to observe ischemia-induced arrythmias; however, a longer duration is necessary to see ischemia-induced infarct areas in the heart. It would be interesting to investigate whether SUM would be able to decrease the size of infarct area during longer durations of ischemia. In addition, the lack of molecular mechanisms underlying the effects of SUM concerning IPC in this protection is a limitation of the study. We hope that this study will lead to future research with SUM in different ischemic conditions.

CONCLUSIONS

In conclusion, the results of the study show that bolus injections of SUM alone protects the rat heart against IR injury by decreasing the incidence of arrhythmia. SUM is cardioprotective against arrhythmias in rats subjected to IR injury but not as protective as in IPC. However, the preventive effect of SUM against VF may be predictive for cardioprotection in ischemic conditions. Further studies are needed to elucidate which mechanisms of IPC interfere with SUM.

ACKNOWLEDGEMENTS

This study was supported by Başkent University Research Fund (DA 11/11). We thank GlaxoSmithKline (Turkey) for their generous gift of SUM and Seda Cal and Erkan Ermis (biologists of the Pharmacology Department); Adem Kurtçuoğlu and Sezai Kolçuk (Experimental Animals Production and Research Center Unit) for their technical assistance, and Yasemin Özerdem, Güldeniz Uzar, İdil Bahar Abdulazizoğlu, Cemre Çavuşoğlu, Gökçe Yağmur Efendi, and Hamit Koç (undergraduate students of Başkent University Medical Faculty) for observing as part of their education.

Conflict of Interest: No conflict of interest was declared by the authors.

REFERENCES

1. Ramage AG, Villalón CM. 5-hydroxytryptamine and cardiovascular regulation. Trends Pharmacol Sci. 2008;29:472-481.
2. Villalón CM, De Vries P, Saxena PR. Serotonin receptors as cardiovascular targets. Drug Discovery Today. 1997;2:294-300.
3. Weiss O. Ueber die Wirkungen von Blutserum-Injectionen ins Blut. Archiv für die Gesamte Physiologie des Menschen und der Thiere. 1896;65:215-230.
4. Hoyer D, Clarke DE, Fozard JR, Hartig PR, Martin GR, Mylecharane EJ, Saxena PR, Humphrey PP. International Union of Pharmacology classification of receptors for 5-hydroxytryptamine (Serotonin). Pharmacol Rev. 1994;46:157-203.
5. Duquesnoy C, Mamet JP, Sumner D, Fuseau E. Comparative clinical pharmacokinetics of single doses of sumatriptan following subcutaneous, oral, rectal and intranasal administration. Eur J Pharm Sci. 1998;6:99-104.
6. Villalón CM, Centurión D. Cardiovascular responses produced by 5-hydroxytriptamine: a pharmacological update on the receptors/mechanisms involved and therapeutic implications. Naunyn Schmiedebergs Arch Pharmacol. 2007;376:45-63.
7. Mueller L, Gallagher RM, Ciervo CA. Vasospasm-induced myocardial infarction with sumatriptan. Headache. 1996;36:329-331.
8. Laine K, Raasakka T, Mäntynen J, Saukko P. Fatal cardiac arrhythmia after oral sumatriptan. Headache. 1999;39:511-512.
9. Lynch JJ Jr, Stump GL, Kane SA, Regan CP. The prototype serotonin 5-HT 1B/1D agonist sumatriptan increases the severity of myocardial ischemia during atrial pacing in dogs with coronary artery stenosis. J Cardiovasc Pharmacol. 2009;53:474-479.
10. Kemp BK, Cocks TM. Effects of U46619 on contractions to 5-HT, sumatriptan and methysergide in canine coronary artery and saphenous vein *in vitro*. Br J Pharmacol. 1995;116:2183-2190.

11. Ferdinandy P, Schulz R, Baxter GF. Interaction of cardiovascular risk factors with myocardial ischemia/reperfusion injury, preconditioning, and postconditioning. Pharmacol Rev. 2007;59:418-458.

12. Krzeminski TF, Mitrega K, Porc M, Zorniak M, Ryszka F, Ostrowska Z, Kos-Kudła B. Differential action of two prolactin isoforms on ischemia and re-perfusion-induced arrhythmias in rats *in vivo*. J Endocrinol Invest. 2011;34:206-215.

13. Baller D, Bretschneider HJ, Hellige G. A critical look at currently used indirect indices of myocardial oxygen consumption. Bas Res Cardiol. 1981;76:163-181.

14. Fawaz G, Tutunji B. Ouabain-induced ventricular tachycardia and its effect on the performance and metabolism of the dog heart. Br J Pharmacol Chemother. 1959;14:355-357.

15. Spokes RA, Middlefell VC. Simultaneous measurement of plasma protein extravasation and carotid vascular resistance in the rat. Eur J Pharmacol. 1995;281:75-79.

16. Johnson DE, Rollema H, Schmidt AW, McHarg AD. Serotonergic effects and extracellular brain levels of eletriptan, zolmitriptan and sumatriptan in rat brain. Eur J Pharmacol. 2001;425:203-210.

17. Ahmed LA, Salem HA, Attia AS, Agha AM. Comparative study of the cardioprotective effects of local and remote preconditioning in ischemia/reperfusion injury. Life Sci. 2012;90:249-256.

18. Walker MJ, Curtis MJ, Hearse DJ, Campbell RW, Janse MJ, Yellon DM, Cobbe SM, Coker SJ, Harness JB, Harron DW, et al. The Lambeth Conventions: guidelines for the study of arrhythmias in ischaemia infarction, and reperfusion. Cardiovasc Res. 1988;22:447-455.

19. Ravingerová T, Matejíková J, Pancza D, Kolár F. Reduced susceptibility to ischemia-induced arrhythmias in the preconditioned rat heart is independent of PI3-kinase/Akt. Physiol Res. 2009;58:443-447.

20. Macintyre PD, Bhargava B, Hogg KJ, Gemmill JD, Hillis WS. The effect of i.v. sumatriptan, a selective 5-HT1-receptor agonist on central haemodynamics and the coronary circulation. Br J Clin Pharmacol. 1992;34:541-546.

21. Macintyre PD, Bhargava B, Hogg KJ, Gemmill JD, Hillis WS. Effect of subcutaneous sumatriptan, a selective 5HT1 agonist, on the systemic, pulmonary, and coronary circulation. Circulation. 1993;87:401-405.

22. Newman CM, Starkey I, Buller N, Seabra-Gomes R, Kirby S, Hettiarachchi J, Cumberland D, Hillis WS. Effects of sumatriptan and eletriptan on diseased epicardial coronary arteries. Eur J Clin Pharmacol. 2005;61:733-742.

23. Lewis PJ, Barrington SF, Marsden PK, Maisey MN, Lewis LD. A study of the effects of sumatriptan on myocardial perfusion in healthy female migraineurs using 13NH3 positron emission tomography. Neurology. 1997;48:1542-1550.

24. Bax WA, Renzenbrink GJ, Van Heuven-Nolsen D, Thijssen EJ, Bos E, Saxena PR. 5-HT receptors mediating contractions of the isolated human coronary artery. Eur J Pharmacol. 1993;239:203-210.

25. Huffmyer J, Raphael J. Physiology and pharmacology of myocardial preconditioning and postconditioning. Semin Cardiothorac Vasc Anesth. 2009;13:5-18.

26. Murry CE, Richard VJ, Reimer KA, Jennings RB. Ischemic preconditioning slows energy metabolism and delays ultrastructural damage during a sustained ischemic episode. Circ Res. 1990;66:913-931.

Turk J Pharm Sci 2018;15(3):333-338
DOI: 10.4274/tjps.20982

ORIGINAL ARTICLE

Synthesis and Evaluation of a New Series of Thiazolyl-pyrazoline Derivatives as Cholinesterase Inhibitors

Yeni Tiyazolil-Pirazolin Türevlerinin Sentezi ve Kolinesteraz İnhibitörleri Olarak Değerlendirilmesi

Halide Edip TEMEL[1], Mehlika Dilek ALTINTOP[2]*, Ahmet ÖZDEMİR[2]

[1]Anadolu University, Faculty of Pharmacy, Department of Biochemistry, Eskişehir, Turkey
[2]Anadolu University, Faculty of Pharmacy, Department of Pharmaceutical Chemistry, Eskişehir, Turkey

ABSTRACT

Objectives: In recent years, the design of anticholinesterase agents based on molecular hybridization of pharmacologically active scaffolds has attracted a great deal of interest in medicinal chemistry. For this purpose, we aimed to design and synthesize anticholinesterase agents based on the molecular hybridization of thiazole and pyrazoline scaffolds.

Materials and Methods: New thiazolyl-pyrazoline derivatives were synthesized via the ring closure reaction of 3-(2-furyl)-5-(1,3-benzodioxol-5-yl)-1-thiocarbamoyl-4,5-dihydro-1*H*-pyrazole with 2-bromo-1-arylethanone derivatives. The compounds were investigated for their inhibitory effects on AChE and BuChE using a modification of Ellman's spectrophotometric method. As a part of this study, the compliance of the compounds to Lipinski's rule of five was evaluated. The physicochemical parameters (log P, TPSA, nrotb, molecular weight, number of hydrogen bond donors and acceptors, molecular volume) were calculated using Molinspiration software.

Results: 2-[5-(1,3-Benzodioxol-5-yl)-3-(2-furyl)-4,5-dihydro-1*H*-pyrazol-1-yl]-4-(naphthalen-2-yl)thiazole was found to be the most effective AChE inhibitor (38.5±2.85%), whereas 2-[5-(1,3-benzodioxol-5-yl)-3-(2-furyl)-4,5-dihydro-1*H*-pyrazol-1-yl]-4-(4-fluorophenyl)thiazole was found as the most potent BuChE inhibitor (43.02±2.71%) in this series. These compounds only violated one parameter of Lipinski's rule of five. On the basis of Lipinski's rule, they were expected to have reasonable oral bioavailability.

Conclusion: In the view of this study, the structural modification of the identified compounds is on-going for the generation of new cholinesterase inhibitors with enhanced efficacy.

Key words: Benzodioxole, cholinesterases, Lipinski's rule of five, pyrazoline, thiazole

ÖZ

Amaç: Son yıllarda, medisinal kimyada farmakolojik olarak aktif halkaların moleküler hibridizasyonuna dayalı antikolinesteraz ajanların tasarımı ilgi çekmektedir. Bu amaçla, burada tiyazol ve pirazolin halkalarının moleküler hibridizasyonuna dayalı antikolinesteraz ajanlar tasarlamayı ve sentezlemeyi hedefledik.

Gereç ve Yöntemler: 3-(2-Furil)-5-(1,3-benzodioksol-5-il)-1-tiyokarbamoil-4,5-dihidro-1*H*-pirazolün 2-bromo-1-ariletanon türevleri ile halka kapanma reaksiyonuyla yeni tiyazolil-pirazolin türevleri sentezlendi. Bileşikler, Ellman'ın spektrofotometrik yönteminin bir modifikasyonu kullanılarak AChE ve BuChE üzerindeki inhibe edici etkileri için araştırıldı. Bu çalışmanın bir parçası olarak, bileşiklerin Lipinski'nin beş kuralına uyumluluğu değerlendirildi. Fizikokimyasal parametreler (log P, TPSA, nrotb, molekül ağırlığı, hidrojen bağı donörlerinin ve alıcılarının sayısı, molekül hacmi) Molinspiration yazılımı kullanılarak hesaplandı.

Bulgular: Bu seride, 2-[5-(1,3-benzodioksol-5-il)-3-(2-furil)-4,5-dihidro-1*H*-pirazol-1-il]-4-(4-florofenil)tiyazol en güçlü BuChE inhibitörü (%43.02±2.71) olarak bulunurken, 2-[5-(1,3-benzodioksol-5-il)-3-(2-furil)-4,5-dihidro-1*H*-pirazol-1-il]-4-(naftalen-2-il)tiyazolün en etkili AChE inhibitörü (%38.5±2.85) olduğu bulundu. Bu bileşikler, Lipinski'nin beş kuralının sadece bir parametresini ihlal ettiler. Lipinski'nin kuralına dayanarak, makul oral biyoyararlanıma sahip olmaları beklenmektedir.

Sonuç: Bu çalışmanın ışığında, etkinliği arttırılmış yeni kolinesteraz inhibitörlerinin üretilmesi için tanımlanmış bileşiklerin yapısal modifikasyonu devam etmektedir.

Anahtar kelimeler: Benzodioksol, kolinesterazlar, Lipinski'nin 5 kuralı, pirazolin, tiyazol

*Correspondence: **E-mail:** mdaltintop@anadolu.edu.tr, **Phone:** +90 535 258 67 35 **ORCID-ID:** orcid.org/0000-0002-8159-663X
Received: 08.09.2017, **Accepted:** 30.11.2017

INTRODUCTION

Alzheimer's disease (AD), a progressive multifarious neurodegenerative disorder, is the leading cause of dementia in older people worldwide. The incidence of AD is predicted to increase dramatically in the future, as the average age of the population increases. Although extensive efforts have been devoted to the discovery of anti-AD drugs for almost a century, donepezil, galantamine, rivastigmine (cholinesterase inhibitors) and memantine (*N*-methyl-D-aspartate receptor antagonist) are the only drugs currently used for the management of AD. These agents only provide symptomatic relief but do not halt the progression of the disease.[1-5]

The development of new potent anti-AD drugs is a difficult and time-consuming process, and many molecules reaching clinical trials simply fail. Most phase 2 clinical trials ending with a positive outcome do not succeed in phase 3, often due to serious adverse effects or lack of therapeutic efficacy.[6,7]

Acetylcholinesterase (AChE) is a highly viable target for the design and development of potent anti-AD agents due to its role in the pathogenesis of AD.[1-8] On the other hand, in progressed AD, the level of AChE in the brain declines to 55-67% of normal values, whereas the level of butyrylcholinesterase (BuChE) increases to 120% of normal levels, indicating that BuChE plays a pivotal role for acetylcholine (ACh) hydrolysis in the late stage of AD. As a result, selective inhibition of BuChE has emerged as a promising therapeutic approach to elevate ACh level in progressed AD.[9,10]

Thiazole has been recognized as a promising scaffold for the design and development for central nervous system (CNS) active agents. There are thiazole-based CNS drugs currently used as therapeutic agents for the treatment of various CNS disorders and a number of thiazole derivatives are in clinical trials.[11] Diverse modifications of the thiazole ring at various positions have led to a variety of thiazole-based CNS agents as AChE and BuChE inhibitors, secretase inhibitors, monoamine oxidase (MAO) inhibitors, neuronal nitric oxide synthase inhibitors, ACh receptor ligands, adenosine receptor ligands, dopamine receptor ligands, serotonin receptor ligands, glutamate receptor ligands, ɣ-aminobutyric acid receptor ligands, opioid receptor ligands, neuroprotective and anticonvulsant agents.[11-14] Acotiamide has been reported to be a promising thiazole-based agent for the treatment of functional dyspepsia in clinical trials. Acotiamide enhances ACh release in the enteric nervous system through AChE inhibition and M1/M2 muscarinic receptor antagonism.[15]

Pyrazoline has also attracted a great deal of interest as an indispensable scaffold due to its diverse therapeutic applications extending from CNS applications to antimicrobial therapy.[16,17] Diversely substituted pyrazolines embedded with a variety of functional groups have been reported to inhibit MAOs and cholinesterases, molecular targets important for the treatment of neurodegenerative disorders such as Parkinson's disease and AD.[16-23]

Prompted by the aforementioned findings and in the continuation of our ongoing research on thiazoles[24] and pyrazolines[25] as cholinesterase inhibitors, we designed a new series of thiazolyl-pyrazoline derivatives based on the molecular hybridization of thiazole and pyrazoline scaffolds.[26] A facile and versatile synthetic route was used to prepare the title compounds and their inhibitory effects on AChE and BuChE were investigated. A computational study for the prediction of Absorption, Distribution, Metabolism and Excretion (ADME) properties of all compounds was also performed.

MATERIALS AND METHODS

Chemistry

All reagents were purchased from commercial suppliers and were used without further purification. Melting points (MP) were determined on an Electrothermal 9100 MP apparatus (Weiss-Gallenkamp, Loughborough, UK). ^{1}H-NMR spectra were recorded on a Bruker spectrometer (Bruker, Billerica, MA, USA). Mass spectra were recorded on an Agilent LC-MSD-Trap-SL Mass spectrometer (Agilent, Minnesota, USA). Elemental analyses (C, H, N) were performed on a Perkin Elmer EAL 240 elemental analyzer (Perkin-Elmer, Norwalk, CT, USA) and the results were within ±0.4% of the theoretical values. Thin layer chromatography (TLC) was performed on TLC Silica gel 60 F_{254} aluminium sheets (Merck, Darmstadt, Germany) to check the purity of the compounds.

General procedure for the synthesis of the compounds

*1-(2-furanyl)-3-(1,3-benzodioxol-5-yl)-2-propen-1-one (**1**)*

A mixture of 2-acetylfuran (0.06 mol), 1,3-benzodioxole-5-carboxaldehyde (0.06 mol) and 40% (w/v) sodium hydroxide (10 mL) in ethanol (30 mL) was stirred at room temperature for about 24 h. The resulting solid was washed, dried, and crystallized from ethanol.[27,28]

*3-(2-furanyl)-5-(1,3-benzodioxol-5-yl)-1-thiocarbamoyl-4,5-dihydro-1H-pyrazole (**2**)*

A mixture of compound **1** (0.03 mol), thiosemicarbazide (0.036 mol) and sodium hydroxide (0.075 mol) was refluxed in ethanol (30 mL) for 12 h. The product was poured into crushed ice. The precipitate was filtered and crystallized from ethanol.[29]

*2-[5-(1,3-benzodioxol-5-yl)-3-(furan-2-yl)-4,5-dihydro-1H-pyrazol-1-yl]-4-(aryl)thiazole (**3a-g**)*

A mixture of compound **2** (0.01 mol), 2-bromo-1-arylethanone (0.01 mol) in ethanol (20 mL) was refluxed for 10 h. After cooling, the precipitate was collected by suction filtration. The product was crystallized from ethanol.[29]

*2-[5-(1,3-benzodioxol-5-yl)-3-(furan-2-yl)-4,5-dihydro-1H-pyrazol-1-yl]-4-(4-(methylsulfonyl)phenyl)thiazole (**3a**)*

Yield: 76%; MP: 178-179°C.

^{1}H-NMR (400 MHz, DMSO-d_6) δ (ppm): 2.99-3.00 (1H, m), 3.22 (3H, s), 3.92 (1H, dd, *J*=17.36, 11.16 Hz), 5.57 (1H, dd, *J*=11.52, 5.96 Hz), 5.93 (2H, s), 6.65 (1H, s), 6.87-6.95 (4H, m), 7.59 (1H, s), 7.86 (3H, d, *J*=8.72 Hz), 7.94 (2H, d, *J*=7.44 Hz).

Elemental analysis calculated (Anal. calcd) for $C_{24}H_{19}N_3O_5S_2$ (%): C, 58.40; H, 3.88; N, 8.51. Found (%): C, 58.45; H, 3.89; N, 8.58.

MS (ESI) *m/z*: 494 $[M+H]^+$.

*2-[5-(1,3-benzodioxol-5-yl)-3-(furan-2-yl)-4,5-dihydro-1H-pyrazol-1-yl]-4-(4-(trifluoromethyl)phenyl)thiazole (**3b**)*

Yield: 80%; MP: 77-78°C.

^{1}H-NMR (400 MHz, DMSO-d_6) δ (ppm): 3.12-3.13 (1H, m), 3.90 (1H, dd, *J*=18.32, 12.20 Hz), 5.57 (1H, dd, *J*=11.48, 5.96 Hz), 5.94 (2H, s), 6.65 (1H, s), 6.86-6.96 (4H, m), 7.55 (1H, s), 7.69 (2H, d, *J*=8.12 Hz), 7.88-7.92 (3H, m).

Anal. calcd for $C_{24}H_{16}F_3N_3O_3S$ (%): C, 59.62; H, 3.34; N, 8.69. Found (%): C, 59.57; H, 3.39; N, 8.78.

MS (ESI) *m/z*: 484 $[M+H]^+$.

*2-[5-(1,3-benzodioxol-5-yl)-3-(furan-2-yl)-4,5-dihydro-1H-pyrazol-1-yl]-4-(4-fluorophenyl)thiazole (**3c**)*

Yield: 81%; MP: 89-90°C.

^{1}H-NMR (400 MHz, DMSO-d_6) δ (ppm): 3.10-3.11 (1H, m), 3.89 (1H, dd, *J*=17.76, 11.80 Hz), 5.55 (1H, dd, *J*=11.52, 5.92 Hz), 5.94 (2H, s), 6.64-6.65 (1H, m), 6.85-6.94 (4H, m), 7.14-7.28 (3H, m), 7.71-7.75 (2H, m), 7.86-7.87 (1H, m).

Anal. calcd for $C_{23}H_{16}FN_3O_3S$ (%): C, 63.73; H, 3.72; N, 9.69. Found (%): C, 63.69; H, 3.77; N, 9.63.

MS (ESI) *m/z*: 434 $[M+H]^+$.

*2-[5-(1,3-benzodioxol-5-yl)-3-(furan-2-yl)-4,5-dihydro-1H-pyrazol-1-yl]-4-(2,6-difluorophenyl)thiazole (**3d**)*

Yield: 78%; MP: 137-138°C.

^{1}H-NMR (400 MHz, DMSO-d_6) δ (ppm): 3.13-3.14 (1H, m), 3.93 (1H, dd, *J*=17.73, 11.82 Hz), 5.58 (1H, dd, *J*=11.70, 6.30 Hz), 5.98 (2H, s), 6.67-6.69 (1H, m), 6.88-6.98 (4H, m), 7.10-7.21 (2H, m), 7.26-7.34 (1H, m), 7.83-7.90 (2H, m).

Anal. calcd for $C_{23}H_{15}F_2N_3O_3S$ (%): C, 61.19; H, 3.35; N, 9.31. Found (%): C, 61.13; H, 3.42; N, 9.33.

MS (ESI) *m/z*: 452 $[M+H]^+$.

*2-[5-(1,3-benzodioxol-5-yl)-3-(furan-2-yl)-4,5-dihydro-1H-pyrazol-1-yl]-4-(2,5-dimethoxyphenyl)thiazole (**3e**)*

Yield: 77%; MP: 113-114°C.

^{1}H-NMR (400 MHz, DMSO-d_6) δ (ppm): 3.03-3.04 (1H, m), 3.68 (3H, s), 3.76 (3H, m), 3.88 (1H, dd, *J*=17.84, 12.24 Hz), 5.50 (1H, dd, *J*=11.52, 7.08 Hz), 5.94 (2H, s), 6.64-6.65 (1H, m), 6.75-6.94 (5H, m), 7.07-7.19 (2H, m), 7.38-7.41 (1H, m), 7.87 (1H, s).

Anal. calcd for $C_{25}H_{21}N_3O_5S$ (%): C, 63.15; H, 4.45; N, 8.84. Found (%): C, 63.11; H, 4.42; N, 8.85.

MS (ESI) *m/z*: 476 $[M+H]^+$.

*2-[5-(1,3-benzodioxol-5-yl)-3-(furan-2-yl)-4,5-dihydro-1H-pyrazol-1-yl]-4-[4-(morpholin-4-yl)phenyl]thiazole (**3f**)*

Yield: 78%; MP: 210-211°C.

^{1}H-NMR (400 MHz, DMSO-d_6) δ (ppm): 3.01-3.02 (1H, m), 3.08 (4H, bs), 3.69 (4H, s), 3.87 (1H, dd, *J*=17.60, 12.72 Hz), 5.54 (1H, dd, *J*=12.44, 5.20 Hz), 5.93 (2H, s), 6.59-6.64 (3H, m), 6.80-6.94 (6H, m), 7.55 (1H, s), 7.86 (1H, s).

Anal. calcd for $C_{27}H_{24}N_4O_4S$ (%): C, 64.78; H, 4.83; N, 11.19. Found (%): C, 64.72; H, 4.88; N, 11.16.

MS (ESI) *m/z*: 501 $[M+H]^+$.

*2-[5-(1,3-benzodioxol-5-yl)-3-(furan-2-yl)-4,5-dihydro-1H-pyrazol-1-yl]-4-(naphthalen-2-yl)thiazole (**3g**)*

Yield: 83%; MP: 153-154°C.

^{1}H-NMR (400 MHz, DMSO-d_6) δ (ppm): 3.09 (1H, dd, *J*=17.76, 2.72 Hz), 3.78 (1H, dd, *J*=17.96, 11.48 Hz), 5.80 (1H, dd, *J*=11.12, 2.68 Hz), 5.94 (2H, s), 6.59-6.87 (6H, m), 7.06 (1H, s), 7.19 (1H, s), 7.69 (1H, s), 7.81 (1H, s), 7.88 (1H, s), 7.95 (2H, d, *J*=8.80 Hz), 8.16-8.19 (1H, m).

Anal. calcd for $C_{27}H_{19}N_3O_3S$ (%): C, 69.66; H, 4.11; N, 9.03. Found (%): C, 69.75; H, 4.29; N, 9.06.

MS (ESI) *m/z*: 466 $[M+H]^+$.

Determination of AChE and BuChE inhibitory activity

The inhibitory effects of compounds **3a-g** on AChE and BuChE were determined using Ellman's method[30] with minor modifications (electric eel AChE enzyme was used instead of bovine AChE enzyme and buffer was added as 2.4 mL instead of 3 mL).[31] The compounds were dissolved in DMSO and tested at the final concentration range 5-80 µg/mL. Twenty microliters of enzyme (AChE or BuChE, 1 U/mL) and 10 µL sample were added to 2.4 mL buffer, the mixture was incubated at 37°C for 15 min. After 15 min incubation, 50 µL of 0.01 M 5,5'-dithiobis(2-nitrobenzoic acid) (DTNB) and 20 µL of 75 mM acetylthiocholine iodide or 25 mM butyrylthiocholine iodide were added, and the final mixture was incubated at room temperature for 30 min. A blank was prepared using 10 µL of DMSO instead of the test sample, with all other procedures similar to those used in the case of the sample mixture. Absorbances were measured at 412 nm and 37°C using polystyrene cuvettes with a spectrophotometer (UV-1700, Shimadzu). The experiment was performed in triplicate. Galantamine was used as a positive control. Data are expressed as mean ± standard deviation. The inhibition (percent) of AChE or BuChE was calculated using the following equation:

$$I\ (\%) = 100 - (OD_{sample} / OD_{control}) \times 100$$

In silico prediction of ADME parameters

The physicochemical parameters [logarithm of octanol/water partition coefficient (log P), topological polar surface area (TPSA), number of rotatable bonds (nrotb), molecular weight, number of hydrogen bond donors and acceptors, molecular volume] of compounds **3a-g** were calculated using Molinspiration software.[32-35]

There was no need for ethics committee approval because our work only included *in vitro* and *in silico* studies.

RESULTS AND DISCUSSION

The synthesis of thiazole derivatives (**3a-g**) followed the general pathway outlined in Scheme 1. The base-catalyzed Claisen-Schmidt condensation of 2-acetylfuran with 1,3-benzodioxole-5-carboxaldehyde gave 1-(2-furanyl)-3-(1,3-benzodioxol-5-yl)-2-propen-1-one (**1**), which underwent a subsequent cyclization reaction with thiosemicarbazide in the presence of sodium hydroxide affording 3-(2-furanyl)-5-(1,3-benzodioxol-

5-yl)-1-thiocarbamoyl-4,5-dihydro-1*H*-pyrazole (**2**). Finally, new thiazolyl-pyrazoline derivatives (**3a-g**) were synthesized *via* the ring closure reactions of compound **2** with 2-bromo-1-arylethanone derivatives.

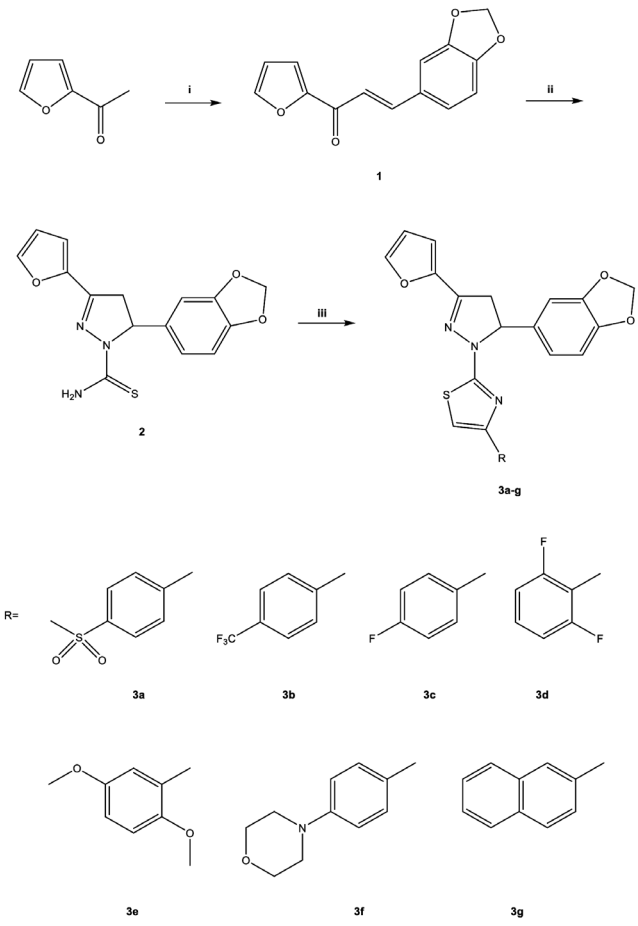

Scheme 1. The synthetic route for the preparation of compounds **3a-g**. Reagents and conditions: (i) 1,3-benzodioxole-5-carboxaldehyde, 40% (w/v) NaOH, ethanol, rt, 24 h; (ii) thiosemicarbazide, NaOH, ethanol, reflux, 12 h; (iii) 2-bromo-1-arylethanone, ethanol, reflux, 10 h

The inhibitory effects of compounds **3a-g** on AChE and BuChE were determined using a modification of Ellman's spectrophotometric method (Table 1). Galantamine was used as a positive control. According to the results, compounds **3a-g** showed less ChE inhibitory activity than galantamine.

Compounds **3a**, **3b**, **3e**, **3f** and **3g** showed less than 50% AChE inhibition at 80 µg/mL, whereas compounds **3c** and **3d** showed no inhibitory activity against AChE. Compound **3g** was identified as the most potent AChE inhibitor (38.5±2.85%) in this series. This outcome indicated that naphthalene ring enhanced the inhibitory activity against AChE. The increased activity can be attributed to its high lipophilicity due to the presence of naphthalene moiety.

Compounds **3a**, **3f** and **3g** showed no inhibitory activity against BuChE, whereas the other compounds showed BuChE inhibitory activity ranging from 43.02 to 21.44%. The most selective BuChE inhibitor was found as compound **3c** (43.02±2.71%) followed by compound **3d** (38.52±3.33%). This outcome pointed out the importance of fluoro substituent for BuChE inhibitory activity.

Table 1. The inhibitory effects of compounds 3a-g on AChE and BuChE

Compound	Inhibition% (80 µg/mL)	
	AChE	BuChE
3a	8.60±1.29	---
3b	29.57±2.31	24.24±2.62
3c	---	43.02±2.71
3d	---	38.52±3.33
3e	25.62±3.23	21.44±2.85
3f	19.79±0.41	---
3g	38.5±2.85	---
Galantamine	(97.17±0.48)[a]	(80.98±0.22)[a]

---: No inhibition. [a]Inhibition% at 16 µg/mL, AChE: Acetylcholinesterase, BuChE: Butyrylcholinesterase

Table 2. Pharmacokinetic parameters important for bioavailability of compounds 3a-g

Compound	Molecular properties[a]							
	MW	Log P	TPSA	nrotb	HBA	HBD	Volume	Violations
3a	493.57	4.00	94.24	5	8	0	397.15	0
3b	483.47	6.03	60.10	5	6	0	380.45	1
3c	433.46	5.30	60.10	4	6	0	354.08	1
3d	451.45	5.37	60.10	4	6	0	359.02	1
3e	475.53	5.17	78.57	6	8	0	400.25	1
3f	500.58	5.08	72.57	5	8	0	427.29	2
3g	465.53	6.32	60.10	4	6	0	393.15	1

[a]Molecular properties were calculated using Molinspiration software.
MW: Molecular weight, log P: The logarithm of octanol/water partition coefficient, TPSA: Topological polar surface area, nrotb: Number of rotatable bonds, HBA: Number of hydrogen bond acceptors, HBD: Number of hydrogen bond donors

As a part of this study, Molinspiration software was used to determine their physicochemical parameters (log P, TPSA, nrotb, molecular weight, number of hydrogen bond donors and acceptors, molecular volume) for the evaluation of the compliance of the compounds to Lipinski's rule of five.[32] This rule states that most 'drug-like' molecules have log P ≤5, molecular weight ≤500, number of hydrogen bond acceptors ≤10, and number of hydrogen bond donors ≤5. Compounds violating more than one of these rules may have bioavailability problems.[32-35] According to *in silico* studies, compounds **3b**, **3c**, **3d**, **3e**, and **3g** only violated one parameter of Lipinski's rule of five, whereas compound **3a** did not violate Lipinski's rule (Table 2). On the basis of Lipinski's rule of five, they were expected to have good oral bioavailability. On the other hand, compound **3f** violated two parameters of Lipinski's rule of five, and therefore it can be concluded that compound **3f** may have bioavailability problems.

CONCLUSIONS

In the current work, new thiazolyl-pyrazoline derivatives were synthesized and investigated for their *in vitro* inhibitory effects on AChE and BuChE. Moreover, the compliance of the compounds to Lipinski's rule of five was evaluated. Naphthalene-substituted compound **3g** was the most potent AChE inhibitor (38.5±2.85%), whereas fluoro-substituted compound **3c** was the most effective BuChE inhibitor (43.02±2.71%) in this series. In the view of this work, the structural modification of the identified compounds is on-going for the generation of new anticholinesterase agents with enhanced efficacy and selectivity.

Conflict of Interest: No conflict of interest was declared by the authors.

REFERENCES

1. Kumar A, Singh A, Ekavali. A review on Alzheimer's disease pathophysiology and its management: an update. Pharmacol Rep. 2015;67:195-203.
2. Guzior N, Wieckowska A, Panek D, Malawska B. Recent Development of multifunctional agents as potential drug candidates for the treatment of Alzheimer's disease. Curr Med Chem. 2015;22:373-404.
3. Silva T, Reis J, Teixeira J, Borges F. Alzheimer's disease, enzyme targets and drug discovery struggles: From natural products to drug prototypes. Ageing Res Rev. 2014;15:116-145.
4. Anand R, Gill KD, Mahdi AA. Therapeutics of Alzheimer's disease: Past, present and future. Neuropharmacology. 2014;76:27-50.
5. Tayeb HO, Yang HD, Price BH, Tarazi FI. Pharmacotherapies for Alzheimer's disease: Beyond cholinesterase inhibitors. Pharmacol Ther. 2012;134:8-25.
6. Godyn J, Jonczyk J, Panek D, Malawska B. Therapeutic strategies for Alzheimer's disease in clinical trials. Pharmacol Rep. 2016;68:127-138.
7. Sikazwe D, Yendapally R, Ramsinghani S, Khan M. Alzheimer's drug discovery maze: A snap view of the past decade's diverse pharmacological targets for the disorder. Mini-Rev Med Chem. 2017;17:305-318.
8. Wang Y, Wang H, Chen HZ. AChE inhibition-based multi-target-directed ligands, a novel pharmacological approach for the symptomatic and disease-modifying therapy of Alzheimer's disease. Curr Neuropharmacol. 2016;14:364-375.
9. Li Q, Yang H, Chen Y, Sun H. Recent progress in the identification of selective butyrylcholinesterase inhibitors for Alzheimer's disease. Eur J Med Chem. 2017;132:294-309.
10. Greig NH, Utsuki T, Yu Q, Zhu X, Holloway HW, Perry T, Lee B, Ingram DK, Lahiri DK. A new therapeutic target in Alzheimer's disease treatment: attention to butyrylcholinesterase. Curr Med Res Opin. 2001;17:159-165.
11. Mishra CB, Kumari S, Tiwari M. Thiazole: A promising heterocycle for the development of potent CNS active agents. Eur J Med Chem. 2015;92:1-34.
12. Ayati A, Emami S, Asadipour A, Shafiee A, Foroumadi A. Recent applications of 1,3-thiazole core structure in the identification of new lead compounds and drug discovery. Eur J Med Chem. 2015;97:699-718.
13. Sun ZQ, Tu LX, Zhuo FJ, Liu SX. Design and discovery of novel thiazole acetamide derivatives as anticholinesterase agent for possible role in the management of Alzheimer's. Bioorg Med Chem Lett. 2016;26:747-750.
14. D'Ascenzio M, Chimenti P, Gidaro MC, De Monte C, De Vita D, Granese A, Scipione L, Di Santo R, Costa G, Alcaro S, Yáñez M, Carradori S. (Thiazol-2-yl) hydrazone derivatives from acetylpyridines as dual inhibitors of MAO and AChE: synthesis, biological evaluation and molecular modeling studies, J Enzyme Inhib Med Chem. 2015;30:908-919.
15. Zala AV, Walker MM, Talley NJ. Emerging drugs for functional dyspepsia. Expert Opin Emerg Drugs. 2015;20:221-233.
16. Shaaban MR, Mayhoub AS, Farag AM. Recent advances in the therapeutic applications of pyrazolines. Expert Opin Ther Pat. 2012;22:253-291.
17. Alex JM, Kumar R. 4,5-Dihydro-1H-pyrazole: an indispensable scaffold. J Enzyme Inhib Med Chem. 2014;29:427-442.
18. Kumar S, Bawa S, Drabu S, Kumar R, Gupta H. Biological activities of pyrazoline derivatives -A recent development. Recent Pat Anti-Infect Drug Discov. 2009;4:154-163.
19. Secci D, Bolasco A, Chimenti P, Carradori S. The state of the art of pyrazole derivatives as monoamine oxidase ınhibitors and antidepressant/anticonvulsant agents. Curr Med Chem. 2011;18:5114-5144.
20. Ucar G, Gokhan N, Yesilada A, Bilgin AA. 1-N-Substituted thiocarbamoyl-3-phenyl-5-thienyl-2-pyrazolines: A novel cholinesterase and selective monoamine oxidase B inhibitors for the treatment of Parkinson's and Alzheimer's diseases. Neurosci Lett. 2005;382:327-331.
21. Jayaprakash V, Yabanoglu S, Sinha N, Ucar G. Pyrazoline-based mycobactin analogues as dual inhibitors of mao/cholinesterase. Turk J Biochem. 2010;35:91-98.
22. Mishra N, Sasmal D. Additional acetyl cholinesterase inhibitory property of diaryl pyrazoline derivatives. Bioorg Med Chem Lett. 2013;23:702-705.
23. Shah MS, Khan SU, Ejaz SA, Afridi S, Rizvi SUF, Najam-ul-Haq M, Iqbal J. Cholinesterases inhibition and molecular modeling studies of piperidyl-thienyl and 2-pyrazoline derivatives of chalcones. Biochem Biophys Res Commun. 2017;482:615-624.
24. Turan-Zitouni G, Ozdemir A, Kaplancikli ZA, Altintop MD, Temel HE, Çiftçi GA. Synthesis and biological evaluation of some thiazole derivatives as new cholinesterase inhibitors. J Enzyme Inhib Med Chem. 2013;28:509-514.
25. Altintop MD, Özdemir A, Kaplancikli ZA, Turan-Zitouni G, Temel HE, Çiftçi GA. Synthesis and biological evaluation of some pyrazoline derivatives bearing a dithiocarbamate moiety as new cholinesterase inhibitors. Arch Pharm (Weinheim). 2013;346:189-199.

26. Havrylyuk D, Roman O, Lesyk R. Synthetic approaches, structure activity relationship and biological applications for pharmacologically attractive pyrazole/pyrazoline-thiazolidine-based hybrids. Eur J Med Chem. 2016;113:145-166.

27. Özdemir A, Altıntop MD, Kaplancıklı ZA, Zitouni GT, Çiftçi GA, Demirci F. Synthesis and biological evaluation of a new series of pyrazolines as new anticandidal agents. Pharm Chem J. 2014;48:605-614.

28. Özdemir A. Synthesis and antimicrobial activity of some pyrazoline derivatives bearing amide moiety. Marmara Pharm J. 2013;17:187-192.

29. Altıntop MD, Özdemir A, Turan-Zitouni G, Ilgın S, Atlı Ö, Demirel R, Kaplancıklı ZA. A novel series of thiazolyl-pyrazoline derivatives: Synthesis and evaluation of antifungal activity, cytotoxicity and genotoxicity. Eur J Med Chem. 2015;92:342-352.

30. Ellman GL, Courtney KD, Anders V Jr, Feather-Stone RM. A new and rapid colorimetric determination of acetylcholinesterase activity. Biochem Pharmacol. 1961;7:88-95.

31. Turan-Zitouni G, Altıntop MD, Özdemir A, Kaplancıklı ZA, Çiftçi GA, Temel HE. Synthesis and evaluation of bis-thiazole derivatives as new anticancer agents. Eur J Med Chem. 2016;107:288-294.

32. http://www.molinspiration.com. (Accessed August 2017).

33. Lipinski CA, Lombardo F, Dominy BW, Feeney PJ. Experimental and computational approaches to estimate solubility and permeability in drug discovery and development settings. Adv Drug Deliv Rev. 2001;46:3-26.

34. Veber DF, Johnson SR, Cheng HY, Smith BR, Ward KW, Kopple KD. Molecular properties that influence the oral bioavailability of drug candidates. J Med Chem. 2002;45:2615-2623.

35. Gabr MT, El-Gohary NS, El-Bendary ER, El-Kerdawy MM, Ni N. Synthesis, in vitro antitumor activity and molecular modeling studies of a new series of benzothiazole Schiff bases. Chinese Chem Lett. 2016;27:380-386.

Turk J Pharm Sci 2018;15(3):339-346
DOI: 10.4274/tjps.02486

ORIGINAL ARTICLE

The Glucose Lowering Effect of *Zornia gibbosa* Span Extracts in Diabetic Rats

Diyabetik Sıçanlarda *Zornia gibbosa* Span Ekstrelerinin Glukoz Düşürücü Etkisi

Mallikarjuna Rao TALLURI[1]*, Rajananda Swamy TADI[2], Ganga Rao BATTU[2], Mohammad ZUBAIR[3]

[1]Anacipher Clinical Research Organisation, Department Bio-Analytical, Telangana, India
[2]Andhra University, College of Pharmaceutical Sciences, Department of Pharmacognosy and Phytochemistry, Andra Pradesh, India
[3]University of Tabuk, Faculty of Medicine, Department of Medical Microbiology, Tabuk, Kingdom of Saudi Arabia

ABSTRACT

Objectives: Diabetes mellitus is a chronic, lifelong condition that affects our body physiology. Untreated diabetes mellitus causes diseases such as diabetic retinopathy, diabetic nephropathy and diabetic neuropathy, auto immune diseases, polyuria, polydipsia, loss of weight, and cardiovascular diseases. The use of medications for the treatment of diabetes mellitus causes adverse effects with long-term use, and sometimes leads to death. Today, researchers are working on the discovery of new anti-diabetes drugs from plants with low or no adverse effects. From this point of view, the present work was conducted to evaluate the anti-diabetic activity of *Zornia gibbosa* Span.

Materials and Methods: This acute toxicity study was conducted for ethyl acetate and ethanol (70%v/v) extracts of *Z. gibbosa* as per OECD guidelines. The anti-diabetic activity of selected plant extracts were tested using alloxan-induced diabetes in a rat model.

Results: No mortality was observed in the administered doses of *Zornia gibbosa* Span extracts. The tested extracts significantly ($p \leq 0.01$) restored the physiologic changes that occurred due to the alloxan-induced diabetes mellitus. The hydroalcoholic extracts at 500 mg/kg body weight concentration showed more activity compared with other extracts at different concentrations along with standard drug (glibenclamide). *Zornia gibbosa* significantly decreased glucose concentrations and restored the altered enzymes levels caused by damage to different organs by diabetes.

Conclusion: The results of the present study indicate that *Z. gibbosa* has a significant anti-diabetic activity. Therefore, it may be capable of use as an alternate medicine along with allopathic medicine in the treatment of diabetes as well as its health problems.

Key words: *Zornia gibbosa* Span, diabetes mellitus, alloxan, glibenclamide

ÖZ

Amaç: Diyabet, vücudumuzun fizyolojisini etkileyen, yaşam boyu kronik bir hastalıktır. Tedavi edilmeyen diabetes mellitus, diyabetik retinopati, diyabetik nefropati ve diyabetik nöropati, otoimmün hastalıklar, ploiüri, polidipsi, kilo kaybı ve kardiyovasküler hastalıklar gibi hastalıklara neden olur. Diabetes mellitus tedavisinde kullanılan ilaçlar, uzun süreli kullanımda yan etkilere neden olur, bazen ölüme yol açar. Günümüzde araştırmacılar, yan etkileri düşük veya hiç olmayan bitkilerden hareketle yeni anti-diyabetik ilaçların keşfedilmesi üzerinde çalışmaktadır. Bu açıdan, mevcut çalışmada, *Zornia gibbosa* Span'ın anti-diyabetik etkinliğinin değerlendirilmesi amaçlanmıştır.

Gereç ve Yöntemler: Akut toksisite çalışması OECD kılavuzlarına göre *Z. gibbosa*'nın etil asetat ve etanol (%70 v/v) ekstreleri için yürütülmüştür. Seçilen bitki ekstrelerinin anti-diyabetik aktivitesi, sıçanlar üzeinde oluşturulan alloksan-nedenli diyabet modeli kullanılarak değerlendirilmiştir.

Bulgular: *Zornia gibbosa* Span ekstrelerinin uygulanan dozlarında herhangi bir ölüm görülmemiştir. Ekstreler, alloksan-nedenli diabetes mellitus nedeniyle oluşan fizyolojik değişiklikleri önemli ölçüde ($p \leq 0.01$) iyileştirmiştir. 500 mg/kg konsantrasyonundaki sulu-alkollü ekstreler, standart ilaç (glibenklamid) ile birlikte farklı konsantrasyonlardaki diğer ekstrelerle karşılaştırıldığında, daha yüksek aktivite göstermiştir. *Z. gibbosa* glukoz konsantrasyonunu önemli ölçüde düşürmüş ve diyabetin değişik organlara hasar vermesi nedeniyle değişen enzim düzeylerini iyileştirmiştir.

Sonuç: Bu çalışmanın sonuçları, *Z. gibbosa*'nın önemli anti-diyabetik etkiye sahip olduğunu göstermektedir. Bu nedenle, diyabet tedavisinde ve diyabetin neden olduğu diğer sağlık problemlerinde *Z. gibbosa*'nın allopatik tıp ile birlikte kullanılabileceği ortaya konulmuştur.

Anahtar kelimeler: *Zornia gibbosa* Span, şeker hastalığı, alloksan, glibenklamid

*Correspondence: **E-mail:** tmrao1987@gmail.com, **Phone:** +91 9032146226 **ORCID-ID:** orcid.org/0000-0002-9242-709X
Received: 12.09.2017, **Accepted:** 09.11.2017

INTRODUCTION

Glucose is a simple sugar found in all foods and an essential nutrient that provides energy for the proper functioning of body cells. However, it cannot be delivered alone to cells and it needs insulin to aid its transport into the cells. Insulin is a hormone produced by specialized cells (β-cells) of the pancreas. Without insulin, cells become ravenous for glucose because carbohydrates are broken down in the small intestine and the glucose in digested food is then absorbed by the intestinal cells into the bloodstream, and is carried by the bloodstream to all cells in the body where it is used.[1,2] High blood sugar levels over a prolonged period causes diabetes mellitus (DM). DM is a chronic, lifelong condition that affects our body's ability to use the energy found in food. There are three major types of DM. One is type 1 DM, which results from the pancreas's failure to produce enough insulin. In type 2 DM, either the amount of insulin produced is not enough for the body's needs, or the body's cells are resistant to it, and finally the third is gestational diabetes, which occurs in pregnant women.[3-6]

Globally, an estimated 415 million people have DM.[7] In the last three years, 1.5 to 5 million deaths occurred per year due to DM. All three forms of DM increase the risk of long-term complications.[8,9] The main complication due to DM is damage in the blood vessels. Untreated DM affects primary organs of the body such as the eyes, kidneys, and nerves by causing diseases diabetic retinopathy, diabetic nephropathy and diabetic neuropathy, auto immune diseases, polyuria, polydipsia, loss of weight, and cardiovascular diseases. Low levels of insulin cause the liver to turn fatty acids into ketone bodies for fuel instead of glucose, which causes ketosis. This in turn decreases the blood pH levels, which causes severe dehydration, hypotension, and finally death. These evets mainly occur in type 1 DM.[1,10-12]

DM is a chronic disease, for which there is no cure, mainly for type 1 DM.[1] Blood sugar levels of patients with type 2 DM and gestational DM can be controlled with a healthy diet, exercise, weight loss, and use of appropriate medications, but there is no cure.[2] Blood glucose (sugar) levels of patients with type 1 DM are controlled by taking insulin. Patients with type 2 and gestational DM use oral medications such as biguanides (metformin),[13] sulfonylureas (tolbutamide, glibenclamide, glimepiride), and thiozolidinediones (pioglitazone, rosiglitazone). The use of these medications causes adverse effects with long-term use,[14,15] sometimes causing severe acute diseases and lead to death. The adverse effects are mainly rapid or shallow breathing; painful or difficult urination; anxiety; blurred vision; chest discomfort; depression; irregular, pounding, or racing heartbeat or pulse; behavior changes similar to being drunk, difficulty with concentrating, drowsiness; lack or loss of strength; and restless sleep. Therefore, safer and more effective anti-diabetic drugs are still urgently needed.[16]

Natural products, mainly herbal medicines, have been playing an important role in treating diabetes around the world for centuries particularly in Asia, India, and Africa.[17,18] Many researchers are working on the discovery of new anti-diabetes drugs and have reported many new plants and their extracts' anti-diabetic activity using advancements of novel technology.[19,20] These findings provide valuable leads for the development of new isolated compounds for the treatment of diabetes.[21] However, there are still many medicinal plants available to screen for their biologic activities for disease including diabetes. Many pharmaceutical companies and academic laboratories are engaged in the discovery of new targets, pathways, and treatments for diabetes to supplement the current chemotherapies.[22] From this point of view, the present work was conducted to evaluate the anti-diabetic activity of *Zornia gibbosa* (*Z. gibbosa)* based on its traditional use. *Z. gibbosa* is an annual herb belonging to the family fabaceae. It has around 70 species in the *Zornia* genus, commonly known as Nellujollusoppu, and it grows at high altitudes i.e. 450-2000 m around India. It has been used in folklore medicine for the treatment of different ailments.[23-25]

MATERIALS AND METHODS

Reagents and chemicals

All reagents used for the present study were of analytical grade. Diagnostic kits were purchased from Span Diagnostics Ltd, Gujarat, India. Alloxan monohydrate was from Sigma chemicals, St Louis, USA, and Glibenclamide from Avantis Pharma Ltd.

Plant material and preparation of extracts

The plant material, *Z. gibbosa,* was collected at Guntur, Andhra Pradesh, India. The authentication of the plant was performed by Rtd. Prof. M. Venkaih, Department of Botany, Andhra University, Visakhapatnam (AU/DP&P/BGR/72). The plant material aerial parts were separated and shade dried at room temperature and powdered. The powdered material was used for extraction separately with ethyl acetate and hydroalcoholic (Hyd. ext) using the maceration process. The extracted solvents were concentrated to dryness under vacuum using a rotavapour.

Selection of animals

Healthy male and female albino rats of weighing between 180-250 g aged 60-90 days were used for the study. The rats were housed under standard light and humidity and were supplied proper food and water ad libitum.

Acute toxicity studies

The acute toxicity study was conducted for ethyl acetate and ethanol (70% v/v) extracts of *Z. gibbosa* as per Organisation for Economic Co-operation and Development (OECD) guidelines 420 (OECD.2001) and regulations of the Institutional Animal Ethics Committee (Reg no. 516/01/A/CPCSEA). The male albino rats were divided into two groups of 6 animals. They were maintained for one week before the experiment under room temperature and allowed free access to water and diet. The animals were subjected to an acute toxicity study using each extract at a dose of 2000 mg/kg orally in 2 groups at regular time intervals, *i.e.*, 1, 2, 4, 8, 12 and 24 h. During this time, the animals were under observation to note different conditions such as skin changes, morbidity, aggressiveness, oral secretions, sensitivity to sound and pain, respiratory movements, and mortality.

Grouping of animals for glucose lowering test

The experimental design consisted of 48 rats divided into eight groups. Group 1 received 0.1 mL of normal saline; the blood glucose of the rats was elevated by the administration of 100 mg/kg body weight of alloxan monohydrate intraperitoneally after an overnight fast but with access to drinking water, except groups 1. The animals were then housed in a controlled facility and allowed to drink 5% glucose solution to overcome the hypoglycemia. The hyperglycemic state was confirmed by the measurement of fasting blood glucose concentration using a glucometer with blood collected by tail vein puncture. Rats with blood glucose ≥200 mg/dL after 72 h were considered diabetic and used for the research.[26,27] Group 2: normal rats treated with the ethanol (70% v/v) extract 500 mg/kg body weight to determine the effect of the extract on normal blood glucose levels. Group 3: diabetic untreated (animals were treated with 100 mg/kg body weight of alloxan monohydrate); group 4: diabetic animals treated with standard drug (5 mg/kg body weight of glibenclamide); group 5: diabetic animals treated with 250 mg/kg body weight of ethyl acetate extract orally; group 6: diabetic animals treated with 500 mg/kg body weight of ethyl acetate extract orally; group 7: diabetic animals treated with 250 mg/kg body weight of ethanol (70% v/v) extract orally, and group 8: diabetic animals orally treated with 500 mg/kg body weight of ethanol (70% v/v) extract of *Z. gibbosa.*

Treatment with extract and standard drug

Extracts of *Z. gibbosa* and glibenclamide (standard drug) were dissolved in 10 mL normal saline (0.9% NaCl) before oral administration. Respective doses of extract and standard drug were then administered to the rats once daily in the morning (09:00-10:00 AM) for twelve days and the blood glucose was checked every four days. On the seventeenth day, the rats were fasted for 12 h and euthanized. Blood samples were collected by carotid puncture into heparinized tubes, centrifuged at 1000 r/min for 5 min, and the clear serum supernatant was used immediately for the assessment of the lipid profile, and liver and kidney function tests.

Serum biochemical parameters

The biochemical parameters that were investigated includes: alanine aminotransferase (ALT), aspartate aminotransferase (AST), alkaline phosphatase (ALP), total bilirubin, total protein, and creatinine using Span diagnostics Ltd. kits, and serum electrolytes (K^+, Cl^-, Na^+) were determined using Randox diagnostic kits.

Plasma lipid profiles

The plasma total cholesterol, triglyceride (TG), high-density lipoprotein (HDL), and low-density lipoprotein (LDL) were determined using Randox diagnostic kits. The absorbance was determined and calculated using a fully-smart semi-automated analyzer, BS Biosciences.

Statistical analysis

Results are expressed in mean±standard error of mean using ordinary two-way analysis of variance using GraphPad Prism-6 software. The results of $p<0.01$ were considered as significant.

RESULTS

Acute toxicity of the selected plant extracts was tested as per OECD guidelines. There were no behavior signs such as alertness, motor activity, breathlessness, restlessness, diarrhea, tremor, convulsion, and coma observed at the administered doses. The rats were physically active and no deaths were recorded in present study of extracts treated at 2000 mg/kg body weight. Therefore, the LD50 is greater than 2000 mg/kg body weight.

The glucose levels were decreased in all tested groups compared with the untreated diabetes group, which continued to have elevated levels until the animals were sacrificed. Among all doses of tested extracts, hyd. ext at 500 mg/kg body weight showed better activity in the reduction of elevated glucose levels (Figure 1) and retained the body weight of the rats (Figure 2) as the treatment moved forward, except in the diabetic untreated group. No hyperglycemia or hypoglycemia was observed in the rats treated only with the extracts.

ALT, AST, ALP, total bilirubin, total protein, creatinine levels were significantly elevated in the diabetic animals. The various doses of extracts and standard drug significantly ($p<0.01$) restored the ameliorated levels of ALT, AST, ALP, total bilirubin, total protein, creatinine levels. Normal levels of ALT and ALP levels showed a normoglycemic condition. The hydroalcoholic extract at 500 mg/kg body weight showed better activity in the increase of reduced ALT and creatinine levels as well as the reduction of increased AST, ALP, albumin and total protein levels (Figure 3, 4).

The electrolyte levels (sodium, chloride, and potassium) were varied in the diabetes-induced groups, extracts of *Z. gibbosa* significantly adjusted the electrolyte levels at the tested doses, as much as standard drug (Figure 5).

LDL, TG, and cholesterol levels were increased, whereas HDL levels were decreased in the diabetic animals. The extracts of *Z. gibbosa* and standard drug significantly decreased levels of LDL, TG, and cholesterol, and increased the HDL levels ($p<0.01$) (Figure 6).

DISCUSSION

DM is caused by failure to maintain a stable level of blood glucose in the face of normal fluctuations of supply and demand. The secretary product of pancreatic β-cells, insulin, is central in the pathophysiology of DM.[28] Type 1 DM, or insulin-dependent DM, results from an absolute deficiency of insulin due to autoimmunologic destruction of the insulin-producing pancreatic β-cells.[29] In type 2 DM, or non-insulin-dependent DM, muscle and fat cells are 'resistant' to the actions of insulin and compensatory mechanisms that are activated in the β-cells to secrete more insulin are not sufficient to maintain blood glucose levels within a normal physiologic range.[30,31]

DM is characterized by chronic hyperglycaemia and it leads to the development of different physiologic changes in the body, and finally causes diseases.[32-35] In the present study, alloxan induction was used to cause DM in the animals. It leads to

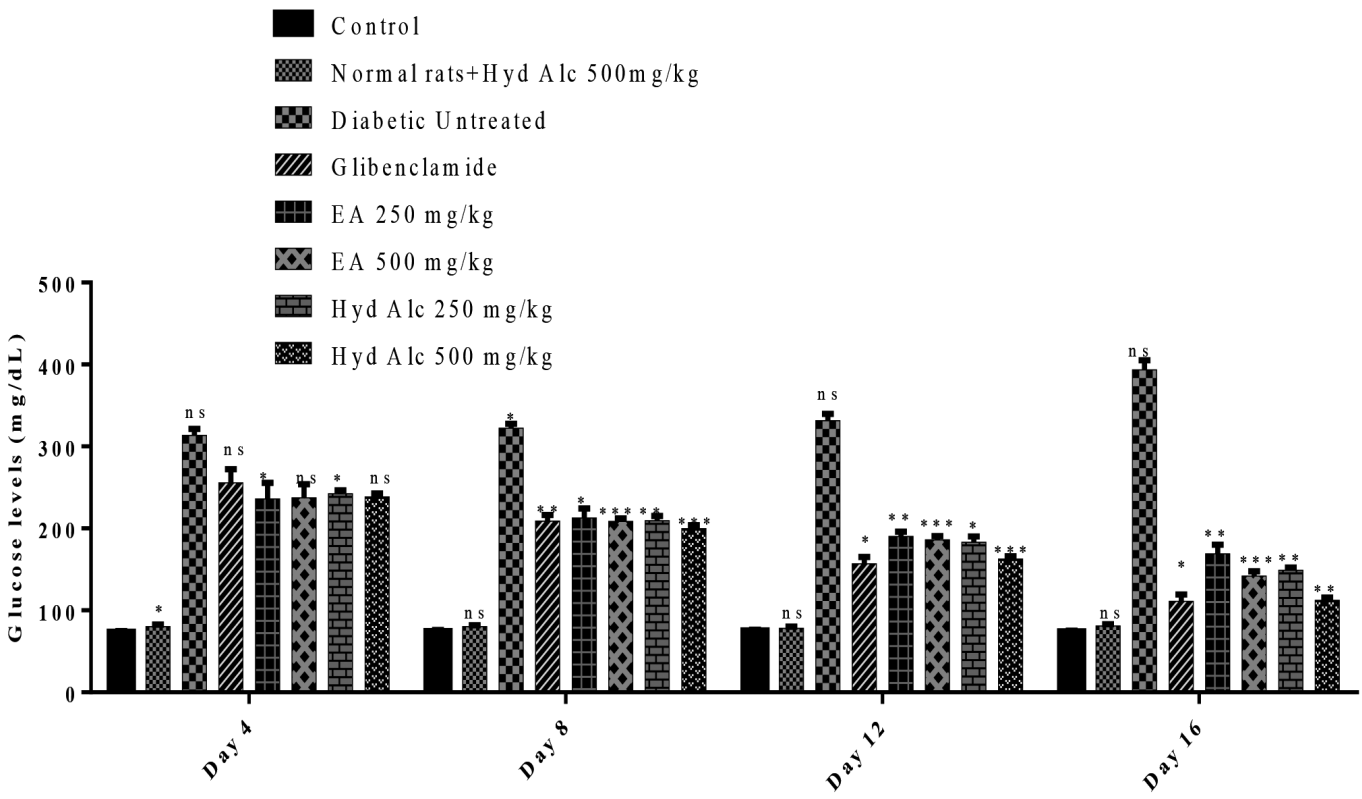

Figure 1. Glucose levels of rats in different groups

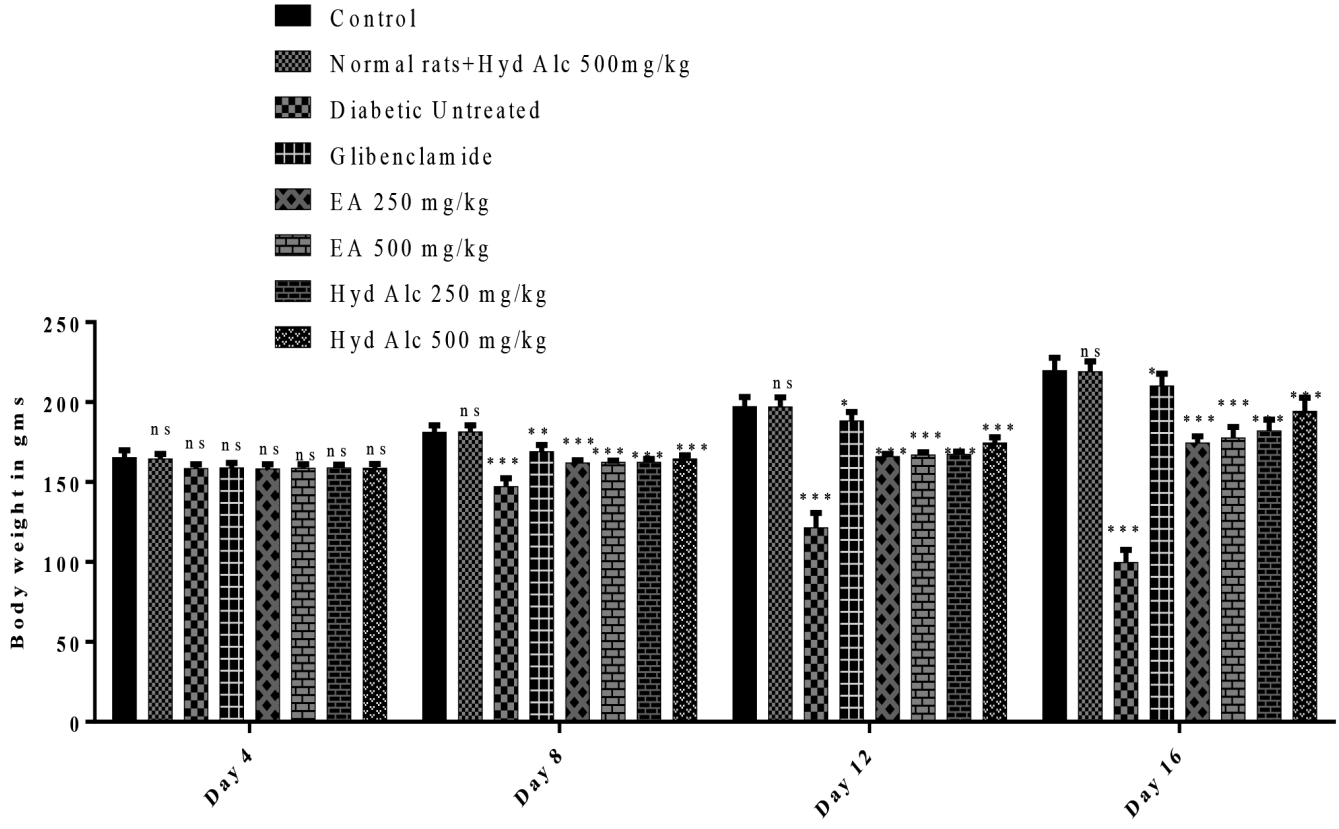

Figure 2. Body weight of the rats in different groups

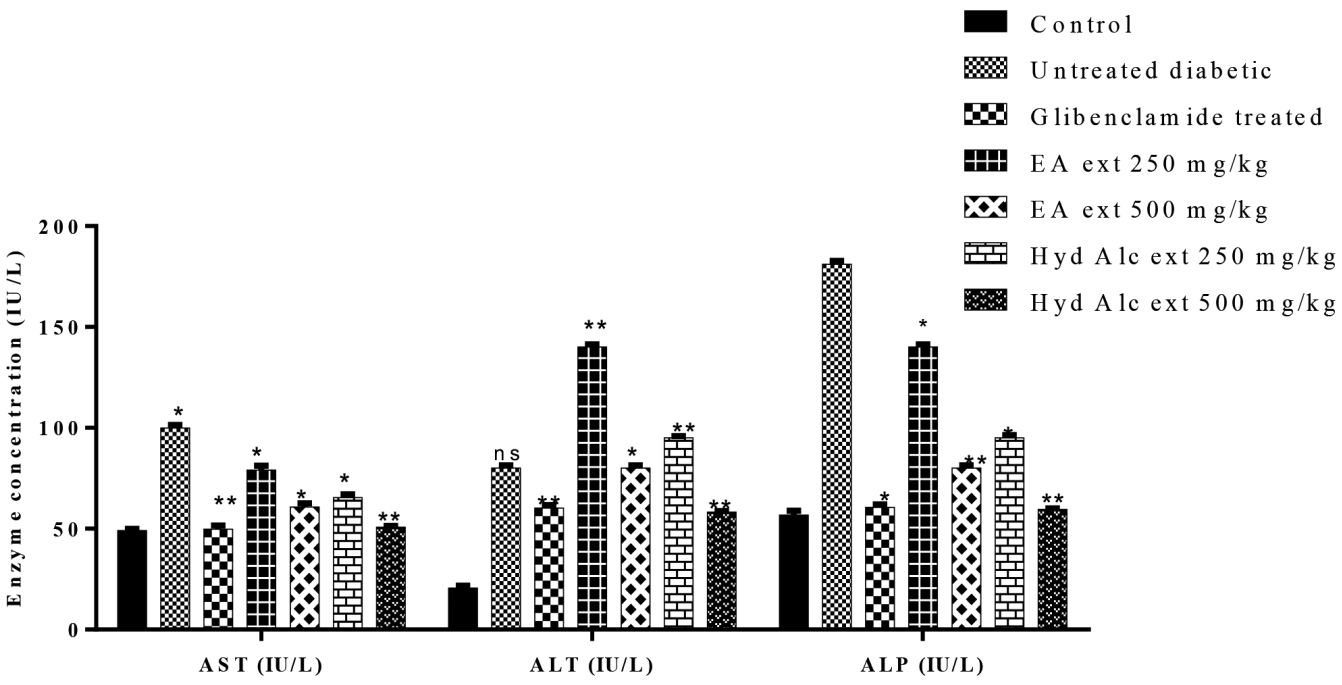

Figure 3. Effect of *Z. gibbosa* extracts on AST, ALT, ALP levels in alloxan-induced diabetic rats

AST: Aspartate aminotransferase, ALT: Alanine aminotransferase, ALP: Alkaline phosphatase

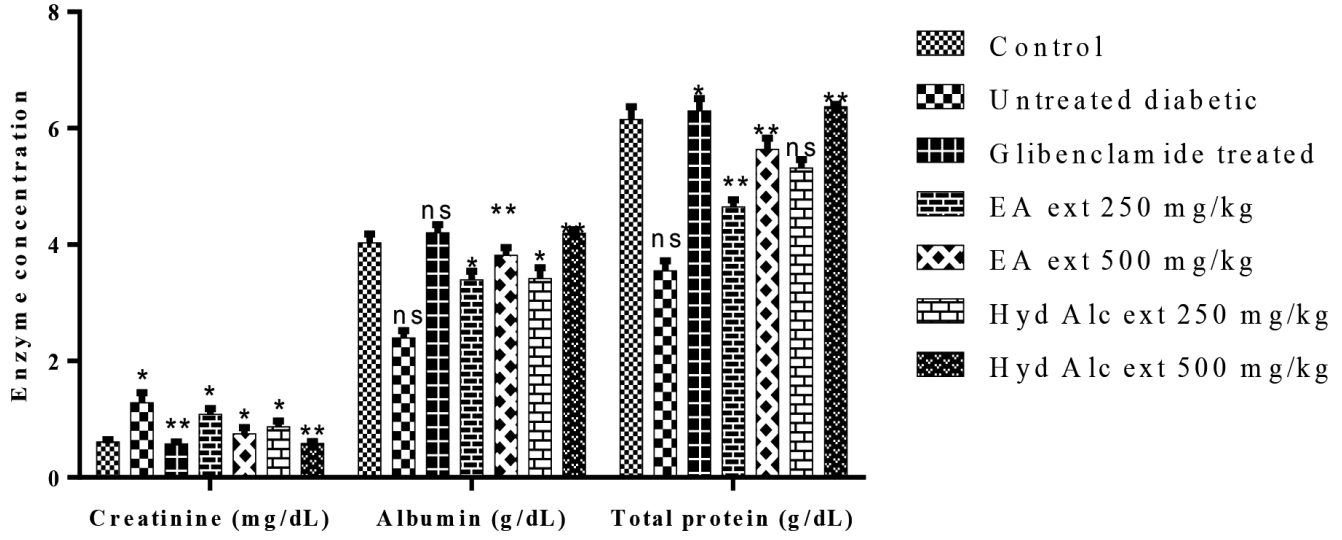

Figure 4. Effect of *Z. gibbosa* extracts on creatinine, albumin and total protein levels in alloxan-induced diabetic rats

variations in their body physiologic condition[36,37] by causing necrosis to the pancreatic β-cells,[38-40] this leads to a reduction in insulin production and finally altering enzymatic levels in different organ's functions in the body such as the kidneys and liver (Figure 3 to Figure 6). The tested extracts of *Z. gibbosa* showed a significant reduction of the increased blood glucose levels (Figure 1). The reduction of glucose levels by *Z. gibbosa* may have been through protection of the β-cells from undergoing necrosis.[1,2] The weight loss also observed after diabetic induction was probably due to excessive breakdown of tissue proteins and lipid for energy to maintain the body organs' function, but after treatment with the extracts of *Z. gibbosa*, the animals started to regain their body weight (Figure 2). The gained body weight may be due to improved metabolic activities with normal levels of glucose in the body.

Insulin helps glucose uptake in muscle and fat and inhibits hepatic glucose production. Insulin also stimulates cell growth, differentiation, and promotes the storage of substrates in fat and muscle by stimulating lipogenesis, glycogen, and protein synthesis, and inhibiting lipolysis, glycogenolysis, and protein

breakdown. Insulin deficiency (type 1 DM) or resistance (type 2 DM) results in profound deregulation of these processes, and produces elevations in fasting and postprandial glucose and lipid levels.[41-43] In the present study, elevations in electrolytes, albumin, and creatinine levels were also observed in the alloxan-induced diabetic rats and *Z. gibbosa* extracts significantly reinstated altered electrolytes, albumin, and creatinine levels in the diabetic rats (Figure 4, 5). This means that *Z. gibbosa* extracts have the ability to protect nephron function and increase electrolyte absorption in renal tubules.[44]

The enzyme levels of AST, ALT, ALP, and bilirubin indicate the functioning of the liver in the body[45,46] and alterations in these enzymes were observed in the alloxan-induced diabetic rats, which indicates that DM affects the functions of organs.[47] *Z. gibbosa* extracts significantly revised the reduced or increased enzymes levels of the liver and its function (Figure 3) due to DM, possibly through regeneration of damaged functions due to DM.

DM causes diabetic dyslipidemia, i.e. low-density cholesterol levels (LDL) and increases TG and high-density cholesterol levels (HDL), which increases the risk for heart disease and stroke.[48,49] Variations in these levels (lipid profile) were observed in the present experiment and the variations were restored in the *Z. gibbosa* extract-treated groups compared with the diabetic untreated group (Figure 6). This might be due to reduced hepatosynthesis of triglycerols or reduced

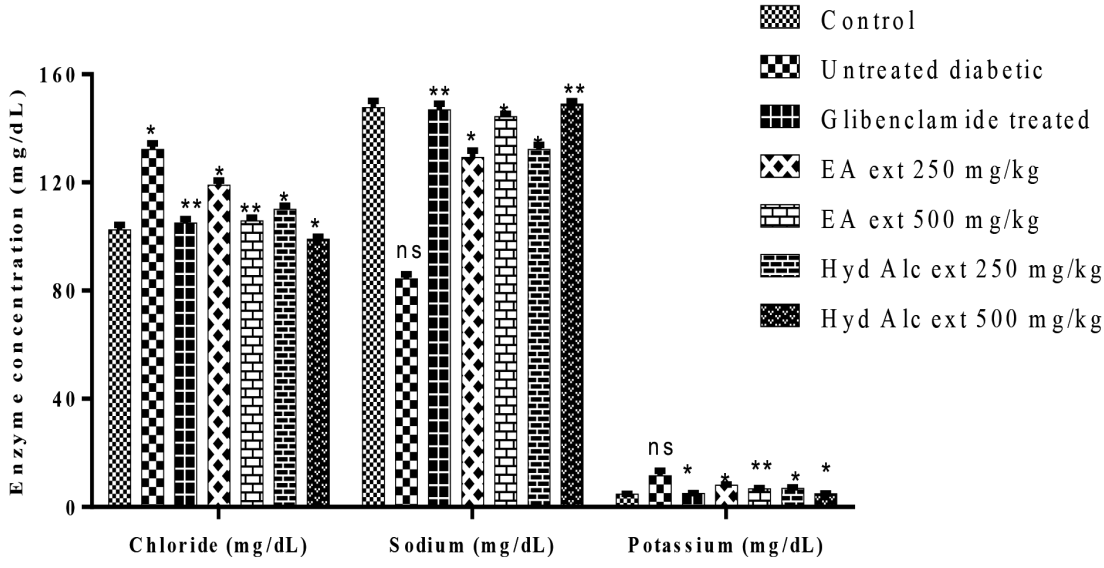

Figure 5. Effect of *Z. gibbosa* extracts on chloride, sodium and potassium levels in alloxan-induce diabetic rats

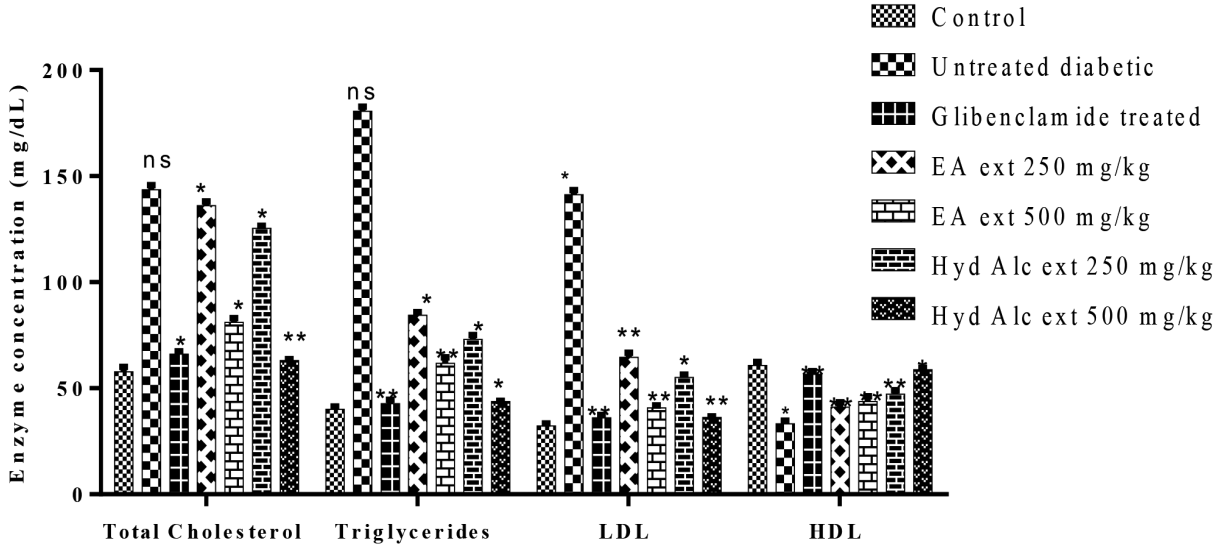

Figure 6. Effect of *Z. gibbosa* extracts in total cholesterol, triglycerides, LDL and HDL levels in alloxan-induced diabetic rats

LDL: Low-density lipoprotein, HDL: High-density lipoprotein

lipolysis because deficiency of insulin enhanced the hydrolysis of triacylglycerols.[50,51] The increased HDL levels in *Z. gibbosa* extract-treated groups indicates that these have the ability to suppress the enzymes' action responsible for LDL formation (3-hydroxy-3-methylglutaryl coenzyme A reductase) in the diabetic condition.[52] From the above results, it can be summarized that, the tested extracts of *Z. gibbosa* have the ability to restore physiologic changes that occur due to the diabetes-like reduction in glucose concentrations, gaining of body weight, and failure of organs such as the kidneys and liver.

CONCLUSIONS

DM is a well-known chronic disorder around the world with various late complications such as retinopathy, neuropathy, and nephropathy. *Z. gibbosa* has significant antidiabetic activity (glucose lowering). Therefore, it can be used as an adjuvant medicine along with allopathic medicine in the treatment of diabetes as well as for its late complications. A further study is underway in our laboratory to isolate the active principle and to study the mechanism of its action.

ACKNOWLEDGEMENTS

The authors acknowledge the authorities of AU College of Pharmaceutical Sciences for providing the necessary facilities.

Conflict of Interest: No conflict of interest was declared by the authors.

REFERENCES

1. Bell GI, Polonsky KS. Polonsky, Diabetes mellitus and genetically programmed defects in beta-cell function. Nature. 2001;414:788-791.
2. Mathis D, Vence L, Benoist C. beta-Cell death during progression to diabetes. Nature. 2001;414:792-798.
3. World Health Organization. Definition, diagnosis and classification of diabetes mellitus and its complications. Part 1: Diagnosis and classification of diabetes mellitus. Geneva; 1999.
4. Diabetes Fact sheet N°312. WHO. October 2013. Archived from the original on 26 Aug 2013. Retrieved 25 March 2014.
5. National Institute for Health and Clinical Excellence. Clinical guideline 66: Type 2 diabetes. London, 2008.
6. The American Diabetes Association Complete Guide to Diabetes, 3rd ed. Alexandria, VA: American Diabetes Association, 2002.
7. World Health Organization. Global status report on noncommunicable diseases 2010. Geneva, 2011.
8. International Diabetes Federation. p. 13. Retrieved 21 Mar 2016.
9. The top 10 causes of death Fact sheet N°310". World Health Organization; 2013.
10. Mathers CD, Loncar D. Projections of global mortality and burden of disease from 2002 to 2030. PLoS Med. 2006;3:442.
11. Morrish NJ, Wang SL, Stevens LK, Fuller JH, Keen H. Mortality and causes of death in the WHO Multinational Study of Vascular Disease in Diabetes. Diabetologi. 2001;44(Suppl 2):14-21.
12. Roglic G, Unwin N, Bennett PH, Mathers C, Tuomilehto J, Nag S, Connolly V, King H. The burden of mortality attributable to diabetes: realistic estimates for the year 2000. Diabetes Care. 2005;28:2130-2135.
13. Howlett HC, Bailey CJ. A risk-benefit assessment of metformin in type 2 diabetes mellitus. Drug Saf. 1999;20:489-503.
14. Krentz AJ, Bailey CJ. Oral antidiabetic agents: current role in type 2 diabetes mellitus. Drugs. 2005;65:385-411.
15. Stein SA, Lamos EM, Davis SN. A review of the efficacy and safety of oral antidiabetic drugs. Expert Opin Drug Saf. 2013;12:153-175.
16. Chang CL, Lin Y, Bartolome AP, Chen YC, Chiu SC, Yang WC. Herbal Therapies for Type 2 Diabetes Mellitus: Chemistry, Biology, and Potential Application of Selected Plants and Compounds. Evid Based Complement Alternat Med. 2013;2013:378657.
17. Jia W, Gao W, Tang L. Antidiabetic herbal drugs officially approved in China. Phytotherapy Res. 2003;17:1127-1134.
18. Hays NP, Galassetti PR, Coker RH. Prevention and treatment of type 2 diabetes: current role of lifestyle, natural product, and pharmacological interventions. Pharmacol Ther. 2008;118:181-91.
19. Jung M, Park M, Lee HC, Kang YH, Kang ES, Kim SK. Antidiabetic agents from medicinal plants. Curr Med Chem. 2006;13:1203-1218.
20. Gershell L. Type 2 diabetes market. Nat Rev Drug Discov. 2005;4:367-368.
21. Salimifar M, Fatehi-Hassanabad Z, Fatehi M. A review on natural products for controlling type 2 diabetes with an emphasis on their mechanisms of actions. Curr Diabetes Rev. 2013;9:402-411.
22. Carpino PA, Goodwin B. Diabetes area participation analysis: a review of companies and targets described in the 2008-2010 patent literature. Expert Opin Ther Pat. 2010;20:1627-1651.
23. Pullaiah T, Ramakrishnaiah V, Sandhya Rani S, Rao PN. Flora of Guntur District Andhra Pradeh, India. Regency Publications; New Delhi; 2001:140.
24. Sawant BV, Bairy TS. Phyto-Pharmacognostical study of *Zornia gibbosa* Span (Samyojaki). Research & Reviews: A Journal of Pharmacology. 2013;3:24-32.
25. Sawant BV, Bairy TS, Shrikanth P Acharya. Analgesic Activity and Acute Toxicity Study of *Zornia gibbosa* Span (Samyojaki) in Mice. Research & Reviews: A Journal of Pharmacology. 2014;4:1-4.
26. Pari L, Amarnath Satheesh M. Antidiabetic activity of Boerhavia diffusa L. effect on hepatic key enzymes in experimental diabetes. J Ethnopharmacol. 2004;91:109-113.
27. Yadav JP, Saini S, Kalia AN, Dangi AS. Hypoglycemic and hypolipidemic activity of ethanolic extract of Salvadora oleoides in normal and alloxan-induced diabetic rats. Indian J Pharmacol. 2008;40:23-27.
28. Expert Committee on the Diagnosis and Classification of Diabetes Mellitus. Report of the expert committee on the diagnosis and classification of diabetes mellitus. Diabetes Care. 2001;26(Suppl 1):5-20.
29. Atkinson MA, Eisenbarth GS. Type 1 diabetes: new perspective on disease pathogenesis and treatment. Lancet. 2001;358:221-229.
30. Cavaghan MK, Ehrmann DA, Polonsky KS. Interactions between insulin resistance and insulin secretion in the development of glucose intolerance. J Clin Invest. 2000;106:329-333.
31. Kahn SE. Clinical review 135: The importance of b-cell failure in the development and progression of type 2 diabetes. J Clin Endocrinol Metab. 2001;86:4047-4058.

32. Diabetes Control and Complications Trial Research Group, Nathan DM, Genuth S, Lachin J, Cleary P, Crofford O, Davis M, Rand L, Siebert C. The effect of intensive treatment of diabetes on the development and progression of long-term complications in insulin-dependent diabetes mellitus. N Engl J Med. 1993;329:977-986.

33. Wei M, Gaskill SP, Haffner SM, Stern MP. Effects of diabetes and level of glycemia on all-cause and cardiovascular mortality. The San Antonio Heart Study. Diabetes Care. 1998;7:1167-1172.

34. Ebara T, Conde Karin, Kako Y, Liu Y, Xu Y, Ramaksishnan R, Goldberg IJ, Shachter NS. Delayed catabolism of apoB-48 lipoproteins due to decreased heparan sulfate proteoglycan production in diabetic mice. J Clin Invest. 2000;105:1807-1818.

35. Ginsberg HN. Insulin resistance and cardiovascular disease. J Clin Invest. 2000;106:453-458.

36. Williams SB, Goldfine AB, Timimi FK, Ting HH, Roddy MA, Simonson DC, Creager MA. Acute hyperglycemia attenuates endothelium-dependent vasodilation in humans *in vivo*. Circulation. 1998;97:1695-1701.

37. Du XL, Edelstein D, Rossetti L, Fantus IG, Goldberg H, Ziyadeh F, Wu J, Brownlee M. Hyperglycemia-induced mitochondrial superoxide overproduction activates the hexosamine pathway and induces plasminogen activator inhibitor-1 expression by increasing Sp1 glycosylation. Proc Nat Acad Sci USA. 2000;97:12222-12226.

38. Kliber A, Szkudelski T, Chichlowska J. Alloxan stimulation and subsequent inhibition of insulin release from *in situ* perfused rat pancreas. J Physiol Pharmacol. 1996;47:321-328.

39. Goldner MG, Gomori G. Studies on the mechanism of alloxan diabetes. Endocrinology. 1944;35:241-248.

40. Tasaka Y, Inoue Y, Matsumoto H, Hirata Y. Changes in plasma glucagon, pancreatic polypeptide and insulin during development of alloxan diabetes mellitus in dog. Endocrinol Jpn. 1988;35:399-404.

41. Klip A, Paquet MR. Glucose transport and glucose transporters in muscle and their metabolic regulation. Diabetes Care. 1990;13:228-243.

42. Brüning JC, Michael MD, Winnay JN, Hayashi T, Hörsch D, Accili D, Goodyear LJ, Kahn CR. A muscle-specific insulin receptor knockout exhibits features of the metabolic syndrome of NIDDM without altering glucose tolerance. Mol Cell. 1998;2:559-569.

43. Abel ED, Peroni O, Kim JK, Kim YB, Boss O, Hadro E, Minnemann T, Shulman GI, Kahn BB. Adipose-selective targeting of the GLUT4 gene impairs insulin action in muscle and liver. Nature. 2001;409:729-733.

44. Day A, Mayne P, Mayne PD. Clinical chemistry in diagnosis and treatment. 6th ed. London; CRC Press; 1994.

45. LaRosa JC, Grundy SM, Waters DD, Shear C, Barter P, Fruchart JC, Gotto AM, Greten H, Kastelein JJ, Shepherd J, Wenger NK; Treating to New Targets (TNT) Investigators. Intensive lipid lowering with atorvastatin in patients with stable coronary disease. N Engl J Med. 2005;352:1425-1435.

46. Snow V, Aronson MD, Hornbake ER, Mottur-Pilson C, Weiss KB; Clinical Efficacy Assessment Subcommittee of the AmericanCollege of Physicians. Lipid control in the management of type 2 diabetes mellitus: a clinical practice guideline from the American College of Physicians. Ann Intern Med. 2004;140:644-650.

47. Green RM, Flamm S. AGA technical review on the evaluation of liver chemistry tests. Gastroenterology. 2002;123:1367-1384.

48. Pfeffer MA, Keech A, Sacks FM Cobbe SM, Tonkin A, Byington RP, Davis BR, Friedman CP, Braunwald E, et al. Safety and tolerability of pravastatin in long-term clinical trials: prospective Pravastatin Pooling (PPP) Project. Circulation. 2002;105:2341-2346.

49. Heart Protection Study Collaborative Group. MCR/BHF Heart Protection Study of cholesterol lowering with simvastatin in 20,536 high-risk individuals: a randomised placebo-controlled trial. Lancet. 2002;360:7-22.

50. Gagne C, Bays HE, Weiss SR, Mata P, Quinto K, Melino M, Cho M, Musliner TA, Gumbiner B; Ezetimibe Study Group, et al. Efficacy and safety of ezetimibe added to ongoing statin therapy for treatment of patients with primary hypercholesterolemia. Am J Cardiol. 2002;90:1084-1091.

51. Crouse JR. Hypertriglyceridemia: a contraindication to the use of bile acid binding resins. Am J Med. 1987;83:243-248.

52. Saltiel AR, Kahn CR. Insulin signalling and the regulation of glucose and lipid metabolism. Nature. 2001;414:799-806.

Turk J Pharm Sci 2018;15(3):347-353
DOI: 10.4274/tjps.16779

ORIGINAL ARTICLE

Anatomic Studies on *Verbascum pestalozzae* Boiss. and *Verbascum pycnostachyum* Boiss. & Heldr.

Verbascum pestalozzae Boiss. ve *Verbascum pycnostachyum* Boiss. & Heldr. Üzerinde Anatomik Araştırmalar

Sevim KÜÇÜK[1]*, Melike Belkıs GÖKÇE[1], Ramazan Süleyman GÖKTÜRK[2]

[1]Anadolu University, Faculty of Pharmacy, Pharmaceutical Botany, Eskişehir, Turkey
[2]Akdeniz University, Faculty of Science, Department of Biology, Antalya, Turkey

ABSTRACT

Objectives: The genus *Verbascum L*. (Scrophulariaceae) known as "sığır kuyruğu" in Anatolia is represented by 248 species, 193 of which are endemic. The flowers contain essential oil, mucilage, and glycosides. Some species of *Verbascum* have some folkloric uses as expectorants, sedatives, and treatment for dysmenorrhea and rheumatalgia. Its use for healing wounds in animal care has also been reported. In this study, the anatomic structures of root, stem, and leaves of *Verbascum pestalozzae* Boiss. and *Verbascum pycnostachyum* Boiss. & Heldr. are given for the first time. According to the results, some of the differences between stem and leaf anatomic features of these species were described and the data were supported by detailed photographs.

Materials and Methods: Specimens were collected from C3 Antalya: Voucher specimens of *V. pestalozzae* and *V. pycnostachyum* were deposited in the Herbarium of the Biology Department, Akdeniz University in Antalya, Turkey and Herbarium of the Faculty of Pharmacy, Anadolu University in Eskişehir, Turkey. The materials were identified as *V. pestalozzae* and V. *pycnostachyum* using flora of Turkey and the East Aegean islands. For anatomic studies, samples were collected from the natural habitats and kept in 70% alcohol. In the research, root, stem and leaves of mature and flowered plants were used. Investigations were performed on the cross-sections of the root, the flowering stem, and the leaf. The anatomic structures of the species were drawn using a Leitz SM-LUX binocular microscope. All sections were embedded in glycerin gelatin and stained using Sartur reactive, and photographs were taken through a light microscope (Olympus BX51T).

Results: The cross sections taken from root, stem, and leaves of *V. pestalozzae* and *V. pycnostachyum* were examined and the anatomic features belonging to these plants were determined and compared.

Conclusion: The anatomic properties belonging to the two species were generally compatible with findings of Metcalfe and Chalk and others signified in the genus. We believe that our results provide additional evidence for taxonomists to help separate the species. The lack of a taxonomic, morphologic, and anatomic study on the species made it important for the systematic introduction of the research.

Key words: Scrophulariaceae, *Verbascum*, anatomy, endemic

ÖZ

Amaç: Anadolu'da "Sığır kuyruğu" olarak adlandırılan *Verbascum L.* (Scrophulariaceae) cinsi, ülkemizde 193'ü endemik olmak üzere 248 tür ile temsil edilmektedir. Çiçekleri müsilaj, uçucu yağ ve glikozitler taşır. Bazı *Verbascum* türleri halk arasında göğüs yumuşatıcı ve balgam söktürücü olarak, adet sancısını gidermede, yatıştırıcı, romatizma ağrılarını giderici ve ayrıca hayvan yaralarını tedavi etmekte kullanılmaktadır. *Verbascum pestalozzae* Boiss. ve *Verbascum pycnostachyum* Boiss. & Heldr. türlerinin kök, gövde ve yaprak anatomik yapıları ilk kez bu çalışmada verilmiştir. Araştırmalar sonucunda türlerin gövde ve yaprak anatomik özellikleri belirlenmiş ve veriler detaylı fotoğraflarla desteklenmiştir. Gen merkezi Anadolu olmasına rağmen *Verbascum* ile ilgili yeterli çalışmaların bulunmaması ve taşıdığı sekonder metabolitler ile potansiyel bir tıbbi bitki olması çalışmanın önemini artıracaktır.

Gereç ve Yöntemler: *V. pestalozzae* ve *V. pycnostachyum*'a ait örnekler C3 Antalya'dan toplanmış, Akdeniz Üniversitesi Biyoloji Bölümü ve Anadolu Üniversitesi Eczacılık Fakültesi Herbaryumu'na konulmuştur. Türlerin teşhisi Türkiye florası ve Doğu Ege adaları kullanılarak belirlenmiştir. Anatomik çalışmalar için, örnekler doğal habitatlardan toplanmış ve %70 alkolde tutulmuştur. Araştırmada, olgun ve çiçekli bitkilerin kök, gövde ve yaprakları kullanılmıştır. Kök, çiçekli gövde ve yaprak kesitleri üzerinde incelemeler yapılmış. Türlerin anatomik yapılarının çizimleri Leitz SM-LUX binoküler mikroskop kullanılarak yapılmıştır. Kesitler gliserin jelatin ile daimileştirilip, Sartur reaktifiyle boyanmış ve fotoğraflar ışık mikroskobu (Olympus BX51T) ile çekilmiştir.

*Correspondence: E-mail: salan@anadolu.edu.tr, Phone: +90 545 299 72 14 ORCID-ID: orcid.org/0000-0002-3594-0364
Received: 11.08.2016, Accepted: 18.05.2017

Bulgular: *V. pestalozzae* ve V. *pycnostachyum*'un kök, gövde ve yapraklarından alınan kesitler incelenmiş ve bu bitkilere ait anatomik özellikler karşılaştırılmıştır.

Sonuç: İki türe ait anatomik özellikler genellikle Metcalfe ve Chalk ve diğer çalışmalarda belirtilen bulgularla uyumludur. Sonuçlarımızın, taksonomistlere ek kanıt sağladığına ve türlerin ayrılmasına yardımcı olabileceğine kanısındayız. Türler üzerinde taksonomik, morfolojik ve anatomik bir çalışma olmaması, araştırmanın sistematik olarak tanıtımı için önemli hale getirmiştir.

Anahtar kelimeler: Scrophulariaceae, *Verbascum*, anatomi, endemik

INTRODUCTION

The genus *Verbascum* Linnaeus (1753: 177) (excl. *Celsia* Linnaeus 1753: 621) (Scrophulariaceae) has about 360 species from all over the world (Heywood 1993, Mabberley 2008). Represented with 248 species in Turkey, the genus has been divided into 13 partly artificial groups with 130 additional hybrids. Among them, 193 species are endemic to Turkey, with an endemism percentage of about 80%. The genus *Verbascum* L. (Scrophulariaceae) known as "Sığır Kuyruğu" in Anatolia.[1-5]

Many plant species among the flora of Turkey play important roles in traditional medicine. There are approximately 9300 plant species in Turkish flora, some of which are widely used in folkloric medicine due to their antimicrobial and anticarcinogenic properties.[6,7] One of the well-known *Verbascum* species is *V. thapsus* L., which has been used for the treatment of several diseases including asthma, spasmodic cough, migraine, and earache. Moreover, *V. thapsus, V. fruticulosum* Post, *V. undulatum* Lam. and *V. georgicum* Bentham have anti-malarial and anti-viral effects, which have been investigated in both *in vitro* and *in vivo* studies.[6]

It is reported that leaves and flowers of *Verbascum* species have expectorant, mucolytic, and demulcent properties, and they are used to treat respiratory disorders such as bronchitis, dry coughs, tuberculosis, and asthma in Anatolia.[8,9] *Verbascum* species are also used to treat hemorrhoids, rheumatic pain, superficial fungal infections, wounds and diarrhea. Furthermore, these species demonstrate several inhibitory activities against the murine lymphocytic leukemia and influenza viruses A2 and B. Macerated oil prepared from the flowers is used for reducing earache, and applied externally for eczema and other types of inflammatory skin disorders.[10]

Verbascum species have some folkloric uses such as a sedative, and treatment for dysmenorrhea and rheumatalgia. Its use for healing wounds has also been reported in animal care. Iridoid and neolignan type glycosides, oleanan type terpenes, flavonoids, polysaccharides, saponins, steroids and alkaloids were major compounds isolated from *Verbascum* species.[11] In several bioactivity studies on *Verbascum* sp., anti-proliferative,[12] anti-inflammatory,[13] antioxidant,[14,15] anti-histaminic, anti-fungal, anti-bacterial,[16] wound healing,[17] anti-microbial[18] and anti-cancer effects[19] have been shown in crude extracts of roots, leaves, flowers, and aerial parts.

Verbascum genus is one of the largest genus with regard to the number of species in Turkey and is also known for several problems in diagnosis and taxonomy.

In addition, the anatomic structures of root, stem and leaves of and *Verbascum pestalozzae* Boiss. (endemic), "Boz Sığır Kuyruğu" and *Verbascum pycnostachyum* Boiss. & Heldr. "Eğirdir Sığır Kuyruğu"[2,4] are given in this study for the first time.

EXPERIMENTAL

Plant material

The flowering aerial parts of *Verbascum pestalozzae* were collected from C3 Antalya: Konyaaltı, Doyran, between Saklıkent and Karçukuru (36^0 49' 01'' N, 30^0 21' 54'' E), on lime stone rocks, 2100 m, 17.07.2008, ESSE 15069! Göktürk 7338; *Verbascum pycnostachyum* were collected from C3 Antalya, between Korkuteli and Fethiye (37° 02' 53'' N, 30° 06' 26 '' E), steppe, 1370 m above the sea level, at the end of July 2007, Eskişehir (ESSE) 14730!, Göktürk 6093; (Figures 1-3). Voucher specimens of *V. pestalozzae* and *V. pycnostachyum* were deposited in the Herbarium of the Biology Department, Akdeniz University in Antalya, Turkey and Herbarium of the Faculty of Pharmacy, Anadolu University in ESSE, Turkey. The materials were identified as *V. pestalozzae* and *V. pycnostachyum* using flora of Turkey and the East Aegean islands.[2]

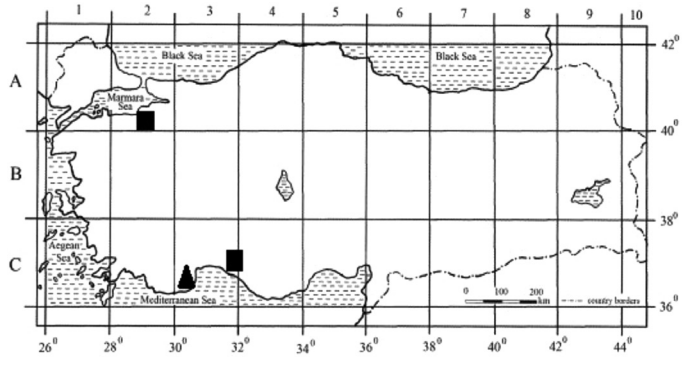

Figure 1. Distribution map of *V. pestalozzae* (▲) and *V. pycnostachyum* (■) in Turkey

Figure 2. *V. pestalozzae*

Anatomical

For anatomic studies, samples were collected from the natural habitats and kept in 70% alcohol. In the research, root, stem, and leaves of mature and flowered plants were used. Investigations were performed on the cross-sections of the root, the flowering stem, and the leaf. The anatomic structures of glandular and covering hairs were drawn using a Leitz SM-LUX binocular microscope. All sections were embedded in glycerin gelatin and stained using Sartur reactive, and photographs were taken through a light microscope (Olympus BX51T).

RESULTS AND DISCUSSION

The cross sections taken from root, stem, and leaves of *V. pestalozzae* and *V. pycnostachyum* were examined and the anatomic features belonging to these plants were determined and compared (Figures 4-10, Table 1).

Figure 3. *V. pycnostacyum* habit (picture: R.S. Göktürk)

Root

The root in both species is composed of periderm on the outside and felloderm where 4-5 radial rows are broken down and felloderm with 2-3 rows of tissue. Outer felloderm cells are tissue debris of the primary cortex that has been shattered or crushed in place. Secondary phloem formed of elliptical-shapeless, round-shaped, irregular-arranged and 4-6 row cells under the periderm is taken part. Cambium is uncertain. The secondary xylem part covers a large area and consists of tracheal elements with large and small sizes in a

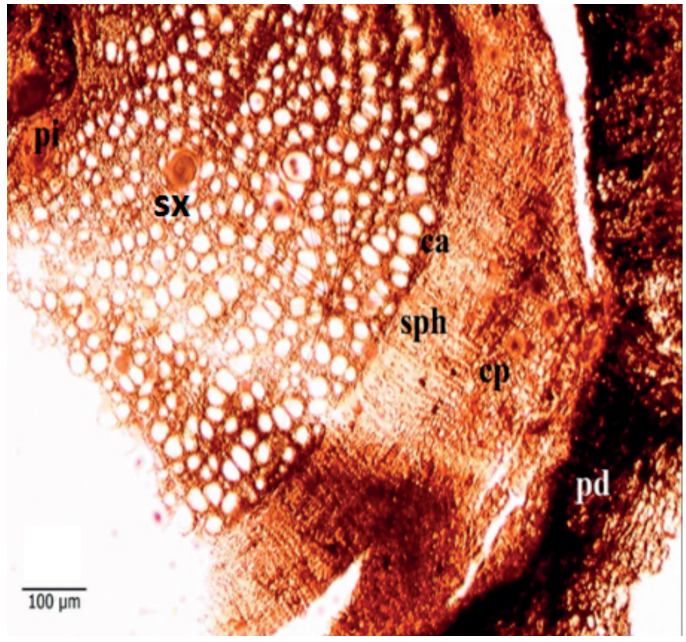

Figure 4. *V. pestalozzae*; cross-section of root

cp: Cortex parenchym, pd: Peridermis, pi: Pith, sph: Secondary phloem, sx: Secondary xylem

Table 1. Anatomic differences of the species

		V. pestalozzae	*V. pycnostachyum*
Root	**Pith**	**Parenchymatic**	**Parenchymatic**
Stem	Sclerenchyma	3-6 celled	1-5 celled
	Phloem	Thick, 3-8 celled	Thick, 8-15 celled
Leaf		Abaxial surface is projected under the vascular bundle	Protrusion
	Vascular bundles	Crescent-shaped	Horne shaped
	Upper parenchymatic cells	5-6 celled	25-30-celled
	Lower epidermis parenchymatic cells	5-10 celled	10-15 celled
Eglandular hairs in the stem and leaf		Candelabriform, stellate, multicellular	Candelabriform, stellate, multicellular
Glandular hairs in the stem and leaf		Head 1 stalk 2 celled; Head 2 stalk 1 celled; Head 3 stalk 2 celled; Head 1 stalk 3 celled; Head 2 stalk 3 celled; pellucid glands	Head 1 stalk 1 celled Head 2 stalk 1 celled Head 3 stalk 2 densely

sclerenchymatic tissue. Medullary rays are 2-3 rows of cells. The pith region, covering a narrow area, is parenchymatic in *V. pestalozzae* and *V. pycnostacyum* (Figures 4, 7).

Stem

When cross-sections were taken on the stems of two *Verbascum* species, secondary growth was observed. The epidermis is formed by a single-row, thick membrane elliptic or round cells. The upper and lower walls are thick but the lateral sides are thin. Its upper surface is covered with cuticle (Figures 5, 8). Covering hair and glandular trichomes were observed. Covering hairs of *V. pestalozzae* are candelabriform, stellate, and multicellular. Glandular trichomes were of 6 types; head 1 stalk 2 celled; head 2 stalk 1 celled; head 3 stalk 2 celled; head 1 stalk 3 celled; head 2 stalk 3 celled; pellucid glands (Figures 11b). Covering hairs are candelabriform, stellate, and multicellular in *V. pycnostachyum*. Its glandular trichomes are of three types; head 1 stalk 1 celled, head 2 stalk 1 celled, head 3 stalk 2 celled (dense, Figures 10). Parenchymatic cortex in 5 or 20 rows is found in both species under the epidermis. Collenchyma cells under the epidermis in the primary cortex were seen, and parenchyma cells including oval-shaped chloroplast inside the epidermis were found. Druse crystals were observed in parenchymatic cells. The endodermis, consisting of flattened cells, can hardly be distinguished from the cortex parenchyma. There were large, small, and discontinuous sclerenchyma bunches, 3 or 6 rows in secondary phloem of *V. pestalozzae*, but 1-5 rows in *V. pycnostachyum*. Phloem is much narrower in *V. pestalozzae* with 3-8 rows, but it is much wider in *V.*

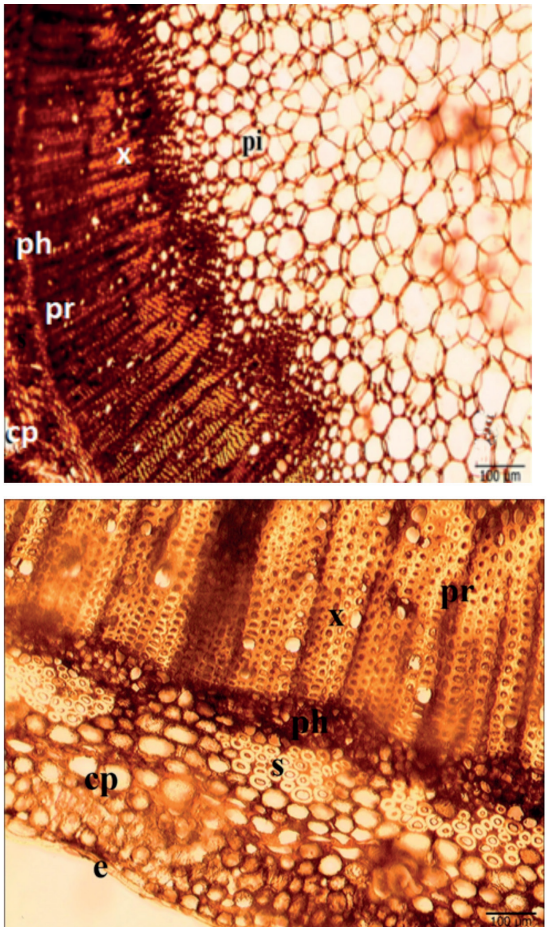

Figure 5. *V. pestalozzae*; cross-section of stem

cp: Cortex parenchym, e: Epidermis, ph: Phloem, pi: Pith, pr: Pith ray, s: Scleranchyma, x: Xylem

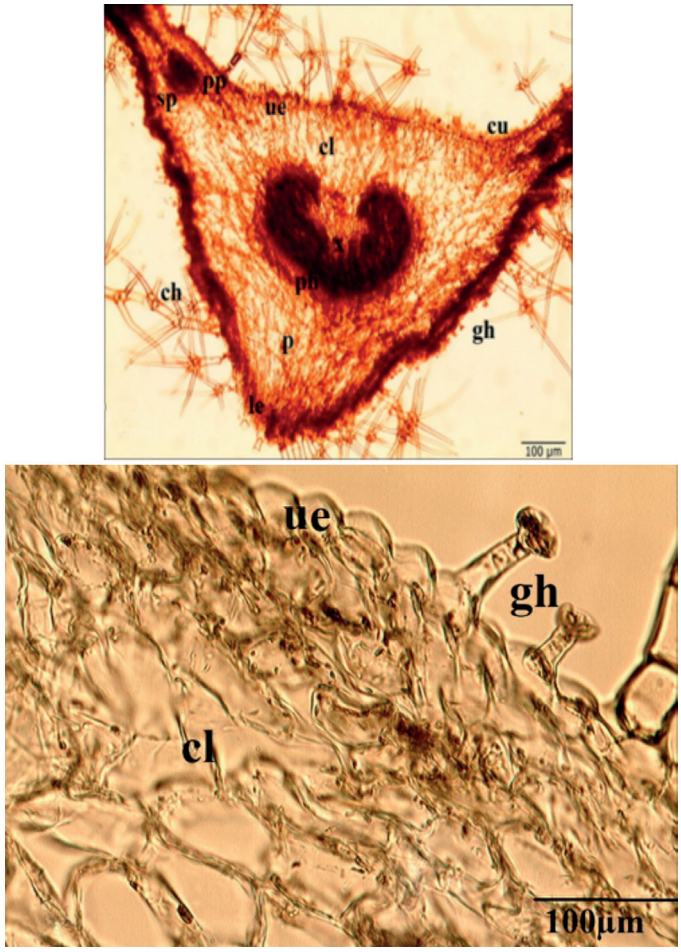

Figure 6. *V. pestalozzae*; cross-section of leaf, respectively

ch: Covering hair, cl: Collenchyma, cu: Cuticle, gh: Glandular hair, p: Parenchyma, ph: Phloem, ue: Upper epidermis, x: Xylem

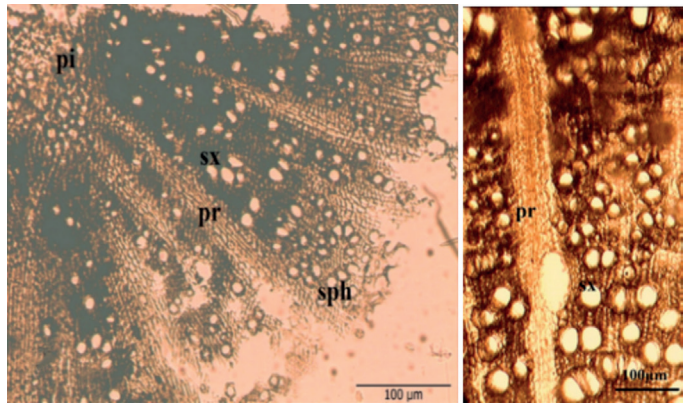

Figure 7. *V. pycnostachyum*; cross-section of root

pi: Pith, pr: Pith ray, sph: Secondary phloem, sx: Secondary xylem

pycnostachyum with 8-15 rows, but has a circle shape consisting of flattened, shapeless or oval cells. Cambium is uncertain. Bunches in both types of secondary xylem narrowed towards the primary xylem. Sclerenchymatic cells in this part, formed from trache and tracheids in both types, created regular rows in a radial direction. Pith bunches were in the form of large polygon or round- shaped and parenchymatic cells where their walls were lignified. Druse crystals were clearly found in these cells (Figures 5, 8).

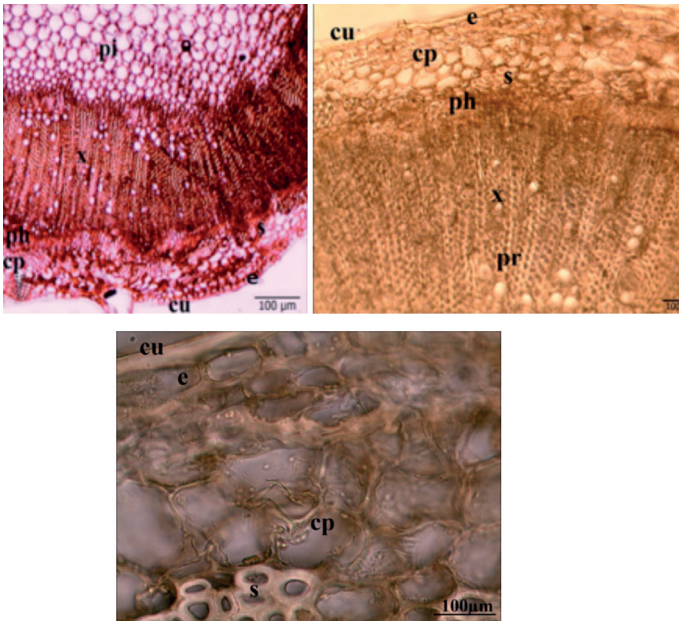

Figure 8. *V. pycnostachyum*; cross-section of stem

cp: Cortex, parenchym, cu: Cuticle, e: Epidermis, ph: Phloem, pi: Pith, pr: Pith ray, s: Scleranchyma, x: Xylem

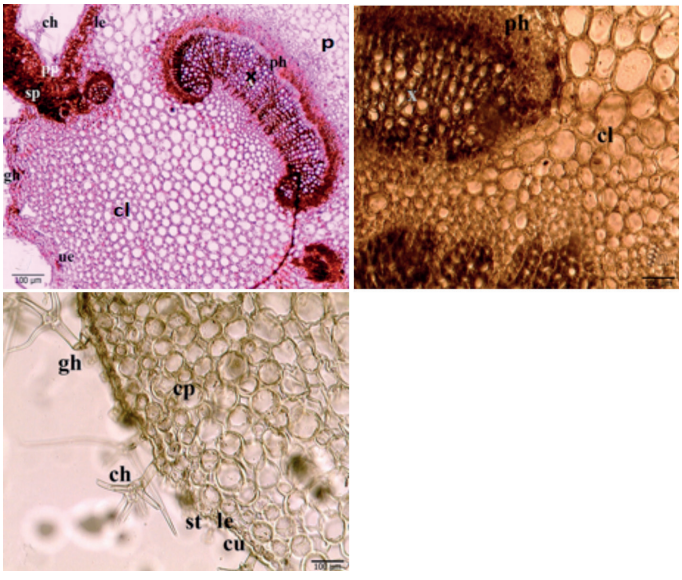

Figure 9. *V. pycnostachyum*; cross-section of leaf, respectively

ch: Covering hair, cl: Collenchyma, cp: Cortex, parenchym, cu: Cuticle, gh: Glandular hair, le: Lower epidermis, p: Parenchyma, ph: Phloem, pp: Palisade parenchyma, st: Sp-spongy parenchyma, ue: Upper epidermis, x: Xylem

Leaf

In the cross-section of the main and inter vascular tissues, the outer and inner layers of *V. pestalozzae* and *V. pycnostachyum* were clearly protrusive. The epidermis includes a single flattened row, rectangular, round or oval-shaped cells. Outer epidermal cells are larger than the inner epidermal cells, covered with a thin cuticle layer, which is curled over. Outer membranes are thicker than inner and longitudinal membranes, but the inner membranes of epidermal cells in the middle vein area became thicker. Covering hairs and glandular hairs were the same as the stem and seen in both epidermis. Covering hairs are candelabriform, stellate, and multicellular in *V. pestalozzae.* Glandular hairs were of 6 types. The covering hairs of *V. pycnostachyum* were candelabriform, stellate, and multicellular. Glandular hairs were of 3 types. Stoma (amphistomatic) found on both surfaces of the leaf were much denser on the lower surface. The transverse cross-section is higher than the epidermal cells (hygromorphic stoma). In all types of mesophyll was arranged as two or three-rows under the outer epidermis. It was formed with plentiful chloroplasted palisade parenchyma and three or five rows of sponge parenchyma, which was underneath (bifacial leaf). Vascular bundles were collateral. These were well developed in a continuous crescent in *V. pestalozzae* but interrupted and horn-shaped in *V. pycnostachyum*. Xylem was located in the upper epidermis, while the floor was located in the lower epidermis. In xylem, tracheal elements are arranged radially and thin-walled parenchymal cells are present. Phloem is placed under the xylem. Clear parenchymatic cells were arranged in 2 or 3 rows under the outer epidermis, five or six rows in *V. pestalozzae* after collenchyma, and 5 or 6 rows in *V. pycnostachyum*. Parenchymatic tissue was found in *V. pycnostachyum* with 25-30 rows under the phloem till the inner epidermis, but much narrower in *V. pestalozzae* with 5-10 rows. Thick lateral veins in both sides of the middle vein were arranged till the edge of palm and the middle vein made a deep outgrowth. The lateral veins had the same anatomical structure as the middle veins, but vascularity was much more reduced (Figures 6, 9-12).

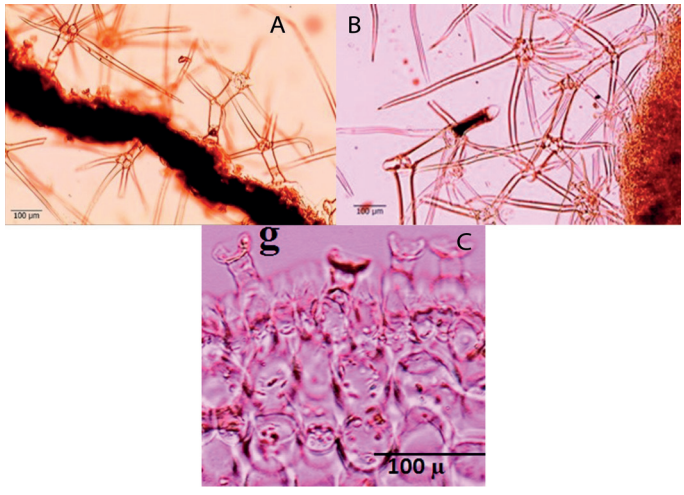

Figure 10. Hairs of stem and leaf. (A) *V. pestalozzae* eglanular hairs of; leaf (B). *V. pycnostachyum* eglandular hairs of leaf, glandular hairs of stem (C)

g: Glandular hairs

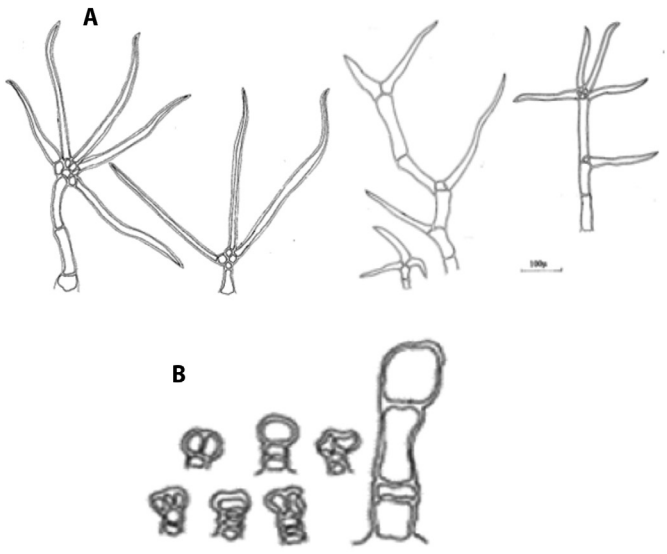

Figure 11. Hairs of stem and leaf of *V. pestalozzae* and *V. pycnostachyum* (A) eglandular hairs (B) glandular hairs

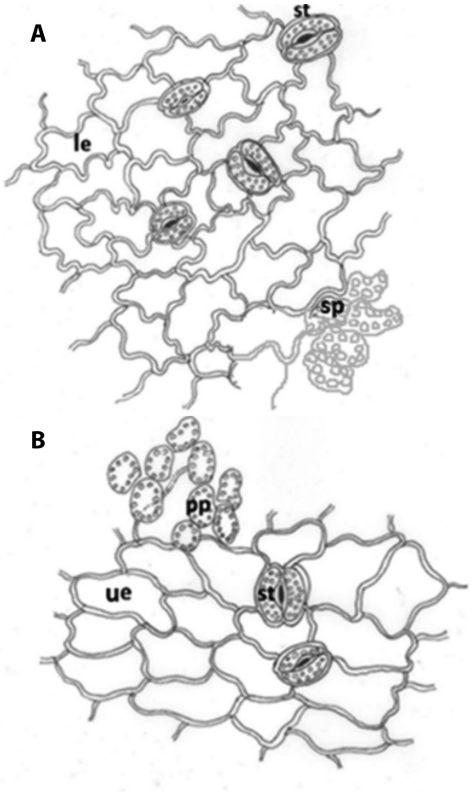

Figure 12. *V. pestalozzae* and *V. pycnostachyum*; (A) surface view of lower epidermis, (B) surface view of upper epidermis

ue: Upper epidermis, le: Lower epidermis, st: Stomata, pp: Palisade parenchima, sp: Spongy parenchima

According to the results, the root, stem, and leaf anatomic structures of each *Verbascum* species, *V. pestalozzae* differs anatomically from each other. These differences can be summarized as follows: in the stem, there are narrower sclerenchymatic cells and phloem than those in the leaf of *V. pestalozzae*; having a protrusion below, continuous crescent vascular bundles, less parenchymatic cells in outer and inner epidermis, stellate type hairs and differences in the number of cells in secretion hairs.

CONCLUSIONS

The anatomic properties belonging to the two species are generally compatible with the findings of Metcalfe and Chalk[20] and others signified in the genus.[21-24] We believe that our results provide additional evidence for taxonomists and can help to separate the species. The lack of a taxonomic, morphologic, and anatomic studies on the species made it important for the systematic introduction of the research.

Conflict of Interest: No conflict of interest was declared by the authors.

REFERENCES

1. Çıngay, B, Karavelioğulları FA, A new species of *Verbascum, V. nihatgoekyigitii* (Scrophulariaceae), from southeastern Anatolia, Turkey. Phytotaxa. 2016;269:287-293.
2. Huber-Morath A, *Verbascum* L. In: Davis PH, ed. Flora of Turkey and The East Aegean Islands, University Press; Edinburgh; 1978;6:453-603.
3. Davis PH, Mill RR, Tan K. Flora of Turkey and The East Aegean Islands (Supplement), Vol.10, University Press; Edinburgh; 1988;(Suppl):190-192.
4. Karavelioğulları FA, *Verbascum L*. İçinde: Güner A, Aslan S, Ekim T, Vural M, Babaç MT, eds. Türkiye Bitkileri Listesi (Damarlı Bitkiler). Nezahat Gökyiğit Botanik Bahçesi ve Flora Araştırmaları Derneği Yayını; İstanbul; 2012:850-870.
5. Karavelioğulları FA, Yüce Babacan E, Başer B. *Verbascum duzgunbabadagensis* (Scrophulariaceae), a new species from eastern Anatolia, Turkey. Phytotaxa. 2014;181:47-53.
6. Şengül M, Ögütçü H, Adıgüzel A, Şahin F, Kara AA, Karaman İ, Güllüce M. Antimicrobial Effects of *Verbascum georgicum* Bentham Extract. Turk J Biol. 2005;2:105-110.
7. Baytop T. Türkiye'de Bitkiler ile Tedavi, 2. Baskı, Nobel Tıp Kitabevleri; İstanbul; 1999:334-335.
8. Tuzlacı E. Şifa Niyetine, Türkiye'nin Bitkisel Halk İlaçları. Alfa Yayınları; İstanbul; 2006:379-383.
9. Senatore F, Rigano D, Formisano C, Grassia A, Basile A, Sorbo S. Phytogrowth-inhibitory and antibacterial activity of *Verbascum sinuatum*. Fitoterapia. 2007;78:244-247.
10. Tatlı İİ, Schuhly W, Akdemir ZS. Secondary metabolites from bioactive methanolic extract of *Verbascum pycnostachyum* Boiss. & Heldr. flowers. H U J Fac Pharm. 2007;27:23-32.
11. Turker AU, Camper ND. Biological Activity of Common Mullein, A Medicinal Plant, J Ethnopharmacol. 2002;82:117-125.
12. Klimek B, Stepien H. Effect of some constituents of mullein (*Verbascum sp.*) on proliferation of rat splenocytes *in vitro*. Eur J Pharm Sci. 1994;2:123.
13. Lee JH, Lee JY, Kang HS, Jeong CH, Moon H, Whang WK, Kim CJ, Sim SS. The effect of acteoside on histamine release and arachidonic acid release in RBL-2H3 mast cells. Arch Pharm Res. 2006;29:508-513.

14. Alan S, Saltan FZ, Göktürk RS, Sökmen MM. Taxonomical Properties of Three *Verbascum L*. Species and Their Antioxidant Activities. Asian J Chem. 2009;21:5438-5452.

15. Quirantes-Piné R, Herranz-Lopez M, Funes L, Borrás-Linares I, Micol V, Segura-Carretero A, Fernández-Gutiérrez A. Phenylpropanoids and their metabolites are the major compounds responsible for blood-cell protection against oxidative stress after administration of Lippia citriodora in rats. Phytomedicine. 2013;20:1112-1118.

16. Abougazar H, Bedir E, Khan, IA, Çaliş I. Wiedemannioside A-E: New Phenylethanoid Glycosides from the Roots of *Verbascum wiedemannianum*, Planta Med. 2003;69:814-819.

17. Mehdinezhad B, Rezaei A, Mohajeri D, Ashrafi A, Asmarian S, Haghdost IS, Hokmabad RV, Safarmashaei S. Comparison of *in vivo* wound healing activity of *Verbascum thapsus* flower extract with zinc oxide on experimental wound model in rabbits. Adv Environ Biol. 2011;5:1501-1509.

18. Dülger B, Kirmizi S, Arslan H, Güleryüz G. Antimicrobial activity of three endemic *Verbascum species*. Pharm Biol. 2002;40:587-589.

19. Korkina LG, Pastore S, Dellambra E, De Luca C. New molecular and cellular targets for chemoprevention and treatment of skin tumors by plant polyphenols: a critical review. Curr Med Chem. 2013;20:852-868.

20. Metcalfe GR, Chalk L. Anatomy of the Dicotyledons. London; Oxford Üniv Press; 1979.

21. Coşkunçelebi K, İnceer H, Beyazoğlu O. *Verbascum varians* Freyn & Sint. var. trapezunticum Murb.(Scrophulariaceae)'un Morfolojik, Anatomik ve Sitolojik Yönden İncelenmesi. Ot Sistematik Botanik Derg. 1999;6:25-34.

22. Çakır T, Bağcı E. *Verbascum anatolicum* (Fisch. & Mey) Hub-Mor. (Scrophulariaceae)'a ait Taksonomik Karakterler Üzerinde Gözlemler. Fırat Üniv Fen ve Müh Bil Dergisi. 2005;17:151-153.

23. Çakır T, Bağcı *E. Verbascum euphraticum* Bentham ve *V. melitenense* Boiss (Scrophulariaceae) Türleri Üzerinde Taksonomik Bir Çalışma. Fırat Üniv Fen ve Müh Bil Dergisi. 2006;18:445-458.

24. Alan S, Gökman AB. Investigation of morphological, morphometric and anatomical characteristics of endemic *Verbascum orgyale* Boiss. & Heldr. Biological Diversity and Conservation. 2015;8:94-103.

Turk J Pharm Sci 2018;15(3):354-359
DOI: 10.4274/tjps.93063

ORIGINAL ARTICLE

Oxidative Stress and Anti-oxidants in Pre and Post-operative Cases of Breast Carcinoma

Operasyon Öncesi ve Sonrası Meme Kanseri Olgularında Oksidatif Stres ve Antioksidanlar

Sohail HUSSAIN[1,2]*, Mohammad ASHAFAQ[2]

[1]Aligarh Muslim University, J.N. Medical College, Department of Biochemistry, Uttar Pradesh, India
[2]Jazan University, Faculty of Pharmacy, Department of Pharmacology and Toxicology, Jazan, Kingdom of Saudi Arabia

ABSTRACT

Objectives: To investigate the existence of oxidative stress in the sera of patients with breast cancer and its effects on the consequent breast cancer.

Materials and Methods: This study included 50 control volunteers, 50 patients with breast cancer, and 50 patients with post-operative breast cancer. Patients with pre-operative cancer were clinically and histopathologically diagnosed for breast carcinoma with stage 0, not having therapeutic history. The control 50 healthy female volunteers had the same socio-economic status, and no history of any cancer. After obtaining consent, venous blood was collected from the volunteers by vein puncture using a 10 mL sterile disposable syringe and needle. About 8 mL of blood was collected, 4 mL of which was poured into a heparinized bulb and 4 mL was allowed to clot. The levels of MDA, NO, GSH, and activities of RBC-SOD (in RBC lysate), NOS, copper and zinc GPx, and CAT, and vitamins A, C, and E metabolites were measured in the sera of each group.

Results: The activities of RBC-SOD and the levels of MDA, NO, as well as the NOS were significantly higher in the sera of all patients with breast cancer as compared with the controls. However, the levels of GSH and vitamins A, C, and E, as well as the activities of copper and zinc GPx and CAT were decreased in patients with breast cancer when compared with the controls.

Conclusion: The study provides further evidence for the presence of oxidative stress in the serum of patients with breast carcinoma. Patients with higher levels of MDA showed deficiencies of antioxidants and trace elements in the serum. A poor dietary antioxidant status and high oxidant levels are associated with the risk of breast cancer, thus suggesting that patients with breast cancer should take nutritive supplements to balance the antioxidant and oxidant levels for better outcomes.

Key words: Breast cancers, oxidants, antioxidants

ÖZ

Amaç: Meme kanserli hastaların serumlarında oksidatif stresin varlığını ve meme kanserine etkilerini araştırmaktır.

Gereç ve Yöntemler: Bu çalışmaya 50 gönüllü kontrol, 50 meme kanseri hastası ve 50 ameliyat sonrası meme kanseri hastası dahil edildi. Bu hastalar, klinik ve histopatolojik olarak evre 0 meme kanseri teşhisi olan ve tedavi almamış hastalardır. Kontrol grubundaki 50 sağlıklı kadın gönüllü aynı sosyo-ekonomik statüye sahipti ve hiçbir kanser öyküsü yoktu. Onam alındıktan sonra, 10 mL'lik steril tek kullanımlık bir şırınga ve iğne kullanılarak venöz ponksiyon ile gönüllülerden venöz kan alındı. Yaklaşık 8 mL kan toplandı, 4 mL'si heparinize bir ampul içerisine alındı ve 4 mL'si pıhtılaşmaya bırakıldı. Her grubun serumunda MDA, NO, GSH ve RBC-SOD (RBC lizat), NOS, bakır ve çinko GPx ve CAT aktiviteleri, A, C ve E vitaminleri ölçüldü.

Bulgular: Meme kanseri olan tüm hastaların serumlarında RBC-SOD aktiviteleri, MDA, NO ve NOS düzeyleri, kontrollere göre anlamlı olarak daha yüksektir. Bununla birlikte, kontrol grubu ile karşılaştırıldığında meme kanseri olan hastalarda GSH, A, C ve E vitaminleri ile bakır ve çinko GPx ve CAT aktiviteleri azalmıştır.

Sonuç: Bu çalışma, meme kanseri hastalarının serumunda oksidatif stresin varlığına yönelik ileri kanıt sunmaktadır. Serumunda daha yüksek seviyelerde MDA bulunan hastaların antioksidan ve eser elementlerinin yetersiz olduğunu göstermiştir. Zayıf antioksidan diyet ve yüksek oksidan düzeyleri meme kanseri riski ile ilişkilidir, bu nedenle meme kanseri olan hastaların daha iyi sonuçlar için antioksidan ve oksidan seviyelerini dengeleyecek besleyici takviyeler almaları gerektiğini düşündürmektedir.

Anahtar kelimeler: Meme kanseri, oksidanlar, antioksidanlar

*Correspondence: **E-mail:** shussainamu@gmail.com, **Phone:** +90 557632511 **ORCID-ID:** orcid.org/0000-0001-6958-6191
Received: 09.02.2017, **Accepted:** 07.09.2017

INTRODUCTION

Breast cancer is one of the most common malignant tumors in women with unknown etiology.[1] Reactive oxygen species (ROS) such as superoxide anion radical ($\downarrow O_2^-$), hydroxyl radicals ($^{\bullet}OH$) and hydrogen peroxide (H_2O_2) are produced during aerobic metabolism.[2] Levels of free radicals are controlled by anti-oxidant enzymes [catalase (CAT), glutathione peroxidase (GPx), superoxide dismutase (SOD)] and anti-oxidants (vitamins E, C, glutathione, carotenoids and flavonoids).[3] Under normal conditions, there is a balance between the activities of anti-oxidant enzymes and intracellular levels of these anti-oxidants. This balance is essential for the survival of organisms and their health. An imbalance between the production and detoxification of ROS results in oxidative stress. ROS has been implicated in the pathogenesis of certain diseases, including cancer.[4,5] It reacts with polyunsaturated fatty acids to induce the release of toxic and reactive aldehyde metabolites such as malondialdehyde (MDA), one of the end products of lipid peroxidation (LPO). MDA may be involved in tumor promotion because it can interact with the functional groups of a variety of cellular compounds.[6] To control the over production of ROS, cells protect themselves against oxidative damage by antioxidant detoxifying mechanisms, which helps to lower ROS concentrations in the body. SOD catalyzes the dismutation of $O_2\downarrow$ into H_2O_2, and CAT is responsible for the detoxification of H_2O_2 to oxygen and water.[7] Glutathione acts as a reducing agent that maintains enzymes in an active state as an antioxidant.[8] The main protective roles of glutathione against oxidative stress are: (i) to act as a cofactor for several detoxifying enzymes such as glutathione reductase and GPx against oxidative stress; (ii) to participate in amino acid transport through the plasma membrane; (iii) to scavenge the ($^{\bullet}OH$) and singlet oxygen, detoxifying the H_2O_2 and lipid peroxides by the catalytic action of GPx, and (iv) to regenerate the most important antioxidants back to their active forms.[8,9] Nitric oxide (NO) acts as an intracellular second messenger and provides an efficient system for cellular regulation, interaction, and defense. Its role strictly depends on the chemical reactivity with oxygen and metals. Recent studies revealed that the involvement of altered NO levels was associated in the pathogenesis of cervical cancer (CaCx).[10] Some findings have shown that concentration of NO higher or lower than the basal level caused a tumorigenic effect in CaCx.[11] In addition to the body defense mechanism, there are vitamins that provide the body with much needed immunity and a mechanism of self-defense to fight against various pathogens. Studies indicate that the level of these antioxidants in the body decrease in carcinogenesis. The level of vitamin E was found to vary in cervical carcinogenesis.[12] Vitamin C has free radical scavenging property, it directly reacts with hydroperoxides and plays an important role in sparing vitamin E. Thus, the role of vitamin C is very important in the treatment of cancer.[12,13] Strong oxidizing agent such as NO, interacts with organic substances and with the support of transition metal like copper which creates more reactive species such as ($^{\bullet}OH$).[14] Zinc is an integral part of biomembranes, it may be involved in the control of membrane integrity, stability, and LPO -related injuries. Zinc plays an inhibitory role in RNA and DNA polymerase, phosphodiesterase, and an activating effect on the membrane-bound enzyme, adenylcyclase, and there is suggested role of zinc in carcinogenesis.[15] The levels of LPO and antioxidant status in patients with breast cancer after surgery remain unknown. To address these issues, the levels of oxidants and antioxidants in the patients with breast cancer were examined during and after tumor removal.

MATERIALS AND METHODS

The present study was conducted in the Department of Biochemistry, Jawaharlal Nehru Medical College, Aligarh Muslim University, Aligarh, Uttar Pradesh, India. This study included 50 control volunteers, 50 patients with breast cancer, and 50 patients with post-operative breast cancer. Further, the women were within the age group of 35-65 years and were from the same demographic area. Patients with pre-operative cancer were clinically and histopathologically diagnosed for breast carcinoma with stage 0, not having therapeutic history. The 50 healthy female control volunteers were from the same socio-economic status, had no history of smoking, alcoholism, and any cancer. Volunteers/patients with a history of smoking, alcoholism, and other diseases that induce oxidative stress such as diabetes mellitus, pulmonary diseases, and respiratory diseases were excluded from the study. The study was approved by the institutional ethics committee and written informed consent was received from the patients. After obtaining consent, venous blood was collected from the volunteers/patients under aseptic conditions by veinpuncture usinga 10 mL sterile disposable syringe and needle. About 8 mL of blood were collected, 4 mL of which was poured into a heparinized bulb and 4 mL was allowed to clot. Serum and plasma were separated by centrifugation at 3000 rpm for 10 min at room temperature. The plasma pellets were taken as a source of red blood cells (RBCs). The samples were stored at 4°C before analysis and all the samples were analyzed on the day of collection.

Assay of LPO

Measurement of MDA in serum was estimated using the thiobarbituric acid (TBA) method.[16,17] MDA, which is a stable end product of fatty acid peroxidation, reacts with TBA at acidic conditions to form a complex that has a maximum absorbance at 535 nm. A 300 µL sample was mixed with 1.5 mL of 0.05 mol/L HCl and 0.5 mL of 0.67% TBA and then mixed and boiled well in water at (95°C) for 30 min. After cooling, the products were extracted with 2 mL of 15% butanol and centrifuged at 2500 rpm at (4°C) for 30 min. The rate of LPO was expressed as MDA formed per hour per milligram of protein using the molar extinction coefficient of 1.56×10^5 mol/L^{-1} cm^{-1}.

Assay of SOD

SOD activity was estimated using a commercial Ransod kit (Randox Laboratories, UK). This method is based on the generation of $^{\cdot}O_2$ produced by xanthine and xanthine oxidase,

which react with phenyl tetrazolium chloride to form a red formazan dye. RBC-SOD activity was measured in RBC hemolysate through the degree of reaction inhibition. The results are expressed as U/mL. RBC-SOD was assessed using Winterbourn's method, which is based on the ability of SOD to inhibit the reduction of nitroblue tetrazolium by superoxide, which is generated by the reaction of photo-reduced riboflavin and oxygen.[18]

Assay of CAT

CAT activity was measured by monitoring the decrease in absorption of H_2O_2 at 240 nm.[19] One hundred microliters of serum was added to a 0.5 mL quartz cuvette containing 400 µL of 20 mM H_2O_2 in phosphate-buffered saline (25°C) and mixed thoroughly by pipetting. The absorbance was monitored immediately at 240 nm for three minutes at one-minute intervals. CAT activity was measured for each sample and the rate in mAU/min/mg protein was averaged.

Assay of GSH

GSH status analyses were assayed from blood samples obtained through a venous arm puncture and the serum was separated by centrifugation.[20] After the separation, the buffy coat was removed and the packed cells were washed 3 times with physiologic saline. One hundred-microliter aliquots of washed RBCs were added to 300 mL ice-cold 5% metaphosphoric acid. To completely precipitate proteins, the samples were vortexed and incubated on ice for 10 min. After centrifugation at 4°C at 12000 rpm for 10 min, the supernatants were filtered through a 0.2 mm filter and diluted 5 times before being injected into the capillary electrophoresis system.

GPx assay

GPx activity was assayed according to the method of Haque et al.[21] The assay mixture consisted of 0.1 M phosphate buffer (pH 7.4), 1 mM EDTA, 1 mM sodium azide, 1 mM GSH, 0.2 mMNADPH, 0.25 mM H_2O_2, and 0.1 mL sera. Oxidation of NADPH was recorded spectrophotometrically at 340 nm. The enzyme activity was calculated as nanomoles of NADPH oxidized per minute per milligram of protein using a molar extinction coefficient of 6.22×10^3 M^{-1} cm^{-1}.

NO assay

Serum was deproteinized first to convert NO to nitrate, the stable product of NO. The nitrate present in the filtrate was then reduced to nitrite, which was measured by diazotization of sulphanilamide and coupled with naphthylethylene diamine, as in Najawa and Cortas's method.[22]

Inducible NO (iNOS) assay

iNOS synthase activity was measured *in vitro* in blood lymphocytes (suspended in MEM @ 1×10^6 viable cells/mL) using arginine and Greiss reagent with the method of Stuehr and Marletta.[23] The optical density of the citrulline formed was determined spectrophotometerically with a ultraviolet-visible spectrophotometer (Shimazu) at 540 nm against a control.

Assay of vitamins

Serum vitamin C was estimated by the method of Kyaw[24], where phosphotungstic acid was first deproteinized and then reacted with ascorbic acid to produce a blue color. Vitamins A and E were measured using high-performance liquid chromatography (HPLC) as per the modified method of Omu et al.[25]. In brief, α-tocopherol acetate and retinol acetate were pipetted into an Eppendorf tube. Blood serum was added and vortexed; the hexane extract of vitamin A and E was taken out in a glass tube, dried under nitrogen stream, and dissolved into methanol. Finally, this preparation was injected into an HPLC fitted with reverse phase of column C18. The vitamins were eluted with methanol at a flow rate of 1.5 mL/min for 15 minutes. The peak heights and curve areas of vitamin A, E, and acetates were measured to calculate the amount of these vitamins in the serum with an ultraviolet detector at 292 nm.

Assay of trace elements

Copper and zinc in serum were estimated by using an atomic absorption spectrophotometer.

Statistical analysis

The experimental data are expressed as mean±standard deviation. In this study, p values of $p<0.05$ were considered significant. Statistical analysis was performed using the STATGRAPHICS plus statistical package.

RESULTS

The results showed that the level of MDA was increased significantly in all groups of patients with breast cancer as compared with the controls ($p<0.05$). The MDA level was decreased 13.81% in post-operative patients as compared with pre-operative patients. On the other hand, the activity of RBC-SOD was significantly increased in pre-operative and post-operative patients ($p<0.05$) as compared with controls, but its activity in post-operative patients was decreased 34.69% compared with pre-operative patients (Table 1). However, the activity of CAT was decreased significantly in all groups of patients with breast cancer compared with the controls ($p<0.05$), but this activity in post-operative patients was increased 23.13% compared with pre-operative patients (Table 1).

The contents of GSH was increased 23.52% in the post-operative group compared with the preoperative group. The level of NO was decreased 24.32% in the post-operative group when compared with the pre-operative group, and iNOS activity was also decreased 38.01% in the post-operative group as compared with the pre-operative group (Table 1). Significantly decreased RBC-SOD activity ($p<0.05$) and plasma levels of vitamins C, A, and E ($p<0.05$) were observed in all patients with cancer when compared with the healthy controls. It was observed that the concomitant decline in the activity of RBC-SOD and levels of vitamins were associated with the progression of cancer, but the levels of all vitamins were not significant in post-operative patients (Table 2). The Cu/Zn ratio was also found to be significantly ($p<0.05$) lower in post-operative patients when compared with the pre-operative.

Table 1. Serum levels of oxidants and antioxidative enzymes in control and in patients with breast cancer before and after surgery

Parameters	Control	Pre-operative	Post-operative	Percentage change in post-operative group
NO (μM/L)	36.56±6.13	78.34±12.79* (114.44%)	59.28±11.61# (-24.33 %)	↓24.33*
iNOS (nmoles/mL/min)	1.19±0.53	3.92±0.77* (229.41%)	2.43±0.51# (-38.01%)	↓38.01*
MDA (μM/L)	2.13±0.69	3.098±1.02* (45.07)	2.67±0.94# (13.81)	↓13.81
SOD (U/mL)	390.99±58.76	712.43±154.87* (82.21)	465.88±113.57# (34.69)	↓34.69*
RBC-SOD (units/mg)	362513±217.9	2387.34±398.97* (99.24)	2669.48±276.9# (10.56)	↑10.56
GSH (mM/L)	0.64±0.1017	0.39±0.1943* (-39.06%)	0.51±0.3109# (30.77)	↑30.77%
GPx (U/L)	26673.37±3994.56	8304.40±1856* (-68.86)	10234.43±2743# (18.85)	↑18.85
CAT (U/mL)	78.68±8.51	44.98±16.78* (-42.83)	58.52±21.79# (23.13)	↑23.13*

*: Significant changes, pre-oprative vs control, #: Significant changes post-operative vs pre-oprative, ↑: Increase, ↓: Decrease, GPx: Glutathione peroxidase, CAT: Catalase, GSH: Glutathione, RBC-SOD: Red blood cell-superoxide dismutase, MDA: Malondialdehyde, NO: Nitric oxide, iNOS: Inducible nitric oxide

Table 2. Serum levels of vitamins and trace elements incontrols and in patients with breast cancer before and after surgery

	Control	Pre-operative	Post-operative	Percentage change in post-operative group
Vitamin A (mg/dL)	38.76±4.61	32.99±6.33	34.81±4.19	↑5.22**
Vitamin C (mg/dL)	1.84±0.09	0.98±0.08	1.02±0.14	↑39.2**
Vitamin E (mg/dL)	81.2±0.89	6.32±0.91	7.14±0.72	↑11.4**
Serum copper (μg%)	114.04±12.79	168.6±9.89	142.5±8.16	↓15.48**
Serum zinc (μg%)	106.7±9.74	70.92±11.83	81.91±19.11	↑13.41**

**: Significant changes, ↑: Increase, ↓: Decrease

DISCUSSION

Increased oxidative stress and LPO are implicated in carcinogenic processes. The magnitude of this damage depends on ROS levels and on the body defense mechanisms against them, which are mediated by various cellular antioxidants.[8,26] MDA is produced by the oxidation of polyunsaturated fatty acids in membranes induced by free radicals, and is an indicator of oxidative damage. Many studies have examined the possibility of a connection between LPO and cancer.[6,27] Higher plasma MDA levels have been reported in patients with cancer than in controls.[27] However, lower LPO measured in plasma using TBA-reactive substances has also been reported in breast cancer groups compared with controls.[28] Our findings are in agreement with most earlier studies that suggested that there might be some accumulation of ROS, which causes significantly higher LPO at cellular and molecular levels. ROS derived from $NO^{\bullet}$ and released from inflammatory cells. Radical can act on neighboring dividing epithelial cells, leading to somatic mutations in crucial cancer-causing genes.[29] $NO^{\bullet}$ produced in solid tumors has been implicated in enhanced vascular permeability, and increased tumor blood flow, and hence sustained tumor growth.[30] GSH, as a reductant, is very important in maintaining the stability of erythrocyte membranes. It is implicated in the cellular defense against xenobiotics and deleterious compounds such as free radicals and hydroperoxides.[31] GSH in the nucleus also maintains the redox state of critical protein sulphydryls that are necessary for DNA repair and expression.[8] A decrease in blood GSH in circulation has been reported in several diseases including malignancies.[32] The lower GSH levels in patients with breast cancer supports the hypothesis that glutathione status is inversely related in malignant transformation.[33] Several studies have reported decreased levels of GSH in the blood of patients with breast cancer compared with control subjects.[34,35] Our results showed that there were significant decreases in blood GSH levels in patients with breast cancer compared with the control subjects. The decrease in GSH concentration can be explained by decreased GSH synthesis and/or increased GSH consumption in the removal of peroxides and xenobiotics. Cells have strong endogenous antioxidant defenses against increased LPO, ROS, and NO. SOD and CAT are the first line of defense against superoxide and H_2O_2.[36,37] The significant increase in SOD activities indicates the formation of more superoxide radicals and their removal because SOD metabolizes superoxide radicals.[38] Furthermore, the decrease in activity of SOD might be due to an association with free radical generation, which causes damage to enzymes by cross linking or damaging the nuclear DNA, leading to mutations. It may also be due to a scarcity of trace elements such as zinc and manganese, which act as cofactors for this enzyme.[39] However, the significant decrease in CAT activity indicates the toxicity produced by H_2O_2.[27] Studies have shown that oxidants may activate gene expression through antioxidant responsive elements,[40] which explains the enhanced enzyme activities. Our data showed a significant increase in SOD and a decrease in

CAT activities in patients with breast cancer compared with the controls. A substantial increase in GSH level and increase CAT activity were found in the postoperative patients, which might be due to the free radical scavenging property. The decreased levels of vitamin C may be associated with its action as an antioxidant where it gets used. Its synergism with vitamin E and A helps in sparing vitamin E, and during this process, vitamin C gets used,[12,13] which is seen through the significant decline in plasma ascorbic acid. A negative correlation between vitamin C and MDA was noted, thereby leading to the conclusion that free radicals are scavenged by ascorbic acid and thus get utilized. Copper can interact directly with the bases of DNA at G-C sites.[41] The addition of copper to DNA *in vitro* mediates more extensive DNA base damage, inducing more mutations.[42] Copper may also elaborate other free radical species such as •OH; therefore, the inactivation/loss of certain tumor suppressor genes can lead to the initiation and/or progression of carcinogenesis. The elevation in copper levels may be due to mobilization of copper from tissue to serum.[42]

Zinc is used for cell growth and maintains the integrity of the membrane. However, cancerous cells may consume the zinc present in the circulation for tumor growth and maintain membrane integrity.[43] This might be a possible reason for the depletion of zinc in breast cancer. The increased ratio of Cu/Zn is due to the significant decrease in Zn and concomitant increase in copper. Therefore, in the pre-operative group, the ratio of Cu/Zn was increased as compared with the controls. As this ratio is altered, this could be considered as a risk factor for tumor growth or carcinogenesis.

CONCLUSIONS

In conclusion, breast cancer is related to an increase of oxidants in serum with concomitant decrease of antioxidant defense capacity. Overall, our data support the importance of endogenous antioxidant in the etiology of breast cancer across all levels of predicted risk. There are some significant differences in the oxidant and antioxidant status in the blood of patients with breast cancer before and after surgery. Prospective studies in a larger population should be conducted to confirm our present findings.

ACKNOWLEDGEMENTS

The author thanks to Aligarh Muslim University, Aligarh, Uttar Pradesh, India, for financial assistance.

Conflict of Interest: No conflict of interest was declared by the authors.

REFERENCES

1. Jemal A, Tiwari RC, Murray T, Ghafoor A, Samuels A, Ward E, Feuer EJ, Thun MJ; American Cancer Society. Cancer statistics, 2004. CA Cancer J Clin. 2004;54:8-29.
2. Rajneesh CP, Manimaran A, Sasikala KR, Adaikappan P. Lipid peroxidation and antioxidant status in patients with breast cancer. Singapore Med J. 2008;49:640-643.
3. Hou MF, Lin SB, Yuan SS, Tsai SM, Wu SH, Ou-Yang F, Hsieh JS, Tsai KB, Huang TJ, Tsai LY. The clinical significance between activation of nuclear factor kappa B transcription factor and overexpression of HER-2/neu oncoprotein in Taiwanese patients with breast cancer. Clin Chim Acta. 2003;334:137-144.
4. Tsai LY, Lee KT, Liu TZ. Evidence for accelerated generation of hydroxyl radicals in experimental obstructive jaundice of rats. Free Radic Bio Med. 1998;24:732-737.
5. Polat MF, Taysi S, Gul M, Cikman O, Yilmaz I, Bakan E, Erdogan F. Oxidant/antioxidant status in blood of patients with malignant breast tumor and benign breast disease. Cell Biochem Funct. 2002;20:327-331.
6. Vaca CE, Wilhelm J, Harms-Ringdahl M. Interaction of lipid peroxidation products with DNA. A review. Mutat Res. 1988;195:137-149.
7. Gönenç A, Erten D, Aslan S, Akinci M, Simşek B, Torun M. Lipid peroxidation and antioxidant status in blood and tissue of malignant breast tumor and benign breast disease. Cell Biol Int. 2006;30:376-380.
8. Estrela JM, Ortega A, Obrador E. Glutathione in cancer biology and therapy. Crit Rev Clin Lab Sci. 2006;43:143-181.
9. Bakan N, Taysi S, Yilmaz O, Bakan E, Kuşkay S, Uzun N, Gündoğdu M. Glutathione peroxidase, glutathione reductase, Cu-Zn superoxide dismutase activities, glutathione, nitric oxide and malondialdehyde concentrations in serum of patients with chronic lymphocytic leukemia. Clin Chim Acta. 2003;338:143-149.
10. Beevi SS, Rasheed MH, Geetha A. Evidence of oxidative and Nitrosative stress in patients with Cervical squamous cell carcinoma. Clin Chim Acta. 2007;375:119-123.
11. Ioannidis I, Batz M, Paul T, Korth HG, Sustmann R, Groot HD. Enhanced release of nitric oxide causes increased cytotoxicity of s-nitro-N-acetyl-DL-penicillamine and sodium nitroprusside under hypoxic condition. Biochem J. 1998;318:789-795.
12. Niki E. Action of ascorbic acid as a scavenger of active stable oxygen radicals. Am J Clin Nutr. 1991;54:195-145.
13. Head KA. Ascorbic acid in the prevention and treatment of cancer. Altern Med Rev. 1998;3:174-186.
14. Gorodetsky R, Fuks Z, Sulkes A, Ginsburg H, Weshler Z. Correlation of erythrocyte and plasma levels of zinc, copper and iron with evidence of metastatic spread in cancer patients. Cancer. 1985;55:779-787.
15. Morton KS. Role of trace elements in cancer. Cancer Research. 1975;35:3481-3487.
16. Tsai LY, Lee KT, Tsai SM, Lee SC, Yu HS. Changes of lipid peroxide levels in blood and liver tissue of patients with obstructive jaundice. Clin Chim Acta. 1993;215:41-50.
17. Buege JA, Aust SD. Microsomal lipid peroxidation. Methods Enzymol. 1978;52:302-310.
18. Winterbourn CC, Hawkins RE, Brian M, Carrell RW. The estimation of red cell superoxide dismutase activity. J Lab Clin Med. 1975;85:337-341.
19. Aebi H. Catalase *in vitro*. Methods Enzymol. 1984;105:121-126.
20. Carru C, Zinellu A, Pes GM, Marongiu G, Tadolini B, Deiana L. Ultrarapid capillary elec-trophoresis method for the determination of reduced and oxidized glutathione in red blood cells. Electrophoresis. 2002;23:1716-1721.
21. Haque R, Bin-Hafeez B, Parvez S, Pandey S, Sayeed I, Ali M, Raisuddin S. Aqueous extract of walnut (*Juglans regia* L.) protects mice against cyclophosphamide induced biochemical toxicity. Hum Exp Toxicol. 2003;22:473-480.

22. Cortas NK, Wakid NW. Determination of inorganic nitrate in serum and urine by kinetic cadmium reduction method. Clin Chem. 1990;36:1440-1443.

23. Stuehr DJ, Marletta MA. Synthesis of nitrite and nitrate in murine macrophage cell lines. Cancer Res. 1987;47:5590-5594.

24. Kyaw A. A simple colorimetric method for ascorbic acid determination in blood plasma. Clin Chim Acta. 1978;86:153-157.

25. Omu AE, Fatinikun T, Mannazhath N, Abraham S. Significance of Simultaneous Determination of serum and seminal plasma a tocopherol and retinol l in infertile men by high- performance liquid chromatography. Andrologia. 1999;31:347-354.

26. Z Zengin E, Atukeren P, Kokoglu E, Gumustas MK, Zengin U. Alterations in lipid peroxidation and antioxidant status in different types of intracranial tumors within their relative peritumoral tissues. Clin Neurol Neurosurg. 2009;111:345-351.

27. Gönenç A, Erten D, Aslan S, Akinci M, Simşek B, Torun M. Lipid peroxidation and antioxidant status in blood and tissue of malignant breast tumor and benign breast disease. Cell Biol Int. 2006;30:376-380.

28. Kumaraguruparan R, Subapriya R, Viswanathan P, Nagini S. Tissue lipid peroxidation and antioxidant status in patients with adenocarcinoma of the breast. Clin Chim Acta. 2002;325:165-170.

29. Hussain SP, Hofseth LJ, Harris CC. Radicals causes of cancer. Nat Rev Cancer. 2003;3:276-285.

30. Tamir S, Burney S, Tannenbaum SR. DNA damage by nitric oxide. Chem Res Toxicol. 1996;9:821-827.

31. Pastore A, Federici G, Bertini E, Piemonte F. Analysis of glutathione: Implication in redox and detoxification. Clin Chim Acta. 2003;333:19-39.

32. Yeh CC, Hou MF, Tsai SM, Lin SK, Hsiao JK, Huang JC, Wang LH, Wu SH, Hou LA, Ma H, Tsai LY. Superoxide anion radical, lipid peroxides and antioxidant status in the blood of patients with breast cancer. Clin Chim Acta. 2005;361:104-111.

33. Kumaraguruparan R, Subapriya R, Kabalimoorthy J, Nagini S. Antioxidant profile in the circulation of patients with fibroadenoma and adenocarcinoma of the breast. Clin Biochem. 2002;35:275-279.

34. Lamari F, La Schiazza R, Guillevin R, Hainque B, Foglietti MJ, Beaudeux JL, Bernard M. Biochemical exploration of energetic metabolism and oxidative stress in low grade gliomas: Central and peripheral tumor tissue analysis. Ann Biol Clin (Paris). 2008;66:143-150.

35. M. Gago-Dominguez X, Jiang X, Esteban Castelao J. Lipid peroxidation and the protective effect of physical exercise on breast cancer. Med Hypotheses. 2007;68:1138-1143.

36. Nair U, Bartsch H, Nair J. Lipid peroxidation induced DNA damage in cancer prone inflammatory diseases: A review of published adduct types and levels in humans. Free Radic Biol Med. 2007;43:1109-1120.

37. Khanzode SS, Muddeshwar MG, Khanzode SD, Dakhale GN. Antioxidant enzymes and lipid peroxidation in different stages of breast cancer. Free Radic Res. 2004;8:81-85.

38. Aggarwal S, Subberwal M, Kumar S, Sharma M. Brain tumor and role of betacarotene, a-tocopherol, superoxide dismutase and glutathione peroxidase. J Cancer Res Ther. 2006;2:24-27.

39. Manoharan S, Kolanjiappan K, Kayalvizhi M. Enhanced Lipid peroxidation and impaired enzymatic antioxidant activities in the erythrocytes of the patients with cervical carcinoma. Cell Mol Bio Lett. 2004;9:699-707.

40. Gago-Dominguez M, Castelao JE, Pike MC, Sevanian A, Haile RW. Role of lipid peroxidation in the epidemiology and prevention of breast cancer. Cancer Epidemiol Biomarkers Prev. 2005;14:2829-2839.

41. Chen CA, Hwang JL, Kuo TL, Hsieh CY, Huang SC. Serum copper and zinc levels in patients with cervical cancer. J Formos Med Assoc. 1990;89:677-682.

42. Singh M, Dwivedi S, Singh G, Bajpai M. Serum copper levels in different stages of carcinoma. Ind J Matern Child Health. 1990;1:12-14.

43. Beerheide W, Bernard HU, Tan YJ, Ganesan A, Rice WG, Ting AE. Potential drugs against cervical cancer. Zinc-ejecting inhibitors of the human papillomavirus Type 16 E6 oncoprotein. J Natl Cancer Inst. 1999;91:1211-1220.

Turk J Pharm Sci 2018;15(3):360-363
DOI: 10.4274/tjps.64936

ORIGINAL ARTICLE

Comparative Characteristics of Anti-depressant, Anti-hypoxic Action, and Effect on the Physical Endurance of *Scutellaria baicalensis* Drugs

Scutellaria baicalensis (Çin Takkesi) İlaçlarının Anti-Depresan, Anti-Hipoksik ve Fiziksel Dayanıklılık Üzerine Etkilerinin Karşılaştırmalı Özellikleri

Anatolii MATVIYCHUK, Galina SLIPCHENKO*, Yurii STOLETOV, Galina BELIK, Olena RUBAN, Sergii KUTSENKO

National University of Pharmacy, Department of Industrial Technology of Drugs, Kharkov, Ukraine

ABSTRACT

Objectives: The influence of original drugs from *Scutellaria baicalensis* (SB) Georgi (dry extract, powder of rhizomes and roots, tablets "Scutex" on the basis of the dry extract and capsules "Scutella", which contain powder of rhizomes with roots) was studied on depressive behavior, physical endurance and anti-hypoxic activity in mice.

Materials and Methods: The used dry extract SB (SBDE), powder of roots and rhizomes from SB (SBRP), tablets from dry extract of SB named "Scutex", and hard gelatin capsules from the crushed root of SB named "Scutella" were obtained from National University of Pharmacy, Department of Industrial Technology of Drugs. In the experiment, 94 random-breed white male mice weighing 20-29 g were used and kept in standard sanitary and laboratory conditions.

Results: The experiments revealed that SBDE had anti-depressant action. Powder from rhizomes and roots of SB and "Scutella" capsules had anti-hypoxic action. All test drugs showed no influence on the physical endurance of mice. These results suggest the possible use of SBDE as an anti-depressant drug, and rhizomes with roots and "Scutella" capsules as an anti-hypoxic remedy.

Conclusion: SBDE at a dose 50 mg/kg shows anti-depressant activity that exceeds the activity of the comparison drug "Bilobil". SBDE, SBRP, "Scutex" tablets and "Scutella" capsules do not affect the physical endurance of mice. SBDE at a dose 50 mg/kg and SBRP at a dose of 173 mg/kg and 260 mg/kg exhibit anti-hypoxic activity. "Scutex" tablets show no anti-hypoxic action and "Scutella" capsules cause probable anti-hypoxic action that exceeds the effect of the reference drug "Bilobil".

Key words: *Scutellaria baicalensis*, anti-depressive action, physical endurance, anti-hypoxic activity

ÖZ

Amaç: Orijinal *Scutellaria baicalensis* (SB) Georgi ilaçlarının (kuru ekstresi, rizom ve kök tozları, kuru ekstre bileşimli "Scutex" tabletleri ve rizom ve kök tozu taşıyan "Scutella" kapsülleri) depresif davranış, fiziksel dayanıklılık ve anti-hipoksik aktivite üzerine etkisi sıçanlar üzerinde test edilmiştir. Deneyler, SB'nin kuru ekstresinin anti-depresan etkiye sahip olduğunu ortaya koymuştur.

Gereç ve Yöntemler: SB kuru ekstresi (SBDE), SB köklerinden (SBRP) ve rizomlarından elde edilen toz, "Scutex" kodlu SB'nin kuru ekstresinden elde edilen tabletler ve "Scutella" kodlu SB'nin ezilmiş kökünden elde edilen sert jelatin kapsüller, Ulusal Eczacılık Üniversitesi, İlaçların Endüstriyel Teknolojisi Anabilim Dalı'nda hazırlandı. Deneyde 20-29 g ağırlığındaki, rastgele-ırk, beyaz erkek sıçanlar kullanıldı ve standart sağlık ve laboratuvar koşullarında tutuldu.

Bulgular: Deneyler SB'nin kuru ekstresinin anti-depresan etkiye sahip olduğunu ortaya çıkarmıştır. SB rizom ve kök tozunun ve "Scutella" kapsüllerinin anti-hipoksik etkisi vardır. Test edilen ilaçlardan hiçbiri sıçanların fiziksel dayanıklılığı üzerinde etki göstermemiştir. Bu sonuçlar, SB'nin kuru ekstresinin anti-depresan ilaç, kök, rizomlar ve "Scutella" kapsüllerinin anti-hipoksik ilaç olarak kullanımını önermektedir.

Sonuç: SBDE 50 mg/kg'lık bir dozda, karşılaştırma ilacı "Bilobil" etkisini aşan anti-depresan aktivite gösterir. SBDE, SBRP, "Scutex" tabletleri ve "Scutella" kapsülleri sıçanların fiziksel dayanıklılığını etkilemez. SBDE, 50 mg/kg dozunda ve SBRP'de 173 mg/kg ve 260 mg/kg dozunda anti-hipoksik aktivite gösterir. "Scutex" tabletleri anti-hipoksik etki göstermez ve "Scutella" kapsülleri referans ilaç "Bilobil" etkisini aşan muhtemel anti-hipoksik etkilere neden olur.

Anahtar kelimeler: *Scutellaria baicalensis*, anti-depresan etki, fiziksel dayanıklılık, anti-hipoksik aktivite

***Correspondence: E-mail:** galinaslipchenko@ukr.net, **Phone:** +380957355942 **ORCID-ID:** orcid.org/0000-0002-4783-7460
Received: 31.03.2017, **Accepted:** 05.10.2017

INTRODUCTION

The creation of new effective drugs based on plant material is relevant and a priority direction of modern pharmacy. Herbal origin preparations have recently become very popular due to the variety of therapeutic effects provided by both individual substances and complex compounds found in plant material. *Scutellaria baicalensis* (SB) Georgi (Lamiaceae family) is a promising source of biologically active substances. The main biologically active substances of SB are flavonoids and flavonoid glycosides such as baicalin, baicalein, scutellarin, oroxylin, wogonin, apigenin, and others. In traditional Chinese medicine, roots of SB have long been used for hypertension, epilepsy, nervousness, sleep disorders. Recently, the psychotropic and cerebroprotective action of SB drugs has been investigated, including in neurodegenerative diseases, and CNS lesions of ischemic genesis.[1-6] It has been proved that preparations of raw SB (dry extract, "Scutex" tablets and "Scutella" capsules) show anxiolytic and anti-amnestic effects.[7,8] In view of the above, there is a need for the expediency of comprehensive comparative pharmacological studies of SB dry extract, powder of roots and rhizomes of SB and preparations based on them as potential psychotropic drugs. The purpose of the study was to evaluate the possible anti-depressant properties and anti-hypoxic action of the dry extract, powder of roots and rhizomes of SB and also "Scutex" tablets based on dry extract SB (SBDE) and hard gelatin capsules "Scutella", which contain powder of rhizomes with roots of SB, on the physical endurance of mice.

MATERIALS AND METHODS

The used SBDE, powder of roots and rhizomes from SB (SBRP), tablets from dry extract of SB named "Scutex", and hard gelatin capsules from the crushed root of SB named "Scutella" were obtained from National University of Pharmacy's Department of Industrial Technology of Drugs. In the experiment, 94 random-breed white male mice weighing 20-29 g were used and kept in standard sanitary and laboratory conditions. During the experiments, the animals were in the vivarium at 19-24°C, humidity was under 50%, the natural light mode was "day-night". The animals were housed in plastic cages and fed a standard diet. The experimental studies were performed in accordance with the "general ethical principles of animal experiments" (Ukraine, 2001) in accordance with the "European Convention for the Protection of vertebrate animals used for experimental and other scientific purposes". SBDE was used in doses of 25 mg/kg, 50 mg/kg, 75 mg/kg; SBRP was used in doses of 87 mg/kg (25 mg/kg in terms of baicalin), 173 mg/kg (50 mg/kg in terms of baicalin) and 260 mg/kg (75 mg/kg in terms of baicalin); "Scutex" tablets and "Scutella" hard gelatin capsules were used in doses of 320 mg/kg (50 mg/kg in terms of baicalin) and 260 mg/kg (75 mg/kg in terms of baicalin), respectively. SBDE, SBRP, crushed tablet mass "Scutex" and the contents of the "Scutella" capsules were dissolved in water and administered to the mice through intragastric probes in a volume of 0.1 mL for 10 g mass once per day for 5-8 days last 30-60 minutes before experiment. The control group was injected with the same amount of pooled tap water. The reference product-"Bilobil" (KRKA, Slovenia) at a dose of 100 mg/kg, was dissolved in water and injected in the same mode.[9] All behavioral tests were conducted sequentially, synchronously with the appropriate control, because the effects depended on chronopharmacologic factor. The study of the anti-depressant properties of SBDE, SBRP, "Scutex" and "Scutella" drugs and reference drug were conducted using the mice tail suspension test (despair behavior).[10] The anti-hypoxic effect was evaluated on the model of normobaric hypoxic hypoxia with hypercapnia.[11] The impact of the studied substances on the physical endurance of mice was studied through a test of swimming with load.[10]

Statistical analysis

The results were examined statistically using STATISTICA 8.0 software by evaluating the reliability of differences between the comparison groups using Student's t parametric criterion in cases of normal distribution, nonparametric Mann-Whitney U criterion in its absence. The difference was considered statistically significant at $p \leq 0.05$.

RESULTS AND DISCUSSION

Results of anti-depressant activity of SBDE in terms of the immobilization test (tail suspension test) are shown in Table 1. The obtained results indicate that SBDE at a dose of 50 mg/kg increased latent time of frozen mice hanging 1.7 times or by 68% compared with control ($p \leq 0.05$); amount of frozen hangs decreased 1.2 times or by 18%; the overall duration of frozen hangs decreased 1.5 times or by 35% ($p \leq 0.05$). The reference drug "Bilobil" in a dose of 100 mg/kg increased the latency time of frozen hangs 1.4 times or by 39% ($p \leq 0.05$), and total duration of frozen hangs tendentiously decreased 1.2 times. The action of SBDE exceeded the effect of the reference drug "Bilobil" 1.2 times by an increase in latency for frozen hangs. Therefore, SBDE possesses antidepressant action. The next step was to study the anti-depressant activity of SBRP in doses of 173 mg/kg and 260 mg/kg. SBRP in both doses had no significant effect on quantitative parameters of depressive behavior (Table 1). "Scutex" tablets and "Scutella" capsules also showed no probable anti-depressant activity (Table 1). They only biased the increased latent time of frozen hangs and reduced their total duration. On the other hand, the effect of the drug *Ginkgo biloba* ("Bilobil") on depressive behavior was weak and unstable, as in the different series of experiments it either increased latency time of immobilization or tendentiionally reduced its total duration, or had no significant effect. All drugs of SB; SBDE, SBRP, "Scutex" tablets, and "Scutella" capsules, as well as "Bilobil" had no effect on the physical endurance of mice in the test of swimming to exhaustion (Table 2). This was evidenced by the unchanged swimming time compared with the controls. Results of the study regarding the anti-hypoxic properties of SBDE in normobaric hypoxic hypoxia with hypercapnia model demonstrated an increased life expectancy of the mice of 1.3 times compared with the controls (Table 3), indicating a distinct anti-hypoxic effect of the drug. In the group of animals treated with the comparator, no statistically significant differences as compared with the controls were observed. SBRP at a dose

Table 1. Influence of dry extract *Scutellaria baicalensis* and reference drug "Bilobil" on despair behavior in mice immobilization test conditions (tail suspension test)

Group, dose, n	Latent time of frozen hanging, s	Number of frozen hangs	Total duration of frozen hangs, s
Control (1), n=6	42.8±3.70	13.5±1.60	108.7±7.00
"Bilobil" 1, 100 mg/kg, n=6	59.5±5.70*	13.5±2.00	93.3±6.00
SBDE, 50 mg/kg, n=9	71.9±5.90*	11.1±2.00	70.6±5.50*
Control (2), n=8	42.13±12.73	11.25±1.29	108.13±18.85
"Bilobil" (2), 100 mg/kg, n=7	34.14±6.75	11.43±0.87	128.14±9.69
SBRP, 173 mg/kg, n=7	98.43±28.82	7.71±1.58	93±20.22
SBRP, 260 mg/kg, n=7	63.14±9.04	8±0.72	102.29±8.90
Control (3), n=6	35.50±5.81	10.67±1.36	103.83±20.6
"Bilobil" (3), 100 mg/kg, n=6	54.00±13.50	12.67±1.61	103.67±16.01
"Scutex", 320 mg/kg, n=6	102.33±40.18	7.50±2.55	58.0±19.04
Control (4), n=7	41.30±6.13	12.35±0.98	111.84±22.6
"Bilobil" (4), 100 mg/kg, n=6	52.22±10.11	12.71±1.25	101.22±17.5
"Scutella", 260 mg/kg, n=6	55.42±12.05	9.13±1.18	104.17±19.04

S: Seconds; mg/kg: milligrams of drug per kilogram of animal weight, *: Statistically significant differences (p≤0.05 as for appropriate control), SBDE: Dry extract *Scutellaria baicalensis*, SBRP: Powder of roots and rhizomes from *Scutellaria baicalensis*

Table 2. The impact of *Scutellaria baicalensis* drugs and reference drug "Bilobil" on physical endurance of mice by swimming with load test

Group, dose, n	Time of swimming to exhaustion, min
Control (1)	3.44±0.33
SBDE, 50 mg/kg	3.41±0.34
"Bilobil" (1), 100 mg/kg	3.40±0.27
Control (2)	6.01±0.50
SBRP, 173 mg/kg	7.92±0.91
SBRP, 260 mg/kg	6.73±0.75
"Bilobil" (2), 100 mg/kg	6.05±0.42
Control (3)	3.60±0.23
"Scutex" 320 mg/kg	3.64±0.20
"Bilobil" (3), 100 mg kg	3.68±0.43
Control (4)	5.81±0.52
Scutella, 260 mg/kg	6.15±0.56
"Bilobil" 100 mg/kg	6.26±0.42

All values are mean±standard deviations of six experiments, SBDE: Dry extract *Scutellaria baicalensis*, SBRP: Powder of roots and rhizomes from *Scutellaria baicalensis*

Table 3. Impact of dry extract *Scutellaria baicalensis*, powder of roots and rhizomes from *Scutellaria baicalensis*, "Scutex", "Scutella" and "Bilobil" on life expectancy in mice under normobaric hypoxic hypoxia with hypercapnia

Group, dose, n	Life span, min
Control (1), n=8	24.47±1.67
SBDE, 50 mg/kg, n=8	32.03±2.18*
"Bilobil" (1), 100 mg/kg, n=6	30.07±4.14
Control (2), n=8	23.62±1.11
SBRP, 173 mg/kg, n=6	30.87±3.17*
SBRP, 260 mg/kg, n=7	38.73±3.79*#
"Bilobil" (2), 100 mg/kg, n=7	30.96±1.49*
Control (3), n=6	17.89±0.60
"Scutex" 320 mg/kg, n=6	21.81±2.36
"Bilobil", 100 mg/kg, n=5	20.27±1.06
Control (4), n=7	22.77±0.84*
Scutella, 260 mg/kg, n=6	36.99±3.98
"Bilobil" (4), 100 mg/kg, n=6	29.96±1.31*

mg/kg: milligrams of drug per kilogram of animal weight. All values are mean±standard deviations; number of experiments for each group is mentioned win the table, *Significant differences from control indicator of corresponding series of experiments (p<0.05), #Significant differences with the rate of animals treated with "Bilobil" (p<0.05), in the corresponding series of experiments, SBDE: Dry extract *Scutellaria baicalensis*, SBRP: Powder of roots and rhizomes from *Scutellaria baicalensis*

of 173 mg/kg significantly increased the life duration of mice by 1.3 times compared with the control. Similar results were observed when the reference drug "Bilobil" was administered. Influenced by SBRP at a dose of 260 mg/kg, the lifespan of the mice increased 1.6 times compared with the controls, which is 33% more than in the background of SBRP at a dose of 173 mg/kg (Table 3). Accordingly, SBRP at a dose of 260 mg/kg has the most significant anti-hypoxic effect in terms of normobaric hypoxic hypoxia with hypercapnia and exceeds the effect of comparison drug, and at a dose of 173 mg/kg SBRP acts at the level of reference drug. "Scutex" tablets only showed a tendency to increase the life duration of mice by 21.9% compared with the controls. "Bilobil" also showed a tendency to increase lifespan of mice by 13.3% as compared with the control group. "Scutella" capsules (Table 3) significantly increased the lifespan of mice by 1.6 times compared with the controls. Under the influence of "Bilobil", there was also an increase in life expectancy of mice of 1.3 times compared with the control group. Thus, we can conclude that "Scutella" revealed anti-hypoxic action and had an advantage over the reference "Bilobil" drug. The anti-hypoxic effect of the latter was not stable, however, because in different experiments it was revealed either on a statistically significant level or biased.

CONCLUSIONS

SBDE at a dose 50 mg/kg shows anti-depressant activity that exceeds the activity of the comparison drug "Bilobil". SBRP at doses of 173 mg/kg and 260 mg/kg, as well as "Scutex" tablets and "Scutella" capsules have no anti-depressant action. SBDE, SBRP, "Scutex" tablets and "Scutella" capsules have not effect on the physical endurance of mice. SBDE at a dose 50 mg/kg and SBRP at a dose of 173 mg/kg and 260 mg/kg exhibit anti-hypoxic activity exceeding the activity of the reference drug "Bilobil". "Scutex" tablets show no anti-hypoxic action and "Scutella" capsules cause probable anti-hypoxic action that exceeds the effect of the reference drug "Bilobil".

Conflict of Interest: No conflict of interest was declared by the authors.

REFERENCES

1. Yakovleva GP, Blinova KF. Encyclopedic Dictionary of medicinal plants and products of animal origin. Belodubovskaya GA, Zabinkova NN, eds. St. Petersburg; Utchebnaja kniga; 1999:1-407.
2. Ibrahimova VS. Chinese medicine. Methods of diagnosis and treatment. Pharmaceuticals. Acupuncture therapy. Antares. 1994:426-429.
3. Arnal-Shnebellen B, Goetz P. Encyclopedia of medicinal plants (translated from French). Grassar E, Yunen M, eds. Riderz Daydzhest; 2004:1-352.
4. Shang Y, Zhang H, Cheng J, Miao H, Liu Y, Cao K, Wang H. Flavonoids from *Scutellaria baicalensis* Georgi are effective to treat cerebral ischemia/reperfusion. Neural Regen Res. 2013;8:514-522.
5. Lu JH, Ardah MT, Durairajan SS, Liu LF, Xie LX, Fong WF, Hasan MY, Huang JD, El-Agnaf OM, Li M. Baicalein inhibits formation of α-synuclein oligomers within living cells and prevents Aβ peptide fibrillation and oligomerisation. Chembiochem. 2011;12:615-624.
6. Xiong Z, Jiang B, Wu PF, Tian J, Shi LL, Gu J, Hu ZL, Fu H, Wang F, Chen JG. Antidepressant effects of a plant-derived flavonoid baicalein involving extracellular signal-regulated kinases cascade. Biol Pharm Bull. 2011;34:253-259.
7. Slipchenko GD, Shtrygol SY, Kudina OV, Taran AV, Ruban OA. The comparative pre-clinical study of psychotropic properties of the medicines from *Scutellaria baicalensis* Georgi. Pharmacology and Drug Toxycology. 2016;4-5:41-49.
8. Shtrygol SY, Slipchenko GD, Kudinov AV, Matviichuk AV, Ruban OA. Comparative clinical trials of antiamnestic properties of *Scutellaria baicalensis* drugs. Phitoterapiya Chasopis. 2016;4:17-20.
9. Tsyvunin VV, Shtrygol SY, Prokopenko YS. Neuroprotective properties of dry extracts of *Fumaria schleicheri* and *Ocimum basilicum*. Reviews on clinical pharmacology and Drug Therapy. 2013;11:66-71.
10. Stefanov OV. Preclinical study of drugs (1st ed). Kyiv; Avitsena; 2001:1-528.
11. Mironov AN. Guidance on conducting the preclinical studies of pharmaceuticals. (1st ed) Moscow; Griff & Co; 2012:1-944.

Turk J Pharm Sci 2018;15(3):364-369
DOI: 10.4274/tjps.94695

ORIGINAL ARTICLE

The Apoptotic and Anti-apoptotic Effects of Pendimethalin and Trifluralin on A549 Cells *In Vitro*

Pendimetalin ve Trifluralinin Apopitotik ve Anti-Apopitotik Etkilerinin A549 Hücrelerinde *İn Vitro* Değerlendirilmesi

Zehra SARIGÖL-KILIÇ, Ülkü ÜNDEĞER-BUCURGAT*

Hacettepe University, Faculty of Pharmacy, Department of Pharmaceutical Toxicology, Ankara, Turkey

ABSTRACT

Objectives: Pendimethalin and trifluralin are commonly used in many countries to control broadleaf weeds and grassy weed species because of their inhibitor effects on growth and cell division. In this study, we examined the apoptotic and anti-apoptotic potentials of pendimethalin and trifluralin on A549 human non-small lung cancer cells with several concentrations *in vitro*.

Materials and Methods: The expression levels of apoptosis-related genes *BCL-2, BAX, CAS3, CAS9, P53, BIRC*, and *PPIA* were examined using quantitative RT-PCR after 24 h treatment of 1, 10, 50, 100 and 500 µM pendimethalin and trifluralin.

Results: The effects of pendimethalin were found more repressive than trifluralin on all studied concentrations. Twenty-four hours' exposure with 100 µM pendimethalin and trifluralin altered the gene expressions, suppressing apoptosis and allowing cancer cells to grow and proliferate.

Conclusion: Care should be taken not to exceed the permissible values and residue limits in food during pendimethalin and trifluralin use in order to reduce the possible carcinogenic effects on humans.

Key words: Pendimethalin, trifluralin, apoptosis, A549, gene expressions

ÖZ

Amaç: Pendimetalin ve trifluralin birçok ülkede, büyüme ve hücre bölünmesi üzerindeki inhibitör etkileri nedeniyle, geniş yapraklı yabani otları ve çimenli ot türlerini kontrol etmek amacıyla yaygın şekilde kullanılmaktadır. Bu çalışmada, pendimetalin ve trifluralinin apoptotik ve anti-apoptotik potansiyelleri, A549 insan küçük olmayan akciğer kanseri hücreleri üzerinde çeşitli konsantrasyonlarda *in vitro* incelendi.

Gereç ve Yöntemler: Apoptoz ile ilişkili genler *BCL-2, BAX, CAS3, CAS9, P53, BIRC* ve *PPIA*'nın ekspresyon seviyeleri, 24 saat 1, 10, 50, 100 ve 500 µM pendimetalin ve trifluralin uygulamasından sonra kantitatif RT-PCR ile incelendi.

Bulgular: Çalışılan tüm konsantrasyonlarda pendimetalinin etkileri trifluralinin etkilerine kıyasla daha fazla baskılayıcı bulundu. 100 µM pendimetalin ve trifluraline 24 saat boyunca maruz bırakılan hücrelerde gen ifadesi, apoptozu baskılayacak ve kanser hücrelerinin büyüme ve çoğalmasına yol açacak şekilde değişikliğe uğradı.

Sonuç: Pendimethalin ve trifluralinin insanlar üzerindeki olası kanserojenik etkilerini azaltabilmek için, kullanımları sırasında izin verilen değerlerin ve gıdalar üzerindeki kalıntı limitlerinin aşılmamasına dikkat edilmelidir.

Anahtar kelimeler: Pendimetalin, trifluralin, apopitoz, A549, gen ifadesi

*Correspondence: **E-mail:** uundeger@hacettepe.edu.tr, **Phone:** +90 535 368 53 91 **ORCID-ID:** orcid.org/000-0002-6692-0366
Received: 20.07.2017, **Accepted:** 17.08.2017

INTRODUCTION

Dinitroaniline herbicides were first discovered when dye and dye chemical intermediates were being evaluated. Chemicals in the dinitroaniline herbicide family essentially have a bright yellow color depending on the two nitro groups of the phenyl ring. They are generally referred to as "yellow compounds". The most important and the first herbicide in the dinitroaniline family is trifluralin, which became known in 1963.[1] Dinitroaniline herbicides are separated into two groups as methylaniline herbicides and sulfonyllanine herbicides. Pendimethalin and trifluralin are herbicidal compounds in the group of methylaniline.[2] Herbicides such as pendimethalin and trifluralin are used to control broadleaf weeds and grassy weed species in cabbage, celery, corn, cotton, garlic, lettuce, radish, rice, sorghum, tobacco, brassicas, carrots, cereals, citrus, onions, peas, peanuts, pome fruits, potatoes, soybeans, stone fruits, and tomatoes. Both herbicide compounds are also used in Turkey. Pendimethalin is used for growing apples, walnuts, hazelnuts, peanuts, potatoes, soy, citrus, grapes and asiatic seeds; trifluralin is used for growing cotton, soybean, sunflower seeds, sugar cane, citrus, tomatoes, peppers, onions, aubergine beans, carrots, cumin, and sesame in Turkey.[3]

Dinitroaniline group herbicide compounds pendimethalin and trifluralin can cause nitrosamine synthesis in animals and humans. Nitrozamines are highly reactive, harmful chemical species. They can act as carcinogenic substances by removing amino groups from the nucleotide bases of DNA. At the same time, they can act as toxic alkylating agents.[2] For these reasons, cancer is the suspected health effect and the risk of dietary exposure to pendimethalin and trifluralin. Pendimethalin and trifluralin are also present as contaminants in soil, ground water, surface water, and air because of the widespread use of various formulations.[4] Pendimethalin is classified as a slightly toxic compound (class 3) to mammals. Trifluralin has no acute toxicity on oral, dermal, and ocular exposures to mammals; although it is highly toxic to cold and warm water aquatic organisms as reported by the United States Environmental Protection Agency. Pendimethalin and trifluralin have also been classified as a group C-possible human carcinogen.[5]

Apoptosis, programmed cell death, is defined by important morphologic changes; blebbing, chromatin condensation, nuclear fragmentation, and cell shrinkage. It is an essential process for normal development and also related to chronic diseases with various pathologic situations such as cardiovascular, immunologic, neurodegenerative diseases, and cancer.[6]

Apoptotic mechanism is activated with many biochemicals, the best-defined pathway factors are caspases.[7] *CAS3* is the main protease in the cell death process; *CAS6* and *CAS7* also contribute to the coordination of apoptosis. Thus, these three caspases are known the 'executioner caspases'. In addition, *CAS8* and *CAS9* play a role in the initiation step.[8] When the initiative caspases activate the executioner caspases, the apoptotic process gets started with other enzyme activations.[9] The apoptosis process continues on the extrinsic or intrinsic (mitochondrial) pathway and results in cell death.[10] As well being a programmed process, apoptosis can occur after different kinds of irritations, such as radiation, anticancer drugs that cause DNA damage, and deprivation of cytokines that provide survival signals.[11]

In addition to enzymatic changes, the apoptotic pathway is directly related to some gene expressions. As an example, *BCL-2* family proteins control the intrinsic pathway on the antiapoptotic side; however, *BAX* and BAK proteins are promoters of cell death.[12,13] One of the most important proteins at the cell cycle checkpoint is the *P53* tumor suppressor protein, which can be activated by DNA damage, hypoxia, and apoptosis.[14]

Pesticides are known to lead cells to apoptosis in both the intrinsic and extrinsic pathways.[15-17] The compounds mainly enhance mitochondrial oxidative stress mediators and activate the cytochrome-C pathway, resulting in intrinsic apoptosis.[18,19] Dinitroaniline herbicides are used as weed controllers. Their mechanisms of action are based on cell division and decreasing cell elongation and growth with mitotic disruption during mitosis.[20,21]

In this study, we measured the expression levels of *P53*, *BAX, BCL-2, CAS3, CAS9, BIRC*, and *PPIA* (housekeeping) genes related to apoptosis on A549 human lung carcinoma cells after exposure to pendimethalin and trifluralin, which are two commonly used dinitroaniline herbicides.

MATERIALS AND METHODS

Solution preparation

Pendimethalin is highly soluble in oil and organic solvents.[22] The solution was prepared in a dimethyl sulfoxide (DMSO):olive oil (1:3, v/v) mix. Trifluralin is soluble in organic solvents and less soluble in water.[23] The trifluralin solution was prepared in PBS (1% DMSO).

Dulbecco's Modified Eagle's medium with 10% fetal calf serum and a 1% penicillin-streptomycin mixture were used as the cell culture medium.

Cell culture and treatment

A549 cells were cultured in a 25-cm^2 cell culture flask and transferred to a 75-cm^2 flask after 24 h under the conditions of 5% CO_2 and 37°C. After 24 hours, the cells were harvested and transferred to 6-well plates as 10,000 cell/2 mL medium of each. Cell counts were performed using Tripan blue (0.4% w/v in distilled water) in a Neubauer Chamber. One day later, when the cell count multiplied 2 folds and reached 20,000/well, pendimethalin and trifluralin solutions were added to the wells, the final concentrations were 1, 10, 50, 100 and 500 µM. These concentrations were chosen according to their 50% inhibitory concentration (IC_{50}) and toxicity levels.[24-27] The cells were incubated for 24 hours and harvested from the wells and centrifuged at 1200 rpm for 5 min.

RNA isolation, cDNA synthesis and gene expression

RNA isolation were performed using an RNeasy Mini Kit, QIAGEN in accordance with the manufacturer's instructions. In brief, after centrifugation, the cell suspension was filtrated

from the gDNA eliminator column, then transferred and attached to the RNeasy spin column and washed with the solutions as instructed.

The amount and quality of the eliminated RNA samples were measured using Maestrogen Nanodrop. For this measurement, 1 µL of the sample was loaded to the base portion fiber terminal. All the samples' OD 260/280 ratios were found in the range of 1.6-1.8.

The cDNA synthesis was performed from the RNA samples with RT² First Strand Kit, QIAGEN as per the manufacturer's instructions. The RNA samples were denaturized at 42˚C for 5 min in a real-time quantitative reverse transcription polyeramse chain reaction (qRT-PCR) device. The samples were placed on a cold surface to protect the linearity. Then reverse-transcription enzymes were added and the cDNA synthesis process was performed at 42˚C for 15 minutes and 90˚C for 5 minutes. Newly synthesized cDNA samples were stored at -20˚C. The PCR primers used in this study are listed in Table 1.

To measure the expression levels of apoptosis-related genes, cDNA samples were mixed with RT² qPCR primers (*BCL-2, BAX, CAS3, CAS9, P53*, *BIRC* and *PPIA*), RT² SYBR Green qPCR mastermix, and expression was performed using the qRT-PCR device under the conditions of hold 95˚C 15 min, cycle 95˚C 15 sec and 60˚C 30 sec, for 40 cycles. The results were recorded at 60˚C. The threshold limit was set to 0.05 and the Ct values of the samples were calculated.

The results of this article were prepared on performed *in vitro* cultured cells study. Therefore, there is no need for ethics committee approval.

Statistical analysis

Statistics of the Ct values were prepared with an internet-based program RT² Profiler PCR Data Analysis 3.5. ΔΔCt was used to interpret the gene expression data.[28] All experiments were performed twice.

RESULTS

The average Ct (mean), average ΔΔCT, and fold regulation (up-down regulation) values of the A549 cell line after exposure to pendimethalin and trifluralin for 24 h were calculated. ΔCt calculation was preferred to normalize the raw data and Ct value of the housekeeping gene, *PPIA*, was used as the normalization factor. Fold regulation is the ratio of the relative gene expression between the housekeeping gene and the treatment group. This calculation illustrated the up- and down-regulated expressions within $p<0.05$ significance. The formulas used for the calculations were as follows:

ΔCt = Ct (gene of interest) - average [Ct (housekeeping / reference gene)]

ΔΔCt = ΔCt (test group n) - ΔCt (control group)

Average ΔCt = [ΔCt (sample 1) + ΔCt (sample 2) + ... ΔCt (sample n)] / n samples

Average ΔΔCt = $2^{(-\text{Average } \Delta Ct)}$

Fold regulation = $2^{(-\Delta\Delta Ct)}$

The results are presented in Tables 2-7.

Due to the fold regulation results of trifluralin, all gene expressions were down-regulated at the examined concentrations (1-500 µM). However, pendimethalin showed different regulation profiles in the same genes. The concentrations of 100 and 500

Table 1. The PCR primers used in this study

P53	5′-CCCAGCCAAAGAAGAAACCA-3′ (fwd)
	5′-TTCCAAGGCCTCATTCAGCT-3′(rv)
BIRC5	5′-AGAACTGGCCCTTCTTGGAGG-3′(fwd)
	5′-CTTTTTATGTTCCTCTATGGGGTC-3′(rv)
BAX	5′-TGCTTCAGGGTTTCATCCAG-3′(fwd)
	5′-GGCGGCAATCATCCTCTG-3′(rv)
BCL-2	5′-AGGAAGTGAACATTTCGGTGAC-3′(fwd)
	5′-GCTCAGTTCCAGGACCAGGC-3′(rv)
CAS3	5′-ACATGGCGTGTCATAAAATACC-3′(fwd)
	5′-CACAAAGCGACTGGATGAAC-3′(rv)
CAS9	5′-CCAGAGATTCGCAAACCAGAGG-3′(fwd)
	5′-GAGCACCGACATCACCAAATCC-3′(rv)
Housekeeping ***PPIA***	5′-AAGGGTTCCTGCTTTCAC-3′(fwd)
	5′-GGACCCGTATGCTTTAGG-3′(rv)

Table 2. Average Ct values of pendimethalin

AVG Ct pendimethalin

Symbol	Control	PM 500	PM 100	PM 50	PM 10	PM 1
BAX	19.48	34.74	33.89	25.66	23.81	19.97
BCL-2	26.87	30.87	30.88	29.97	28.94	24.98
BIRC5	25.79	33.95	*N/A	31.78	29.99	22.99
P53	20.35	34.43	34.85	26.59	26.04	19.93
CAS3	22.79	*N/A	*N/A	28.57	25.94	22.05
CAS9	24.27	*N/A	33.31	30.22	25.7	22.9
PPIA	25.03	*N/A	*N/A	27.48	26.36	22.27

*N/A greater than 35

Table 3. Average ΔΔCt values of pendimethalin

$2^{(-\text{Average } \Delta Ct)}$ pendimethalin

Symbol	Control	PM 500	PM 100	PM 50	PM 10	PM 1
BAX	47.01	1.20	2.17	3.53	5.86	4.92
BCL-2	0.28	17.57	17.39	0.18	0.17	0.15
BIRC5	0.59	2.07	1.00	0.05	0.08	0.61
P53	25.72	1.49	1.11	1.86	1.24	5.06
CAS3	4.74	1.00	1.00	0.47	1.33	1.16
CAS9	1.69	1.00	3.24	0.15	1.58	0.65
PPIA	1.00	1.00	1.00	1.00	1.00	1.00

Table 4. Fold regulation (up-down) values of pendimethalin

Up-down regulation (comparing to control group) pendimethalin					
	PM 500	PM 100	PM 50	PM 10	PM 1
Symbol	Fold regulation	Fold regulation	Fold regulation	Fold regulation	Fold regulation
BAX	-39.1245*	-21.7057*	-13.3152*	-8.0278*	-9.5467*
BCL	62.6829**	62.0345**	-1.5692***	-1.6818***	-1.834***
BIRC5	3.4943**	1.6876***	-11.6318	-7.336	1.0281***
P53	-17.2677*	-23.1831*	-13.8326*	-20.6776*	-5.0806*
CAS3	-4.7404*	-4.7404*	-10.0561*	-3.5554*	-4.0699*
CAS9	-1.6935***	1.9119***	-11.2746*	-1.0718***	-2.6208*
PPIA	1	1	1	1	1

*Down regulated expression compared with the control group (*PPIA*) p<0.05
**Up regulated expression compared with the control group (*PPIA*) p<0.05
***No significant changes observed compared with the control group

Table 5. Average Ct values of trifluralin

AVG Ct trifluralin						
Symbol	Control group	TF 500	TF 100	TF 50	TF 10	TF 1
BAX	19.48	22.83	18.29	18.12	18.79	18.35
BCL	26.87	28.78	25.21	25.78	26.36	25.97
BIRC5	25.79	29.42	24.85	24.52	24.49	23.77
P53	20.35	24.86	19.87	19	19.7	19.33
CAS3	22.79	26.05	21.41	21.9	22.77	22.33
CAS9	24.27	26.12	22.55	22.65	23.21	23.16
PPIA	25.03	24.96	20.74	20.26	20.94	21.07

Table 6. Average ΔΔCt values of trifluralin

$2^{(-\text{Average }\Delta Ct)}$ trifluralin						
Symbol	Control group	TF 500	TF 100	TF 50	TF 10	TF 1
BAX	47.01	4.38	5.45	4.42	4.44	6.61
BCL-2	0.28	0.07	0.05	0.02	0.02	0.03
BIRC5	0.59	0.05	0.06	0.05	0.09	0.15
P53	25.72	1.07	1.83	2.39	2.35	3.35
CAS3	4.74	0.47	0.63	0.32	0.28	0.42
CAS9	1.69	0.45	0.28	0.19	0.21	0.24
PPIA	1.00	1.00	1.00	1.00	1.00	1.00

µg/mL, *BCL-2* gene, and on 500 µg/mL *BIRC5* gene expressions were found up-regulated compared with the *PPIA* control gene, whereas other concentrations of pendimethalin the examined genes are down-regulated.

DISCUSSION

Pesticide use has brought about both positive and negative results on human health and the environment. They led to an increase of the amount and quality of agricultural products, along with various health problems and disruption of the soil and water.

In this study, we determined the changes of apoptosis-related gene expressions with dinitroaniline herbicides. After 24 h of incubation, at the concentration of 100 µM, pendimethalin significantly down-regulated *BAX*, *P53*, and *CAS3*. Although *CAS9* levels showed no significant change, *BCL-2* and *BIRC5* levels were up-regulated with pendimethalin exposure. On the other hand, trifluralin exposure down-regulated all examined gene levels at all concentrations. It has been shown that *P53* is essential for normal cell apoptosis regulation because of its ability to control *BAX* regulation - the proapoptoic member of the *BCL-2* family.[29] Decreased *P53* levels gave rise to cellular viability, lifespan, and chromosomal instability.[30] It can be stated that increased *BCL-2* expressions come with a decrease of *P53* and *BAX* levels and prevent A549 cells from entering apoptosis. Also, *BAX* can induce caspase activation and increase cellular reactive oxygen species (ROS) by caspase cleavage.[31] Studies demonstrated that *CAS3* activation mediated the *BAX*-mediated pro-oxidant effects[32] and had an important role on inducing apoptosis via the mitochondrial cascade.[33] In our study, *CAS3* expressions were found down-regulated with *BAX*, which in turn lowered the probability of apoptosis on A549 non-small lung cancer cells.

Table 7. Fold regulation (up-down) values of trifluralin

Up-down regulation (comparing to control group) trifluralin					
	TF 500	TF 100	TF 50	TF 10	TF 1
Symbol	Fold regulation	Fold regulation	Fold regulation	Fold regulation	Fold regulation
BAX	-10.7406*	-8.6338*	-10.6295*	-10.5927*	-7.1107*
BCL-2	-3.9449*	-6.2118*	-12.8616*	-12.0003*	-8.3397*
BIRC5	-13.0412*	-10.2319*	-11.3137*	-6.9644*	-3.8504*
P53	-24.0006*	-14.0744*	-10.7406*	-10.9283*	-7.6741*
CAS3	-10.091*	-7.5685*	-14.7741*	-16.8538*	-11.3137*
CAS9	-3.7842*	-5.9587*	-8.8766*	-8.1965*	-7.1851*
PPIA	1	1	1	1	1

*Downregulated expression compared with the control group (PPIA) p<0.05
**Upregulated expression compared with the control group (PPIA) p<0.05
***No significant changes observed compared with the control group

Caspases can initiate the degradation phase of apoptosis with DNA fragmentation and blebbing.[34] *CAS9* inhibition was shown to decrease the ROS production in mitochondria,[35] and the up-regulation resulted with induced ROS production and activation of *CAS3* and *CAS7*.[36]

BIRC5 (survivin) showed different effects with herbicide exposure at the concentration of 100 µM. Although pendimethalin caused up-regulation, trifluralin exposure down-regulated *BIRC5* levels significantly. It is known that *BIRC5* is responsible for cell division regulation during the G_1-S phase and it is also considered for anticancer therapies.[37] Expressed levels of *BIRC5* were found higher than in normal healthy cells in various tumors such as lung, breast, ovarian, and prostate cancers.[38-41] One study stated that *BIRC5* silencing suppressed cell proliferation in A549 non-small lung cancer cells.[38] Compared with our results, we can state that even though pendimethalin reduced apoptotic cycles with *BIRC5* up-regulation, trifluralin exposure could not deactivate programmed cell death in A549 cells at the *BIRC5* level.

CONCLUSIONS

According to our findings and those of previous studies, pendimethalin and trifluralin exposure resulted with reduced-apoptosis, which in turn lead to tumor growth in A549 cells *in vitro*. As stated before, both herbicides significantly changed the expression levels, but pendimethalin had more effects on anti-apoptosis than trifluralin. This study found that tumor suppression genes can be altered by environmental exposure and further studies will enlighten us about the connection between dinitroaniline herbicides and lung cancer.

ACKNOWLEDGEMENTS

This work was supported by the Hacettepe BAP under Grant number 1603.

Conflict of Interest: No conflict of interest was declared by the authors.

REFERENCES

1. Wallace DR. Trifluralin in Encyclopedia of Toxicology. In: Wexler P, ed. Encyclopedia of Toxicology, 3rd ed. Oxford; Academic Press; 2014:388-389.
2. Agronomy 317, Intro to Weeds, "Dinitroanilines", Accessed: 03.02.1017, Available via "http://agron.iastate.edu/-weeds/Ag317-99/manage/herbicide/dnas.html".
3. T.C. Milli Eğitim Bakanlığı, Çevre Sağlığı, Pestisitler, 850 CK 0054, Ankara, 2012.
4. Kegley S, Hill B, Orme S. Pendimethalin. PAN Pesticide Database, Pesticide Action Network, North America, San Francisco, CA. Accessed 23.12.2015, Available via" http://www.pesticideinfo.org".
5. US Environmental Protection Agency (US EPA), R.E.D. Facts: Pendimethalin, US EPA; Washington DC; 1997.
6. Zimmermann KC, Green DR. How cells die: Apoptosis pathways. J Allergy Clin Immunol 2001;108:99-103.
7. Martin SJ, Green DR. Protease activation during apoptosis: death by a thousand cuts? Cell. 1995;82:349-352.
8. McIlwain DR, Berger T, Mak TW. Caspase functions in cell death and disease. Cold Spring Harb Perspect Biol. 2013;5:a008656.
9. Riedl SJ, Shi Y. Molecular mechanisms of caspase regulation during apoptosis. Nat Rev Mol Cell Biol. 2004;5:897-907.
10. Vermeulen K, Van Bockstaele DR, Berneman ZN. Apoptosis: mechanisms and relevance in cancer. Ann Hematol. 2005;84:627-639.
11. Kataoka S, Tsuruo T. Physician Education: Apoptosis. Oncologist. 1996;1:399-401.
12. Wei MC, Zong WX, Cheng EH, Lindsten T, Panoutsakopoulou V, Ross AJ, Roth KA, MacGregor GR, Thompson CB, Korsmeyer SJ. Proapoptotic BAX and BAK: a Requisite Gateway to Mitochondrial Dysfunction and Death. Science. 2001;292:727-730.
13. Cory S, Adams JM. The Bcl2 family: regulators of the cellular life-or-death switch, Nat Rev Cancer. 2002;2:647-656.
14. Hussain SP, Harris CC. Molecular epidemiology of human cancer: contribution of mutation spectra studies of tumor suppressor genes. Cancer Res. 1998:58:4023-4037.

15. Chi CC, Chou CT, Liang WZ, Jan CR. Effect of the pesticide, deltamethrin, on Ca2+ signaling and apoptosis in OC2 human oral cancer cells. Drug Chem Toxicol. 2014;37:25-31.

16. Raszewski G, Lemieszek MK, Lukawski K, Juszczak M, Rzeski W. Chlorpyrifos and cypermethrin induce apoptosis in human neuroblastoma cell line SH-SY5. Basic Clin Pharmacol Toxicol. 2015;116:158-167.

17. Jang Y, Lee AY, Jeong SH, Park KH, Paik MK, Cho NJ, Kim JE, Cho MH. Chlorpyrifos induces NLRP3 inflammasome and pyroptosis/apoptosis via mitochondrial oxidative stress in human keratinocyte HaCaT cells. Toxicology. 2015;338:37-46.

18. Banerjee BD, Seth V, Ahmed RS. Pesticide-induced oxidative stress: perspectives and trends. Rev Environ Health. 2001;16:1-40.

19. Li Q, Kobayashi M, Kawada T. Carbamate pesticide-induced apoptosis and necrosis in human natural killer cells. J Biol Regul Homeost Agents. 2014;28:23-32.

20. Nick P. Control of plant shape, In Plant Microtubules: Potential for Biotechnology. Nick P, ed. Berlin- Heidelberg; Springer Berlin-Heidelberg; 2000:25-50.

21. Tresch S, Plath P, Grossmann K. Herbicidal cyanoacrylates with antimicrotubule mechanism of action. Pest Manag Sci. 2005;61:1052-1059.

22. EXTOXNET, Extension Toxicology Network Pesticide Information Profiles: Pendimethalin, 1996a. Accessed 23.12.2015, Available via http://extoxnet.orst.edu/pips/pendimet.htm

23. EXTOXNET. Extension Toxicology Network Pesticide Information Profiles: Trifluralin, 1996b. Accessed 23.12.2015, Available via http://extoxnet.orst.edu/pips/triflura.htm

24. Dimitrov BD, Gadeva PG, Benova DK, Bineva MV. Comparative genotoxicity of the herbicides Roundup, Stomp and Reglone in plant and mammalian test systems. Mutagenesis. 2006;21:375-382.

25. Patel S, Bajpayee M, Pandey AK, Parmar D, Dhawan A. In vitro induction of cytotoxicity and DNA strand breaks in CHO cells exposed to cypermethrin, pendimethalin and dichlorvos. Toxicol In Vitro. 2007;21:1409-1418.

26. Zaidenberg A, Marra C, Luong T, Gomez P, Milani L, Villagra S, Drut R. Trifluralin toxicity in a Chagas disease mouse model. Basic Clin Pharmacol Toxicol. 2007;101:90-95.

27. Weir SM, Yu S, Salice CJ. Acute toxicity of herbicide formulations and chronic toxicity of technical-grade trifluralin to larval green frogs (Lithobates clamitans). Environ Toxicol Chem. 2012;31:2029-2034.

28. Livak KJ, Schmittgen TD. Analysis of Relative Gene Expression Data Using Real-Time Quantitative PCR and the 2–(-Delta Delta C(T)) Method. Methods. 2001;25:402-408.

29. Fridman JS, Lowe SW. Control of apoptosis by p53. Oncogene. 2003;22:9030-9040.

30. Lowe SW, Lin AW. Apoptosis in cancer. Carcinogenesis. 2000;21:485-495.

31. Ricci JE, Munoz-Pinedo C, Fitzgerald P, Bailly-Maitre B, Perkins GA, Yadava N, Scheffler IE, Ellisman MH, Green DR. Disruption of mitochondrial function during apoptosis is mediated by caspase cleavage of the p75 subunit of complex I of the electron transport chain. Cell. 2004;117:773-786.

32. Kirkland RA, Franklin J. Bax and caspases regulate increased production of mitochondria-derived reactive species in neuronal apoptosis: LACK of A role for depletion of cytochrome c from the mitochondrial electron transport chain. Biochem Biophys Rep. 2015;4:158-168.

33. Chakraborty S, Mazumdar M, Mukherjee S, Bhattacharjee P, Adhikary A, Manna A, Chakraborty S, Khan P, Sen A, Das T. Restoration of p53/miR-34a regulatory axis decreases survival advantage and ensures Bax-dependent apoptosis of non-small cell lung carcinoma cells. FEBS Lett. 2014;588:549-559.

34. Srinivasula SM, Ahmad M, Fernandes-Alnemri T, Alnemri ES. Autoactivation of procaspase-9 by Apaf-1-mediated oligomerization. Mol Cell. 1998;1:949-957.

35. Cepero E, King AM, Coffey LM, Perez RG, Boise LH. Caspase-9 and effector caspases have sequential and distinct effects on mitochondria. Oncogene. 2005;24:6354-6366.

36. Brentnall M, Rodriguez-Menocal L, De Guevara RL, Cepero E, Boise LH. Caspase-9, caspase-3 and caspase-7 have distinct roles during intrinsic apoptosis. BMC Cell Biol. 2013;14:1-9.

37. Wheatley SP, McNeish IA. Survivin: a protein with dual roles in mitosis and apoptosis. Int Rev Cytol. 2005;247:35-88.

38. Monzo M, Rosell R, Felip E, Astudillo J, Sanchez JJ, Maestre J, Martin C, Font A, Barnadas A, Abad A. A novel anti-apoptosis gene: Re-expression of survivin messenger RNA as a prognosis marker in non-small-cell lung cancers. J Clin Oncol. 1999;17:2100-2104.

39. Tanaka K, Iwamoto S, Gon G, Nohara T, Iwamoto M, Tanigawa N. Expression of survivin and its relationship to loss of apoptosis in breast carcinomas. Clin Cancer Res. 2000;6:127-134.

40. Krajewska M, Krajewski S, Banares S, Huang X, Turner B, Bubendorf L, Kallioniemi OP, Shabaik A, Vitiello A, Peehl D, Gao GJ, Reed JC. Elevated expression of inhibitor of apoptosis proteins in prostate cancer. Clin Cancer Res. 2003;9:4914-4925.

41. Xing J, Jia CR, Wang Y, Guo J, Cai Y. Effect of shRNA targeting survivin on ovarian cancer. J Cancer Res Clin Oncol. 2012;138:1221-1229.

Turk J Pharm Sci 2018;15(3):370-375
DOI: 10.4274/tjps.37132

ORIGINAL ARTICLE

Investigation of Antimicrobial Activities of Some Herbs Containing Essential Oils and Their Mouthwash Formulations

Uçucu Yağ İçeren Bazı Bitkilerin ve Gargara Formülasyonlarının Antimikrobiyal Aktivitelerinin Araştırılması

Büşra KULAKSIZ[1]*, Sevda ER[2], Neslihan ÜSTÜNDAĞ-OKUR[3], Gülçin SALTAN-İŞCAN[4]

[1]Biruni University, Department of Pharmacognosy, İstanbul, Turkey
[2]Anadolu University, Yunus Emre Vocational School for Health Services, Department of Medical Services and Techniques, Eskişehir, Turkey
[3]İstanbul Medipol University, Department of Pharmaceutical Technology, İstanbul, Turkey
[4]Ankara University, Department of Pharmacognosy, Ankara, Turkey

ABSTRACT

Objectives: The aim of this study was to prepare pharmaceutical formulations of mouthwashes and to examine the antimicrobial activities of essential oils obtained from plants used traditionally in Turkey for oral infections.

Materials and Methods: Essential oils were obtained from herbal drugs using water distillation with Clevenger apparatus. The antimicrobial capacities of mouthwash formulations containing a mixture of essential oils with proportions of 4.5% and 9.0% were examined using disc diffusion and microbroth dilutions.

Results: The inhibition zone diameters were determined to vary between 7 and 59 mm. The static and cidal activity was generally 50% and greater than 50% when pure essential oil samples were applied on microorganism specimens. Formulation F2, which contained a mixture of essential oils with proportions of 4.5%, showed 6.25% minimum bactericidal effect on *Staphylococcus aureus* ATCC 25923, and 3.125% the minimum inhibitory concentration and minimum bactericidal concentration on all other microorganisms. The antimicrobial effect of pure essential oil samples applied on microorganisms was lower than of mouthwashes formulations; the antimicrobial effect of F2, which contained a mixture of essential oils with proportions of 4.5% was higher than formulation F1, which contained a mixture of essential oils with proportions of 9%.

Conclusion: The results obtained by these methods allow us to conclude that the essential oils and the prepared F1 and F2 mouthwash formulations exerted activity against microorganisms affecting the oral cavity. The F2 formulation also had significant antimicrobial activity on the tested microorganisms.

Key words: Antimicrobial activity, *Laurus nobilis* L., *Origanum vulgare* L. ssp. *hirtum*, *Rosmarinus officinalis* L., *Salvia fruticosa* Mill.

ÖZ

Amaç: Türkiye'de halk arasında yaygın olarak kullanılan bitkilerden elde edilen uçucu yağların antimikrobiyal etkilerini araştırmak ve bu etkilerden yola çıkarak ağız enfeksiyonlarında kullanılmak üzere gargara formülasyonu hazırlamaktır.

Gereç ve Yöntemler: Uçucu yağlar, bitkilerden (*Origanum vulgare* L. ssp. *hirtum*, *Rosmarinus officinalis* L., *Laurus nobilis* L., *Salvia fruticosa* Mill.) su distilasyonu metodu ile Clevenger apareyi kullanılarak elde edilmiştir. Elde edilen uçucu yağlar ve %4.5 ve %9.0 oranlarında uçucu yağların karışımını içeren gargara formülasyonlarının antimikrobiyal aktiviteleri disk difüzyon metodu ve mikrobroth dilüsyon metodu ile araştırılmıştır.

Bulgular: Bu çalışmada antimikrobiyal aktivite disk difüzyon metodu ve mikrobroth dilüsyon metoduyla değerlendirilmiştir. İnhibisyon zon çaplarının 7-59 mm arasında değişkenlik gösterdiği belirlenmiştir. Uçucu yağlar, mikroorganizmalar üzerine saf olarak uygulandığında statik ve sidal etkinliğin genellikle %50 ve %50'nin üzerinde olduğu gözlenmiştir. %4.5 oranında uçucu yağ karışımı içeren F2 formülasyonunun *Staphylococcus aureus* ATCC 25923 üzerindeki minimum bakterisidal etkisinin %6.25 olduğu ve diğer tüm mikroorganizmalar üzerinde minimum inhibitör konsantrasyon ve minimum bakterisidal konsantrasyonunun %3.125 olduğu bulunmuştur. Uçucu yağ örneklerinin mikroorganizmalar üzerine saf olarak uygulandığında gösterdikleri antimikrobiyal etkinin, gargara formülasyonlarına göre daha düşük olduğu; ayrıca %4.5 oranında uçucu yağ karışımı

*Correspondence: E-mail: bkulaksiz@biruni.edu.tr, Phone: +90 538 251 20 71 ORCID-ID: orcid.org/0000-0002-6466-3271
Received: 21.08.2017, Accepted: 23.11.2017

içeren F2 formülasyonunun, %9.0 oranında uçucu yağ karışımı içeren F1 formülasyonuna göre test edilen tüm mikroorganizmalar üzerine daha yüksek antimikrobiyal etkiye sahip olduğu bulunmuştur.

Sonuç: Elde edilen sonuçlar uçucu yağların karışımı ile hazırlanan F1 ve F2 formülasyonlarının, test edilen mikroorganizmalara karşı antimikrobiyal etkiye sahip olduğunu ortaya koymuştur. Ayrıca çalışma sonucunda F2 formülasyonunun test edilen mikroorganizmalar üzerinde önemli oranda antimikrobiyal aktiviteye sahip olduğu rapor edilmiştir.

Anahtar kelimeler: Antimikrobiyal aktivite, *Laurus nobilis* L., *Origanum vulgare* L. ssp. *hirtum*, *Rosmarinus officinalis* L., *Salvia fruticosa* Mill.

INTRODUCTION

Diseases that affect the buccal cavity and teeth are a current public health concern. Mouth bacteria have been linked to plaque, tooth decay, and toothache. Plaque, which is a layer that forms on the surface of a tooth, principally at its neck, is composed of bacteria in an organic matrix that has been linked to gingivitis, periodontal disease, or dental carries.[1] Patient compliance and acceptance is extremely important for oral topical products. Ointments, creams, and some emulsions are rarely used for oral topical treatment, the patients have lower acceptance for application of ointments in the mouth.[2] Nowadays, mouthwash is one of the oral formulations that are available in the market. A mouthwash is identified as a non-sterile liquid solution used mostly for its deodorant, refreshing or antiseptic action, and also these rinses aim to decrease oral bacteria, eliminate food particles, temporarily decrease bad breath and offer a pleasant taste.[3] Mouthwashes are very useful in the reduction of microbial plaques.[4] It is important to make sure that formulated aqueous mouthwashes provide a comfortable feeling in the mouth during use, and it must have a pleasant flavor to obtain consumer acceptance.

Plants have been used for centuries in herbal tea preparations, as spices, and for therapeutic purposes.[5] The number of plants used for therapeutic purposes and spices is reported to be around 20,000. It is estimated that the number of plant species used for medical purposes in the world is 350,000 and 5% of these are formed by aromatic plants.[6,7] Herbal products have recently experienced more thorough investigation for their potential in preventing oral illnesses, particularly plaque-related diseases, such as dental caries.[8] Natural substances obtained from medicinal plants and used in alternative medicine were reported to possess antibacterial activity. The development of antibiotic resistant strains in recent years has become a serious health problem. In this direction, the antimicrobial effects of plant extracts and essential oils obtained from various parts of the plant against bacteria and fungus became important.[9] Researchers are trying to pay more attention to these natural products aiming to find an effective antimicrobial mouthwash that has the advantage of decreasing the adverse effects of synthetic products. The use of natural antimicrobials may conduce to control the disordered growth of oral microbiota, thus overwhelming problems caused by species resistant to conventional antimicrobials.[10,11] Natural materials have proved antibacterial action, mainly because most plants used in alternative medicine are composed of flavonoids, which act on bacterial cells disrupting the cytoplasmic membrane and inhibiting the enzymatic activity.[12]

Turkey is a Mediterranean country that is rich in medicinal and aromatic plants. Most of these are used in local folk tradition for many purposes.[13] *Laurus nobilis* L. is a plant belonging to the Lauraceae family, which comprises approximately 2500 species. The genus *Laurus* is found in Europe and consists of two species, *Laurus azorica* and *Laurus nobilis*. Leaves of the plant, which are not shed during winter, are 5-10 cm long, 2-5 cm wide, and green in color. The fruits are small and olive-like.[14,15] The antimicrobial, analgesic, anti-inflammatory, acetylcholine esterase inhibiting properties of the essential oil of *Laurus nobilis* L. have been reported.[15,16]

There are four reports on the essential oil content and composition of *Origanum vulgare* L. ssp. *hirtum* of Turkish origin. This plant is known in Turkey as "İstanbul kekiği" and is widely used as thyme in the Marmara and Thrace regions.[17,18]

Rosemary (*Rosmarinus officinalis* L.), belonging to the Lamiaceae family, is a pleasant smelling perennial shrub that grows in several regions around the world. It is known as "Biberiye, Kuşdili" in Turkey.[13,19] Sage is one of the most valued herbs known for its essential oil richness and its plethora of biologically active compounds extensively used in folk medicine. Sages are cultivated in many countries. The garden sage (*Salvia officinalis* L.) is grown in Canada, the United States of America, Spain, Italy, Greece, Albania, Germany, France, Turkey, and England.[20]

Essential oils are volatile and oily mixtures with a strong odor, consisting of a large number of chemical compounds that give off the characteristic odor and color of the plant, which can be obtained from aromatic plants or from various herbal sources by methods such as water or hydro distillation. Essential oils can be found in different parts such as the root, stem, leaf, fruit, seed, wood, crust, bud, rhizome, and flower. Also, they are found in particular secretory canals such as the secretory trichome, secreting vesicle, or parenchyma and epidermal cells in the plants, depending on the family.[5,21,22]

Essential oils so called because they are fragrant, and "volatile oil" and "etheric oil" because they are volatile and easily evaporate.[6,21] The term "essential oil" was derived from the effective ingredient of the drug "Quinta essential", named by Paracelsus von Hohenheim in the 16th century.[23] Aromatic materials have been used scientifically and commercially for many purposes such as cosmetics, medicine, the food industry, perfumery, aromatherapy, and phytotherapy for many years.[21] Essential oils contain terpenic hydrocarbons and their oxygenated derivatives, as well as a small amount of volatile aliphatic hydrocarbons and mixtures of aromatic substances derived from phenylpropene. They consist of a many compounds that have different structures containing different functional groups. These functional groups also determine the characteristic chemical properties of volatile oils. Essential oils contain phenylpropene as well as terpenes. Terpenes are present in much greater amounts than phenylpropenes, and phenylpropenes are responsible for the odor and taste of essential oil.[6,7]

Hence, the purpose of the present study was to prepare and evaluate antimicrobial activities of mouthwashes.

Ethics committee approval was not required for the study.

EXPERIMENTAL

The plant materials were provided from the market and identified in Pharmaceutical Botanical Department, İstanbul University Faculty of Pharmacy. Plant materials were determined as *Origanum vulgare* L. ssp*. hirtum, Laurus nobilis* L.*, Rosmarinus officinalis* L.*, Salvia fruticosa* Mill. Voucher specimens were kept in Medipol University.

In this study, sodium chloride, sodium bicarbonate, sodium saccharin, and ethanol were purchased from Sigma Aldrich (Germany).

Obtaining essential oil

Plant materials were hydro distilled for 4 hours using a Clevenger apparatus. The temperature of the heater was set at 100±2˚C. The obtained essential oils were dried over anhydrous sodium sulfate and stored at 4˚C.[24] Plant materials and plant registration numbers are shown in Table 1.

Preparation of mouthwashes

The mouthwash was prepared according to Table 2. Mouthwash solutions were formulated 4.5-9% of essential oil, 1-2% of *Origanum vulgare* L. ssp*. hirtum* and *Salvia fruticosa* Mill, 2-4% of *Rosmarinus officinalis* L., and 0.5-1% of *Laurus nobilis* L. Ethanol, sodium chloride, and sodium bicarbonate were also added to the formulations. Saccharine sodium was used as a sweetener. Essential oils were weighed and dissolved in a part of the ethanol and the other ingredients were added gradually with the aid of a mechanical stirrer at 500 rpm for 30 mins. The mixture was filtered and the filtrate volume was made up to 10 mL with distilled water. No preservative was necessary to be added due to the high content of ethanol (>15%) in the formulations.[25]

Determination of pH

The pH of the mouthwashes was determined using a calibrated pH meter (Mettler Toledo, Switzerland). Determinations were performed three times and an average of these determinations was taken as the pH of the prepared mouthwashes.

Determination of antimicrobial activity of essential oils and mouthwash formulations

Kirby-Bauer disc diffusion method

The Kirby-Bauer disc diffusion method was used to determine the antimicrobial susceptibilities of microorganisms to essential oils. Antimicrobial activities of sage, rosemary, bay, and thyme essential oils were determined against various microorganisms (*Staphylococcus aureus* ATCC 25923*, Staphylococcus epidermidis* ATCC 12228*, Enterococcus faecalis* ATCC 29212*, Bacillus cereus* DSM 4312, *Escherichia coli* ATCC 25922, and *Candida albicans* ATTC 10231). For this purpose, the bacteria were incubated in Brain Heart Infusion Agar (BHI) medium at 37˚C, for 24 hours. *Candida albicans* was incubated in Sabouraud Dextrose Agar (SDA) medium at 30˚C, for 48 hours. After incubation, the microorganisms were adjusted to 0.5 McFarland turbidity standard (10^8 CFU/mL) in 0.85% physiologic saline. The prepared microbial suspension was seeded on the Mueller Hinton Agar (MHA) medium with a swab. Petri dishes were allowed to stand for 15 mins to dry. At the end of the period, aseptic conditions, taking discs prepared from Whatman 42 number filter paper using a pen, 10 µL of essential oil was dropped onto the disks and the disks were placed on the Petri dishes. After placement of the disks, the Petri dishes were allowed to stand for 15 mins, the bacterial specimens were incubated for 24 hours, and the yeast specimens were incubated for 48 hours. After the incubation, the zone diameters around the discs were measured using a scale and recorded, and the results were evaluated. The experiment was performed in double parallel.[11]

Microbroth dilution method

The microbroth dilution method was applied to determine minimum inhibitory concentrations (MIC) and minimum bactericidal concentrations (MBC) of F1 and F2 mouthwashes and essential oil samples. For this purpose, 100 µL double-strength Mueller Hinton Broth medium for antibacterial activity and SDA medium for antifungal activity were added (100 µL) to each well of a 96-well plate. One hundred microliters of the essential oil samples and formulation samples were added and 50% dilutions were made. Subsequently, bacterial specimens (*Staphylococcus aureus* ATCC 25923, *Salmonella typhi* ATCC 14028, *Escherichia coli* ATCC 25922) incubated in BHI medium at 37˚C for 24 hours, and yeast specimen (*Candida albicans* ATTC 10231) incubated in Sabouraud Dextrose Broth medium at 30˚C for 48 hours were adjusted to a 0.5 McFarland turbidity standard (10^8 CFU/mL) in the 0.85% physiologic saline. Microorganism samples adjusted the McFarland turbidity and was added 100 µL to wells. The wells only containing the medium were used as a negative control, and the wells containing the microorganisms and the medium were used as positive controls. After incubation, MICs and minimum cidal concentrations were determined and recorded. The experiment was conducted in double parallel.[12]

RESULTS AND DISCUSSION

In current study, the *Origanum vulgare* L. ssp*. hirtum, Laurus nobilis* L.*, Rosmarinus officinalis* L. and *Salvia fruticosa* Mill. essential oils were collected (Table 1) and mouthwash formulations were prepared according to Table 2. There are studies showing antimicrobial activities of volatile oils obtained from various plants and spices.[26] Essential oils contain different components and therefore the antibacterial effect ratings vary depending on the variety and amount of the compounds. Essential oils have antimicrobial effects on various Gram (+) and Gram (-) bacteria and many other microorganisms. Carvacrol and thymol break down the bacterial membrane thus releasing membrane-related substances from the cell, terpenoids and phenylpropanoids have been reported to reach more internal parts of the cell by penetrating the bacterial wall due to their lipophilic nature. It is known that plant extracts and essential oils have antimicrobial effects on Gram (+) and Gram (-) bacteria, as well as against various fungi.[27]

In a study, Al-Howiriny extracted the essential oil of *Salvia lanigera* and reported that it had a good inhibitory effect against *Mycobacterium smegmatis*, *Candida albicans*, and *Candida vaginalis*.[28] Holley and Patel[29] showed that essential oils obtained from *Coriandrum sativum*, *Cinnamomum zeylanicum*, *Cymbopogon citratus*, *Satureja montana* (Coriander, cinnamon, lemon grass, geysey) were effective against *Aspegillus niger*, *Candida albicans, Rhizopus oligosporus*, and showed that essential oils obtained from *Thymus vulgaris, Pimpinella anisum, Cinnamomum zeylanicum* plants (thyme, anise and cinnamon) had fungicidal activity against *Aspergillus flavus, Aspargillus parasiticus, Aspergillus ochraceus,* and *Fusarium moniliforme*. Also, they showed that thyme essential oil was fungi toxic. This effect was thought to be due to the hydrogen bonds formed between the hydroxyl groups of phenolic compounds in the volatile oil composition and the active part of the target enzymes.[30] Another study showed that the essential oil obtained from *Rosmarinus officinalis* were effective against *Staphylococcus aureus, Salmonella typhi, Escherichia coli,* and *Pseudomonas aeruginosa*.[31]

For many centuries, plants have been used to provide food flavor and aroma, to extend the shelf-life of foods, and to treat diseases. The antimicrobial effects of plants that have been used for many years as traditional medicine have been investigated from the beginning of the 20th century. Due to the increase in antibiotic resistant infections in recent years, there is a growing interest in natural compounds and essential oils obtained from plants in particular.[7,32] In this study, the *Origanum vulgare* L. ssp. *hirtum, Laurus nobilis* L., *Rosmarinus officinalis* L. and *Salvia fruticosa* Mill. essential oils were collected and used to prepare mouthwash formulations. Flavors are added to the formulas to improve consumer acceptability of the mouthwash ingredients. In this study, saccharine sodium was used as a sweetener. Sodium bicarbonate was used the F1 and F2 formulations. Several studies have shown that bicarbonate is one of the salivary components that potentially modify the formation of caries. It increases the pH in saliva, and in this way, creates a hostile environment for the growth of aciduric bacteria. Sodium bicarbonate can also change the virulence of the bacteria that cause tooth decay. Animal studies have shown that dentifrices containing sodium bicarbonate reduce the amounts of both *Streptococcus sobrinus* and *Streptococcus mutans*, and this may reduce caries. Studies on humans showed a statistical reduction in the number of mutant streptococci. Sodium bicarbonate can also prevent caries by reducing enamel solubility and increase remineralization of enamel.[33]

Antimicrobial activities of essential oil samples were determined by disc diffusion assays. Furthermore, the antimicrobial activities of the F1 and F2 mouthwashes and essential oil samples were determined using microbroth dilutions. The antimicrobial activities of the tested samples against various microorganisms (*Staphylococcus aureus* ATCC 25923, *Streptococcus epidermidis* ATCC 12228, *Enterococcus faecalis* ATCC 29212, *Bacillus cereus* DSM 4312, *Escherichia coli* ATCC 25922 and *Candida albicans* ATTC 10231) are given in Table 3. According to these results, the diameters of the zones ranged between 7 and 59 mm (Table 3).

Bacillus sp., *Enterococcus* sp., *Salmonella* sp., *Staphylococcus* sp., *Streptococcus* sp., and *Candida* sp. are found in the oral microbiome. Therefore, we worked with these bacteria in our study.[34,35]

Origanum vulgare L. ssp. *hirtum* essential oil had the largest inhibition zone (59 mm) on *Candida albicans* ATTC 10231 and *Salvia fruticosa* Mill. essential oil had the smallest inhibition zone (7 mm) on *Staphylococcus aureus* ATCC 25923 and *Bacillus cereus* DSM 4312; *Rosmarinus officinalis* essential oil had the

Table 1. Plant materials and plant registration numbers

Turkish name	Latin name	Plant registration numbers
Kekik	*Origanum vulgare* subsp. *hirtum*	BK 1001
Defne	*Laurus nobilis* L.	BK 1002
Biberiye	*Rosmarinus officinalis* L.	BK 1003
Adaçayı	*Salvia fruticosa* Mill.	BK 1004

Table 2. Amount of Ingredients used to prepare 10 mL of mouthwash formulations (F1 and F2)

Ingredient/mouthwash formulations		F1	F2	Blank formulation
Essential oil	***Origanum vulgare* subsp. *hirtum***	2%	1%	-
	Salvia fruticosa	2%	1%	-
	Rosmarinus officinalis	4%	2%	-
	Laurus nobilis	1%	0.5%	-
NaCl		0.1%	0.1%	0.1%
$NaHCO_3$		0.05%	0.05%	0.05%
Sodium saccharine		0.01%	0.001%	0.001%
Ethyl alcohol		60%	60%	60%
Distilled water		q.s.10 mL	q.s.10 mL	q.s.10 mL

Table 3. Determination of antimicrobial activity using disc diffusion. Values are given in millimeters

Microorganism/plants	*S. aureus* ATCC 25923	*S. epidermidis* ATCC 12228	*E. faecalis* ATCC 29212	*B. cereus* DSM 4312	*E. coli* ATCC 25922	*C. albicans* ATTC 10231
O. vulgare* subsp. *hirtum	43	37	21	37	39	59
S. fruticosa	7	-	-	7	9	-
R. officinalis	7	9	-	9	9	9
L. nobilis	13	9		9	11	9

smallest inhibition zone (7 mm) on *Staphylococcus aureus* ATCC 25923. As a result of the study, the essential oil obtained from *Origanum vulgare* subsp. *hirtum* showed the largest zone diameter in the tested microorganisms (Table 3).

The antimicrobial activity results determined using microbroth dilutions against various microorganisms (*Staphylococcus aureus* ATCC 25923, *Salmonella typhi* ATCC 14028, *Escherichia coli* ATCC 25922 and *Candida albicans* ATTC 10231) are given in Table 4. According to these results, the static and cidal activity was generally 50% and more than 50% when pure essential oil samples were applied on microorganism specimens. the MIC of the essential oil *Salvia fruticosa* Mill. was registered as 6.25% on *Escherichia coli* ATCC 25922 and *Salmonella typhi* ATCC 14028.

Formulation F1 contained 9.0% of essential oil and it was observed that the MIC and bactericidal concentration were 25% on *Escherichia coli* ATCC 25922 and *Salmonella typhi* ATCC 14028, 50% on *Staphylococcus aureus* ATCC 25923, and was over 50% on *Candida albicans* ATCC 10231. The F2 formulation contained 4.5% of essential oil in its composition, has been found that was 6.25 % the minimum bactericidal activity on *Staphylococcus aureus* ATCC 25923. Also, the F2 formulation were 3.125% the MIC and MBC on all other microorganisms. The solvent formulation did not exhibit antimicrobial activity (Table 4).

In this study, the antimicrobial effects of essential oils obtained from *Origanum vulgare* L. ssp. *hirtum*, *Salvia fruticosa, Rosmarinus officinalis*, and *Laurus nobilis* by water distillation were investigated on various microorganisms *(Staphylococcus aureus* ATCC 25923, *Staphylococcus epidermidis* ATCC 12228, *Enterococcus faecalis* ATCC 29212, *Bacillus cereus* ATCC DSM 4312, *Escherichia coli* ATCC 25922 and *Candida albicans* ATTC 10231) using the disc diffusion method. According to the results, most of the tested plant materials were observed to have antimicrobial activity against microorganisms. The greatest antimicrobial activity was against *Candida albicans* ATTC 10231 strains by *Origanum vulgare* subsp. *hirtum* essential oil. In addition, the lowest antimicrobial activity was found with *Salvia fruticosa* essential oil against *Staphylococcus aureus* ATCC 25923 and *Bacillus cereus* DSM 4312 bacteria. The lowest antimicrobial activity of *Rosmarinus officinalis* essential oil was against *Staphylococcus aureus* ATCC 25923 bacteria. Accordingly, *Origanum vulgare* subsp. *hirtum* essential oil was detected as having the strongest antimicrobial activity against the tested microorganisms.

According to the results of the microbroth dilution test, the essential oil samples showed antimicrobial activity at a certain rate against the tested microorganisms (*Staphylococcus aureus* ATCC 25923, *Salmonella typhi* ATCC 14028, *Escherichia coli* ATCC 25922, and *Candida albicans* ATTC 10231). The antimicrobial effect that essential oils showed separately on microorganisms was less effective than the mouthwash formulation. The antimicrobial effect of pure essential oil samples applied on microorganisms was lower than in mouthwash formulations; the antimicrobial effect of formulation F2, which contained mixture of essential oils with proportions of 4.5%, was higher than formulation F1, whose essential oils had a proportion of 9%.

CONCLUSIONS

In this study, essential oils and essential oil-containing mouthwashes were successfully prepared. The results obtained by these methods allow us to conclude that the essential oils and prepared F1 and F2 mouthwash formulations exerted activity against the tested microorganisms, which affect the oral cavity. It was also concluded that static and cidal activity on the microorganisms of formulation F2 were markedly higher than in formulation F1. The static and cidal activity was generally 50% and more than 50% when pure essential oil samples were applied on microorganism specimens. Formulation F2, which contained 4.5% essential oils, had a 6.25% minimum bactericidal effect on *Staphylococcus aureus* ATCC 25923 and 3.125% MIC and minimum bactericidal concentration on all other microorganisms.

Formulation F2 contained less essential oil than formulation F1, yet the antibacterial and antifungal effect on the microorganisms of F2 was markedly higher than in F1.

The pH of a formulation is important for patient compliance. The pH of the prepared mouthwashes ranged between 7.37 and 7.63. The pH of the formulations was appropriate for mucosal delivery because they were iso-hydric. This indicated the non-irritancy of the formulation in oral mucosa.

Table 4. Determination of antimicrobial activity using microbroth dilutions

Microorganisms/plants	*E. coli* ATCC25922		*S. typhi* ATCC 14028		*S. aureus* ATCC 25923		*C. albicans* ATCC 10231	
	MIC	MBC	MIC	MBC	MIC	MBC	MIC	MFC
O. vulgare* subsp. *hirtum	>50%	>50%	>50%	>50%	>50%	>50%	>50%	>50%
S. fruticosa	6.25%	>50%	6.25%	>50%	>50%	>50%	>50%	>50%
R. officinalis	50%	50%	50%	50%	>50%	>50%	50%	50%
L. nobilis	50%	50%	50%	50%	>50%	>50%	50%	50%
F1	25%	25%	25%	25%	50%	50%	>50%	>50%
F2	3.125%	3.125%	3.125%	3.125%	3.125%	6.25%	3.125%	3.125%

MIC: Minimum inhibition concentration, MBC: Minimum bactericidal concentration, MFC: Minimum fungicidal concentration

ACKNOWLEDGEMENTS

The authors would like to thank to Emre Şefik Çağlar for assistance during the experiments and Prof. Şükran Kültür and Onur Altınbaşak for identifying plant samples.

Conflict of Interest: No conflict of interest was declared by the authors.

REFERENCES

1. Okpalugo J, Ibrahim K, Inyang US. Toothpaste formulation efficacy in reducing oral flora. Trop J Pharm Res. 2009;8:71-77.
2. Aslani A, Zolfaghari B, Davoodvandi F. Design, formulation and evaluation of an oral gel from Punica granatum flower extract for the treatment of recurrent aphthous stomatitis. Adv Pharm Bull. 2016;6:391-398.
3. Jayana R, Shree BVS, Rao DG, Nagar P. Clinical features, diagnosis and management of oral lichen planus in children. Journal of Dentistry and Oral Bioscience. 2012;3:47-50.
4. Salehi P, Momeni Danaie Sh. Comparison of the antibacterial effects of persica mouthwash with chlorhexidine on Streptococcus mutans in orthodontic patients. DARU Journal of Pharmaceutical Sciences. 2006;14:178-182.
5. Karankı E. Ülkemizde yaygın olarak kullanılan bazı baharatların antimikrobiyal aktivitesinin belirlenmesi. Niğde Üniversitesi Fen Bilimleri Enstitüsü, Yüksek Lisans Tezi, Niğde, 2013.
6. Tisserand R, Young, R. Essential Oil Composition. In: Williamson EM, ed. Essential Oil Safety. Kanada; Elsevier; 2014.
7. Toroğlu S, Dığrak M, Çenet M. Baharat olarak tüketilen *Laurus nobilis* ve *Zingiber officinale* Roscoe bitki uçucu yağlarının antimikrobial aktiviteleri ve antibiyotiklere *in vitro* etkilerinin belirlenmesi. Kahramanmaraş Sütçü İmam Üniversitesi Fen ve Mühendislik Dergisi. 2006;1:20-26.
8. Yamaguti-Sasaki E, Ito LA, Canteli VC, Ushirobira TM, Ueda-Nakamura T, Dias Filho BP, Nakamura CV, de Mello JC. Antioxidant capacity and *in vitro* prevention of dental plaque formation by extracts and condensed tannins of *Paullinia cupana*. Molecules. 2007;12:1950-1963.
9. Ertürk R, Çelik C, Kaygusuz R, Aydın H. Ticari olarak satılan kekik ve nane uçucu yağlarının antimikrobiyal aktiviteleri. Cumhuriyet Tıp Dergisi. 2010;32:281-286.
10. Kaewnopparat S, Dangmanee N, Kaewnopparat N, Srichana, T, Chulasiri M, Settharaksa S. *In vitro* probiotic properties of *Lactobacillus fermentum* SK5 isolated from vagina of a healthy woman. Anaerobe. 2013;22:6-13.
11. Chmit M, Kanaan H, Habib J, Abbass M, Mcheik A, Chokr A. Antibacterial and antibiofilm activities of polysaccharides, essential oil, and fatty oil extracted from *Laurus nobilis* growing in Lebanon. Asian Pac J Trop Med. 2014;7:546-552.
12. Nascimento GGF, Locatelli J, Freitas PC, Silva GL. Antibacterial activity of plant extracts and phytochemicals on antibiotic-resistant bacteria. Braz J Microbiol. 2000;31:247-256.
13. Özcan MM, Chalchat JC. Chemical composition and antifungal activity of rosemary (*Rosmarinus officinalis* L.) oil from Turkey. Int J Food Scie Nutr. 2008;59:691-698.
14. Baytop T. Therapy with medicinal plants in Turkey (Past and Present) Nobel Tıp Press; 2000:13-31.
15. Sahin Başak S, Candan F. Effect of *Laurus nobilis* L. Essential oil and its main components on α-glucosidase and reactive oxygen species scavenging activity. Iran J Pharm Res. 2013;12:367-379.
16. Sayyah M, Saroukhani G, Peirovi A, Kamalinejad M. Analgesic and anti-inflammatory activity of the leaf essential oil of *Laurus nobilis* Linn. Phytother Res. 2003;17:733-736.
17. Lawrence BM. The botanical and chemical aspects of Oregano. Perf Flav. 1984:41-51.
18. Başer KHC, Özek T, Kürkçüoglu M, Tümen G. The essential oil of *Origanum vulgare* subsp. *hirtum* of Turkish origin. Journal of Essential Oil Research. 1994;6:31-36.
19. Akgül A. Spice science and technology. Turkish Association of food Technologists. 1993:3.
20. Özcan MM Figueredo G, Chachat JC, Chalard P, Juhaimi FYA, Ghafoor K, Babiker EE. Chemical constituents in essential oils of *Salvia officinalis* l. and *Salvia fruticosa* Mill. Z Arznei- Gewürzpfl A. 2015;20:181-184.
21. Yaylı N, Uçucu Yağlar ve Tıbbi Kullanımları, 1. İlaç kimyası, Üretimi, Teknolojisi, Standardizasyonu Kongresi, Antalya; Türkiye; 29-31 Mart 2013.
22. Ozdikmenli S, Zorba NN. Uçucu yağların *Staphylococcus aureus* üzerine etkisi. Türk Tarım-Gıda Bilim ve Teknoloji Dergisi. 2014;2:228-235.
23. Burt S. Essential oils: Their antibacterial properties and potential applications in foods- a review. Int J Food Microbiol. 2004;94:223-253.
24. Chen Z, He B, Zhou J, He D, Deng J, Zeng R. Chemical compositions and antibacterial activities of essential oils extracted from *Alpinia guilinensis* against selected foodborne pathogens. Ind Crop Prod. 2016;83:607-613.
25. Allen LV. Ansel's Pharmaceutical dosage forms and drug delivery systems, 9th ed. Wolters Kluwer; 2011:358-371.
26. Çelik E, Çelik YG. Bitki Uçucu Yağlarının Antimikrobiyal Özellikleri. Orlab On-Line MikrobiyolojiDergisi. 2007;5:1-6.
27. Beyaz M. Esansiyel yağlar: Antimikrobiyal, antioksidan ve antimutajenik aktiviteleri. Akademik Gıda Dergisi. 2014;12:45-53.
28. Howiriny TAA. Composition and antimicrobial activity of the essential oil of Salvia lanigera. Pak J Biol Sci. 2003;6:133-135.
29. Holley RA, Patel D. Improvement in shelf-life and safety of perishable foods by plant essential oils and smoke antimicrobials. Food Microbiol. 2005;22:273-292.
30. Evren M, Tekgüler B. Uçucu yağların antimikrobiyel özellikleri. Orlab On-Line Mikrobiyoloji Dergisi. 2011;9:28-40.
31. Barbosa LN, Probst Ida S, Andrade BF, Alves FC, Albano M, da Cunha Mde L, Doyama JT, Rall VL, Fernandes Júnior A. *In vitro* antibacterial and chemical properties of essential oils including native plants from Brazil against pathogenic and resistant bacteria. J Oleo Scie. 2015;64:289-298.
32. Aydın DB. Bazı tıbbi ve baharatların gıda patojenleri üzerine antibakteriyel etkisinin araştırılması. Kafkas Üniversitesi Veteriner Fakültesi Dergisi. 2008;14:83-87.
33. Legier-Vargas K, Mundorff-Strestha SA, Featherstone JBD, Gwinner LM. Effects on sodium bicarbonate dentifrice on the levels of cariogenic bacteria in human saliva. Caries Res. 1995;29:143-147.
34. Wade WG. The oral microbiome in health and disease. Pharmacol Res. 2013;69:137-143.
35. Seville LA, Patterson AJ, Scott KP, Mullany P, Quail MA, Parkhill J, Ready D, Wilson M, Spratt D, Roberts AP. Distribution of Tetracycline and Erythromycin Resistance Genes Among Human Oral and Fecal Metagenomic DNA. Microb Drug Resist. 2009;15:159-166.

Turk J Pharm Sci 2018;15(3):376-381
DOI: 10.4274/tjps.74936

ORIGINAL ARTICLE

Levels of Heavy Metals and Ochratoxin A in Medicinal Plants Commercialized in Turkey

Türkiye'de Satılan Tıbbi Bitkilerde Ağır Metal ve Okratoksin A Seviyeleri

Hakan ÖZDEN[1]*, Sibel ÖZDEN[2]

[1]İstanbul University, Faculty of Science, Department of Biology, Division of Botany, İstanbul, Turkey
[2]İstanbul University, Faculty of Pharmacy, Department of Pharmaceutical Toxicology, İstanbul, Turkey

ABSTRACT

Objectives: The aim of this study was to determine the levels of Pb, Cd, and OTA in frequently used medicinal plants.

Materials and Methods: Twenty-one samples of linden, chamomile, and sage were obtained during the spring and summer period of 2016 from local markets and traditional bazaars in İstanbul, Turkey. Microwave-assisted digestion was applied for the preparation of the samples and the ICP-OES was used for the determination of Pb and Cd. Determination of OTA was performed using HPLC-FLD after immunoaffinity column clean-up.

Results: OTA was detected in only one chamomile sample with a low concentration level of 0.034 µg/kg. According to the results of ICP-OES analysis, Pb in the concentration range of 4.125-6.487 mg/kg, 3.123-5.769 mg/kg and 3.229-5.985 mg/kg and Cd in the concentration range of 0.324-0.524 mg/kg, 0.365-0.51 mg/kg and 0.321-0.474 mg/kg was found in linden, chamomile, and sage teas, respectively.

Conclusion: We indicated that levels of Pb and OTA were found below the maximum permissible level whereas high levels of Cd were observed in medicinal plants, which may not pose a health risk for consumers according to the exposure assessment. However, it is suggested that other mycotoxins and heavy metal contents should be carefully considered in medicinal plants.

Key words: Lead, cadmium, OTA, linden, chamomile, sage

ÖZ

Amaç: Bu çalışmanın amacı, sıklıkla kullanılan tıbbi bitkilerde Pb, Cd ve OTA seviyelerinin araştırılmasıdır.

Gereç ve Yöntemler: Toplam 21 adet ıhlamur, papatya ve adaçayı örnekleri 2016 yılının bahar ve yaz aylarında İstanbul Türkiye'de geleneksel pazar ve marketlerden satın alındı. Örnekler mikrodalga parçalama yöntemi uygulanarak hazırlandı ve kurşun ve kadmiyum analizi ICP-OES cihazı kullanılarak gerçekleştirildi. OTA tayini immünoafinite kolonu ile temizlemenin ardından HPLC-FLD ile gerçekleştirildi.

Bulgular: OTA sadece 1 adet papatya örneğinde düşük konsantrasyonda (0.034 µg/kg) tayin edildi. ICP-OES analizi sonuçlarına göre; ıhlamur, papatya ve adaçayı örneklerinde sırasıyla kurşun 4.125-6.487 mg/kg, 3.123-5.769 mg/kg ve 3.229-5.985 mg/kg konsantrasyon aralığında; kadmiyum 0.324-0.524 mg/kg, 0.365-0.51 ve mg/kg 0.321-0.474 mg/kg konsantrasyon aralığında bulundu.

Sonuç: Tıbbi bitkilerde Pb ve OTA seviyeleri maksimum izin verilen seviyelerin altında bulunmuş olup, yüksek seviyelerde bulunan Cd seviyelerinin yapılan maruziyet değerlendirmesine göre tüketici sağlığında risk oluşturmayacağı gösterilmektedir. Bununla birlikte, tıbbi bitkilerde diğer mikotoksinler ve ağır metal seviyelerinin dikkatle izlenmesi gerektiği önerilmektedir.

Anahtar kelimeler: Kurşun, kadmiyum, OTA, ıhlamur, papatya, adaçayı

INTRODUCTION

Herbs play an important role in various traditional medicine and recently they are increasingly being used in primary health care interventions. However, there has been increasing concern over the safety and toxicity of natural herbs. Similar to agricultural products, herbs may be subjected to natural and chemical contamination during one or more stages of the supply chain. Medicinal plants are naturally contaminated with mycotoxins during the harvesting, storage, and distribution of these products. Besides, herbs may be subjected to chemical residues from heavy metals.

*Correspondence: E-mail: ozdenh@istanbul.edu.tr, Phone: +90 532 355 88 59 ORCID-ID: orcid.org/0000-0001-7084-3829
Received: 04.09.2017, Accepted: 26.10.2017

Ochratoxin A (OTA) is a toxic secondary metabolite, mainly produced by several *Aspergillus* and *Penicillium* species under diverse environmental conditions. OTA has received increased attention worldwide due to the deleterious effects to health of humans and animals.[1,2] OTA can be found as a natural contaminant in a variety of foods including cereals, wine, grapes and its products, dried fruits, cacao, coffee, and spices.[2]

Some heavy metals, particularly arsenic (As), lead (Pb), cadmium (Cd), and mercury (Hg) have no biologic roles in living organisms and contaminate environments. Many of these metals have toxic effects and cause developmental disorders. Due to their widespread occurrence, toxicity, and persistence in the environment, they should be considered as a potential hazardous threat to human health and crop plants.

Control of chemical hazards in herbs during the food chain is important for quality control and protection of human health. Food safety authorities are responsible for checking product compliance with the legal limits. So far, there has been very little published information on the occurrence of heavy metals and OTA in medicinal plants in Turkey.[3-10] Data are needed to assess the contamination of heavy metals and OTA in widely-consumed medicinal plants and to estimate the exposure to the Turkish population. Therefore, the aim of the present study was to investigate the contamination of Pd, Cd, and OTA in selected medicinal plants such as linden, sage, and chamomile, which are widely consumed in Turkey and exported worldwide, and to evaluate their potential risk to humans. The results of this study would contribute to pollution control and the risk management of heavy metals and OTA in medicinal plants.

MATERIALS AND METHODS

Chemicals

Ultrapure water was used in all experiments obtained using a Milli-Q system (Millipore, Bedford, MA, USA). Analytical grade chemicals were obtained from Merck (Darmstadt, Germany) and Riedel-de Haën (Seelze, Germany).

The metal standard solutions of Cd and Pb for the calibration curves were prepared by diluting a stock solution of 1000 µg/mL, which was obtained from VHG labs (Manchester, NH, USA). All plastics and glassware were properly cleaned by soaking them in 2 M nitric acid and rinsed thoroughly with deionized water prior to use.

For OTA analysis, high-performance liquid chromatography (HPLC) standard solutions in the final concentrations ranges from 0.03 to 10 µg/kg, which are equivalent to 1 g medicinal plant samples, were prepared in methanol:water (1:1, v/v) by serial diluting the stock standard solution of OTA (50 ng/µL in benzene:acetic acid; 99:1, v/v) which was obtained from Supelco (Cat. no: 46912). Phosphate-buffered saline (PBS), pH 7.4, for the extraction in the OTA analysis was prepared as previously described.[11]

Sample collection

A total of 21 unpacked samples of linden (n=7), chamomile (n=7), and sage (n=7) were collected randomly in April and July 2016 from traditional bazaars in Istanbul, Turkey. Some of the studied characteristics of the medicinal plants are given in Table 1. The taxonomic identity of each botanical samples was confirmed by the Department of Botany, Science Faculty, İstanbul University. The dried materials were ground using a Waring Blender (Conair Corp., Stamford, CT, USA) and the ground samples were sealed in plastic packages and kept at room temperature until they were analyzed.

Pd and Cd analysis in medicinal plants

Dried and homogenized medicinal plant materials were weighed as 0.1-0.3 g and placed in Teflon containers (DAP 60, Berghof instruments GmbH, Eningen, Germany). The plant material was wet-digested with 8 mL of 65% nitric acid in a microwave oven (150-190˚C) (Berghof MWS-4 device, Berghof instruments GmbH, Eningen, Germany). After the digestion procedure, the Teflon containers were allowed to cool and the suspensions were diluted with deionized water to 25 mL. The material was passed through syringe-type filters (Chromafil PET-45/25, Macheerey Nagel GmbH, Düren, Germany), and they were then ready for measurement. Samples were run on an inductively-coupled plasma with optical emission spectrometry (Pelkin Elmer Optima 7000 DV, Waltham, MA, USA) for analysis on two different elements of Pb (k: 220,353 nm) and Cd (k: 214,440 nm).[12,13] Measurements were performed in triplicate and the mean value was calculated on a dry weight basis (mg/kg, dw). Standard calibration curves were constructed at concentrations of 0.25; 0.5; 1; 2; 3; 5 mg/kg for Cd and 0.4; 1; 2; 3; 5; 10 mg/kg for Pb. Blanks were also run with standard solutions and all samples were checked for any loss and cross-contamination.

OTA analysis in medicinal plants

Sample extraction and immunoaffinity clean-up

The immunoaffinity columns (OchraTest™) were purchased from VICAM (Watertown, MA, USA). Medicinal plants were extracted according to Trucksess et al.[14] with some modifications. In a 20-mL centrifuge tube, 5 g of sample, 1 g of NaCl, and 25 mL of methanol (0.5%) $NaHCO_3$ (70:30, v/v) solution were added and mixed on a vortex mixer. Then, the mixture was shaken at 400 rpm for 15 min and centrifuged at 3000 rpm for 15 min. Five milliliters of the supernatant was diluted with 20 mL PBS buffer containing 1% Tween 20. The diluted extract was centrifuged at 3000 rpm for 15 min. Afterwards, 20 mL of the supernatant (20 mL=1 g sample equivalent) was passed through an OchraTest™ immunoaffinity column at a flow rate of 1 drop/second until air came through the column. The column was washed with 10 mL of PBS buffer containing 1% Tween 20 and 10 mL of purified water, and dried under vacuum. OTA was eluted by passing 1.5 mL of methanol through the column and the eluate was then diluted with 1.5 mL of purified water. One hundred microliters of the aliquot was injected into an HPLC analyzer equipped with fluorescence detection (FLD).

HPLC-FLD analysis and method validation

The chromatographic analysis was performed as previously described using an LC-20A Shimadzu (Kyoto, Japan) liquid chromatographic system coupled with an RF-10A XL FLD.[11]

Confirmation of OTA in positive samples was achived following the method of Zimmerli and Dick[15] by formation of the methyl ester derivative.

Validation of the method was performed according to our previous paper.[11] In the present study, we established the calibration curve with six levels of OTA in the range of 0.03-10 µg/kg. Recovery experiments and precision analysis of the method were performed on OTA-free blank medicinal plant samples by spiking with the OTA standard solutions in order to obtain final concentrations of 0.5 and 1 µg/kg.

RESULTS AND DISCUSSION

Pb and Cd levels in medicinal plants

Linearity was assessed using Cd (0.25-5 mg/kg) and Pb (0.4-10 mg/kg) calibration curves at the six concentrations with a correlation coefficient r^2=0.9987 and 0.9926, respectively. For the instrumental sensitivity, the limit of detections (LOD; signal-to noise ratio=3) were obtained as 0.013 and 0.13 mg/kg and the limit of quantifications (LOQ; signal-to-noise ratio=10) were 0.039 and 0.39 mg/kg of Cd and Pb, respectively for each matrix.

We analyzed 21 medicinal plants including linden (n=7), chamomile (n=7) and sage (n=7) unpacked samples collected from traditional bazaars in Istanbul. As shown in Table 2, the medicinal plants contained Cd and Pb in the following concentration range of 0.321-0.524 mg/kg and 3.123-6.487 mg/kg, respectively. Cd levels exceeded the maximum permissible level (0.3 mg/kg) in all medicinal plants; however, Pb levels were lower than the maximum permissible level (10 mg/kg) set by the Food and Agriculture Organization and World Health Organisation for medicinal plants.[16] A number of studies have been conducted to determine the contamination of heavy metals in spices and botanicals. The available data on the contamination of heavy metals in analyzed medicinal plants in Turkey are summarized in Table 3. Our results are consistent with the study from Ozcan and Akbulut[5] who reported that Cd was found in the concentration range of 0.61-1.05 mg/kg, which exceeded the maximum permissible level in medicinal plants,

Table 1. Some characteristics of the studied medicinal plants

Common name	Scientific name	Turkish name	Used part	Origin
Linden	*Tilia argentea*	Ihlamur	Dried inflorescence	Anatolia
Chamomile	*Anthemis cretica* subsp *anatolica*	Papatya	Leaf and flowers	Anatolia
Sage	*Salvia fructicosa*	Adaçayı	Leaf	Anatolia

Table 3. Available data on the contamination of heavy metals in analyzed medicinal plants in Turkey

Sample	Cd (mg/kg)	Pb (mg/kg)	Reference
Sage	-	0.51	Ozcan[3]
Chamomile	0.44	0.72	Başgel and Erdemoğlu[4]
Linden	n.d.	0.26	
Sage	n.d.	1.14	
Chamomile	1.05	2.73	Ozcan and Akbulut[5]
Lime flower	0.66	0.43	
Sage (*S. aucheri*)	0.79	1.24	
Sage (*S. fructicosa*)	0.61	0.46	
Linden	<LOD (0.025)		Sekeroglu et al.[6]
Chamomile	0.126		
Chamomile (*Matricaria chamomilla*)	0.12	0.12	Leblebici et al.[7]
Linden (*Tilia platyphyllos*)	0.02	0.12	
Sage (*Salvia officinalis*)	0.04	1.36	
Chamomile	0.14	0.07	Bilgic Alkaya et al.[8]
Linden	0.16	0.11	
Sage	0.16	0.16	
Linden	4.35	n.d.	Tercan et al.[9]
Sage	n.d.	n.d.	
Sage (*Salvia officinalis* L.)	0.17	0.039	Ozyigit et al.[10]

n.d.: Not detected, Pb: Lead, Cd: Cadmium, LOD: Limit of detections

Table 2. Contamination of heavy metals in the analyzed medicinal plants

Medicinal plant	No. of samples	No. of samples with heavy level	Range of contamination (mg/kg)		Mean of contamination (mg/kg) ± SD*	
			Cd	Pb	Cd	Pb
Linden	7	7	0.324-0.524	4.125-6.487	0.395±0.08	4.357±1.11
Chamomile	7	7	0.365-0.51	3.123-5.769	0.422±0.04	4.374±0.77
Sage	7	7	0.321-0.474	3.229-5.985	0.423±0.05	4.43±0.81

*SD: Standard deviation, Pb: Lead, Cd: Cadmium

whereas Pb was found in the concentration range of 0.43-2.73 mg/kg, which is below the maximum permissible level. In contrast, Bilgic Alkaya et al.[8] detected Cd and Pb at low levels (<0.16 mg/kg for Cd and <1.36 mg/kg for Pb) in medicinal plants.

The results of worldwide studies in the analyzed medicinal plants are summarized in Table 4. In the United Arab Emirates, Dghaim et al.[24] showed that 55% of chamomile samples contained Cd (0.82 mg/kg) above the maximum level (0.3 mg/kg).[16] Dghaim et al.[24] also reported that 44% of chamomile samples contained Pb (5.37-11.40 mg/kg) and 100% of sage samples contained Pb (12.66-21.76 mg/kg) above the maximum permissible level (10 mg/kg).[16]

Table 4. Available data on the contamination of heavy metals in analyzed medicinal plants around the world

Sample	Cd (mg/kg)	Pb (mg/kg)	Reference
Chamomile (packed sample)	0.094	0.242	Abou-Arab et al.[17]
Chamomile (non-packed sample)	0.211	0.308	
Linden blossom	0.088	0.096	
Linden blossom	0.141	0.121	
Chamomile	1.3	6.19	Abou-Arab and Abou Donia[18]
Sage (*Saliva officinalis*)	0.01	0.8	Chizzola et al.[19]
Matricaria recutita	0.23	0.31	
Chamomile	0.05	1.34	Dogheim et al.[20]
Chamomile (*Matricaria chamomilla*)	0.017	0.128	Alwakeel[21]
Sage	0.017	0.134	
Sage (*Saliva officinalis*)	n.d. (<0.002)	n.d. (<0.05)	Darwish[22]
Lime	0.36	2.30	Nordin and Selamat[23]
Musk lime	1.22	2.44	
Chamomile	0.82	5.37-11.40	Dghaim et al.[24]
Sage	0.88	12.66-21.76	
Chamomile blossom	0.22	0.62	Mirosławski and Paukszto[25]

n.d.: Not detected, Pb: Lead, Cd: Cadmium

The European Food Safety Authority (EFSA)[26] established that the tolerable weekly intake for Cd was 2.5 µg/kg bw per week. We calculated the weekly intake of Cd (µg/kg bw per week) considering the mean daily consumption of teas as 2.3 g for Middle Eastern (GEMS/Food Regional Diets)[27] for an adult with a mean body weight of 70 kg and the maximum level of Cd (0.524 mg/kg) found in the linden samples. Accordingly, the highest value for the estimated human weekly Cd intake in this study is 0.121 µg/kg per week, thus representing 4.82% of the tolerable weekly intake as established by EFSA.[26]

OTA in medicinal plants

For the method validation, linearity was assessed using an OTA calibration curve at the six concentrations (0.03-10 µg/kg) with a correlation coefficient r^2=0.9998. LOD was obtained as 0.01 µg/kg and the LOQ level was 0.03 µg/kg of OTA for each matrix. The extraction recoveries are presented in Table 5. The average recoveries at the concentrations of 0.5 and 1 µg/kg were 98.9-87.3%, 99.8-98.9%, and 97.6-92.4% for linden, chamomile and sage, respectively, with a relative standard deviation less than 9.6%.

As shown in Table 6, OTA was determined in only one chamomile sample at a concentration of 0.34 µg/kg. OTA was detected in two chamomile samples and one linden sample under the LOQ level (0.03 µg/kg). We found very low levels of OTA in linden, chamomile, and sage plants under the limit of 15 µg/kg for spices regulated by European Commission (EU)[28] and the Turkish Ministry of Agriculture and Rural Affairs (Turkish Food Codex Legislation 2011/28157).[29]

Table 5. Recovery data for OTA in medicinal plants (n=4)

	Spiking level (mg/kg)	Recovery (%, mean ± SD)	RSDr (%)
Linden	0.5	98.9±4.8	4.8
	1	87.3±5.5	6.4
Chamomile	0.5	99.8±2.2	2.2
	1	98.9±7.7	7.7
Sage	0.5	97.6±0.9	0.9
	1	92.4±8.9	9.6

SD: Standard deviation, RSDr: Relative standard deviation, OTA: Ochratoxin A

Table 6. Occurrence of OTA in the analyzed medicinal plants

Medicinal plants	No. of samples	No. of samples with OTA level (%)[a]			Range of contamination (µg/kg)	Mean of contamination[b] (µg/kg)
		<LOD	LOD-LOQ	>LOQ		
Linden	7	6 (85.7%)	1 (14.3%)	-	-	-
Chamomile	7	4 (57.1%)	2 (28.6%)	1 (14.3%)	0.034	0.034
Sage	7	7 (100%)	-	-	-	-

[a]Percentage of contamination. [b]Mean contamination of positive samples, LOD: Limit of detections, LOQ: Limit of quantifications, OTA: Ochratoxin A

To our knowledge, there are no studies on the occurrence of OTA in medicinal herbs including linden, chamomile, and sage in Turkey. Only one study in Turkey from Tosun and Arslan[30] reported that Aflatoxin B1 was determined in linden (60%), chamomile (100%), and sage (100%), with mean concentrations of 14 µg/kg, 28.7 µg/kg, and 8.9 µg/kg, respectively, and some medicinal plants were found to be contaminated with AFB1 above the EU limits of 5 µg/kg for AFB1 and 10 µg/kg for total aflatoxins in spices in 2010.[31] Omurtag and Yazicioğlu[32] presented fumonisin b1 (FB1) and fumonisin b2 (FB2) levels in medicinal plants and they showed no contamination of FB1 and FB2 in linden, chamomile, and sage medicinal plants.

A few studies have reported the contamination of OTA in linden, chamomile, and sage plants. Halt[33] reported that trace amounts of OTA were detected in medicinal plant materials from *Tilia grandifolia*. Aziz et al.[34] found no OTA in lime tree and chamomile medicinal plants. Santos et al.[35] found that chamomile and sage were contaminated with OTA at concentrations of 0.8-1 µg/kg and 1.1-17.3 µg/kg, respectively.

CONCLUSIONS

In summary, Cd and Pb were detected in the range of 0.321-0.524 mg/kg and 3.123-6.487 mg/kg, respectively. Pb levels were found below the maximum permissible level, whereas high levels of Cd were observed in medicinal plants. According to the exposure assessment for Cd, consumption of the medicinal plants does not represent a threat to human health. Occurrence of OTA contamination in medicinal plants from local bazaars in İstanbul was observed for the first time and OTA was determined in only one chamomile sample (0.34 µg/kg). Although herbs are open to contamination with variable amounts of mycotoxins, we observed the contamination levels of OTA in the studied medicinal plants to be very low. However, further studies covering larger numbers of samples that include other types of medicinal plants in open markets are needed to carefully consider the contamination of other mycotoxins and heavy metals.

ACKNOWLEDGEMENTS

This work was supported by the Research Fund of İstanbul University (project number: BYP-2016-22698). The authors would also like to thank Merve Saman for excellent technical assistance for the extraction of the samples in OTA analysis during the internship period.

Conflict of interest: No conflict of interest was declared by the authors.

REFERENCES

1. European Food Safety Authority (EFSA). 2006. Opinion of the scientific panel on the contaminants in the food chain on a request from the commission related to ochratoxin A in food. EFSA J. 2006;365:1-56.
2. Joint FAO/WHO Expert Committee of Food Additives (JECFA). In the Ochratoxin A paragraph in "Safety evaluations of specific mycotoxins". Prepared by the fifty-sixth meeting of the Joint FAO/WHO Expert Committee on Food Additives; 6-15 Feb; Geneva (Switzerland); 2001.
3. Ozcan M. Mineral contents of some plants used as condiments in Turkey. Food Chem. 2004;84:437-440.
4. Başgel S, Erdemoğlu SB. Determination of mineral and trace elements in some medicinal herbs and their infusions consumed in Turkey. Sci Total Environ. 2006;359:82-89.
5. Ozcan MM, Akbulut M. Estimation of Minerals, Nitrate and Nitrite Contents of Medicinal and Aromatic Plants Used as Spices, Condiments and Herbal Tea. Food Chem. 2007;106:852-858.
6. Sekeroglu N, Ozkutlu F, Kara SM, Ozguven M. Determination of cadmium and selected micronutrients in commonly used and traded medicinal plants in Turkey. J Sci Food Agric. 2008;88:86-90.
7. Leblebici S, Bahtiyar SD, Ozyurt MS. Kütahya aktarlarında satılan bazi tibbi bitkilerin ağır metal miktarlarının incelenmesi. J Institut Sci Technol Dumlupinar University. 2012:1-6.
8. Bilgic Alkaya D, Karaderi S, Erdoğan G, Kurt Cücü A. İstanbul aktarlarında satılan bitkisel çaylarda ağir metal tayini. Marmara Pharm J. 2015;19:136-140.
9. Tercan HS, Ayanoglu F, Bahadirli NP. Determination of Heavy Metal Contents and Some Basic Aspects of Widely Used Herbal Teas in Turkey. Rev Chim. 2016;67:1019-1022.
10. Ozyigit II, Yalcin B, Turan S, Saracoglu IA, Karadeniz S, Yalcin IE, Demir G. Investigation of Heavy Metal Level and Mineral Nutrient Status in Widely Used Medicinal Plants' Leaves in Turkey: Insights into Health Implications. Biol Trace Elem Res. 2018;182:387-406.
11. Tosun A, Ozden S. Ochratoxin A in red pepper flakes commercialised in Turkey. Food Addit Contam Part B Surveill. 2016;9:46-50.
12. Baycu G, Tolunay D, Ozden H, Gunebakan S. Ecophysiological and seasonal variations in Cd, Pb, Zn, and Ni concentrations in the leaves of urban deciduous trees in Istanbul. Environ Pollut. 2006;143:545-554.
13. Sastre J, Sahuquillo A, Vidal M, Rauret G. Determination of Cd, Cu, Pb, and Zn in environmental samples: microwave assisted total digestion versus aqua regia and nitric acid extraction. Anal Chim Acta. 2002;462:59-72.
14. Trucksess MW, Weaver CM, Oles CJ, Fry FS Jr, Noonan GO, Betz JM, Rader JI. Determination of aflatoxins B1, B2, G1, and G2 and ochratoxin A in ginseng and ginger by multitoxin immunoaffinity column cleanup and liquid chromatographic quantitation: collaborative study. J AOAC Int. 2008;91:511-523.
15. Zimmerli B, Dick R. Determination of ochratoxin A at the ppt level in human blood, serum, milk and some foodstuffs by high-performance liquid chromatography with enhanced fluorescence detection and immunoaffinity column cleanup: methodology and Swiss data. J Chromatogr B Biomed Appl. 1995;666:85-99.
16. World Health Organization (WHO). WHO Guidelines for Assessing Quality of Herbal Medicines with Reference to Contaminants and Residues. World Health Organization, Geneva; 2007.
17. Abou-Arab AAK, Soliman Kawther M, Tantawy MEEI, Ismail Badeaa R, Khayria N. Quantity estimation of some contaminants in commonly used medicinal plants in the Egyptian market. Food Chem. 1999;67:357-363.
18. Abou-Arab AAK, Abou Donia MA. Heavy Metals in Egyptian Spices and Medicinal Plants and the Effect of Processing on Their Levels. J Agric Food Chem. 2000;48:2300-2304.
19. Chizzola R, Michitsch H, Franz C. Monitoring of metallic micronutrients and heavy metals in herbs, spices and medicinal plants from Austria. Eur Food Res Technol. 2003;216:407-411.

20. Dogheim SM, Ashraf el MM, Alla SA, Khorshid MA, Fahmy SM. Pesticides and heavy metals levels in Egyptian leafy vegetables and some aromatic medicinal plants. Food Add Contam. 2004;21:323-330.

21. Alwakeel SS. Microbial and heavy metals contamination of herbal medicines. Res J Microbiol. 2008;3:683-691.

22. Darwish MA. Essential Oils Yield and Heavy Metals Content of Some Aromatic Medicinal Plants Grown in Ash-Shoubak Region, South of Jordan. Adv Environ Biol. 2009;3:296-301.

23. Nordin N, Selamat J. Heavy metals in spices and herbs from wholesale markets in Malaysia. Food Addit Contam: Part B Surveill. 2013;6:36-41.

24. Dghaim R, Al Khatib S, Rasool H, Ali Khan M. Determination of heavy metals concentration in traditional herbs commonly consumed in the United Arab Emirates. J Environ Public Health. 2015:973878.

25. Mirosławski J, Paukszto A. Determination of the Cadmium, Chromium, Nickel, and Lead Ions Relays in Selected Polish Medicinal Plants and Their Infusion. Biol Trace Elem Res. 2018;182:147-151.

26. EFSA Panel on Contaminants in the Food Chain (EFSA CONTAM Panel). Scientific opinion on tolerable weekly intake for cadmium. EFSA J. 2011;9:1975.

27. GEMS/ Food Regional Diets (revised). Regional per capita consumption of raw and semi-processed agricultural commodities. Geneva: Food Safety Department, World Health Organization; 2003.

28. European Commission (EC). Commission Regulation (EC) No 105/2010 of 5 February 2010 amending Regulation (EC) No 1881/2006 setting maximum levels for certain contaminants in foodstuffs as regards ochratoxin A. Off J Eur Union. 2010;35:7-8.

29. Turkish Food Codex Legislation. Turkish Republic of Official Gazette. 29.12.2011- 28157; Legislation Number: 5996. Turkish Food Codex Legislation of Food Contaminants. Ankara (Turkey): Prime Ministry Press; 2011.

30. Tosun H, Arslan R. Determination of Aflatoxin B1 Levels in Organic Spices and Herbs. ScientificWorldJournal. 2013;2013:874093.

31. European Commission (EC). Commission Regulation (EC) No 165/2010 of 26 February 2010 amending Regulation (EC) No 1881/2006 setting maximum levels for certain contaminants in foodstuffs as regards aflatoxins. Off J Eur Union L. 2010;50:8-12.

32. Omurtag GZ, Yazicioğlu D. Determination of Fumonisins B1 and B2 in herbal tea and medicinal plants in Turkey by high-performance liquid chromatography. J Food Prot. 2004;67:1782-1786.

33. Halt M. Moulds and mycotoxins in herb tea and medicinal plants. Eur J Epidemiol. 1998;14:269-274.

34. Aziz NH, Youssef YA, El-Fouly MZ, Moussa LA. Contamination of some common medicinal plant samples and spices by fungi and their mycotoxins. Bot Bull Acad Sin. 1998;39:279-285.

35. Santos L, Marin S, Sanchis V, Ramos AJ. Screening ofmycotoxin multicontamination in medicinal and aromatic herbs sampled in Spain. J Sci Food Agric. 2009;89:1802-1807.

Turk J Pharm Sci 2018;15(3):382-385
DOI: 10.4274/tjps.88700

ORIGINAL ARTICLE

Phytotoxicity, Toxicity on Brine Shrimp and Insecticidal Effect of *Chrysophthalmum gueneri* Aytac & Anderb. Growing in Turkey

Türkiye'de Yetişen *Chrysophthalmum gueneri* Aytac & Anderb.'in Fitotoksisitesi, Tuzlu Su Karidesi Üzerine Toksisitesi ve İnsektisidal Etkisi

Fatma AYAZ[1], Nurgün KÜÇÜKBOYACI[2]*, Barış BANİ[3], Bilge ŞENER[2], Muhammad Iqbal CHOUDHARY[4]

[1]Selçuk University, Faculty of Pharmacy, Department of Pharmacognosy, Konya, Turkey
[2]Gazi University, Faculty of Pharmacy, Department of Pharmacognosy, Ankara, Turkey
[3]Kastamonu University, Faculty of Arts and Science, Department of Biology, Kastamonu, Turkey
[4]University of Karachi, International Center for Chemical and Biological Sciences, Karachi, Pakistan

ABSTRACT

Objectives: The aim of this study was to investigate the probable toxicity on brine shrimp, phytotoxicity, and insecticidal activity of *Chrysophthalmum gueneri* Aytac & Anderb.

Materials and Methods: The MeOH (80%) extract obtained from the whole plant of *C. gueneri* was fractionated through subsequent solvent extractions in increasing polarity with *n*-hexane, chloroform, and *n*-butanol. The MeOH (80%) extract and all fractions of *C. gueneri* were evaluated for their biologic activities using *in vitro* screening bioassays such as brine shrimp lethality test and phytotoxicity against *Lemna minor*, as well as insecticidal activity against *Rhyzopertha dominica* and *Tribolium castaneum*.

Results: The findings showed that the *n*-hexane and chloroform fractions of the plant had significant phytotoxic activities with 100% growth inhibition (GI) at 1000 µg/mL against *L. minor*. Moreover, the MeOH (80%) extract (53% GI) and *n*-butanol fraction (46.6% GI) of the plant had moderate phytotoxic activities at 1000 µg/mL. Otherwise, no samples had toxicity on the brine shrimps. In addition, the remaining water fraction had low insecticidal activity with 20% mortality against *T. castaneum*.

Conclusion: Our results show that the *n*-hexane and chloroform fractions of *C. gueneri* had potential phytotoxic effects.

Key words: *Chrysophthalmum gueneri*, Asteraceae, brine shrimp lethality, phytotoxicity, insecticidal activity

ÖZ

Amaç: Bu çalışmanın amacı, *Chrysophthalmum gueneri* Aytac & Anderb.'in tuzlu su karidesi üzerine olası toksisite, fitotoksisite ve insektisidal aktivitesinin incelenmesidir.

Gereç ve Yöntemler: *C. gueneri*'nin tüm bitki kısımlarından hazırlanan metanollü (%80) ekstresi artan polaritede *n*-hekzan, kloroform ve *n*-butanol ile art arda fraksiyonlanmıştır. *C. gueneri*'nin metanollü (%80) ekstresi ve tüm fraksiyonları tuzlu su karidesi letalite testi, *Lemna minor*'e karşı fitotoksisite ile *Rhyzopertha dominica* ve *Tribolium castaneum*'a karşı insektisidal aktiviteleri olmak üzere *in vitro* tarama testleri kullanılarak biyolojik aktiviteleri bakımından incelenmiştir.

Bulgular: Çalışmamızın bulguları bitkinin *n*-hekzan ve kloroform fraksiyonlarının 1000 µg/mL'de %100 büyüme inhibisyonu (Bİ) ile *L. minor*'e karşı önemli fitotoksik aktiviteye sahip olduğunu göstermiştir. Bunun yanı sıra, bitkinin metanol (%80) ekstresi (%53 Bİ) ve *n*-butanol fraksiyonu (%46.6 Bİ) 1000 µg/mL'de orta derecede fitotoksik aktiviteye sahip bulunmuştur. Diğer taraftan, tüm örnekler tuzlu su karidesi üzerinde toksisiteye sahip bulunmamıştır. Ayrıca kalan sulu fraksiyonu %20 mortalite ile *T. castaneum*'a karşı düşük insektisidal aktivite göstermiştir.

Sonuç: Sonuçlarımız *C. gueneri*'nin *n*-hekzan ve kloroform fraksiyonlarının potansiyel fitotoksik etkiye sahip olduğunu ortaya koymuştur.

Anahtar kelimeler: *Chrysophthalmum gueneri*, Asteraceae, tuzlu su karidesi letalitesi, fitotoksisite, insektisidal aktivite

*Correspondence: E-mail: nurgun@gazi.edu.tr, Phone: +90 312 202 31 77 ORCID-ID: orcid.org/0000-0001-5489-3367
Received: 24.10.2017, Accepted: 07.12.2017

INTRODUCTION

Medicinal plants that contain various constituents are the most important sources for developing candidates of new drugs and therapeutic agents. Turkey has a rich, still unexplored medicinal flora. Traditional medicines have been used for the treatment of diseases to develope new biological agents from natural sources. Throughout the study of medicinal plants, finding bioactive components prior to structural elucidation from plant extracts, it is necessary to evaluate their biological activity. For this reason, several bench-top assays such as the brine shrimp lethality test, phytotoxicity, and insecticidal effect can be used as major prescreening assays.[1-4]

The genus *Chrysophthalmum* Schultz Bip., which belongs to the family Asteraceae, tribe Inulaeae, is represented by four species around the world.[5] In Turkey, the genus *Chrysophthalmum* has three species, namely *Chrysophthalmum montanum* (DC.) Boiss., *Chrysophthalmum dichotomum* Boiss. & Heldr. and *Chrysophthalmum gueneri* Aytac & Anderb. growing in Turkey.[6] Among them, *C. gueneri* is an endemic herbaceous plant with linear-lanceolate leaves and slender peduncles that grows around Cirlasun bridge, Alanya, Turkey.[7] To date, no phytochemical data has been reported on *C. gueneri*.

In our ongoing investigations on the genus *Chrysophthalmum*, the cytotoxic activity of *C. gueneri* was tested for the first time against some cancer cell lines using a sulforhodamine B assay.[8] In our previous studies on preliminary screening bioassays such as toxic effect on brine shrimp, phytotoxic and insecticidal activities, the *n*-hexane and chloroform fractions of two species, *C. montanum* and *C. dichotomum*, were found as promising plant sources due to having phytotoxicity and toxicity on brine shrimps.[9,10] Following our studies on *C. gueneri*, we now aimed to evaluate *in vitro* phytotoxicity and toxicity on brine shrimps and the insecticidal effect of the plant.

EXPERIMENTAL

Plant material

The whole plants of *C. gueneri* Aytac & Anderb. were collected from wet places among pine forest around Cirlasun bridge, Antalya, Turkey, at the flowering stage in August 2014. The plant was identified by one of our authors Barış Bani PhD, (Kastamonu University). Voucher specimen (F.A. 46) was deposited at the Herbarium of Gazi University (GAZİ), Ankara, Turkey.

Preparation of extracts

The air-dried whole plants of *C. gueneri* (780 g) were extracted four times (4x4000 mL) with 80% methanol at 25°C by stirring for 2 days. After filtration, the combined methanol extracts were evaporated *in vacuo* at 40°C to dryness. The concentrated MeOH extract (140.0 g, CG) were further fractionated by successive solvent extractions with *n*-hexane (15x250 mL), chloroform (10x250 mL), and *n*-butanol saturated with H_2O (9x250 mL) in a separator funnel. Each extract and remaining water phase (R-H_2O) were evaporated to dryness under reduced pressure to yield "*n*-hexane fraction" (5.6 g, CGH), "$CHCl_3$ fraction" (13.6 g, CGC), "*n*-BuOH fraction" (25.4 g, CGB) and "R-H_2O fraction" (67.0 g, CGR), respectively.

Brine shrimp lethality assay

In this assay, we investigated the toxicity of the test samples on *Artemia saline* (Leach) shrimp larvae. Brine shrimp eggs (50 mg) were sprinkled in a rectangular hatching tank (22x32 cm) half-filled with filtered brine solution. The methanol (80%) extract and subsequent solvent fractions of *C. gueneri* (20 mg) were dissolved in 2 mL of methanol. 10, 100, and 1000 µg/mL concentrations were prepared in three vials from stock solution. The solvent was evaporated overnight. After hatching (2 days), 30 shrimps were added in each vial with a volume adjusted to 5 mL using sea water. Under illumination, the vials were incubated at 25-27°C for 24 h. Other vials were supplemented with reference cytotoxic drug (etoposide: 7.46 µg/mL), and solvent, which served as positive and negative controls, respectively. The survived brine shrimps were counted macroscopically using a magnifying glass against a lit background in each vial and LD_{50} values with 95% confidence intervals were determined using Finney computer software.[11,12]

Pytotoxicity assay

The phytotoxicity assay was conducted for the methanol (80%) extract and subsequent solvent fractions of *C. gueneri* against *Lemna minor* L.[13] The medium was prepared by mixing various inorganic components in 1000 mL distilled water. KOH pellets were added for the adjustment of pH at 6.0-7.0. The extracts (30.0 mg) were dissolved in 1.5 mL of methanol (stock solution). The stock solutions of the extracts were diluted to obtain final concentrations as 10, 100 and 1000 µg/mL (nine flasks, three for each dilution). After evaporating the solvent overnight under sterile conditions, 20 mL medium and 10 plants were added to each flask, each one containing a rosette of two fronds of *L. minor*. Other flasks were supplemented with medium and reference plant growth inhibitor, Paraquate, as negative and positive controls, respectively. All flasks were incubated in a growth cabinet for seven days at 30°C. At the end of the incubation period, the number of fronds per flasks was counted and recorded. The growth regulation (GR) in percentage (%) was determined using the formula given below:

$$GR\ (\%) = \frac{100 - \text{Number of the fronds in the test samples}}{\text{Number of the fronds in the negative control}} \times 100$$

According to the criteria, the GR (%) means low activity in 0-39%, moderate activity in 40-59%, good activity in 60-69%, and significant activity in >70%.

Insecticidal activity

The methanol (80%) extract and subsequent solvent fractions of *C. gueneri* were tested against *Rhyzopertha dominica* and *Tribolium castaneum* using the impregnated filter paper method.[14] To prepare the stock solution, the samples (200 mg) were dissolved in 3 mL of methanol. The samples were applied to filter paper (1019.10 µg/cm^2) of appropriate size (9 cm or 90 mm) on Petri dishes using micropipette. The plates were left for 24 h to evaporate the solvent. The next day, 10 insects of each

species were placed in each plate (test and control) using a clean brush. Permethrin (239.5 µg/cm^2) was used as a positive control; methanol was used as a negative control. The plates were incubated at 27°C for 24 h with 50% relative humidity in the growth chamber.

For the calculation, the number of survivals of each species was counted and mortality (M) (%) was determined using the following formula:

$$M\ (\%) = \frac{100 - \text{Number of insects alive in the test samples}}{\text{Number of insects alive in the control}} \times 100$$

Ethics committee approval was not necessary for this study.

RESULTS AND DISCUSSION

In this study, we examined the methanol (80%) extract and the fractions of *C. gueneri* for their lethality, phytotoxicity, and insecticidal activity with primary screening bioassays. The brine shrimp lethality test on *C. gueneri* was investigated at concentrations of 10, 100 and 1000 µg/mL, using etoposide as a standard drug. All fractions and the methanol extract had no toxicity against the brine shrimps (Table 1).

The phytotoxicity assay is a useful primary screen for weedicide research. It is also observed that natural antitumor compounds can inhibit *Lemna* growth.[13] *C. gueneri* showed variable effects in terms of phytotoxicity against *L. minor.* It was found that the tested samples had dose dependent activity. The *n*-hexane and chloroform fractions of the plant showed significant phytotoxic activities with 100% growth inhibition (GI) at 1000 µg/mL. Moreover, the MeOH extract and *n*-butanol fraction had moderate phytotoxic activities with 53% and 46.6% of GI at 1000 µg/mL, respectively. In addition, low phytotoxicity was found in the remaining water fraction with 31.2% of GI at 1000 µg/mL, followed by the chloroform (21% GI), *n*-hexane (15.4% GI), *n*-butanol (13.3% GI), and methanol (80%) extract (6.2% GI) of the plant at 100 µg/mL. There was no phytotoxicity in any tested samples at 10 µg/mL (Table 2).

The methanol extract and fractions of *C. gueneri* were also screened for their insecticidal effects against *R. dominica* and *T. castaneum* using permethrin as a standard drug. The remaining water fraction had low insecticidal activity with 20% of mortality against *T. castaneum* (Table 3).

Table 1. Toxicity of the extract and fractions of *Chrysophthalmum gueneri*

Samples	No of survivors from 30 shrimps			LD_{50} (µg/mL)
	10 µg/mL	100 µg/mL	1000 µg/mL	
CG	27	27	26	-
CGH	19	15	15	464.2454
CGC	27	25	18	3695.8640
CGB	28	27	24	-
CGR	28	22	23	-

Standard drug: etoposide (LD_{50} =7.46 µg/mL),

Table 2. Phytotoxic activity of the extract and fractions of *Chrysophthalmum gueneri*

Samples	Growth regulation (%)		
	10 µg/mL	100 µg/mL	1000 µg/mL
CG	0	6.2	53.0
CGH	0	15.4	100.0
CGC	0	21.0	100.0
CGB	0	13.3	46.6
CGR	0	0	31.2

Standard drug: paraquate (0.015 µg/mL)

Table 3. Insecticidal activity of the extract and fractions of *Chrysophthalmum gueneri*

Samples (1019.10 µg/cm^2)	*Tribolium castaneum*		*Rhyzopertha dominica*	
	Mortality (%)	Insecticidal activity	Mortality (%)	Insecticidal activity
CG	0	No	0	No
CGH	0	No	0	No
CGC	0	No	0	No
CGB	0	No	0	No
CGR	20	Low	0	No

Reference insecticide: permethrin (239.5 µg/cm^2)

The present paper is the first to present data to show that *C. gueneri* exhibits a variety of phytotoxic and insecticidal biologic activities. According to our results, the *n*-hexane and chloroform fractions of the plant were found as promising samples because they had significant phytoxicity on *L. minor*. In our recent study, *n*-hexane and chloroform fractions of the plant also exhibited cytotoxicity on selected cancer cell lines.[8] Our results also showed that the *n*-hexane and chloroform fractions of *C. gueneri* contained bioactive constituents and these fractions could lead to the discovery of important agents.

CONCLUSIONS

In conclusion, according to conventional herbicides and pesticides, *C. gueneri* could be considered a potential source for developing natural constituents possessing weedicide and insecticide activities with less risk to human health and the environment. Therefore, further investigations are merited in order to identify the responsible bioactive compound(s) in *C. gueneri*.

ACKNOWLEDGEMENTS

This study was supported by TÜBİTAK-2211/A and ICCBS-HEJ.

Conflict of Interest: No conflict of interest was declared by the authors.

REFERENCES

1. Inayatullah S, Irum R, Rehman AU, Chaudhary MF, Mirza B. Biological evaluation of some selected plant species of Pakistan. Pharm Biol. 2007;45:397-403.
2. Ullah R, Ibrar M, Shah S, Hameed I. Phytotoxic, cytotoxic and insecticidal activities of *Calendula arvensis* L. J Biotechnol Pharm Res. 2012;3:104-111.
3. Khuda F, Iqbal Z, Zakiullah, Khan A, Nasir F, Muhammad N, Khan JA, Khan MS. Metal analysis, phytotoxic, insecticidal and cytotoxic activities of selected medicinal plants of Khyber Pakhtunkhwa. Pak J Pharm Sci. 2012;25:51-58.
4. Uddin G, Rehman, TU, Arfan M, Liaqat W, Mohammad G, Choudhary MI, Phytochemical analysis, antifungal and phytotoxic activity of seeds of medicinal plant *Indigofera heterantha* Wall. Middle-East J Sci Res. 2011;8:603-605.
5. Rechinger KH. Chrysophthalmum Schultz-Bip. In Kotschy. In: Rechinger, KH, ed. Flora Iranica 145. Compositae IV-Inuleae. Graz; Akademische Druck und Verlagsanstalt; 1980:131-132.
6. Grierson AJC. Chrysophthalmum Schultz Bip. In: Davis, PH, ed. Flora of Turkey and the East Aegean Islands. Edinburgh; Edinburgh University Press; 1975;5:52-53.
7. Aytac Z, Anderberg AA. A new species of Chrysophthalmum Schultz Bip. (Asteraceae-Inuleae) from Turkey. Bot J Linn Soc. 2001;137:211-214.
8. Ayaz F, Kucukboyaci N, Sarimahmut M, Bani B, Duman H, Ulukaya E, Calis I. Cytotoxic activity of the Genus Chrysophthalmum Schultz Bip. from Turkey against various human cancer cell lines. 3rd EACR-Sponsored Anticancer Agent Development Congress; İzmir, Turkey; 2015:42.
9. Ayaz F, Küçükboyacı N, Duman H, Şener B, Choudhary MI. Cytotoxic, Phytotoxic and Insecticidal Activities of *Chrysophthalmum montanum* (DC.) Boiss. Turk J Pharm Sci. 2017;14:290-293.
10. Ayaz F, Küçükboyacı N, Bani B, Şener B, Choudhary MI. Phytotoxic, cytotoxic and insecticidal activities of *Chrysophthalmum dichotomum* Boiss. and Heldr. Indian J Pharm Educ. 2018;52:467-471.
11. Finny DJ. Probit Analysis. (3rd ed). Cambridge; Cambridge University Press; 1971:333.
12. Meyer BN, Ferrigni NR, Putnam JE, Jacobsen LB, Nicholas DE, McLaughin JL. Brine Shrimp: A convenient general bioassay for active plant constituents. Planta Med. 1982;45:31-34.
13. Rahman AU. Studies in Natural Product Chemistry. The Netherlands; Elsevier Science Publishers BV; 1991;9:383-409.
14. Rahman AU, Choudhary MI, William JT. Bioassay techniques for drug development. The Netherlands; Harward Academic Publisher; 2001:67-68.

2018 Author Index

2018 Author Index

2018 Author Index

2018 Subject Index

NOTES

NOTES